Compositional and structural analysis of selected chromosomal domains from *Saccharomyces cerevisiae*

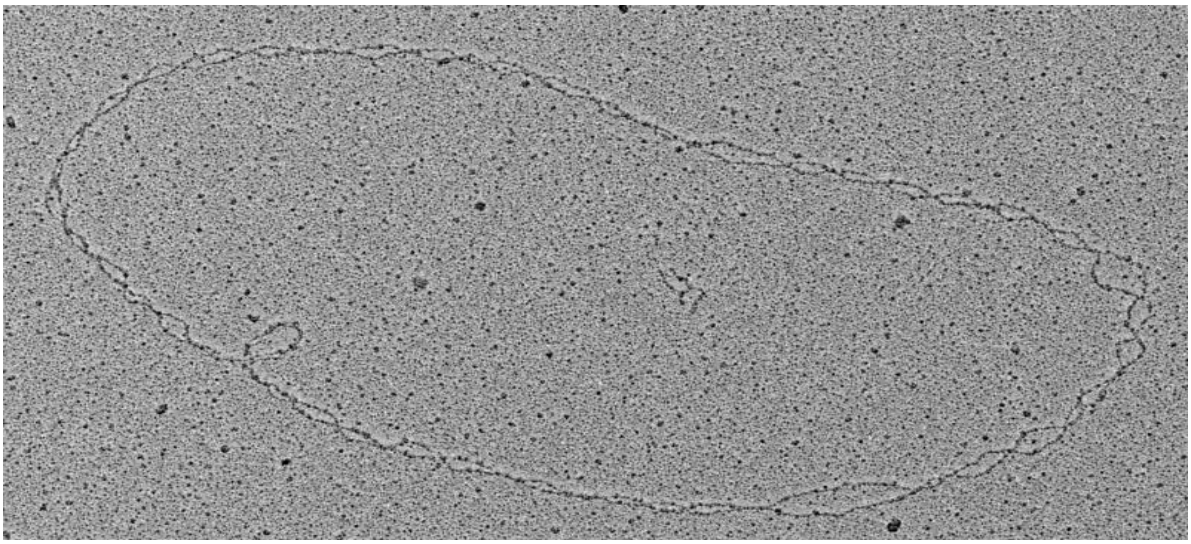

DISSERTATION ZUR ERLANGUNG DES DOKTORGRADES DER
NATURWISSENSCHAFTEN (DR. RER. NAT.)
DER FAKULTÄT FÜR BIOLOGIE UND VORKLINISCHE MEDIZIN
DER UNIVERSITÄT REGENSBURG

vorgelegt von

Stephan Hamperl aus Katzbach

im August 2012

Electron micrograph on the cover visualizes a DNA molecule derived from an ex vivo purified chromatin circle spanning an entire ribosomal DNA repeat.

Das Promotionsgesuch wurde eingereicht am: 23. August 2012

Die Arbeit wurde angeleitet von: PD. Dr. Joachim Griesenbeck

Prüfungsausschuss:

Vorsitzender:	Prof. Dr. Herbert Tschochner
1. Prüfer:	PD. Dr. Joachim Griesenbeck
2. Prüfer:	Prof. Dr. Hinrich Boeger
3. Prüfer:	Prof. Dr. Rainer Deutzmann

Die vorliegende Arbeit wurde in der Zeit von Februar 2009 bis August 2012 am Lehrstuhl Biochemie III des Institutes für Biochemie, Genetik und Mikrobiologie der Naturwissenschaftlichen Fakultät III der Universität Regensburg unter Anleitung von PD Dr. Joachim Griesenbeck im Labor von Prof. Dr. Herbert Tschochner angefertigt.

Ich erkläre hiermit, dass ich diese Arbeit selbst verfasst und keine anderen als die angegebenen Quellen und Hilfsmittel verwendet habe.
Diese Arbeit war bisher noch nicht Bestandteil eines Prüfungsverfahrens.
Andere Promotionsversuche wurden nicht unternommen.

Stephan Hamperl
Regensburg, 23.08.2012

Table of Contents

1 Summary 1

2 Introduction 3

2.1 Chromatin 3

2.1.1 The nucleosome 3

2.1.2 Posttranslational modifications of histones 4

2.1.2.1 Acetylation of histone lysine residues 6

2.1.2.2 Methylation of histone lysine and arginine residues 7

2.1.2.3 Other histone modifications 8

2.1.3 Incorporation of histone variants 9

2.1.4 The positioning of nucleosomes 10

2.1.5 The linker histone H1 and higher order structures of chromatin 11

2.1.6 Non-histone components of chromatin 12

2.2 Compositional and structural analysis of chromatin 12

2.2.1 Reconstitution of chromatin *in vitro* 13

2.2.2 Analysis of DNA-protein interactions *in vivo* 14

2.2.2.1 Chromatin Immunoprecipitation (ChIP) 14

2.2.2.2 DNA adenine methyltransferase identification (DamID) 15

2.2.2.3 Chromatin Endogenous Cleavage (ChEC) 16

2.2.3 Isolation and analysis of *in vivo* assembled chromatin 16

2.2.3.1 Enrichment of chromosomal regions by fractionation 16

2.2.3.2 Purification of yeast mini chromosomes 17

2.2.3.3 Proteomics of isolated chromatin segments 18

2.2.3.4 Purification of defined chromatin domains by site-specific recombination 19

2.3 Chromatin structures at the essential multi-copy rDNA locus and the non-essential single-copy *PHO5* locus 21

2.3.1 Chromatin structure at the yeast rDNA locus 21

2.3.1.1 Cellular localization and chromosomal organization of the multi-copy yeast rDNA locus 22

2.3.1.2 Distinct chromatin structures at the 35S rRNA genes 25
2.3.1.3 Chromatin structure at the intergenic spacer 29
2.3.2 Chromatin structure at the yeast *PHO5* locus 31
2.4 Objectives 32

3 Results 34
3.1 Purification of defined chromosomal domains by site-specific recombination *in vivo* 34
3.1.1 Establishment of yeast strains with a modified rDNA locus competent for excision of distinct rDNA chromatin domains 35
3.1.1.1 Strategy for chromosomal integration and expansion of genetically modified rDNA repeats 35
3.1.1.2 35S rRNA gene chromatin states are established after expansion of the genetically modified rDNA repeats 37
3.1.2 Establishment of a single step purification technique for selected chromosomal domains 40
3.1.2.1 Single-step affinity purification with IgG coupled magnetic beads allows efficient enrichment of rDNA chromatin domains 40
3.1.2.2 LexA-TAP expression level influence the specific enrichment of the targeted domains 42
3.1.2.3 Chromosomal integration of the R recombinase and LexA-TAP expression cassette allows cell growth in complex medium 44
3.1.2.4 Distinct domains of the rDNA locus can be purified from the yeast chromosome 45
3.2 Compositional analysis reveals distinct proteomes for individual rDNA chromatin domains 46
3.2.1 Covalently modified histones are selectively enriched in purifications of distinct rDNA domains 46
3.2.2 Specific non-histone chromatin components are selectively enriched in purifications of distinct rDNA domains 50
3.2.3 Comparative mass spectrometry reveals distinct proteomes for individual rDNA chromatin domains 52
3.2.3.1 Strategy for semiquantitative comparative analysis of rDNA chromatin composition using the iTRAQ technology 52

3.2.3.2 Comparative analysis of proteins co-purifying with LexA-TAP from strains with and without recombined rDNA chromatin domains 53

3.3 Selected complexes and factors identified by the proteome analysis interact with rDNA chromatin *in vivo* 58

3.4 Important structural and conformational chromatin features of specific rDNA chromatin domains are conserved upon isolation 62

3.4.1 Gel filtration analysis of the circular 5S rDNA and E-pro region suggests structural differences 62

3.4.2 Single molecule electron microscopic analysis of 5S rRNA gene circles suggests a heterogeneous population of different chromatin states 64

3.4.3 Restriction endonuclease accessibility analysis of 5S rRNA gene chromatin confirms the results of the single molecule approach 67

3.5 Chromatin domains of single copy genes can be enriched in sufficient amounts and purity to perform mass spectrometric analysis 69

4 Discussion 72

4.1 A single-step purification strategy allows robust enrichment of native rDNA chromatin 72

4.1.1 Yield and specificity of rDNA chromatin isolation procedure compare well with alternative chromatin purification strategies 72

4.1.2 Pol I associated chromatin purified after formaldehyde crosslinking *in vivo* shows similarities and differences when compared to native 35S rRNA gene chromatin 75

4.2 The purification approach allows the unbiased identification of new protein components of chromatin *in vivo* 78

4.3 The native purification strategy is compatible with downstream structural and biochemical analysis of the isolated material 81

4.4 Outlook 82

5 Material and methods 83

5.1 Material 83

5.1.1 Chemicals 83

5.1.2 Buffers and media 83

5.1.3 Nucleic acids 88

5.1.4 Enzymes and polypeptides 106

5.1.5 Antibodies 107
5.1.6 Organisms 107
5.1.7 Equipment 113
5.1.8 Consumables 114
5.1.9 Software 115
5.2 Methods 115
5.2.1 Enzymatic manipulation of DNA 115
5.2.2 Purification of nucleic acids 116
5.2.3 Quantitative and qualitative analysis of nucleic acids 118
5.2.4 Manipulation of *Escherichia coli* 121
5.2.5 Manipulation of *Saccharomyces cerevisae* 121
5.2.6 Formaldehyde crosslinking (FA-X) of yeast cultures 123
5.2.7 Preparation of nuclei 124
5.2.8 Chromatin Endogenous Cleavage (ChEC) 124
5.2.9 DNA workup of ChEC samples 125
5.2.10 Restriction digest and agarose gel electrophoresis of ChEC samples 125
5.2.11 Chromatin Immuno Precipitation (ChIP) 126
5.2.12 Purification of specific chromatin circles from *S. cerevisiae* 127
5.2.13 Endonuclease digestion analysis of purified chromatin domains 129
5.2.14 Micrococcus nuclease digestion of purified chromatin domains 129
5.2.15 Gel filtration chromatography of chromatin circles 130
5.2.16 Protein-biochemical methods 130
5.2.17 Analysis of histone modifications by MALDI TOF/TOF mass spectrometry 134
5.2.18 Comparative iTRAQ MALDI TOF/TOF mass spectrometry 135

6 References 137

7 Abbreviations 158

8 Publications 160

9 Acknowledgements 161

1 Summary

In eukaryotic genomes, chromatin is the template of all nuclear processes including transcription, recombination and replication. Besides the wrapping of DNA in nucleosome core particles, eukaryotic chromatin is associated, interpreted and modified by numerous protein complexes including transcription factors, DNA and RNA metabolizing machineries, architectural proteins and chromatin remodeling and modifying enzymes. To understand how specific genomic loci adopt different functional states, it is critical to characterize the corresponding compositional changes in the local chromatin structure. In this work, a previously established technique based on site specific recombination at defined genomic locations was used to purify selected chromosomal domains from *Saccharomyces cerevisiae* under native conditions. After improvement of yield and purity of the chromatin preparation, the proteomes co-purifying with domains derived from the multi-copy ribosomal DNA locus transcribed by RNA polymerases I, II and III and at an autonomous replication sequence could be defined by comparative mass spectrometry (MS). Many protein components known to interact with the respective chromatin domains were identified as well as several new factors, for which association with rDNA chromatin could be confirmed *in vivo*. Mass spectrometric analysis allowed further to assess the posttranslational modifications of histones associated with the individual domains. In addition, electron microscopic analysis provided single molecule information about nucleosome configurations at 5S ribosomal RNA genes. First statistical analyses indicate a heterogeneous population of chromatin states likely correlating with different stages of transcriptional activity. Finally, the improved protocol was applied to the *PHO5* gene in order to explore the potential of purifying genes that are only present in one copy per cell. The results indicate that *PHO5* associated histone molecules can be enriched in sufficient amounts for MS analysis, opening the door to fully define the specific posttranslational histone modification state at virtually every gene in yeast.

Zusammenfassung

In eukaryotischen Genomen stellt Chromatin die Matrize aller nukleären Prozesse wie Transkription, Rekombination und Replikation dar. Neben dem Aufwickeln der DNA in nukleosomale Kernpartikel, ist eukaryotisches Chromatin assoziiert und wird interpretiert und modifiziert durch zahlreiche Proteinkomplexe, darunter Transkriptionsfaktoren, DNA- und RNA-metabolisierende Maschinerien, strukturelle Proteine und Chromatin-remodulierende und modifizierende Enzyme. Um zu verstehen wie spezifische genomische Loci verschiedene funktionelle Zustände einnehmen, ist es entscheidend, die entsprechenden kompositionellen Änderungen in der lokalen Chromatinstruktur zu charakterisieren. In dieser Arbeit wurde eine bereits etablierte Technik, basierend auf ortspezifischer Rekombination an spezifischen genomischen Loci, verwendet um bestimmte chromosomale Domänen aus der Bäckerhefe *Saccharomyces cerevisiae* unter nativen Bedingungen zu reinigen. Nach Verbesserung von Ausbeute und Reinheit der Chromatin-Präparationen konnten die assoziierten Proteome mit spezifischen Teilbereichen des Multikopien-ribosomalen DNA Lokus, welche von RNA Polymerase I, II und III transkribiert werden, sowie mit einer autonomen Replikationssequenz durch vergleichende Massenspektrometrie (MS) bestimmt werden. Neben vielen bekannten Proteinkomponenten der entsprechenden Chromatindomänen konnten auch mehrere neue Faktoren identifiziert werden, deren Assoziation mit rDNA Chromatin *in vivo* bestätigt werden konnte. Massenspektrometrische Analysen erlaubten weiter die Bestimmung der posttranslationalen Modifikationen von Histonen, die mit den verschiedenen Domänen assoziiert waren. Zusätzlich erlaubten elektronenmikroskopische Analysen Einzelmolekül-Informationen über die Nukleosomenkonfigurationen an 5S ribosomalen RNA Genen zu gewinnen. Erste statistische Analysen deuten auf eine heterogene Verteilung hin, die wahrscheinlich mit verschiedenen transkriptionellen Zuständen korrelieren. Schließlich wurde das verbesserte Protokoll auf das *PHO5*-Gen angewendet, um potentiell Chromatindomänen zu reinigen, die nur einmal pro Zelle existieren. Die Ergebnisse deuten an, dass *PHO5*-assoziierte Histonmoleküle in ausreichenden Mengen für MS-Analysen angereichert werden können. Dies eröffnet die Möglichkeit, den vollständigen posttranslationalen Histonmodifikationszustand jedes Gens in der Hefe zu definieren.

2 Introduction

2.1 Chromatin

The remarkable length and complexity of eukaryotic genomes confronts the cell with several constraints. On the one hand, the genetic information has to be readily accessible for gene expression, and on the other hand, the macromolecular DNA has to be compacted to fit in the limited three-dimensional space of the nuclear subcellular compartment. Cells meet this requirement by assembling the genome into a highly compact but dynamic structure termed chromatin, a complex of nucleic acids and associated proteins (Olins and Olins, 2003). Accordingly, chromatin presents the natural substrate of all DNA template-dependent processes including transcription, replication, recombination, chromosome segregation and DNA repair and thus has to adopt a regulated dynamic structure (Kornberg and Lorch, 1995; Felsenfeld and Groudine, 2003; Khorasanizadeh, 2004; Li et al., 2007; Clapier and Cairns, 2009).

2.1.1 The nucleosome

One of the most direct evidences that eukaryotic DNA is packaged in a repeating unit is derived from electron microscopic studies from nuclei of chicken liver and cultured calf cells (Olins and Olins, 1974; Oudet et al., 1975). The uniformly sized structures with a diameter of 12.4-13nm appeared to correspond to biochemically isolated nucleoprotein complexes released from chromatin which had been identified earlier as the basic repeating unit of chromatin, termed nucleosomes (Hewish and Burgoyne, 1973; Kornberg, 1974). More recently, crystallographic studies have made it possible to visualize the nucleosome core particle with high resolution. Nucleosomes individually assemble 147 DNA base pairs around a core histone octamer. Each octamer is composed of two H3-H4 histone dimers bridged together as a stable tetramer that is flanked by two separate H2A-H2B dimers (Luger et al., 1997; Davey et al., 2002). The histone proteins are highly conserved and share a structured histone fold core consisting of 3 characteristic α-helices. The globular core mediates histone-histone and histone-DNA interactions so that the DNA is wrapped around the octamer in 1.7 turns to form a left-handed superhelix (Figure 1). About 142 hydrogen bonds are formed between the

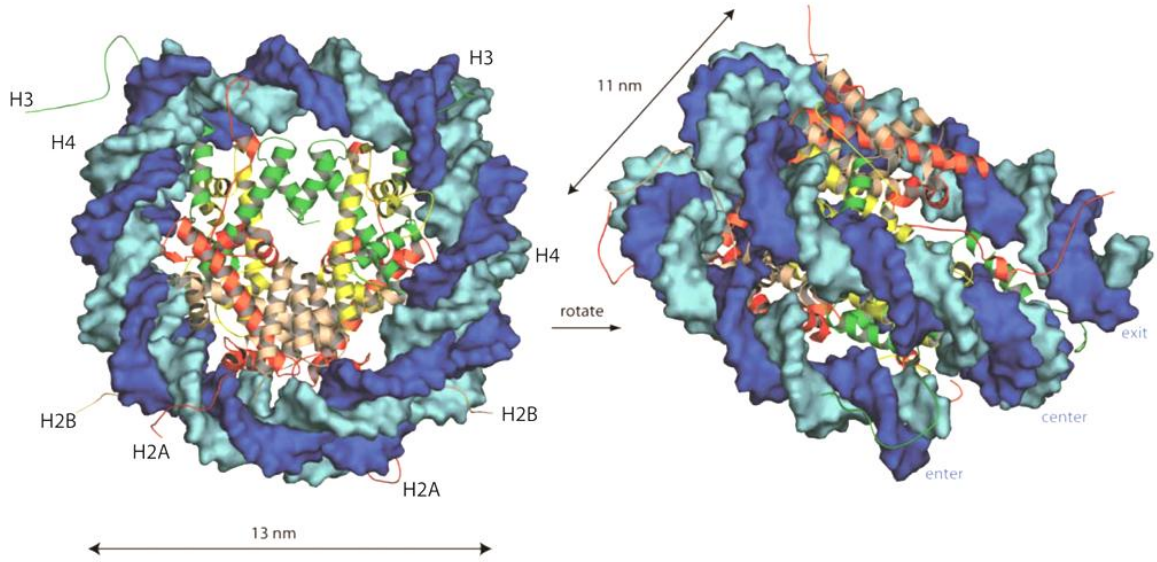

Figure 1 The atomic structure of the nucleosome core particle. 147 bp of DNA (colored in different shades of blue) are wrapped around the histone octamer in 1.7 turns. The histone octamer is composed of two copies of each histone H2A (red), H2B (pink), H3 (green) and H4 (yellow) and forms the nucleosome core particle. Histone tails protrude from the nucleosome core particle (modified from Khorasanizadeh, 2004).

DNA strand and the histone core. Nearly half of these bonds form between the amino acid backbone of the histones and the phosphodiester backbone of the DNA. Additionally, numerous hydrophobic interactions and salt linkages result in a very stable association of the histone octamer with the DNA. The inherent disordered amino-terminal tails of all eight histones, as well as short protease accessible carboxy-terminal domains, extend from the disk-shaped nucleosome surface. (Hacques et al., 1990; Arents et al., 1991). These short tails are 25 to 40 amino acids long and do not contribute significantly to the structure of individual nucleosomes nor to their stability (Luger et al., 1997; Luger and Richmond, 1998). However, *in vitro* removal of the histone tails results in nucleosomal arrays that cannot condense into higher-order structures, indicating that they do play an essential role in controlling the folding of nucleosomal arrays (Carruthers and Hansen, 2000; Peterson and Laniel, 2004; Hizume et al., 2009).

2.1.2 Posttranslational modifications of histones

The histone tails protrude from the nucleosomal cores and are prominent targets for distinct posttranslational modifications (PTMs). Histones are also modified at residues in the globular core. Over one hundred of covalent modifications of histones are described including the acetylation of lysines, the methylation of lysines and arginines, the phosphorylation of serines and threonines, the ubiquitination of lysines, the sumoylation

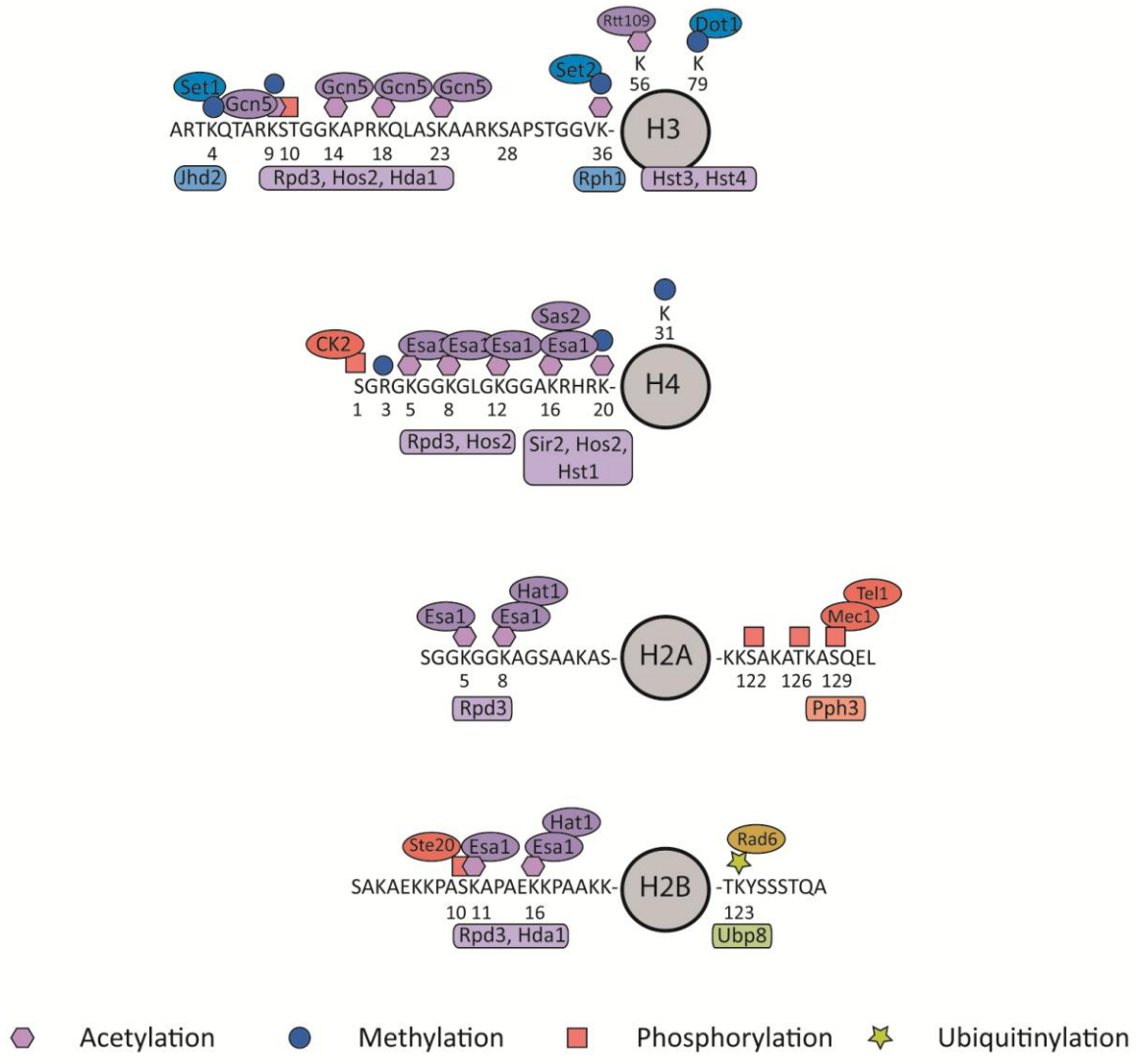

Figure 2 A summary of histone modifications in yeast. The core histone fold domains are indicated as grey circles. The sequences of the N- and C-terminal tails are depicted. The numbers shown under modified residues indicate amino acid positions. The type of modification is indicated by purple hexagons for acetylation, blue circles for methylation, red rectangles for phosphorylation and yellow star for ubiquitination. Mono-,di-, or tri-methylation is not specified. Enzymes that add modifications are shown in the ovals above their sites of action; enzymes that remove modifications are indicated below the tails in boxes (Adapted from Krebs, 2007).

of lysines and the ADP-ribosylation of glutamic acids (Figure 2). New histone marks are still in the process of being identified and 67 new PTMs were recently discovered including crotonylation of lysine residues (Tan et al., 2011).

The possibility to combine a multitude of these histone marks in a combinatorial way led to the proposal of the histone code (Strahl and Allis, 2000; Jenuwein and Allis, 2001). In this hypothesis, the distinct pattern of specific histone marks is thought to mediate interactions with chromatin-modifying effectors which in turn alter chromatin structure with functional consequences for the activity in respective to the genomic target locus. To verify this hypothesis, strong efforts have been directed towards relating histone PTMs with the transcriptional state and identifying the effector modules that recognize

and decrypt different histone marks. However, all chemical modifications of histone tails were shown to be reversible (Bannister et al., 2002; Kubicek and Jenuwein, 2004), indicating that the stability of a certain PTM at a specific locus is limited in time *in vivo*. Moreover, multiple binding partners have been reported for single histone PTMs (Becker, 2006), indicating redundancy and complexity in the recognition of the modified histone tail. Although our knowledge of histone modifications, their effectors and the influence on the transcriptional activity have advanced tremendously, the identified combinations of histone marks have not yet been shown to translate in predictable, defined chromatin states.

2.1.2.1 Acetylation of histone lysine residues

Histone acetylation is catalyzed by histone acetyltransferases (HATs) transfering acetyl groups from acetyl-CoA to the ε-amino side chains of specific lysine residues on all four core histones (Loidl, 1994). This modification appears to be highly dynamic and is reversed by histone deacetylases (HDACs), which remove acetyl groups from lysines. In yeast, histones H3 and H4 can be acetylated on six and five lysine residues in their N-terminal tails, respectively (H3: K9, K14, K18, K23, K36, K56 and H4: K5, K8, K12, K16, K20). H2A can be acetylated at K5 and K8, whereas acetylation of H2B occurs mainly at residues K11 and K16 (Krebs, 2007). Some of the enzymes that add or remove acetyl groups from specific lysine residues of the histone tails are indicated in Figure 2.

It is generally accepted that acetylation results in partial neutralization of the positive charge of the histones, thus decreasing their affinity to negatively charged DNA (Hong et al., 1993) and promoting accessibility of the DNA for transcription activation. Consistent with this observation, deacetylation produces a more compacted structure that is refractory to the binding of factors (Wade, 2001). Acetylation and deacetylation, however, might also regulate gene activity by providing specific binding surfaces for the recruitment of repressors and activators. The bromodomain protein module interacts specifically with acetylated lysine residues of the histone tails (Dhalluin, 1999). This protein domain is found in several transcription factors including the HAT Gcn5 and $TAF_{II}250$, the largest subunit of the TFIID transcription initiation complex (Jacobson et al., 2000).

In addition to targeted modification of nucleosomes at specific promoters, HDACs and HATs modify histone lysine residues throughout the genome in a global and untargeted manner (Krebs et al., 2000; Kuo et al., 2000; Vogelauer et al., 2000). Recent measurements of bulk acetylation levels in yeast suggest that on average, as many as 13 lysines per octamer are acetylated (Waterborg, 2000). Such high overall acetylation

levels are difficult to reconcile with the targeting of HATs to a few specialized sites with high affinity. Dynamic changes in histone acetylation levels may allow gene repression or activation by modulating the level of basal transcription in response to environmental cues. The acetylation state of histone tails was also shown to be implicated in other nuclear processes like DNA replication, DNA repair, transcription elongation and gene silencing (reviewed in Kurdistani and Grunstein, 2003).

2.1.2.2 Methylation of histone lysine and arginine residues

Histone methyltransferases (HMTs) catalyze the transfer of up to three methyl groups from S-adenosyl methionine (SAM) to the same amino group to form mono(me1)-, di(me2)-, or tri(me3)-methylated lysine residues. Methyl groups can be removed by the enzymatic activity of histone demethylases (HDMs). The protein arginine methyltransferases (PRMTs) transfer one or two methyl groups, either symmetrically or asymmetrically, to the ω-guanidino group of arginine residues. Yeast histone H3 has four target sites for HMTs (K4, K9, K36 and K79), whereas vertebrate histone H3 can additionally be methylated at K27. However, the transfer of methyl groups to K20 of histone H4 is well conserved in all eukaryotic cells (Figure 2).

Unlike acetylation and phosphorylation, histone methylation is a relatively stable modification with a slow turnover rate and does not change the charge of the lysine residue at physiological pH. Similar to acetylation marks, methylated lysine residues are recognized by numerous protein domains with high specificity. These protein modules include chromodomains, WD40 domains, PHD domains, Tudor domains or MBT domains with different affinities for mono-, di-, and tri-methylated lysines (Lachner et al., 2001; Huyen et al., 2004; Wysocka et al., 2005; Kim et al., 2006). The development of methods that allow the genome-wide mapping of individual histone modifications made it possible to detect correlations between histone modification patterns and specific states of gene activity (Lee and Mahadevan, 2009). In general, the presence of methyl groups at H3K9, H3K27 and H4K20 overlaps with transcriptional repressed heterochromatic regions of the genome, whereas methylation at H3K4, H3K36 and H3K79 correlates with transcriptional active euchromatin (Zhang and Reinberg, 2001; Kouzarides, 2002; Peterson and Laniel, 2004; Martin and Zhang, 2005). However, the methylation marks are not exclusively linked to the transcriptional state, but were also shown to be implicated in a multitude of other nuclear processes including DNA repair, cell cycle regulation, alternative splicing, recombination and DNA replication (Nguyen and Zhang, 2011; Wagner and Carpenter, 2012).

2.1.2.3 Other histone modifications

Acetylation and methylation of histone residues are the most frequent and intensively studied examples of posttranslational modifications of histone molecules. Nevertheless, other chemical moieties were also shown to influence the nucleosome structure and accessibility of regulatory and enzymatic protein complexes to chromatin templates. One important example is phosphorylation of serine and threonine residues of histone proteins. Importantly, histone H3 is phosphorylated at several sites during mitosis, including serines 10 and 28 and threonines 3 and 11 (Garcia et al., 2005; Bonenfant et al., 2007; Zhou et al., 2008). The hyperphosphorylation of histone H3 during mitosis is conserved in a variety of metazoan, fungi, plants and protozoa and has been linked to a variety of cellular processes including chromosome condensation and segregation, activation of transcription, gene silencing, apoptosis and DNA damage repair (reviewed in Cerutti and Casas-Mollano, 2009).

Ubiquitin, a 76 amino acid protein, is attached to lysine residues of proteins through a series of enzymatic reactions (reviewed in Pickart, 2001). Substrates can be mono- or polyubiquitinated. Whereas polyubiquitination targets proteins for degradation via the 26S proteasome, monoubiquitination generally acts as a tag that marks the substrate protein to signal for a particular function. One well-characterized example of this process in yeast is the monoubiquitination of lysine 123 in the C-terminal tail of histone H2B (Figure 2). The ubiquitin moiety on H2B is dynamically regulated during gene expression in yeast and was linked to contradictory biological outputs including transcriptional activation of specific gene loci (Davie and Murphy, 1990; Davie et al., 1991) and gene silencing at heterochromatin-like regions at telomeres and silent mating type loci (Sun and Allis, 2002). Moreover, ubiquitination is highly dynamic and removed from histones by ubiquitin proteases (UBPs) during metaphase and then reattached to histones at anaphase (Goldknopf et al., 1980; Mueller et al., 1985). Global deubiquitination of H2B also occurs during yeast stationary phase in response to the depletion of glucose from the culture medium (Dong and Xu, 2004).

Other less abundant posttranslational modifications of histone molecules include the transfer of one or several ADP-ribose moieties from NAD^+ to specific amino acid residues by releasing nicotinamide (ADP-ribosylation) (Messner and Hottiger, 2011) and the transfer of Small Ubiquitin-like MOdifier (SUMO) proteins on histone tails in a similar pathway to ubiquitin (Johnson, 2004).

2.1.3 Incorporation of histone variants

In addition to the four canonical histones and their posttranslational modification patterns, the incorporation of certain divergent forms of histones H3 and H2A into nucleosomes additionally increases the complexity of the nucleosome structure. These histone variants appear to be incorporated site specifically into chromatin outside of S phase of the cell cycle replacing the corresponding canonical histones which are deposited onto newly replicated DNA.

In metazoans, three main classes of genes encode for distinct histone H3 proteins: the 'canonical', replication-dependent histone H3, the replication-independent histone variant H3.3, and the centromere specific H3 variant CENP-A (Cse4 in yeast) (Franklin and Zweidler, 1977; Palmer et al., 1987). The H3.3 variant is specifically enriched within actively transcribed genes by a replication-independent replacement process dependent on active transcription (Ahmad and Henikoff, 2002; Schwartz and Ahmad, 2005), although the primary protein sequence shows only subtle difference from canonical H3 in amino acids 87-90 in the histone core region (AAIG vs. SAVM). Interestingly, the yeast species *Saccharomyces cerevisiae* and *Schizosaccharomyces pombe* encode only H3.3-like protein sequences, which may reflect the highly transcribed euchromatic state of their genomes.

Several variants have been described for histone H2A including the well-conserved H2A.Z and H2A.X variants as well as nucleosomes containing the vertebrate specific macro-H2A and H2A-Bbd (Bar-body deficient) histone molecules (West and Bonner, 1980). H2A.X is closely related to canonical H2A with an important C-terminal extension that is mainly involved in DNA repair functions by phosphorylation of a serine residue in response to DNA double strand breaks (Rogakou et al., 1998). A comparison of H2A.Z to canonical H2A reveals a sequence identity of 60% (Wu and Bonner, 1981) with some differences within the histone fold domain and the largest divergence in their C-terminal domains. Several genome wide studies have mapped the binding sites of H2A.Z containing nucleosomes and the variant was found to be enriched in distinct promoter regions (Guillemette et al., 2005; Zhang et al., 2005) that implicated this histone variant in transcriptional activation. However, H2A.Z in yeast was also shown to be important for preventing the spread of silent heterochromatin into active regions near telomeres and silent mating type loci (Meneghini et al., 2003) and other functions are discussed in regard to the folding of the chromatin fiber by facilitating nucleosome-nucleosome interactions (Fan et al., 2002).

2.1.4 The positioning of nucleosomes

Nucleosomes are arranged as a linear array along the DNA polymer, which makes them appear as “beads on the string” by electron microscopy (Olins and Olins, 1974). The string represents short stretches of linker DNA that join adjacent nucleosomes. The size of the linker DNA differs in yeast and higher eukaryotes. Whereas in metazoan species the average nucleosomal repeat length is approximately 190bp, yeast nucleosomes are very closely spaced with an average repeat length of 162±6bp (Hörz and Zachau, 1980), resulting in a linker length of only 15-20bp (White et al., 2001). It is generally accepted that the nucleosomal structure is inhibitory to nuclear processes and thus, the positioning of the nucleosome core particle along the DNA must be carefully regulated to allow or deny access of effector proteins to specific regulatory regions of the genome. The development of microarrays and next-generation sequencing has made it possible to map nucleosome positions on a global scale on many eukaryotic genomes (Tolkunov and Morozov, 2010). The technique is based on extensive digestion of chromatin with micrococcal nuclease (MNase), an endo-exonuclease from *Staphylococcus aureus* with little DNA sequence specificity. In chromatin, the first sites to be cleaved by the enzyme will be located in the unprotected linker DNA, whereas DNA assembled into nucleosomes resists the attack of the nuclease. After prolonged treatment with MNase, the nuclease trims the DNA projecting from each nucleosome until the entire chromatin preparation has been converted to nucleosome core particles. The mononucleosomal-sized DNA fragments (150-200bp) are selected by gel purification. Finally, the collected DNA fragments are mapped to the genome by hybridization with DNA microarrays or high-throughput sequencing (Yuan et al., 2005; Lee et al., 2007; Mavrich et al., 2008). The obtained nucleosome maps showed that nucleosomes are organized in specific patterns around protein-coding genes. The transcription start site (TSS) is preceded by a 150bp long, nucleosome-depleted region (NDR) which is flanked by stably positioned nucleosomes (-1) and (+1), which are enriched in the histone variant H2A.Z (Raisner et al., 2005; Yuan et al., 2005; Lee et al., 2007). With increasing distance from the strongly positioned +1 nucleosome, the precise positioning or phasing of each nucleosome is gradually decreasing such that nucleosomes adapt random positions (Mavrich et al., 2008). The tight wrapping of DNA around the nucleosome core particle led to the suggestion that intrinsic properties of the DNA sequence that promote the bending of the DNA could facilitate both the formation and positioning of a nucleosome core particle (Drew and Travers, 1985). Strong efforts have been directed towards defining the sequence properties and to predict the nucleosome positioning in eukaryotic genomes

(Ioshikhes et al., 2006; Caserta et al., 2009; Kaplan et al., 2009). Distinct sequence motifs that occur in ~10bp intervals include AA/TT dinucleotides facing towards the histone core and GC dinucleotides facing outwards of the circular DNA tract (Drew and Travers, 1985; Boffelli et al., 1991). It is believed that the former pattern allows expansion of the major groove of DNA while the latter pattern allows its contraction to facilitate the overall strong bending of DNA on the surface of nucleosomes. A recent study in yeast showed that the intrinsic DNA sequence preferences of nucleosomes have a dominant role in nucleosome organization *in vivo* (Kaplan et al., 2009). Isolated yeast genomic DNA was reconstituted into chromatin with chicken histones by salt dialysis, followed by genome-wide mapping of reconstituted nucleosomes. The resulting distribution showed a high correlation with nucleosome positions observed *in vivo*, preserving distinct features like the NDR at the 5`end of TSSs and the flanking positions of highly localized nucleosomes. However, the correlation of the maps was not uniform across the genome, and important differences include the increased ordering of nucleosomes in coding regions observed with the *in vivo* map. These positioning differences between *in vivo* and *in vitro* assembled nucleosomes indicate that apart from the intrinsic propensity of certain DNA sequences to form nucleosomes, cellular components such as transcription factors, the transcription initiation machinery and chromatin remodeling machines may also contribute to the chromatin organization *in vivo*.

2.1.5 The linker histone H1 and higher order structures of chromatin

In addition to the four histones forming the octameric core of a nucleosome, the linker histone H1 contributes to chromatin structure. H1 contains a globular histone-fold domain and extended amino- and carboxy-termini and interacts with the linker DNA to juxtapose the entry and exit sites of the nucleosomal DNA. H1 is thought to facilitate and stabilize inter-nucleosomal interactions. The precise location of H1 in the nucleosomal array is still controversial, but H1 containing chromatin shows a distinct higher-order structural folding into a regular 30nm chromatin fiber (reviewed in Woodcock and Ghosh, 2010). Moreover, H1 depletion interferes with chromosome condensation during mitosis (Maresca and Heald, 2006), underscoring an important role of this protein in the formation of higher order structures of chromatin. Despite intense effort and recent success in solving the structure of a tetranucleosome (Schalch et al., 2005), the structural aspects of the 30nm fiber remain elusive because of the compact arrangement

of individual nucleosomes preventing the visualization of the path of the DNA linking each nucleosome by microscopic techniques (Tremethick, 2007). Very little is known about the structural arrangements of chromatin fibers during mitosis that reach their highest compaction state during metaphase chromosome condensation.

2.1.6 Non-histone components of chromatin

Chromatin is defined as the entity of nucleic acids and associated proteins. Apart from histone molecules as the primary protein components, many other protein factors have been identified as *bona fide* constitutents of chromatin, including transcription factors, DNA and RNA metabolizing machineries, architectural proteins and chromatin remodeling and modifying enzymes. The yeast genome, for example, encodes more than 200 DNA-sequence specific transcriptional regulators and genome-wide interaction studies identified more than 11.000 unique interaction sites of transcription factors at promoter regions across the yeast genome (Harbison et al., 2004). The multisubunit RNA and DNA polymerases form a dynamic complex with their DNA template and thus, the elongating nuclear machineries can also be regarded as protein components of chromatin in the course of transcription and replication, respectively. Another important family of abundant and ubiquitous non-histone chromatin proteins is the class of High Mobility Group (HMG) proteins. The three HMG protein families comprise the HMGA proteins containing A/T-hook DNA-binding motifs, HMGB proteins containing HMG-box domain(s), and HMGN proteins containing a nucleosome-binding domain (Banks et al., 2000). The HMG-box is an 80 amino acid domain known to bind certain DNA structures in a sequence-independent manner. The chromatin architectural protein HMGB1 can bind with extremely high affinity to DNA structures that form DNA loops (Stros et al., 2004), while other studies have shown that the HMG-box of different proteins can induce DNA bending (Deckert et al., 1999; Dragan et al., 2004; Phillips et al., 2004). Other DNA-sequence independent chromatin associated proteins include chromatin remodeling and modifying enzymes that allow the dynamic modification of chromatin structure and composition according to the functional state of genomic loci.

2.2 Compositional and structural analysis of chromatin

It is evident that the composition, structure and dynamics of chromatin have a critical influence on all nuclear processes including transcription, replication, recombination and

DNA repair. In order to understand the mechanistic details of these complex processes, it is important to obtain detailed information how composition and posttranslational modification pattern of chromatin influence the structure and functional state of the DNA template.

2.2.1 Reconstitution of chromatin *in vitro*

One approach to analyze biochemical and structural properties of chromatin is the reconstitution of chromatin from naked DNA and purified histones *in vitro*. There are two main approaches currently available to obtain nucleosomal templates from purified components: the ATP-independent random deposition of histone octamers on the DNA and the ATP-dependent periodic assembly of nucleosomal arrays.

Nucleosomes can be assembled by salt-gradient dialysis (Camerini-Otero et al., 1976; Germond et al., 1976). Histones and DNA are combined in the presence of high NaCl concentration and decreasing the salt concentration by dialysis leads to the formation of randomly positioned nucleosomes on the DNA template. The advantage of the salt dialysis technique is the reconstitution of pure chromatin that is devoid of histone chaperones or other large polymers that could interfere with downstream applications. It is important to note, however, that the ATP-independent assembly of chromatin may contain stretches of naked DNA. Instead of a high salt concentration, a histone chaperone that interacts with the core histones and prevents undesired interactions with other molecules present in the assembly reaction can be added. The formation of nucleosomes on the DNA can be facilitated by a wide variety of histone binding proteins (reviewed in Ito et al., 2003), but also polyanions like bulk RNA (Nelson et al., 1981) or polyglutamic acid (Stein et al., 1979) help nucleosome reconstitution *in vitro*.

In order to obtain periodic arrays of nucleosomes, ATP-dependent chromatin assembly can be used with any DNA template of indefinite length. This reaction was first achieved by Worcel and colleagues using a *Xenopus* oocyte extract supplemented with ATP and magnesium ions (Glikin et al., 1984). Similar reactions have been found to occur in crude extracts derived from HeLa cells (Banerjee and Cantor, 1990) or *Drosophila* embryos (Becker and Wu, 1992). Although the chromatin produced from these extracts is almost indistinguishable from bulk native chromatin, the composition and structure is not defined due to the complexity of the extracts.

The use of reconstituted chromatin templates has facilitated the structural and functional studies of the nucleosome. Homogeneity of the chromatin preparations has allowed high resolution of the structure of the nucleosome core particle by crystallography revealing

the role of the histone fold domains in histone–histone and histone–DNA interactions as well as the role of the histone tails protruding outside of the histone octamer (Luger et al., 1997). However, the assembly of nucleosomal arrays *in vitro* has important limitations. First of all, it is unclear if the reconstituted material resembles the native template *in vivo*. Nucleosomes often occupy specific regulatory positions, and their placement may be governed by intracellular chromatin assembly factors or chromatin remodelling complexes not present during the assembly reaction. Moreover, reconstitution of complex chromatin structures including certain epigenetic marks like histone modifications at precise positions is a challenge. Therefore, a deeper knowledge about the composition and structure of chromatin *in vivo* is a prerequisite to guide future *in vitro* reconstitution. To this end, various techniques have been developed to determine the locus-specific association of histones and non-histone proteins with the genomic DNA *in vivo* (see 2.2.2). On the other hand, the isolation and analysis of preassembled chromatin from the cell represents an attractive alternative because the isolated chromatin is likely to more closely reflect the native structure (see 2.2.3).

2.2.2 Analysis of DNA-protein interactions *in vivo*

2.2.2.1 Chromatin Immunoprecipitation (ChIP)

In order to preserve physiologically relevant DNA-protein interactions, different crosslinking reagents and methods like formaldehyde and UV-light were used to covalently link the associated proteins to the DNA *in situ*. Irradiation of living cells with UV light of wavelength near 260nm induces covalent bonds between contact points of nucleic acids and proteins (Gilmour et al., 1991; Carr and Biggin, 1999; Dimitrov and Moss, 2001). Formaldehyde-assisted crosslinking occurs between the exocyclic amino groups and the endocyclic imino groups of DNA bases and the side-chain nitrogen of lysine, arginine and histidine (McGhee and von Hippel, 1975a, 1975b; Chaw et al., 1980). In contrast to UV light as a zero length crosslinker, formaldehyde produces chemical bridges and may also stabilize protein-protein interactions. With the generation of specific antibodies recognizing DNA binding proteins (including histones and their posttranslational modifications), formaldehyde crosslinking in combination with immunoprecipitation has become the dominant method to analyze the localization of post-translationally modified histones and histone variants in the genome, and for mapping DNA target sites for transcription factors and other chromosome-associated proteins *in vivo*. The Chromatin Immuno Precipitation (ChIP) procedure involves the fragmentation of chromatin by enzymatic digestion with MNase or by sonication. The

lysate is cleared by sedimentation and protein-DNA complexes are immunoprecipitated from the supernatant using antibodies to the protein or modification of interest. The precipitated DNA fragments are purified and DNA sequences can be analyzed by (quantitative) PCR, labelling and hybridization to genome-wide or tiling DNA microarrays (ChIP-on-chip, Lee et al., 2006) or high-throughput sequencing (ChIP-seq, Jothi et al., 2008). Although the genome-wide profiling of DNA-binding proteins and histone modifications by ChIP-on-chip and ChIP-seq technologies has produced tremendous progress in our understanding of gene regulatory networks and interaction maps, the result of any ChIP experiment depends crucially on the quality of the antibody and the availability of the epitope on the target molecule in different conditions. Moreover, the use of antibodies has some limitations as a tool for discovering new protein components and/or histone modifications at selected loci, because ChIP requires *a priori* knowledge or educated guess of the protein or modification of interest.

2.2.2.2 DNA adenine methyltransferase identification (DamID)

An alternative method to study DNA-protein interactions in the context of chromatin is DNA adenine methyltransferase identification (DamID) (van Steensel and Henikoff, 2000; van Steensel et al., 2001). A protein of interest is expressed as a fusion protein with the bacterial DNA adenine methyltransferase (Dam). The enzyme catalyzes the transfer of methyl groups to adenine residues in the consensus sequence GATC, which provides a stable tag in local vicinity to the protein binding site because adenine methylation does not occur endogenously in most eukaryotic species. The enzyme is highly active and expression level of the chimeric protein has to be carefully controlled in order to avoid non-specific methylation of DNA by untethered proteins. In order to account for this, a DamID experiment is designed as a comparison between methylation events from the Dam fusion protein and Dam alone. Using the DpnI restriction enzyme that cuts only at methylated GATC sites, target regions of the extracted genomic DNA can be analyzed by PCR-based amplification with specific primer pairs. Alternatively, the genome-wide distribution of adenine methylation marks can be monitored by ligation of the isolated genomic DNA with adapter DNA fragments and PCR with an adapter specific primer pair. The amplified genomic DNA fragments are finally hybridized with a DNA tiling microarray. In contrast to ChIP, DamID does not require a protein-specific antibody and chemical crosslinking with formaldehyde. However, ectopical expression may result in artifactual binding of the Dam fusion protein and DamID is not suitable for the detection of posttranslational modifications. Finally, the technique does not allow

high-resolution mapping of binding sites, because adenine methylation events can extend over a few kilobases from the native binding site (van Steensel et al., 2001).

2.2.2.3 Chromatin Endogenous Cleavage (ChEC)

The Chromatin Endogenous Cleavage (ChEC) method allows localization of chromatin-associated factors on the genomic DNA sequence with high resolution (Schmid et al., 2004). The protein of interest is expressed as a fusion protein with MNase and crosslinked to the respective DNA binding site by treatment of the cells with formaldehyde. MNase activity is strictly dependent on the presence of calcium ions in the millimolar range (Telford and Stewart, 1989) and thus inhibited in the intracellular compartments of most eukaryotic cells. After isolation of crude nuclei, the MNase is activated by addition of Ca^{2+} ions to a final concentration of 2mM. The MNase fusion protein induces double-strand breaks in proximity to the protein binding site. After isolation of genomic DNA, the genomic fragments are linearized with restriction enzymes and separated by agarose gel electrophoresis. Specific cleavage events of the MNase fusion protein can be monitored by Southern blot analysis using the indirect end-labeling method with high resolution of 100-200bp (Schmid et al., 2004; Merz et al., 2008). Genomic regions up to 10kb can be analyzed in a single blot, but distal cleavage sites cannot be quantitatively detected if a strong cleavage site exists closer to the probe. A variation of this method is Chromatin Immuno Cleavage (ChIC). In this approach, a specific antibody to the protein of interest is added to isolated fixed nuclei. Next, a fusion protein consisting of Protein A from *Staphylococcus aureus* and MNase is added in order to tether the nuclease via the Protein A moiety to the primary antibody. Subsequent activation of MNase by addition of calcium ions results in DNA cleavage events in vicinity to the chromatin-bound factor. Similar to ChIP, the outcome of ChIC experiments relies on the quality of specific antibodies. However, it is conceivable to combine ChEC/ChIC with microarray hybridization or high-throughput sequencing to map MNase induced cleavage events on a genome-wide scale (Schmid et al., 2006). However, the technique is not suited to discover new protein interactions and/or histone modifications in an unbiased manner.

2.2.3 Isolation and analysis of *in vivo* assembled chromatin

2.2.3.1 Enrichment of chromosomal regions by fractionation

Early findings indicated that only some of the genomic DNA sequences are transcribed *in vivo* (McConaughy and McCarthy, 1972) and thus, it was expected that the structural

heterogeneity of chromatin is suitable for biochemical fractionation of chromatin based on differential sedimentation and solubility (FRENSTER et al., 1963; Duerksen and McCarthy, 1971; Reeck et al., 1972). Ion exchange chromatography and sucrose gradient centrifugation were successfully applied to fractionate chromatin preparations that differed in their protein content (Reeck et al., 1972) and different fractions were assumed to represent transcriptionally active or inactive chromatin segments (Neelin et al., 1976; Gottesfeld, 1977; Savage and Bonner, 1978). However, the collected fractions represented bulk chromatin fragments from randomly sheared chromosomes and the authors could not distinguish if specific chromosomal regions were enriched in one fraction over the other.

The first specific isolation of native chromatin domains was achieved for the special case of the amplified extrachromosomal nucleoli containing the repetitive ribosomal RNA (rRNA) genes derived from oocytes of the frog *Xenopus laevis*. A simple fractionation protocol by density gradient centrifugation served as the purification strategy. (Higashinakagawa et al., 1977). During the pachytene stage of oogenesis, copies of the rRNA genes become extrachromosomal and replicate independently several thousandfold (Gall et al., 2004). During mid-diplotene, the amplified rRNA genes are packaged in approximately 1500 extrachromosomal nucleoli. After the isolation, it was shown that the purified material was virtually free of nucleic acid sequences other than ribosomal DNA. Further, the nucleoli contained active RNA polymerase I and an enzymatic activity which relaxes superhelical turns of closed circular DNA. Electrophoresis of total nucleolar protein showed most of the proteins to represent ribosomal proteins and chromatin components like histones H2A, H2B, H3 and H4 (Higashinakagawa et al., 1977). It was the first reported case that a single gene was purified in its native chromatin context. However, this procedure is not universally applicable as only rDNA chromatin shows the compartmentalization in nucleoli which was exploited in this study. Additionally, the amplified nucleoli in *Xenopus* represent one of the rare cases that rDNA is present in extrachromosomal copies. Only this situation made it possible to isolate the amplified nucleoli free of any bulk chromosomal DNA.

2.2.3.2 Purification of yeast mini chromosomes

In the past, most methods for chromatin purification were designed to isolate bulk chromatin fragments from randomly sheared chromosomes (Kornberg et al., 1989). After the discovery of certain yeast sequences that allowed DNA to be maintained as episomal, amplified elements (Stinchcomb et al., 1979), genes of interest were cloned into plasmids including such autonomous replication sequences (ARS). It was shown by

nuclease digestion (Pederson et al., 1986) and electron microscopy (Dean et al., 1989) of the purified material that *in vivo*, plasmid DNA was packaged into chromatin.
While the plasmid DNA is amplified up to 80 copies per cell (Simpson et al., 2004) and constitutes about 1% of total yeast DNA, the basic problem is to purify about 1µg plasmid chromatin from about 1mg chromosomal chromatin and 10mg of ribosomes per one litre of yeast cell culture (Kim et al., 2004). Initial protocols involved conventional fractionation of nuclei and subsequent purification by density gradient centrifugation and/or size exclusion chromatography (Dean et al., 1989; Kim et al., 2004). These procedures lead to material that appears to be biochemically pure, but protocols are lengthy, raising concerns about proteolysis or dissociation of chromatin components. Another approach relies on the use of protein-nucleic acid affinity with the *Escherichia coli lac* repressor and operator to achieve a purification of $>10^4$-fold in one single step. A recent study described an efficient single-step method to purify such minichromosomes in its native chromatin context (Unnikrishnan et al., 2010). The authors inserted an array of 8 Lac operator sites in a plasmid containing the TRP1 gene and the efficient, early-firing ARS1 sequence (TALO8). FLAG-epitope tagged Lac repressor was expressed in yeast cells containing the TALO8 minichromosome in order to interact with the Lac operator sites. After lysis of 4 x 10^{10} cells, the minichromosomes were immobilized to protein G magnetic beads crosslinked with anti-FLAG M2 antibodies and washed extensively under stringent salt and detergent conditions. The most abundant proteins present in the elution were the canonical histone proteins and their posttranslational modifications were identified by high resolution mass spectrometry. As replication-associated histone modifications may be in low abundance in bulk histones, the histones purified from the minichromosome system were all in close proximity to the ARS1 region, increasing the chance of identifying modifications specifically enriched in a chromatin structure of active replication. The authors analyzed the cell-cycle specific changes in abundance of histone modifications compared to bulk chromatin and showed that the histone H4 tail is specifically hyperacetylated during S-phase and G2/M-phase and deacetylated upon progression into G1-phase. Besides the core histones, the authors were able to identify other replication factors like minichromosome maintenance (MCM) proteins and subunits of the origin recognition complex (ORC) during S-phase, demonstrating the specificity of the method.

2.2.3.3 Proteomics of isolated chromatin segments

In a new report, Déjardin and Kingston presented a new method termed proteomics of isolated chromatin segments (PICh) for the analysis of proteins associated with specific

chromatin loci (Déjardin and Kingston, 2009). The PICh method relies on nucleic acid probes that recognize specific genomic loci which are then enriched together with their associated proteins. The procedure begins by fixing cells with formaldehyde which stabilizes both protein–protein and protein–DNA interactions. The cells were then lysed and the chromatin was solubilized by sonication. To specifically purify the genomic loci of interest, a 25 base pair probe made of locked nucleic acid (which possesses a higher melting temperature than a regular nucleic acid) linked to a desthiobiotin moiety was used. The probe was efficiently hybridized with the chromatin samples under stringent detergent conditions and then subsequently purified using streptavidin beads and eluted with excess biotin. The purified proteins were resolved on a SDS-PAGE gel and identified by mass spectrometry. This new technique was first applied for the purification of proteins associated with telomeres. Telomeres were selected since they were abundant (100 copies per cell) which reduced the amount of material needed per experiment. The authors used a probe directed at telomere and a probe with the same nucleic acid composition but in a randomized order as a control. The authors purified approximately 200 proteins associated with telomere chromatin, but not with the scrambled probe, from mammalian cells and approximately half of these hits were shared between two different cell lines. A substantial fraction of the proteins identified in these analyses were known to interact with telomeres. For many of the novel proteins purified by PICh, immuno-localization and ChIP supported *in vivo* association with telomeres, clearly demonstrating the strength of the new method. One drawback of the PICh procedure is the amount of starting material needed per experiment. By targeting a specific DNA sequence which is present at a few copies per cell, it becomes extremely difficult to purify sufficient associated proteins for mass spectrometric analysis. Furthermore, this method does not allow the isolation of native chromatin being susceptible to further functional and biochemical analysis.

2.2.3.4 Purification of defined chromatin domains by site-specific recombination

Another approach to purify defined native chromatin fragments from yeast was originally developed by Gartenberg and co-workers (Ansari et al., 1999). The authors made use of the R site-specific recombinase of the yeast *Zygosaccharomyces rouxii* in order to excise specific chromatin domains from their chromosomal context in the form of a closed circle. For inducible expression, yeast cells were transformed with a plasmid carrying the R recombinase coding sequence fused to the *GAL1* promoter. Addition of galactose to the medium resulted in rapid expression of R recombinase. The target sites of the enzyme, termed RS sites, are 31bp long and consist of a 7bp-core, flanked by inverted 12-bp

sequences. When a pair of sites is placed in the same orientation, the intervening DNA is excised and religated into a circle. Thus, if a region of interest is flanked by tandemly oriented RS sites, a specific chromosomal domain is excised from its genomic context. After preparation of whole cell lysate, the excised chromatin domains were separated from bulk chromatin by differential centrifugation. Gartenberg and coworkers applied this method to the *HMR* locus in yeast, a silenced copy of the mating type (*MAT*) locus. This locus is silenced by a heterochromatin-like structure, governed by discrete *cis*-acting regulatory sequences, termed silencers, and a set of *trans*-acting proteins, Sir1-4p. They used recombination *in vivo* to uncouple fragments of the repressed *HMR* locus from silencers and examined the role of the *cis*-acting regulatory elements in persistence of the silenced chromatin. MNase digestion of released chromatin domains demonstrated that the chromatin structure was almost indistinguishable from the chromatin structure at the respective chromosomal location. Therefore, neither recombination nor the chromatin circle isolation seemed to affect the native composition of the domains. Furthermore, Gartenberg and colleagues reported that *SIR* proteins were still associated with the isolated silent mating type domains (Ansari and Gartenberg, 1999; Ansari et al., 1999). Nevertheless, the initial purification strategy by a differential centrifugation step enriches not only for chromatin circles but also for ribosomes, the yeast-specific 2µ circle or high molecular-weight protein complexes (Griesenbeck et al., 2004). Therefore, the obtained fraction was a crude mixture of proteins and nucleic acids with a multitude of enzymatic activities like nucleases, topoisomerases and ATP-dependent chromatin remodelling (Ansari et al., 1999; Griesenbeck et al., 2004). This makes the material unsuitable for a defined functional characterization by biochemical assays. To this end, further purification of the material is required and this was achieved by affinity chromatography of the isolated domains (Griesenbeck et al., 2003). A cluster of *LEXA* binding sequences from *E. coli* was incorporated, such that it is included in the chromatin domain after excision by R recombinase. Furthermore, a recombinant adapter protein was expressed in the yeast strains consisting of the complete LexA protein fused to a C-terminal tandem affinity purification tag (TAP-tag, Rigaut et al., 1999). The artificial protein binds to the *LEXA* binding elements within the excised chromatin domains. After differential centrifugation, the adapter-bound chromatin domains were subjected to a two-step affinity chromatography mediated by the TAP-tag of the adapter. Thus, different chromatin domains could be purified with high specificity and to near homogeneity (Griesenbeck et al., 2003) from the single-copy *PHO5* gene. However, the total amount of contaminating proteins was still significantly above the amount of histones associated with the isolated DNA circle (Griesenbeck et al., 2004).

2.3 Chromatin structures at the essential multi-copy rDNA locus and the non-essential single-copy *PHO5* locus

The composition and structure of chromatin has a critical influence on all nuclear processes accessing DNA, including DNA repair, replication, and transcription. Vice versa nuclear processes induce dynamic changes in chromatin structure. To understand this complex interplay, our research aims to derive a detailed molecular description of chromatin at genes in different transcriptional states. Accordingly, the multicopy rDNA gene cluster and the single-copy *PHO5* locus were chosen as model loci for this work. As outlined below, a common feature of the two genes is that they show a robust chromatin transition when they switch their transcriptional states.

2.3.1 Chromatin structure at the yeast rDNA locus

The eukaryotic ribosome is a complex ribonucleoprotein particle consisting of a large 60S and a small 40S subunit (CHAO and SCHACHMAN, 1956; CHAO, 1957). The large subunit comprises about 46 ribosomal proteins and three ribosomal RNAs (rRNAs) with sedimentation coefficients of 25S (28S for higher eukaryotes), 5.8S and 5S. The small subunit consists of the 18S rRNA and 32 ribosomal proteins (Ben-Shem et al., 2011). In addition to structural components of the ribosome, more than 150 trans-acting ribosome biogenesis factors and about 100 small nucleolar RNAs (snoRNAs) participate in the complex maturation pathway of ribosomes (Venema and Tollervey, 1999; Fromont-Racine et al., 2003; Granneman and Baserga, 2004; Kressler et al., 2010). A high percentage of the cells resources is devoted to ribosome biogenesis (Tschochner and Hurt, 2003) and all three eukaryotic RNA polymerases are involved in this complex process: RNA polymerase II (Pol II) transcribes the genes coding for ribosomal proteins and ribosome biogenesis factors. Synthesis of the smallest rRNA, the 5S rRNA, is performed by RNA polymerase III (Pol III). The other three rRNAs are produced by RNA polymerase I (Pol I) as a primary 35S rRNA transcript, which is further processed by a complex machinery into the mature 18S, 5.8S and 25S rRNAs. As much as 60% of total RNAs in a cell represent descendants of the primary transcript from the rDNA locus (Warner, 1999). In order to meet the cell`s requirement for rRNA during proliferation, the rRNA genes are present in multiple copies arranged in repetitive clusters in all eukaryotic genomes.

2.3.1.1 Cellular localization and chromosomal organization of the multi-copy yeast rDNA locus

Synthesis and processing of rRNAs as well as pre-ribosomal subunit assembly occur in a large sub-nuclear compartment, the nucleolus (Figure 3).

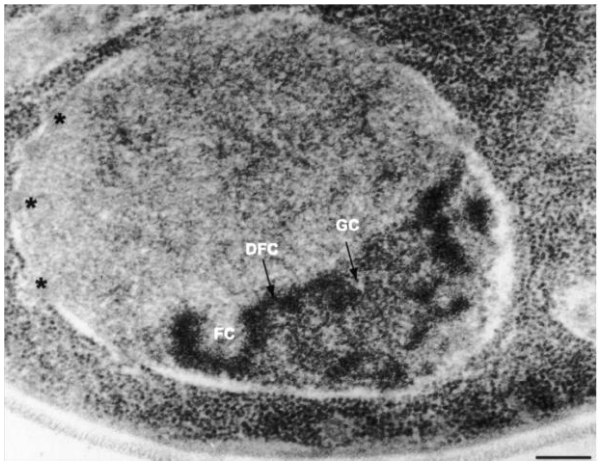

Figure 3. Ultrastructure of the nucleus from *Saccharomyces cerevisiae* The electron micrograph depicts the morphology of a yeast nucleus after cryofixation and freeze-substitution. The nucleus is visualized as a large oval structure surrounded by the nuclear membrane with pores (asterisks). In the nucleolus, three distinct morphological compartments are identified: the fibrillar centres (FC) are detected near the nuclear envelope, surrounded by a dense fibrillar component (DFC) that extends as a network throughout the nucleolar volume. A granular component (GC) is dispersed throughout the rest of the nucleolus. The scale bar represents 200nm (Léger-Silvestre et al., 1999).

Ultrastructural analysis of sectioned yeast nucleoli revealed a crescent-shaped, electron-dense structure with three morphologically different nucleolar compartments: one or more fibrillar centers (FCs) , each bounded by dense fibrillar components (DFCs) and granular components (GCs) constituting the majority of the nucleolus (Koberna et al., 2002; Raska, 2003) (Figure 3). Immunocytological and in situ hybridization studies and the analysis of aberrant morphologies in conditional yeast mutants allowed assigning the structure-function relationship of single nucleolar components (Oakes et al., 1998; Léger-Silvestre et al., 1999; Trumtel et al., 2000). These studies revealed that ribosomal DNA (rDNA) is localised to the FC, whereas Pol I is concentrated at the boundary between the FC and the surrounding DFC, suggesting that this is also the site of rRNA gene transcription. This led to the model that nascent pre-rRNA spreads into the DFC, where early steps of rRNA processing and ribonucleoprotein (RNP) assembly occur. Finally further maturation steps and assembly of ribosomal subunits occur in the GC (Scheer and Hock, 1999).

Besides the morphological clustering of the rRNA genes in the nucleolus, the rRNA genes are also genetically linked by their chromosomal arrangement. The yeast ribosomal DNA locus (rDNA) is located on the right arm of chromosome XII and consists of 150-200 transcription units arranged head to tail in a tandem array

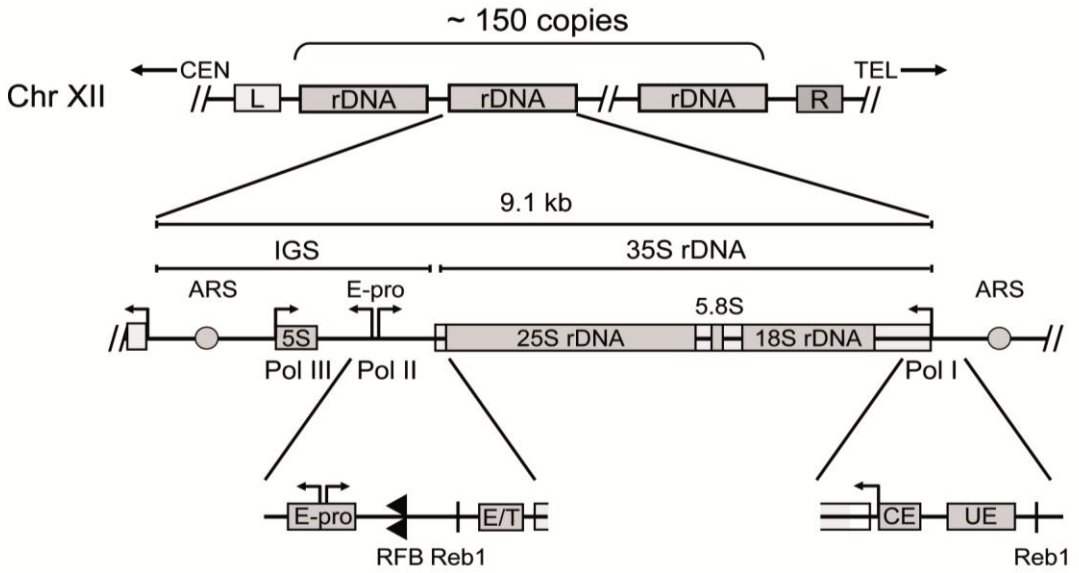

Figure 4 Schematic representation of the rDNA locus in *S. cerevisiae*. 150-200 copies of the rDNA repeats are arranged in tandem on chromosome XII flanked by sequences named L (left) directing towards the centromer (CEN) and R (right) directing towards the telomere (TEL). Each 9.1kb repeat consists of the 35S rDNA transcribed by RNA polymerase I (Pol I), and the RNA polymerase III (Pol III) transcribed 5S rDNA located in the intergenic spacer region (IGS). Arrows mark the transcription start sites and direction. The upstream element (UE) and core element (CE) constitute the Pol I promoter. Transcription termination of the 35S rRNA gene occurs at the enhancer/terminator (E/T) region. Several cis-acting elements have been identified in the intergenic spacer region: an autonomous replication sequence (ARS), the bidirectional Pol II promoter E-pro and the replication fork barrier (RFB). The binding sites of the Reb1 protein are depicted.

(Planta, 1997; Nomura, 2001). Each of these repeated units is composed out of the Pol I transcribed 35S rRNA gene and an intergenic spacer (IGS) region (Figure 4). The IGS contains the 5S rRNA gene transcribed by Pol III in opposite direction (Philippsen et al., 1978). The presence of the 5S rRNA gene within the rDNA unit in *S. cerevisiae* is different from the situation in other eukaryotes, most of which carry 5S rRNA repeats separately from the nucleolar rRNA repeats (Drouin and de Sá, 1995; Geiduschek and Kassavetis, 2001; Haeusler and Engelke, 2006). The 35S rRNA gene is composed of the sequences coding for the mature rRNAs (18S, 5.8S and 25S), which are produced from a large 35S rRNA precursor transcript by complex endo- and exonucleolytic processing events. Pol I transcription of the 35S rDNA is driven by the promoter region, which consists of a bipartite Upstream Element (UE) and a Core Element (CE) including the transcription start site (Musters et al., 1989; Kulkens et al., 1991). The two elements span about 170 bp and represent the binding sites of Pol I specific transcription initiation factors: Upstream Activating Factor (UAF) binds to the UE and consists of the six subunits Rrn5, Rrn9, Rrn10, Uaf30 and the histones H3 and H4 (Keys et al., 1996; Keener et al., 1997). The Core Factor (CF) contains the three subunits Rrn6, Rrn7 and Rrn11 and interacts with the CE (Keys et al., 1994; Lalo et al., 1996). UAF and CF are bridged by TATA-box binding protein (TBP) and

form together the ribosomal gene pre-initiation complex (PIC). In addition, a Terminator element (T) is located at the 3`-end of the 35S rDNA, directly followed by the Enhancer (E), a trans-acting element identified as a positive regulator of Pol I transcription *in vitro* (Elion and Warner, 1986). Nevertheless, Nomura and co-workers could show that deletion of the Enhancer DNA element is dispensable for Pol I transcription *in vivo* (Wai et al., 2001).

Several other *cis*-elements were identified in the IGS region and have been studied extensively. An autonomous replicating sequence (ARS) mediates formation of replication forks in both directions (Linskens and Huberman, 1988). The replication fork moving towards the 3'-end of the preceding 35S rRNA gene is stalled by a DNA element called replication fork barrier (RFB), which is located 3' of the T and E elements described above (see Figure 4), in order to prevent a collision of the replication and the transcription machinery (Brewer and Fangman, 1988; Brewer et al., 1992; Kobayashi et al., 1992). The replication fork moving in the direction of Pol I transcription continues until it fuses with the next stalled replication fork (Lucchini and Sogo, 1994). The RFB is also the binding site for Fob1 (fork blocking protein), a protein implicated in the expansion and contraction of the rDNA locus (Kobayashi et al., 1998). Its presence is known to induce double strand breaks into the rDNA by Fob1-dependent pausing of the DNA replication machinery at RFB sites (Kobayashi et al., 1998, 2004; Burkhalter and Sogo, 2004). In addition to the RFB, the adjacent expansion (EXP) region harbors a bidirectional Pol II promoter (E-pro) which was shown to be required for rDNA repeat expansion (Kobayashi et al., 2001). Transcription at E-pro produces non-coding RNAs and promotes the dissociation of cohesin from neighbouring DNA regions. Cohesin association is suggested to hold sister chromatids in place, preventing unequal recombination and thereby changes in rDNA copy number after the formation of DNA double-strand breaks (Kobayashi et al., 2004). Thus, transcription of E-pro regulates recombination by cohesin dissociation. Interestingly, the NAD^+ dependent histone deacetylase Sir2 (Imai et al., 2000; Landry et al., 2000; Smith et al., 2000) represses the transcriptional activity from E-pro (Kobayashi and Ganley, 2005). The sirtuin Sir2 (silent information regulator 2) is a protein that is reported to be required for transcriptional silencing of Pol II transcription at the silent mating type loci, the telomere regions and the rDNA locus (Gottschling et al., 1990; Bryk et al., 1997; Smith and Boeke, 1997; Imai et al., 2000).

2.3.1.2 Distinct chromatin structures at the 35S rRNA genes

In an exponentially growing yeast cell, ~40 ribosomes are produced every second (Tschochner and Hurt, 2003). Consequently, rRNA genes must be heavily transcribed in order to meet the cell`s requirement of mature rRNAs for ribosome biogenesis. Nevertheless, only a subpopulation of the 35S rRNA genes is transcriptionally active. This state of rDNA is termed “active” or “open” and is virtually devoid of nucleosomes. The other half of the rRNA genes is transcriptionally inactive and packed into a tight array of nucleosomes: Accordingly, this state of rDNA is termed “inactive” or “closed” (Toussaint et al., 2005 and references therein). The coexistence of these two different chromatin states in one cell was a challenge for researchers investigating rDNA chromatin. For example, micrococcal nuclease or DNAse I treatment of isolated nuclei and subsequent Southern blot analysis using a rDNA specific probe, resulted in a faint nucleosomal ladder overlayed by a smear of heterogeneous DNA fragments especially around the site of transcription initiation and upstream in the 5` flanking sequences (Lohr, 1983). The outcome of these experiments supported the hypothesis of two different states, but no more information could be gained by such classical approaches.

The chromatin Miller spreading technique allowed for the first time the visualization of the ultrastructure of eukaryotic genes in its actively transcribed state (Miller and Beatty, 1969; Miller, 1981). After rapid isolation of nuclei from the living cell, the chromatin sample is transferred from isotonic medium to a drop of low salt spreading buffer of alkaline pH. The dispersed chromatin is centrifuged on a carbon coated grid and visualized by electron microscopy (Trendelenburg, 1983). In case of the 35S rRNA genes, the obtained electron micrographs visualize the two states of chromatin: Active rRNA genes are heavily loaded with polymerases (with 40 to 100 molecules on an around 7kb template) and nascent rRNA transcripts increase in size from 5` to 3` in a Christmas tree-like configuration. Highly transcribed genes are interspersed with regions devoid of nascent transcripts, corresponding to non-transcribed rRNA genes (French et al., 2003) (Figure 5A**)**. In this type of analyses it has been observed that the nascent transcripts are co-transcriptionally compacted and cleaved (Osheim et al., 2004). The compaction was attributed to the formation of ribonucleoprotein (RNP) complexes like the small subunit (SSU) processome (Osheim et al., 2004). The SSU processome contains rRNA precursor molecules, the small nucleolar (sno) RNA U3 and specific ribosome biogenesis factors (Dragon et al., 2002). A recent study analyzing the kinetics of pulse-labeling of rRNAs and mathematical modeling provided further evidence that pre-rRNA processing and modification occur during transcription (Kos and Tollervey, 2010). Interestingly, specific SSU processome factors have been identified as rRNA

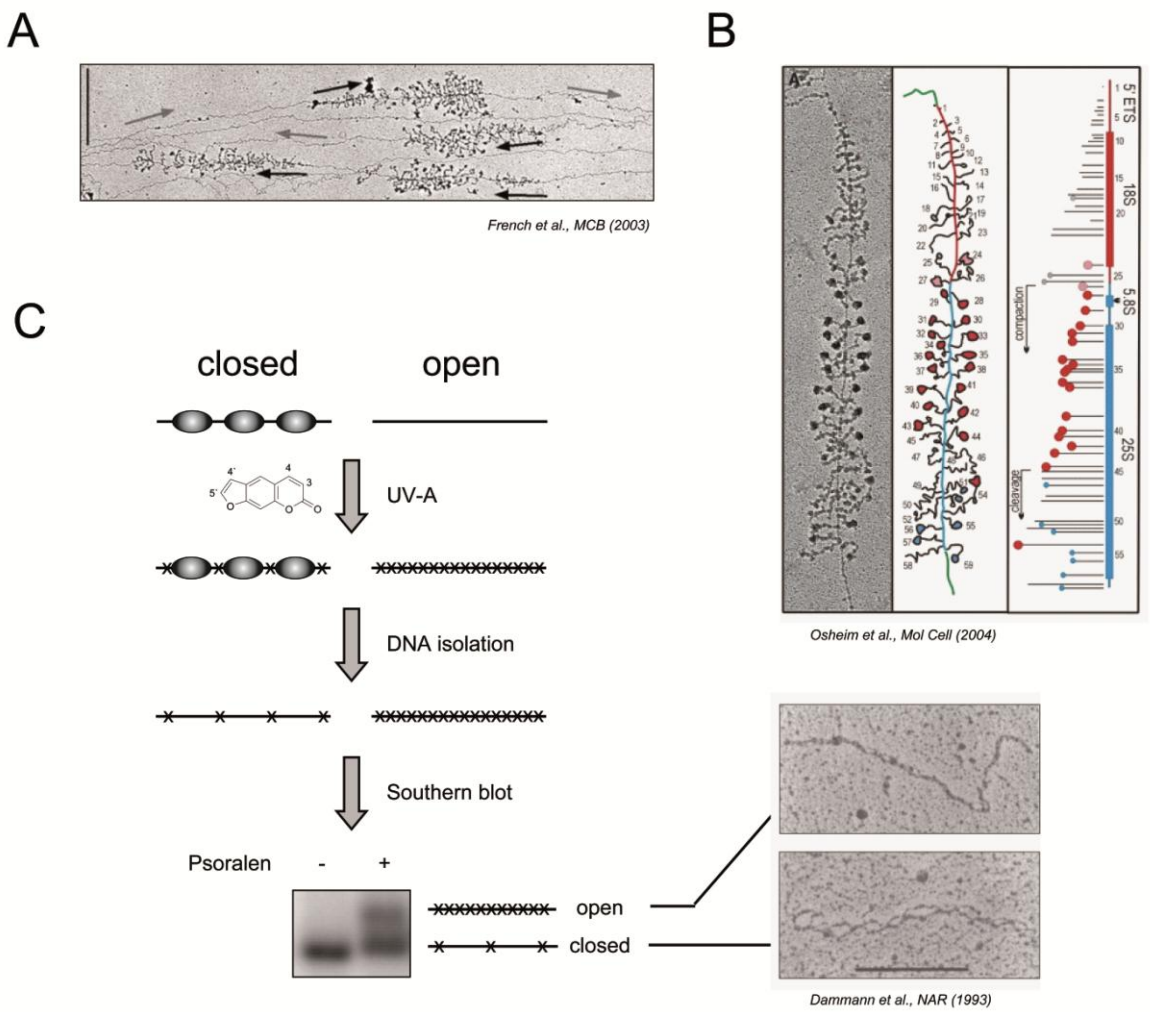

Figure 5 Visualization and analysis of 35S rRNA gene chromatin states by Miller chromatin spreading and psoralen-photocrosslinking A) Electron microscopy analysis of chromatin spreads. View of a chromatin region encompassing tandemly repeated and transcriptionally active rRNA genes which adopt characteristic Christmas-tree like structures. Arrows point in the direction of transcription. A grey arrow depicts a presumably transcriptionally inactive rRNA gene. A black arrow with a pound sign shows a rRNA gene with low Pol I density. The bar represents ~1µm. Picture taken from (French et al., 2003). B) One transcription unit of the rDNA locus is shown. The central string represents the DNA, while the extending strings (some with terminal balls) represent the rRNA. The transcription start site is at the top of the picture. The early terminal balls (depicted in pink and red) represent the SSU processome consisting of the U3 snoRNA and about 40 factors needed for maturation of the SSU. The late terminal balls (depicted in blue) represent probably pre-LSU knobs that form after co-transcriptional cleavage of the rRNA precursor, separating the pre-40S from the pre-60S subunit. Picture taken from (Osheim et al., 2004) C) Psoralen photo-crosslinking analysis of rDNA. Isolated nuclei are photoreacted with psoralen (black crosses), which forms a covalent bond between the two DNA strands. The open, actively transcribed 35S rRNA genes are more accessible to psoralen than the closed, nucleosomal genes (nucleosomes represented as grey ovals). After DNA isolation and restriction enzyme digest, the fragments are separated by agarose gel electrophoresis and analyzed in a Southern blot with a 35S rRNA gene specific probe. The different degree of psoralen incorporation into rDNA leads to separation of fragments originating from the open and the closed rRNA genes (positions indicated on the right of the autoradiograph). Electron micrograph of CsCl purified bands derived from open and closed state of ribosomal DNA under denaturing conditions. The scale bar represents ~1 kb. DNA from the open state is heavily crosslinked and cannot be denatured into single strands. DNA from the closed state can be denatured into single-stranded bubbles with a size of about 150bp (Dammann et al., 1993).

gene chromatin components and were linked to efficient Pol I transcription in yeast and human (Gallagher et al., 2004; Prieto and McStay, 2007). However, the observations in yeast have been challenged by subsequent studies, arguing again for pre-rRNA

mediated recruitment of the respective SSU processome subunits (Wery et al., 2009). Nevertheless, rRNA gene chromatin structure, Pol I transcription and pre-ribosome processing and assembly are strongly interconnected processes (Figure 5B).

Clear evidence for the existence of two different rDNA chromatin states *in vivo* resulted from photo-crosslinking experiments with psoralen (Conconi et al., 1989; Toussaint et al., 2005). Psoralen (4,5`,8-trimethylpsoralen, Figure 5C) is a three ringed furocoumarin, found in many plants serving as a pesticide. Its aromatic ring system intercalates into double stranded nucleic acids and establishes covalent crosslinks between the two DNA strands upon irradiation with long wave UV light. The covalent bonds are formed between the double bonds of psoralen 4´,5´ (furan) and 3,4 (pyrone) and pyrimidine bases. The incorporation of psoralen occurs preferentially in nucleosome free regions or in linker DNA between nucleosomes (Hanson et al., 1976; Cech and Pardue, 1977). Importantly, the integration of psoralen in double stranded DNA does not perturb the general structure of chromatin (Conconi et al., 1984; Gale and Smerdon, 1988). Additionally, psoralen incorporation is neither obstructed by elongating polymerases (Sogo and Thoma, 1989) nor by salt-dependent chromatin condensation (Conconi et al., 1984).

After DNA isolation and digestion with a restriction enzyme, the crosslinked DNA can either be visualized by electron microscopy under denaturing conditions or analysed by Southern blot after native agarose gel electrophoresis (Figure 5C). The migration of psoralen crosslinked DNA in agarose gel electrophoresis is dependent on the amount of psoralen incorporated into the double strand. In the absence of nucleosomes, DNA is heavily crosslinked. As a result the DNA migrates slower in agarose gel electrophoresis because it is less flexible and has a higher molecular weight (termed s-band, *slow migrating band*). Nucleosomal DNA has less psoralen integrated and migrates faster (termed f-band, *fast migrating band*), but still slower than DNA that has not been treated with psoralen (Figure 5C). After psoralen crosslinking analysis, both bands representing the open and closed chromatin state can be observed, when fragments of the Pol I transcribed 35S rRNA gene are investigated (Conconi et al., 1989). Damman and co-workers isolated s- and f-band DNA representing open and closed states of 35S rDNA from an agarose gel and visualized the fragments by electron microscopy in conditions that denature the DNA double strand (Figure 5C right). DNA-fragments derived from the f-band showed single stranded bubbles of about 150 bp size, presumably corresponding to nucleosomal DNA. In contrast, s-band DNA appeared as a rod-like structure of heavily psoralen crosslinked DNA double strands (Dammann et al., 1993, 1995; Lucchini and Sogo, 1994).

The above mentioned analyses provided evidence that the inactive rDNA chromatin state is assembled in a tight array of nucleosomes, whereas the transcriptionally active population is rather free of regularly spaced histone octamers. However, the presence or absence of nucleosomes at actively transcribed 35S rRNA genes is controversially discussed in the literature (Birch and Zomerdijk, 2008; McStay and Grummt, 2008; Németh and Längst, 2008). Psoralen crosslinking studies and the high density of elongating Pol I along the transcribed 35S rDNA sequence seem to be incompatible with nucleosomal structures. Notably, recent studies showed that Pol I transcription in yeast depends on the histones H3 and H4, because depletion of these proteins results in a strong reduction of transcription not only at the level of initiation but also at the level of elongation (Tongaonkar et al., 2005). However, both histones H3 and H4 are known components of the Pol I initiation factor UAF. Thus, histone depletion may likely affect Pol I transcription by inhibiting transcription initiation rather than by the lack of a nucleosomal structure required for efficient elongation. Nevertheless, Proudfoot and co-workers showed by ChIP and MNase digestion of chromosomal DNA that actively transcribed rRNA genes may also adopt a dynamic chromatin structure of unphased nucleosomes (Jones et al., 2007). This study was done using a yeast mutant strain with only 40 copies of rDNA repeats, where all rRNA genes are supposed to be actively transcribed (French et al., 2003). It was also shown that the chromatin remodeling factors Chd1, Isw1 and Isw2 were present across the whole rDNA repeat perhaps to create a dynamic chromatin structure allowing passage of multiple elongating Pol I complexes across the rDNA. However, by combining ChEC with psoralen crosslinking analysis (termed ChEC/psoralen analysis), our laboratory provided further evidence that open rRNA genes are largely devoid of histone molecules. These results are in apparent conflict with the interpretation of the aforementioned ChIP analysis. A simple explanation for the discrepancy could be the presence of a subpopulation of inactive rDNA repeats even in the 40-copy strain used for ChIP analysis (Merz et al., 2008).

Another factor associated with rDNA chromatin is the high-mobility-group (HMG) protein Hmo1. Hmo1 binds throughout the entire 35S rRNA coding sequence, suggesting a possible role in the formation of rDNA specific chromatin (Hall et al., 2006; Berger et al., 2007; Kasahara et al., 2007). Hmo1 associates selectively with the open rRNA gene chromatin (Merz et al., 2008). This is in good agreement with earlier observations providing genetic evidence that Hmo1 assists Pol I during transcription of rDNA (Gadal et al., 2002), although the molecular mechanism of this observation remains unclear. Recently, our laboratory analyzed the dynamics of rDNA chromatin states in course of the cell cycle (Wittner et al., 2011). It was shown that the balance between open and closed rDNA chromatin states can be explained by the interplay between replication and

Pol I transcription. We could further define a function for Hmo1 in preventing replication independent nucleosome assembly at open 35S rRNA genes.
It has been a long-standing question why the cell maintains more than half of the rRNA genes in a transcriptionally inactive state. In fact, yeast mutants with a low copy number of rRNA genes convert all of the 35S rRNA genes in the open state (French et al., 2003). However, these strains were shown to be sensitive to DNA damage (Ide et al., 2010), which led to the conclusion that the balance between open and closed chromatin states of the 35S rRNA genes is important for genome integrity.

2.3.1.3 Chromatin structure at the intergenic spacer

The psoralen gel retardation assay in combination with electron microscopy was used to analyze the chromatin organization of the rDNA IGS regions. A fragment containing the entire ribosomal spacer region revealed a nucleosomal structure for the intergenic spacers (Dammann et al., 1993). Furthermore, limited MNase digestion analysis of rDNA chromatin revealed the existence of five well-positioned nucleosomes in the region between the Pol I promoter region and the 5S rRNA gene. As expected for an origin of replication, the ARS element is located in a nucleosomal linker region (Thoma et al., 1984; Simpson, 1990). In this type of analysis, the intergenic region between the 5S and 35S rRNA genes also displayed a nucleosomal pattern, although nucleosomal particles were less well positioned in this sequence context (Vogelauer et al., 1998).
Psoralen crosslinking in combination with electron microscopy was used to link the nucleosomal organization of the ribosomal IGS region with the transcriptional activity of the 35S rRNA genes. The ribosomal spacers flanking inactive genes showed a regular chromatin structure typical for inactive bulk chromatin. In contrast, spacers flanking active genes displayed a peculiar crosslinking pattern with a heterogeneous size-distribution intermediate between that expected for mono- and di-nucleosomes (Dammann et al., 1993). In addition, this type of analysis revealed a structural link between the transcriptional state of an rRNA gene and its 3´flanking enhancer element. The enhancer regions of transcriptionally active genes were found to be non-nucleosomal, whereas inactive genes were followed by enhancers assembled in regularly spaced nucleosomes. Importantly, the open chromatin structure downstream of active 35S rRNA genes is not dependent on Pol I transcription, because the nucleosome-depleted enhancer region was also established in a Pol I mutant strain. It was suggested that the non nucleosomal enhancer structure downstream of active genes might be related to a function in replication termination with the open enhancer being responsible for the stop of the replication fork

(Dammann et al., 1995). Indeed, later studies confirmed that replication initiation occurs only at ARSs placed downstream of transcriptionally active 35S rRNA genes. Interestingly, the RNA Pol I enhancer contains a weak binding site for the transcription factor Abf1 (ARS-binding factor 1) (Warner, 1989), a multifunctional protein which was shown to enhance the activity of replication origins (Rhode et al., 1992). Since the enhancer elements are always organized in a nucleosome-free structure downstream of transcriptionally active rRNA genes that is highly accessible to transcription factors, it was suggested that the Abf1 binding sites in the rDNA enhancer are able to transactivate the ribosomal origin of replication (Dammann et al., 1995).

In contrast to the 35S rRNA genes, the chromatin structure of the Pol III transcribed 5S rRNA genes remained elusive due to its short length of only 132 nucleotides. Initial mapping of nucleosomes of reconstituted 5S rDNA chromatin *in vitro* and MNase digested yeast chromatin *in vivo* revealed multiple alternative positions of nucleosome core particles, each spaced by one helical repeat (Buttinelli et al., 1993). Transcription of the 5S rRNA gene is dependent on three transcription initiation factors. TFIIIA, which specifically binds the internal promoter of the 5S rRNA gene (Lee et al., 1995) and TFIIIB and C, which are required for transcription of all Pol III genes. TFIIIC comprises six subunits encoded by the genes *TFC1*, *3*, *4*, *6*, *7*, and *8* (Geiduschek and Kassavetis, 2001). The hexameric protein complex is recruited to 5S rRNA genes by interaction with promoter-bound TFIIIA as well as sequences within the gene. TFIIIC recruits the three-subunit TFIIIB complex (Brf1, Bdp1 and Spt15), which binds a conserved upstream regulatory sequence and is necessary and sufficient for Pol III transcription *in vitro* (Kassavetis et al., 1990). Finally, TFIIIB recruits Pol III and catalyzes the open complex formation for transcription initiation and remains bound to the DNA for multiple rounds of initiation (Kassavetis et al., 1990; Goodier et al., 1997). A recent study visualized the transcriptional state of 5S rRNA genes by the chromatin Miller spreading technique on single cells (French et al., 2008). In exponentially growing yeast cells, 20-30% of the short genes were engaged by one to three RNA polymerases, whereas the majority of 5S rRNA genes seem to be transcriptionally inactive under these experimental conditions. Interestingly, the study also showed that the activity of the 5S rRNA gene is largely independent of the activity of the neighboring 35S rRNA gene and vice versa (French et al., 2008).

Taken together, the rDNA locus contains genes transcribed by all three eukaryotic RNA polymerases, as well as regulatory elements necessary for DNA replication, making it an ideal candidate for the study of chromatin structure in relation to the functional state of the locus.

2.3.2 Chromatin structure at the yeast *PHO5* locus

Phosphate is an important nutrient required for cell growth and proliferation (Oshima, 1997). When phosphate is limiting, yeast cells respond by inducing expression of genes to acquire inorganic phosphate from multiple sources. This includes phosphate transporters and non-specific scavenger phosphatases (Ogawa et al., 2000; Springer et al., 2003; Kennedy et al., 2005). Pho5 is a central player in yeast phosphate assimilation because it accounts for more than 90% of the acid phosphatase activity (Svaren and Hörz, 1997). The *PHO5* expression is regulated by two transcription factors Pho2 and Pho4 that bind to the *PHO5* promoter at specific sites termed UASp1 and UASp2 (Figure 6). The exact role of Pho2 in the *PHO5* transition is not clear. Pho2 is a homeodomain protein and was shown to interact and cooperate with Pho4 for binding at UASp1 and for an efficient transactivation at UASp2 (Hirst et al., 1994; Barbaric et al., 1998). Although Pho2 is strictly required for *PHO5* promoter activation, no Pho2 target sites relevant for promoter activation have been located so far. This led to the suggestion that Pho2 acts as a *trans*-acting factor without binding to DNA (Sengstag and Hinnen, 1988). Pho4 is a

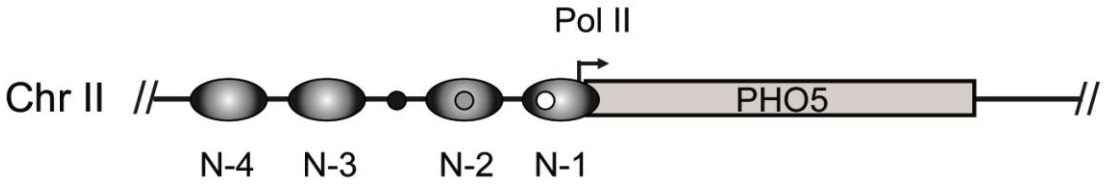

Figure 6 Schematic representation of the *PHO5* locus in *S. cerevisiae*. Grey ovals represent positioned nucleosomes N-1 to N-4 on the promoter under repressing conditions. UASp1, UASp2, and the TATA box are indicated by a small black, gray, and white circle, respectively.

basic helix-loop-helix transcription factor that can be phosphorylated at 5 serine residues by the Pho85-Pho80 complex, a cyclin-dependent kinase (CDK) complex. When phosphate is abundant, Pho4 is constitutively phosphorylated and predominantly located in the cytoplasm. Upon phosphate starvation, Pho4 is not modified by the cyclin-CDK complex and translocates in the hypophosphorylated state from the cytoplasm to the nucleus.

The repressed *PHO5* promoter is packaged in a positioned array of nucleosomes that is interrupted only by a short hypersensitive region containing UASp1 (Almer and Hörz, 1986) (Figure 6). Upon induction of the gene, a 600-bp region of the *PHO5* promoter becomes hypersensitive to nucleases, reflecting a profound alteration in the structure of four nucleosomes (Almer et al., 1986). Binding of Pho4 to both UASp1 and UASp2 is

required for this transition to occur, which appears to be a prerequisite for transcriptional activation (Svaren and Hörz, 1997).

In addition to Pho2 and Pho4, other activities may play roles in the chromatin transition from repressed to activated state at the *PHO5* promoter. The INO80 ATP-dependent chromatin remodeling complex is required for full activation, and the SWI/SNF complex has also been implicated by itself or in association with the histone variant H2AZ (Santisteban et al., 2000; Steger et al., 2003; Brown et al., 2011). Two studies demonstrated that specific nucleosomes are not only remodeled during activation but in fact also displaced from the promoter DNA (Boeger et al., 2003; Reinke and Hörz, 2003). Studies have also pointed out the importance of histone acetylation in *PHO5* regulation; however, none demonstrated an absolute requirement for a specific histone acetyltransferase in the transition from the repressed to the derepressed state. It was shown that the histone H3-specific HAT Gcn5 is not essential for derepression of the *PHO5* gene, but could affect the chromatin structure in a constitutively derepressed *pho80* mutant (Gregory et al., 1998). Although Gcn5 does not affect the final *PHO5*-activated steady-state level, it seems to increase the rate of gene induction by accelerating *PHO5* chromatin remodeling (Barbaric et al., 2001). Deletion of the Rpd3 histone deacetylase loosens the repression by increasing *PHO5* expression in phosphate-rich media, and delays the inactivation after shifting from inducing to non-inducing medium (Svaren and Hörz, 1997; Vogelauer et al., 2000). In addition, the histone acetyltransferases SAGA (Barbaric et al., 2003) and NuA4 (Nourani et al., 2004), and the histone chaperone Asf1 (Adkins et al., 2004; Korber et al., 2006) were shown to be implicated in the regulation of this locus. Recently, the chromatin remodeling complexes Chd1 and Isw1 were shown to selectively remove *PHO5* promoter nucleosomes, without effect on open reading frame nucleosomes (Ehrensberger and Kornberg, 2011), further contributing to the complexity of *PHO5* promoter activation. Taken together, the molecular mechanism of the chromatin transition of the *PHO5* promoter upon induction has still remained an unresolved question despite several decades of intensive research.

2.4 Objectives

In eukaryotic genomes, chromatin is the template of all nuclear processes including transcription, recombination and replication. Besides the wrapping of DNA in nucleosome core particles, eukaryotic chromatin is associated, interpreted and modified

by numerous protein complexes including transcription factors, DNA and RNA metabolizing machineries, architectural proteins, chromatin remodeling and modifying enzymes. To understand how specific genomic loci adopt different functional states, it is critical to characterize the corresponding compositional changes and posttranslational modification pattern in correlation with the functional state of a genomic locus.

Most methods that are currently available to analyze chromatin structure *in vivo* are designed to analyze the association of a protein of interest with a certain genomic DNA fragment. Although current technologies like ChIP allow mapping of DNA target sequences of a specific protein on a genome-wide scale, the analyses are limited to the investigated protein by the use of a specific antibody for ChIP, or by expression of the protein of interest as a Dam- or MNase fusion protein for DamID or ChEC, respectively. Thus, the analysis of chromatin *in vivo* requires *a priori* knowledge or educated guess of the protein or histone modification of interest and is not suited to detect the locus-specific composition of a genomic region of interest in an unbiased manner. Accordingly, the aim of this study was to use site-specific recombination of chromatin segments *in vivo* and subsequent affinity purification as previously reported (Ansari et al., 1999; Griesenbeck et al., 2004; Ehrensberger and Kornberg, 2011) to define the composition, structure and functional state of a specific chromosomal domain purified from yeast bulk chromatin. In the past, the technique allowed specific enrichment of the targeted genomic region of the single copy *PHO5* gene, but the quality and quantity of the samples was not sufficient for identification of associated proteins by MS (Griesenbeck et al., 2003, 2004).

To this end, multiple steps of the purification strategy had to be optimized and were first applied to the multi-copy rDNA gene cluster of yeast. This locus is an attractive target because it is 150-200 fold more abundant than single copy genes and reduces the amount of starting material to obtain purified chromatin in sufficient amount for downstream analyses. Moreover, our current knowledge about the molecular nature of the different 35S rDNA chromatin states, as well as chromatin composition at different elements of the IGS region (e.g. ARS, 5S rRNA gene and E-pro) is still limited. Using this methodology, the aim was to derive an unbiased compositional and structural analysis of these neighboring DNA elements of the rDNA locus by semiquantitative mass spectrometry. Because the native purification strategy is amenable to structural analysis, it was tested if nucleosome positioning on purified chromatin rings could be determined by electron microscopy. Finally, we extended the analysis to the single-copy gene *PHO5* in order to explore if the identification of associated proteins of any genomic locus of interest might be possible, thereby providing an exciting future perspective.

3 Results

3.1 Purification of defined chromosomal domains by site-specific recombination *in vivo*

In this work, specific chromatin segments from yeast cells were isolated by site-specific recombination *in vivo* and subsequent affinity purification to analyze the chromatin at the targeted domain in composition and structure. The purification strategy is depicted in Figure 7 and was originally developed to analyze chromatin associated with the single

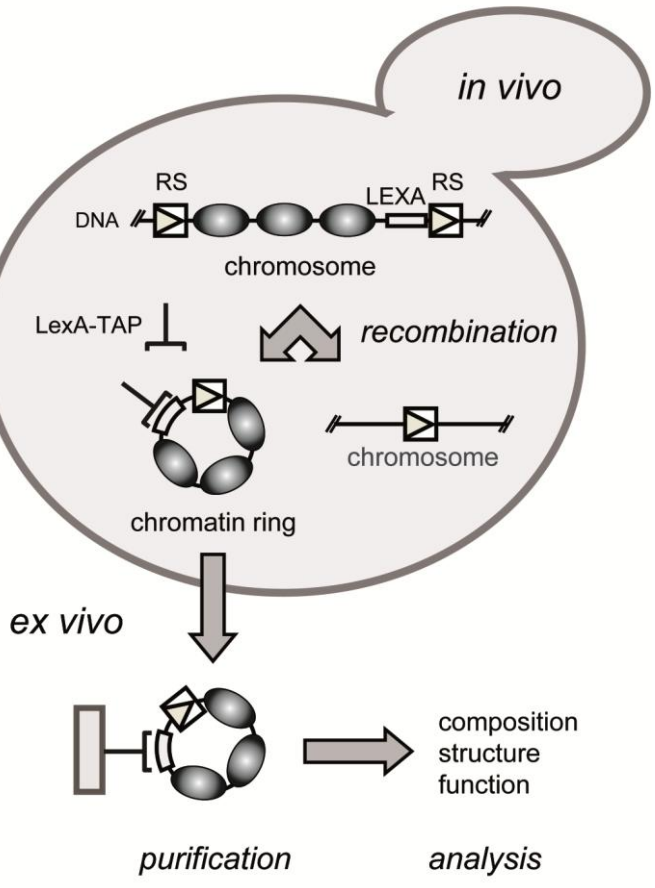

Figure 7 Schematic representation of the purification strategy of specific chromosomal domains. Conditionally expressed R-recombinase excises a genomic locus of interest flanked by RS elements (RS, boxed arrowheads) in form of a chromatin ring. After cell lysis the soluble chromatin rings can be islolated from cellular debris and purified via a recombinant LexA-TAP fusion protein (LexA-TAP, bracket connected to a line), binding to the *LEXA* DNA binding sites (*LEXA*, grey box) as well as to an affinity support (filled rectangle). Filled ovals represent chromatin components.

copy silent mating type and *PHO5* gene loci (Ansari et al., 1999; Boeger et al., 2003; Griesenbeck et al., 2003, 2004). For the isolation of specific chromosomal domains, the chromosomal locus is framed with recognition sites (RS) for the R Recombinase from *Zygosaccharomyces rouxii*. The site-specific recombinase belongs to the integrase family, which also includes the bacteriophage Cre recombinase and the Flp recombinase from *S. cerevisiae*. The mechanism of the enzyme is characterized by a strand exchange mechanism that requires no DNA synthesis or ATP hydrolysis. As in the case of several topoisomerases, the phosphodiester bond energy is conserved in a phospho-protein linkage during strand cleavage and re-ligation (Argos et al., 1986; Gopaul and Duyne, 1999). Additionally, the enzyme works independent of any co-factors or accessory proteins which makes it ideally suited for function in heterologous organisms (Ansari et al., 1999). The R recombinase binds to a pair of target sites and excises the intermediate DNA from its chromosomal context in the form of a closed circular molecule including one of the RS sites. The second RS site stays at its chromosomal position. The reaction is fully reversible and depends on the effective concentrations of educts and products (Gartenberg, 1999). For further purification, three *LEXA* binding clusters are incorporated adjacent to one of the RS sites, such that they are included in the excised chromatin domain. Co-expression of a fusion protein consisting of the bacterial LexA protein fused to a C-terminal TAP tag (LexA-TAP) (Rigaut et al., 1999; Puig et al., 2001) allows the retention of the chromatin circles at an affinity support.

3.1.1 Establishment of yeast strains with a modified rDNA locus competent for excision of distinct rDNA chromatin domains

3.1.1.1 Strategy for chromosomal integration and expansion of genetically modified rDNA repeats

The presence of multiple copies of rDNA repeats in the eukaryotic genomes has been an obvious obstacle for mutational analysis of DNA elements in this locus. To genetically manipulate the multi copy rDNA locus such that every single repeat contains the respective modification, we followed an elegant approach provided by the group of Masayasu Nomura (Wai et al., 2000). Wai and co-workers generated yeast strains in which the rDNA repeats on chromosome XII were completely deleted and replaced by a *URA3* selection marker (Figure 8). Survival of the strains was supported by the presence of a single rDNA repeat on a helper plasmid. This rDNA repeat was under the control of

a *GAL7* promoter and thus transcribed by Pol II. Consequently, the strain could grow on a medium containing galactose but not on a medium containing glucose. This strain was transformed with a DNA fragment containing a modified rDNA gene with introduced pairs of RS sites and *LEXA* binding sites at distinct positions along the rDNA repeat. Counterselection with 5-Fluoroorotic acid (5-FOA) allowed identifying positive clones which had lost the *URA3* gene and integrated the modified rDNA unit by homologous recombination. After several generations, these yeast cells had lost the helper plasmid and the reintegrated rDNA repeat supported growth on medium with glucose as a carbon source. Further analysis showed that the rDNA locus had re-expanded to a wildtype

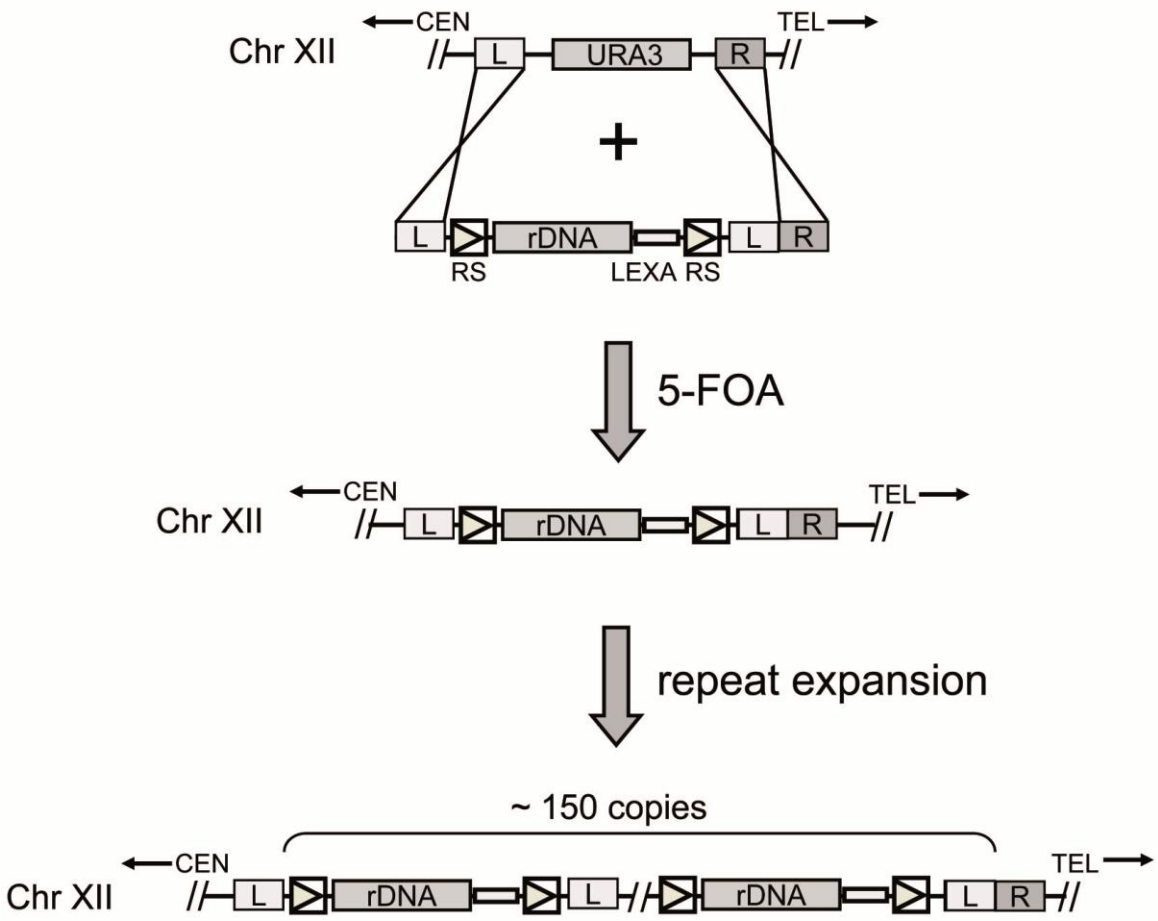

Figure 8 Strategy for the chromosomal integration and expansion of a modified rDNA repeat with pairs of RS sites and *LEXA* binding sites. A schematic representation of the rDNA locus of yeast strain NOY989 is shown. All rDNA repeats are removed from the endogenous locus and replaced by a *URA3* selection marker which is flanked by sequences named L (left) directing towards the centromer (CEN) and R (right) directing towards the telomere (TEL). Integration of a new rDNA repeat and its expansion were carried out using a DNA fragment consisting of a single rDNA unit carrying pairs of RS sites (RS, boxed arrowheads) and a cluster of *LEXA* binding sites (*LEXA*, grey box) with the L sequence added at the left end and the L plus R sequences at the right end. The presence of the L element on the right side of the rDNA was designed to initiate expansion by an unequal crossing-over or a DNA breakage–repair process. Positive clones are selected on 5-Fluoroorotic acid (5-FOA) containing medium to screen for loss of the *URA3* marker. After several generations, the rDNA locus reexpands to a wildtype-copy number of 100-150 with every single repeat containing the RS and *LEXA* binding sites at the respective position along the rDNA repeat. Note that each repeating unit has an extra sequence derived from the L segment in addition to the native 9.1kb rDNA repeat.

copy number of 100-150 again and all expanded rDNA copies had carried the same genetic modifications as the transformed DNA fragment (Figure 8).

This technique was used to construct a library of yeast strains in which either the ARS, the 5S rRNA gene, the E-pro region, the 18S rRNA coding sequence, the 35S rRNA gene or a complete rDNA repeat are flanked by RS elements and include *LEXA* binding sites according to the scheme presented in Figure 9. In this work, the resulting strains will be referred to as the ARS, 5S, E-pro, 18S, 35S and rDNA circle strains, respectively.

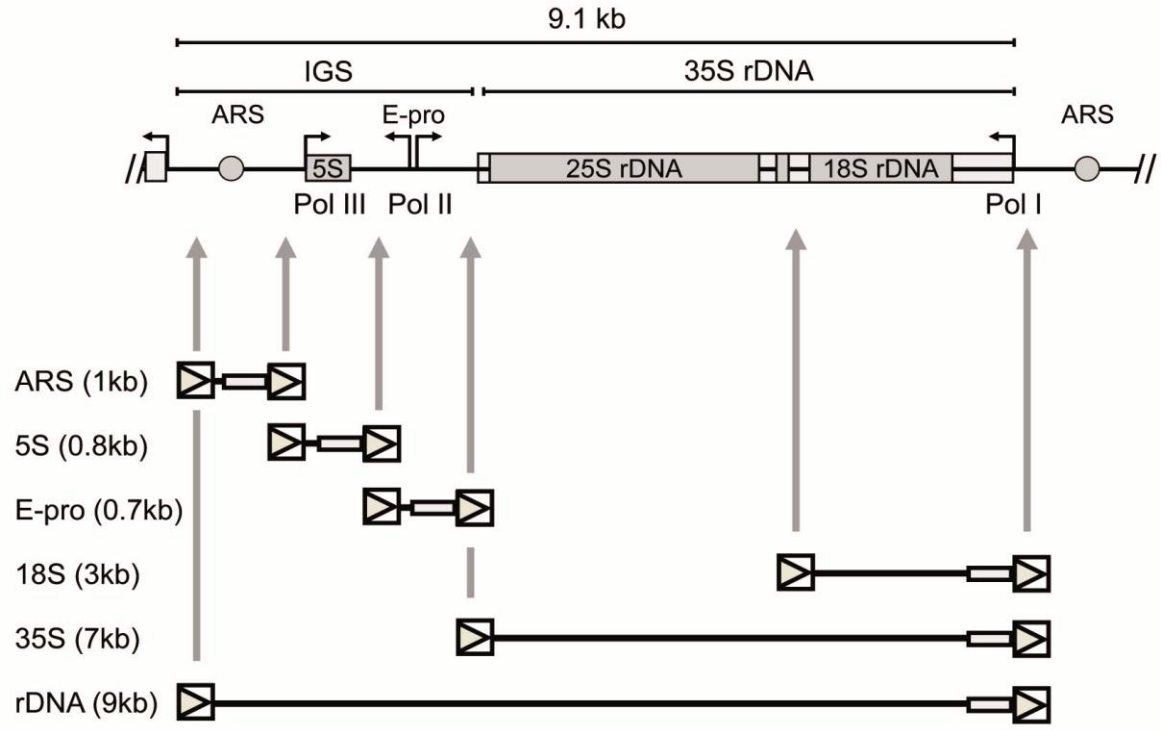

Figure 9 Schematic representation of genetic modifications of the yeast rDNA locus. 35S, 25S, 18S, 5S rRNA coding regions; IGS, intergenic spacer region; ARS, ribosomal autonomous replication sequences (grey circles); E-pro, expansion promoter; arrows indicate transcription start sites used by RNA polymerases I, II, and III (Pol I, II, III) and point in the direction of transcription. Arrows mark the sites of insertion for RS elements and *LEXA* binding sites in the different elements within the rDNA repeat. The description of the respective domain flanked by the RS elements as well as the size of the chromatin ring after recombination (in parentheses) are indicated on the left.

In addition, an isogenic control strain was generated by the same approach. To this end, a native rDNA repeat without RS sites and *LEXA* binding sites was inserted and reexpanded in the same way as for the different circle strains.

3.1.1.2 35S rRNA gene chromatin states are established after expansion of the genetically modified rDNA repeats

In order to ensure that important features of native rDNA chromatin are reestablished after the expansion of the modified rDNA repeats, the rDNA copy number and the

coexistence of the open and closed chromatin states of 35S rRNA genes were analyzed in the circle strains. First of all, none of these yeast strains was displaying any detectable growth defect, suggesting that the integrated RS elements and *LEXA* binding sites in the rDNA locus did not significantly affect rDNA transcription and ribosome production in the

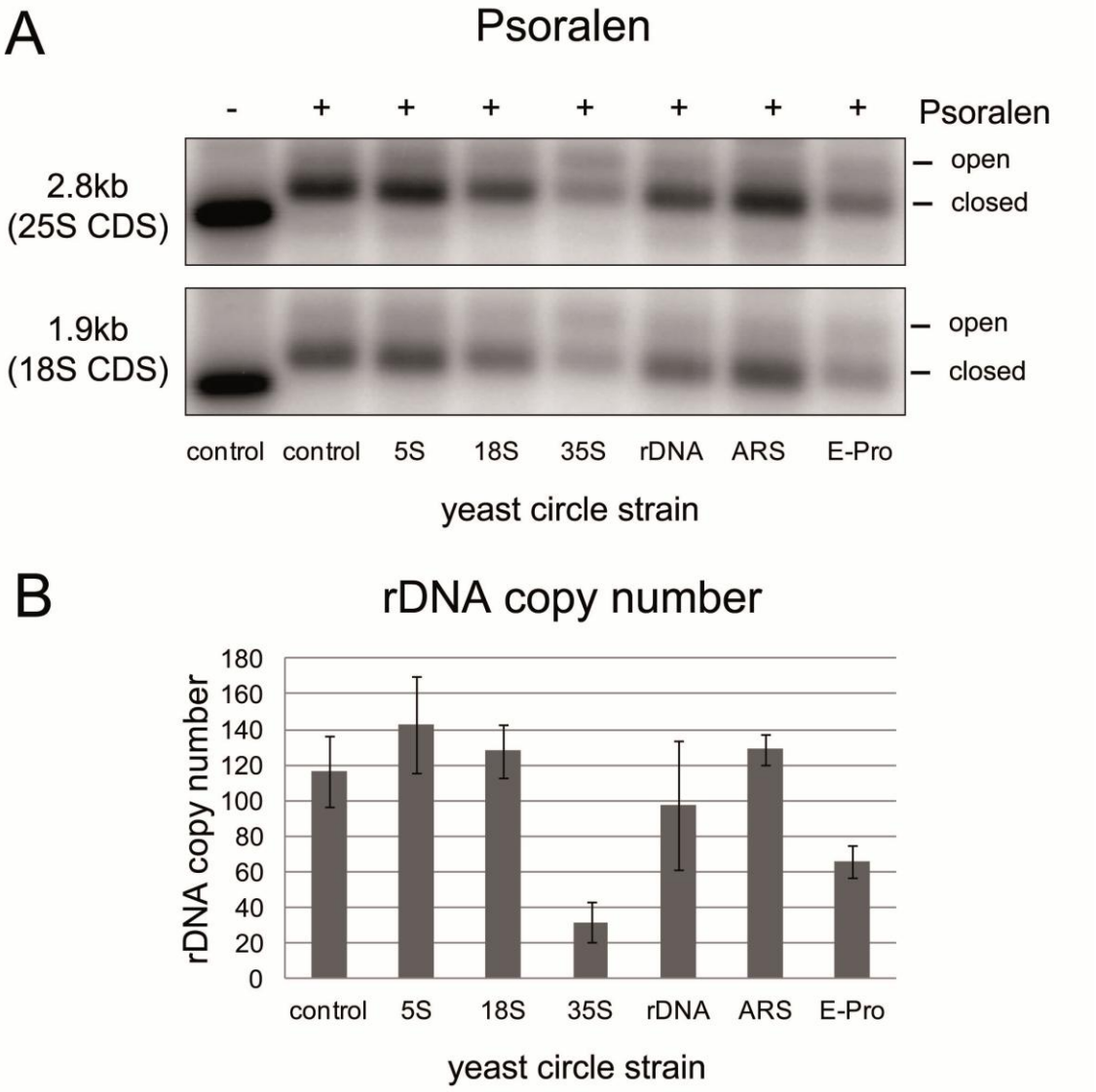

Figure 10 Characterization of rDNA chromatin and rDNA copy number in the yeast circle strains. A) Psoralen crosslinking analysis. Exponentially growing cultures of yeast strains y2378 (control), y2379 (5S), y2380 (18S), y2381 (35S), y2382 (rDNA), y2383 (ARS), y2384 (E-Pro) were crosslinked with formaldehyde. Crude nuclei were prepared and treated with psoralen. DNA was isolated, *Eco*RI digested and analyzed by Southern blot with a probe detecting two different fragments of the 18S and 25S rRNA coding sequence (CDS). Fragments originating from open and closed 35S rRNA genes are indicated. B) Determination of rDNA copy number by quantitative PCR (qPCR). Genomic DNA was isolated from the same yeast strains as described in A). The DNA was analyzed with primer pairs 712/713 or 611/612 and 688/689 amplifying either a region of the 18S rDNA or a region of the single-copy *NOC1* and *PHO5* genes. The relative rDNA copy number was determined by normalizing the ratio of the amount of rDNA to the ratio of the average amount of the two single-copy genes. The average and standard deviations are derived from triplicate qPCRs for each primer pair.

cell. To determine the ratio of open and closed 35S rRNA gene chromatin states in the respective circle strains, exponentially growing cells were treated with formaldehyde and

isolated nuclei were subjected to psoralen crosslinking analysis (Figure 10A). The psoralen incorporation into two different *Eco*RI fragments spanning the regions coding for 18S rRNA and for 25S rRNA, respectively, were investigated by Southern blot analysis. Two distinct bands with different mobilities originating from open or closed 35S rRNA genes could be observed for DNA fragments isolated from cells which had been treated with psoralen (Figure 10A, + psoralen lanes). As a control, the same DNA fragment of the control sample migrated as a single band with higher mobility without psoralen treatment (Figure 10A, – psoralen lane). This result indicates that the open and closed chromatin states of 35S rRNA genes are reestablished upon expansion of a wildtype rDNA repeat (control strain) as well as modified rDNA repeats including RS sites and *LEXA* binding sites (circle strains). Interestingly, the ratio of open to closed copies was elevated in case of the 35S and E-pro circle strains in comparison to the control strain and the other circle strains (Figure 10A, compare lanes 35S and E-Pro with the other + psoralen lanes). The observed difference in psoralen accessibility might be a consequence of different efficiencies of rDNA locus expansion. Thus, the rDNA copy number in the control strain and the circle strains was determined by quantitative PCR (Figure 10B). In good correlation with the psoralen data, the 35S circle strain and the E-pro circle strain showed a significantly reduced rDNA copy number of 32 and 66, respectively, whereas all other investigated strains showed a wildtype number of 100-150 rDNA copies in this type of analysis (Figure 10B). This result suggests that the high ratio of open to closed copies in the 35S and E-pro circle strains is a consequence of reduced rDNA copy number in these strain backgrounds. Further growth of the two strains for several generations in full medium did not lead to an increase of the rDNA copy number (data not shown). One possible explanation for the reduced rDNA copy number in both strains is that the integrated RS sites or *LEXA* binding sites interfere with the expansion of the rDNA locus to a wildtype copy number. Interestingly, the E-pro and 35S circle strains are the only strains carrying an integrated RS site downstream of the 35S rDNA terminator region in close proximity to the replication fork barrier (RFB) (see Figure 9 E-pro and 35S) which was shown to be essential for rDNA repeat expansion (Kobayashi et al., 2001).

Taken together, these results show that the open and closed chromatin states of 35S rRNA genes are reestablished after expansion of the modified rDNA repeats containing RS and *LEXA* binding sites. Besides, the increased percentage of open copies observed in the 35S and E-pro circle strains may be explained by a reduced number of rDNA copies as opposed to a general change of rDNA chromatin structure.

3.1.2 Establishment of a single step purification technique for selected chromosomal domains

Based on an established isolation protocol for single copy genes (Griesenbeck et al., 2004), attempts were made to adapt the technique to the multi-copy rDNA locus and to improve individual steps of the purification in order to increase yield and purity of the targeted chromatin domain.

3.1.2.1 Single-step affinity purification with IgG coupled magnetic beads allows efficient enrichment of rDNA chromatin domains

IgG-sepharose is a widely used affinity matrix for the purification of Protein A- or TAP-fusion proteins from cell extracts. A recently published one-step purification protocol of ribonucleoprotein (RNP) particles in yeast demonstrated that IgG-conjugated magnetic beads allow substantial reduction of background contaminants and high yields in affinity purifications compared to antibody conjugated resins like sepharose (Oeffinger et al., 2007). The magnetic beads have a small diameter (~ 1µm) resulting in a large surface area-to-volume ratio that increases the number of affinity binding sites. Moreover, the beads are impermeable, such that the antibodies are solely conjugated to the bead surface. Unlike permeable resins such as sepharose or agarose, which are in part limited by their pore size, magnetic beads have no theoretical limit to the size of the respective complex targeted for purification. In order to decrease the amount of background contaminants in the purification of rDNA chromatin domains, IgG-conjugated magnetic beads were tested in combination with a slightly modified version of the single-step affinity purification protocol of Oeffinger and co-workers. The general purification scheme of rDNA chromatin domains and a representative nucleic acid and Western blot analysis of different samples taken during the purification of a chromosomal domain spanning the 35S rRNA gene is shown in Figure 11A.

After preparation of whole cell extract, most of the bulk genomic DNA was separated from the soluble recombined rDNA domain by centrifugation (Figure 11B, compare lane 1 **C**ell **E**xtract, with lane 2 **P**ellet after centrifugation). In addition to the 35S rRNA gene circle DNA, the supernatant of the centrifugation contained fragments of genomic DNA, generated by shear force during cell lysis, and RNAs (Figure 11B, lane 3, **IN**put fraction for the affinity purification, note that all DNA samples have been treated with RNAse A before analysis and only trace amounts of degraded RNA fragments are observed). Most of the 35S rRNA gene circle DNA was bound to the IgG coated magnetic beads (Figure

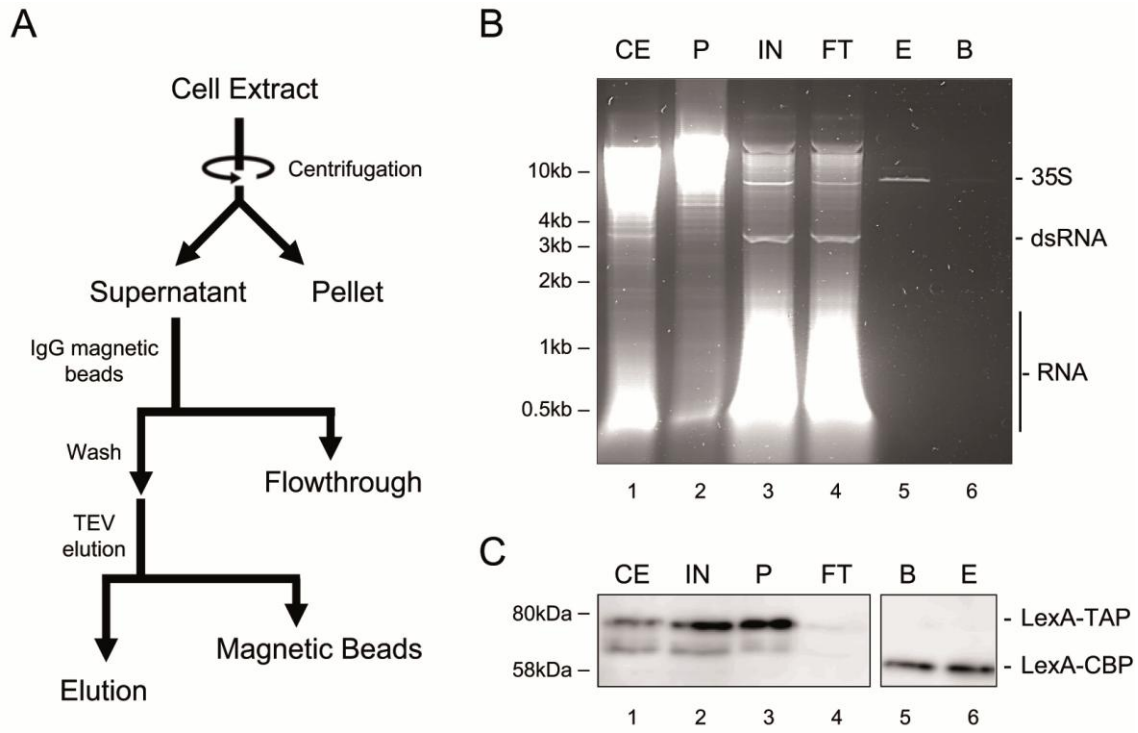

Figure 11 A single step affinity purification protocol with IgG magnetic beads is sufficient to enrich rDNA chromatin domains with high specificity. A) Purification scheme of rDNA chromatin domains. B) Representative DNA analysis of the purification of 35S rRNA gene circles. Purification was performed as described in the Material and Methods section from yeast strain y2381 carrying an rDNA recombination cassette spanning the 35S rRNA gene. DNA was extracted from 0.01% of the crude cell extract (CE), 0.01% of the resulting supernatant (IN) and pellet (P) after centrifugation, 0.01% of the flow-through after binding to IgG coated magnetic beads (FT), and 5% of the beads (B) and released chromatin circles after TEV elution (E). After linearization of the circular 35S rRNA gene circles with SacII, DNA fragments were separated on 1% agarose gel and visualized by SybrSafe stain. Positions of DNA fragments from a size marker are indicated on the left. Position of residual RNA fragments and double-stranded RNA (dsRNA) and the linearized 35S rDNA circle is indicated on the right. C) Representative Western blot analysis of the purification of 35S rRNA gene circles. The same set of samples as described in B) was subjected to 10% SDS-PAGE. After transfer on a PVDF membrane, Western blot analysis with α-PAP antibody recognizing the Prot A-component of the LexA-TAP fusion protein for samples CE, IN, P, FT and with α-CBP antibody recognizing the CBP-component of the LexA-fusion protein for samples B and E was performed. The position of protein bands of a size marker is indicated on the left. The positions of the LexA-TAP fusion protein and the LexA-CBP protein after cleavage within the linker region between the C-terminal protein A moiety and the calmodulin binding peptide of the TAP tag by TEV protease are shown on the right.

11B, compare 35S rRNA gene circle DNA in lane 3 with the circle DNA in lane 4 (**F**low **T**hrough fraction after incubation with the magnetic IgG coated beads)). After washes, the 35S rRNA gene circle could be efficiently eluted under native conditions upon cleavage with TEV protease within the linker region between the C-terminal protein A moiety and the calmodulin binding peptide of the TAP tag (Figure 11B, compare 35S rRNA gene circle DNA in lane 5 **E**lution with the circle DNA in lane 6 **B**eads). The same set of samples derived from an independent purification of 35S rRNA gene circles was subjected to SDS-PAGE and Western blot analysis with antibodies recognizing the Protein A- or CBP-moieties of the TAP-tag of the LexA-fusion protein (Figure 11C). Notably, LexA-TAP migrates as a double band. As shown by MALDI mass spectrometry on the excised protein bands, the higher molecular weight band represents the full length

protein at the expected size, whereas the band with higher electrophoretic mobility represents a degradation product without the LexA moiety of the fusion protein (data not shown). In good correlation with the retention of 35S rDNA chromatin circles, the LexA-TAP fusion protein is efficiently depleted from the supernatant after incubation with IgG magnetic beads (Figure 11C, compare lanes **IN**put of the affinity purification and **F**low **T**hrough after incubation with the affinity resin). Incubation with TEV protease leads to proteolytic digestion of the bait protein at a cleavage site located in the TAP-tag, releasing the LexA-CBP protein and the bound rDNA chromatin circles into the supernatant (**E**lution). The Protein A-tag stays bound to the IgG beads (**B**eads). In these fractions, a CBP antibody could only detect a band corresponding to the size of the LexA-CBP protein, indicating complete TEV cleavage. Substantial amounts of the LexA-CBP protein were released from the IgG beads (Figure 11C, **E**lution), which was sufficient to elute the majority of 35S rDNA chromatin circles from the affinity matrix.
Accordingly, the use of IgG magnetic beads in a single-step affinity purification turned out to be a fast and highly efficient purification strategy for rDNA chromatin domains in comparison to the original protocol (Griesenbeck et al., 2004). The large 35S rDNA chromatin circle with a size of 7kb was specifically retained by binding of the LexA-TAP protein and could be almost completely eluted under native conditions by incubation with TEV protease.

3.1.2.2 LexA-TAP expression level influence the specific enrichment of the targeted domains

The LexA protein is a key transcriptional repressor of the bacterial SOS system involved in DNA repair and maintaining genome integrity (reviewed in Butala et al., 2008). The protein consists of two structurally distinct domains, the N-terminal DNA-binding domain and the C-terminal dimerization domain. LexA interacts with specific DNA sequences via a variant of the classical helix-turn-helix motif (Luo et al., 2001) and the protein binds as a dimer to specific operators named SOS-boxes with the consensus sequence $CTGTN_8ACAG$. However, *in vitro* binding studies with variant consensus sequences showed that, albeit with reduced affinities, the LexA protein is able to bind a large variety of different DNA substrates (Zhang et al., 2010). Consequently, heterologous expression of the LexA-TAP fusion protein in yeast may result in unspecific binding of the protein at weak consensus sequences elsewhere in the yeast genome. In order to test this hypothesis, the LexA-TAP protein was ectopically expressed under control of different native yeast promoters with increasing expression strength including the constitutive

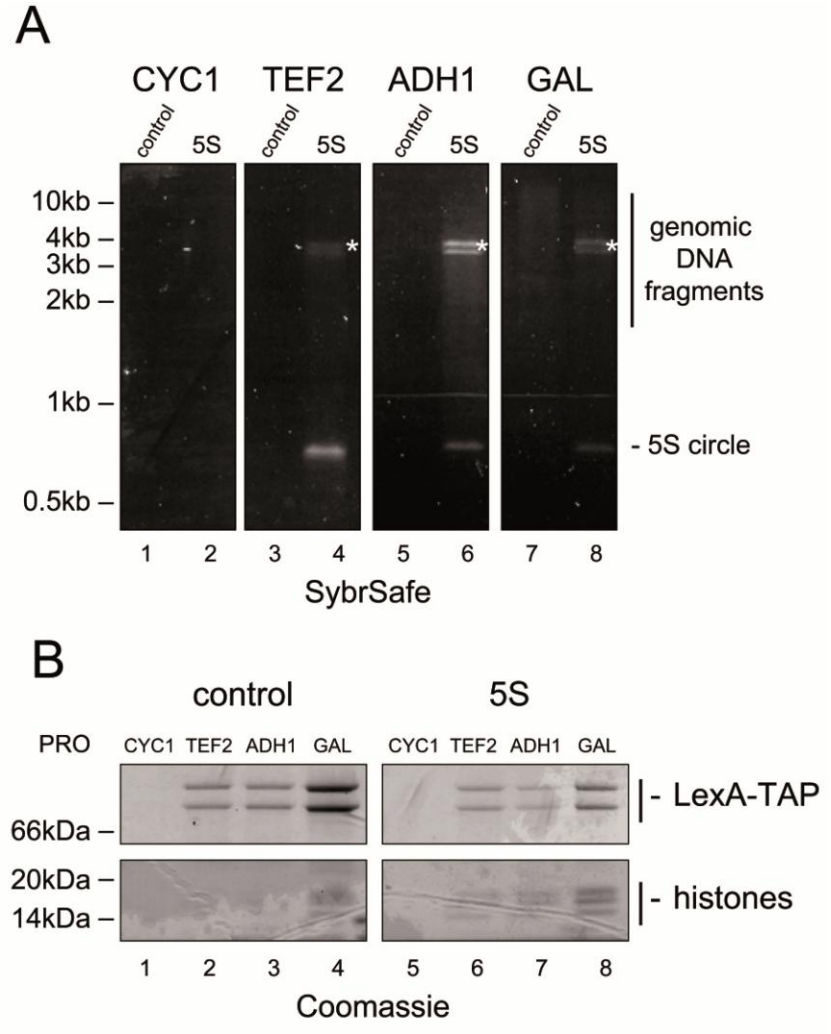

Figure 12 High expression level of the LexA-TAP fusion protein increases the background purification of genomic chromatin fragments. Yeast strains y2124 (control) and y1997 (5S) were transformed with plasmids K2048 (*CYC1*), K2049 (*TEF2*), K2050 (*ADH1*) or K929 (*GAL*). Cells were grown in SCR-LEU medium, recombination was induced by addition of 2% galactose at a cell density of OD_{600} of 0.8. Harvesting of cells, cell lysis and IgG affinity purification was done as described in the Material and Methods section. Proteins and nucleic acids were released from the beads by basic elution (as described in Material and Methods). A) DNA analysis of 5S circle and control purifications with different expression levels of the LexA-TAP protein. DNA was extracted from 10% of elutions. After linearization of the circular 5S rRNA gene circles with *Nco*I, DNA fragments were separated on 1% agarose gel and visualized by Sybr Safe stain. The used promoter is indicated on top of the lanes. Positions of DNA fragments from a size marker are indicated on the left. Position of the *Nco*I linearized 5S rDNA circle and genomic DNA fragments present in the control lane of the *GAL*-dependent expression situation is indicated on the right. Positions of higher-order recombination products are marked by asterisks (see below). B) Protein analysis of 5S circle and control purifications under different promoter strengths for LexA-TAP expression. The rest of the eluates was lyophilized over night in a SpeedVac and the pellets resuspended in SDS-sample buffer. The samples were separated on 4-12% gradient gel and protein bands visualized by colloidal Coomassie staining. The strain and the used promoter is indicated on top of the lanes. The position of protein bands of a size marker is indicated on the left. The positions of the LexA-TAP protein and histones are indicated on the right.

CYC1, *TEF2* and *ADH1* promoters (Mumberg et al., 1995) and the galactose-inducible strong *GAL10* promoter. Plasmids that are competent for episomal expression of LexA-TAP under control of the *CYC1*, *TEF2*, *ADH1* or *GAL1* promoter were transformed in the control strain and the 5S circle strain. Western blot analysis of whole cell extracts showed the expected increasing expression levels of LexA-TAP in the *CYC1*, *TEF2*,

ADH1 and *GAL1* promoter situations (data not shown). After IgG affinity purification, the amount of purified LexA-TAP fusion protein correlated well with the cellular expression levels (Figure 12B LexA-TAP; compare lanes 1 to 4 for the control strain and 5 to 8 for the 5S circle strain). DNA and protein analysis of the affinity-purified samples suggested that overexpression of LexA-TAP mediated by the inducible *GAL10* promoter leads to co-purification of unspecific chromatin fragments. This was shown by the co-purification of genomic DNA fragments (Figure 12A *GAL*, lane 7) and the presence of histone molecules in the control purification (Figure 12B, histones lane 4). *TEF2* and *ADH1* promoter mediated expression of LexA-TAP showed intermediate concentration of the fusion protein (Figure 12B LexA-TAP, lanes 2-3 and lanes 6-7) and specific co-purification of 5S rDNA circles (Figure 12A, lanes 4 and 6) and associated histone molecules, which were absent in the respective control purifications (Figure 12B histones, compare lanes 6-7 with lanes 2-3). The basal expression level of LexA-TAP under control of the *CYC1* promoter showed no specific enrichment of both, 5S rDNA circles (Figure 12A, lane 2) and associated histone molecules (Figure 12B histones, lane 5). This result indicated that the cellular amount of the LexA-TAP fusion protein was not sufficient (Coomassie staining was not sensitive enough to detect the purified fusion protein, Figure 12B, lanes 1 and 5) to allow efficient retention of the multiple copies of 5S chromatin circles on the affinity matrix.

To keep a low background of contaminants in the chromatin preparations, the moderate *TEF2* promoter was used for constitutive expression of the LexA-TAP fusion protein in all subsequent purifications shown in this work. On the other hand, overexpression of LexA-TAP by the *GAL10*-promoter in the control strain generated a tool to purify bulk chromatin fragments from yeast and was used as a control in the analysis of histone modifications (see 3.2.1).

3.1.2.3 Chromosomal integration of the R recombinase and LexA-TAP expression cassette allows cell growth in complex medium

Episomal expression of the heterologous R recombinase and LexA-TAP proteins has important limitations. First, the transformed plasmids have to be maintained in the cell, which is accomplished by a selectable *LEU2* marker gene present on the expression plasmids used in this work. Thus, cells must be grown in minimal medium lacking leucine in order to obtain uniform cell populations including the plasmid resulting in reduced growth rates of the yeast cultures compared to complex medium. Furthermore, episomal vectors are absent from a fraction of cells, even when kept under selective pressure, reducing the overall recombination efficiency (Gartenberg, 2012). To establish yeast

strains carrying a chromosomally integrated expression cassette for R recombinase and LexA-TAP, an integration vector targeting the yeast *URA3* locus was constructed. Yeast strains carrying the chromosomal expression cassette could be cultured in the media of choice and recombination efficiency was greater than observed upon episomal recombinase expression in some cases (data not shown).

3.1.2.4 Distinct domains of the rDNA locus can be purified from the yeast chromosome

rDNA circles could be successfully purified from strains carrying recombination cassettes for either the E-pro region, the 5S rRNA gene, the ARS region, the 18S rRNA coding sequence the 35S rRNA gene, or an entire rDNA repeat (Figure 13, lanes 2-7). In case of the control strain with the same genetic background, carrying a chromosomally integrated expression cassette for R Recombinase and the LexA-TAP protein, but lacking recombination sites and *LEXA* binding sites within the rDNA locus, no significant enrichment of nucleic acids could be observed in such a purification (Figure 13, lane 1 (control)). In many of the rDNA ring purifications, higher molecular weight DNAs were retained on the affinity matrix (Figure 13, lanes 2-5 marked by asterisks). Southern blot analysis confirmed that these nucleic acids originated from higher order recombination products in which single recombination sites had been neglected by the recombinase (data not shown). These recombination products all contained the *LEXA* binding site

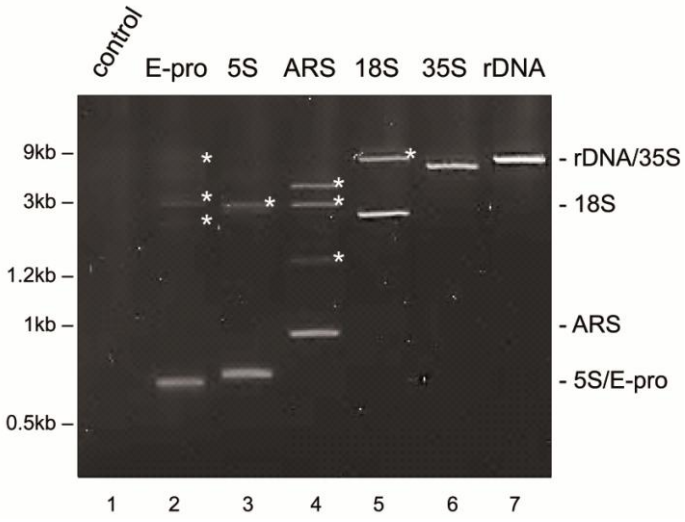

Figure 13 Distinct rDNA domains can be specifically purified from the yeast chromosome. DNA was prepared from chromatin circle preparations from yeast strains y2378, y2384, y2379, y2383, y2380, y2381 and y2382 (the respective purified chromatin domain is indicated on top of each lane), treated with appropriate restriction enzymes (*Nco*I was used for linearization of E-pro, 5S and ARS circles; *Sac*II was used for linearization of control, 18S, 35S and rDNA circles), separated in a 1% agarose gel and visualized with SybrSafe stain. Positions of DNA fragments of a size standard are indicated on the left. Positions of the respective linearized rDNA circles are indicated on the right. Positions of higher-order recombination products are marked by asterisks.

cluster and were therefore specifically bound by the LexA-TAP protein and then enriched on the IgG coated magnetic beads.

Around 200-500ng of purified rDNA chromatin rings could be obtained from one litre of exponentially growing yeast culture (~5 x 10^{10} cells), which corresponds to a recovery between 0.5-5% of the total cellular amount of individual rDNA domains. The efficiency of the purification decreased with the size of the chromatin circles (data not shown). In general, the amounts of purified rDNA chromatin circles proved to be sufficient for downstream analysis of the chromatin composition and structure of the individual rDNA chromatin domains.

3.2 Compositional analysis reveals distinct proteomes for individual rDNA chromatin domains

3.2.1 Covalently modified histones are selectively enriched in purifications of distinct rDNA domains

In order to analyze the protein content of the distinct affinity-purified rDNA chromatin domains, proteins present in the individual chromatin preparations were denatured and separated by SDS-PAGE. Coomassie staining revealed that the LexA-CBP bait protein was similarly enriched in the different purifications including the control purification (Figure 14A, compare lanes 1-6, protein band marked as LexA-CBP on the right). Furthermore, distinct protein bands co-purifying selectively with the rDNA domains were identified as the four canonical histones by mass spectrometry (Figure 14A, bands marked as H3/H2B, H2A and H4 on the right). Interestingly, the chromatin purification of the E-pro region resulted only in a slight enrichment of histone molecules compared to the control purification (Figure 14A, compare lane 2 with lane 1), although the amount of purified E-pro chromatin circles was comparable to the other rDNA chromatin preparations (Figure 13, compare lane 2 with lanes 3-7). A possible explanation is that the E-pro region represents a nucleosome-depleted region. The absence of the histone bands in the control purification argues that the histone molecules co-purified with the individual rDNA chromatin preparations were specifically associated with the enriched subdomains of the rDNA locus. This allowed analyzing potential qualitative and quantitative differences in their posttranslational modification state. Samples of a control purification and purified chromatin domains including the ARS region, the 5S rRNA gene,

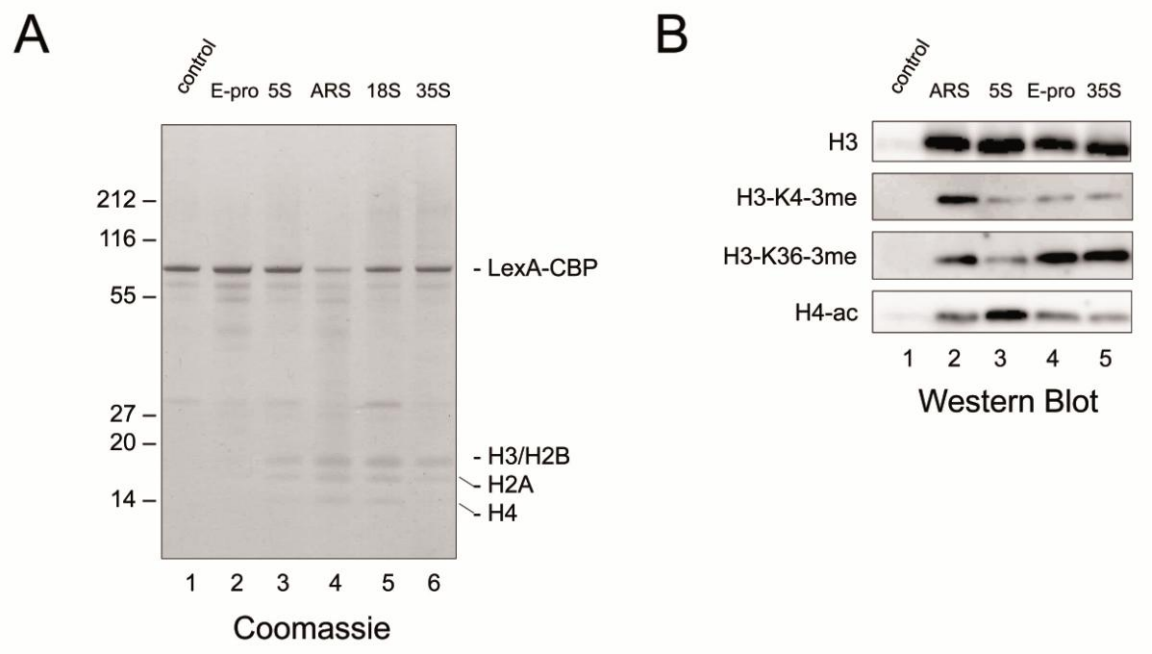

Figure 14 Protein analysis of affinity purified rDNA chromatin domains. A) Proteins associated with affinity purified rDNA circles from yeast strains y2378, y2384, y2379, y2383, y2380 and y2381 (the respective purified chromatin domain is indicated on top of each lane) were separated on a 4-12% NuPAGE Novex Bis-Tris precast gel (Invitrogen) and protein bands visualized by R250 Coomassie blue staining. Positions of marker proteins of a protein size marker are indicated on the left. Positions of the LexA-fusion protein after TEV protease cleavage (LexA-CBP) and histone proteins H3, H2B, H2A and H4 are indicated on the right. B) Western blot analysis of posttranslational modifications of histones associated with affinity purified rDNA circles. Histone proteins present in the respective chromatin preparation (indicated on top of each lane) were separated on a 18% SDS PAGE, transferred on a PVDF membrane and subjected to Western blot analysis with antibodies recognizing an unmodified peptide in the C-terminus of histone H3 (loading control), and the histone modifications H3-K4-3me, H3-K36-3me and acetylated lysine residues of histone H4 (H4-ac).

the E-pro region and the 35S rRNA gene were further subjected to Western Blot analyses (Figure 14B). An antibody raised against the unmodified C-terminus of histone H3 specifically detected similar amounts of the core histone in the chromatin preparations, but not in the control lane (Figure 14B, panel H3, compare lanes 2-5 with lane 1). Interestingly, using an antibody directed against a histone H3 tri-methyl lysine 4 peptide (H3-K4-3me) suggested that this modification is enriched in histone H3 co-purifying with the ARS domain (Figure 14B, panel H3-K4-3me, lane 2). This modification is generally associated with H3 at transcriptional start sites (Pokholok et al., 2005; Barski et al., 2007; Guillemette et al., 2011) and was recently shown to be enriched at DNA replication origins of *Arabidopsis thaliania* (Costas et al., 2011). Histone H3 tri-methylation of lysine 36 (H3-K36-me3) appeared to be enriched in histone molecules co-purifying with E-pro and 35S rRNA gene rings (Figure 14B, panel H3-K36-3me, lanes 4-5). This modification is found within the coding regions of actively transcribed genes (Krogan et al., 2003; Li et al., 2003). Finally, the level of acetylated residues of histone H4 is slightly increased in nucleosomes associated with 5S rRNA genes compared to the other regions within the rDNA locus (Figure 14B, panel H4-ac, compare lane 3 to lanes

2, 4, and 5). Histone H4 acetylation has been found at transcriptionally active somatic 5S rRNA genes in *Xenopus laevis in vivo*, and appears to facilitate binding of the Pol III transcription initiation factor TFIIIA (Howe et al., 1998; Vitolo et al., 2000).
Taken together, these findings show that histone molecules derived from the isolated ARS region, the 5S rRNA gene, the E-pro region and the 35S rRNA gene display differences in their posttranslational modification state.

The use of antibodies to detect specific histone modifications has important limitations because one single histone molecule might carry a multitude of different modifications. Due to the large number of potential modifications it is virtually impossible to raise specific antibodies for each individual combination. Moreover, many modification specific antibodies show a strong interference in epitope binding when combinations of modifications are present within a histone tail. Therefore, mass spectrometry provides a more direct and unbiased technique to study histone modifications. However, trypsin, a protease routinely used for identification of proteins by peptide mass fingerprints, cannot be used for in-gel digestions of histone proteins. Trypsin has a high specificity and hydrolyzes only the peptide bonds in which the carbonyl group is contributed either by an arginine or lysine residue. Histones are rich in lysine residues and most of the resulting tryptic peptides are too small for mass spectrometric identification. In order to circumvent this problem, the histone lysine residues can be derivatised by using propionic anhydride prior to treatment with trypsin (Smith et al., 2003; Taipale et al., 2005). The acid anhydride reacts very efficiently with unmodified or monomethylated ε-amino groups of lysine residues, thereby preventing the tryptic cleavage at the C-terminus of the modified residue. As di- and trimethylation or acetylation of the lysine ε-amino group also prevent the trypsin cleavage, trypsin only cleaves C-terminal of unmodified arginine residues. The resulting peptides are much larger and thus suitable for analysis by MALDI-TOF mass spectrometry (Villar-Garea and Imhof, 2006).
The amounts of histone molecules co-purifying with individual rDNA chromatin domains enabled the analysis of their posttranslational modification state. To this end rDNA chromatin domains containing the ARS, 5S rRNA gene, E-pro, and 18S rRNA coding sequence were purified as described above. A control purification of bulk histone molecules from a yeast strain lacking recombination sites and *LEXA* binding site cluster within the rDNA locus and expressing R recombinase and the LexA-TAP protein under the control of a bi-directional *GAL1-10* promoter was also included (see 3.1.2.2). The

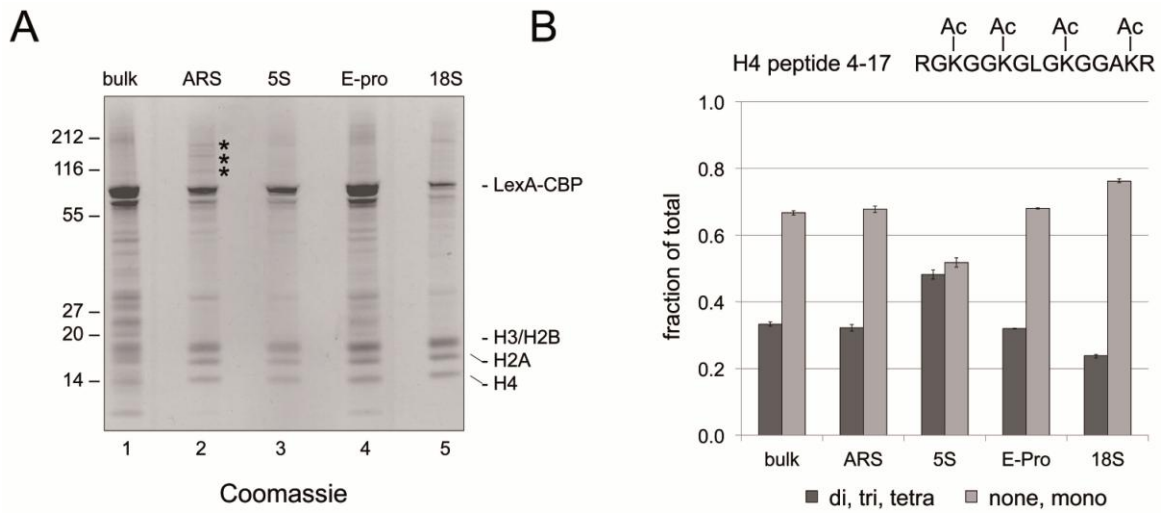

Figure 15 Analysis of posttranslational histone modifications by in-gel tryptic digestion and MALDI TOF/TOF mass spectrometry. A) After transformation of yeast strain y2124 with plasmid K929 and yeast strains y2267, y1997, y2268, y909 with plasmid K2049, the respective chromatin domain (indicated on top of each lane) was purified as described in the Materials and Methods section from each strain. Proteins associated with affinity purified rDNA circles or bulk chromatin were separated on a 4-12% NuPAGE Novex Bis-Tris precast gel (Invitrogen) and protein bands visualized by R250 Coomassie blue staining. Positions of marker proteins of a protein size marker are indicated on the left. Positions of the LexA-fusion protein after TEV protease cleavage (LexA-CBP) and histone proteins H3, H2B, H2A and H4 are indicated on the right. B) The protein bands corresponding to the histones H3/H2B, H2A and H4 were excised from the gel, the lysines within the histone molecules were derivatised with propionic anhydride, in-gel digested with trypsin and analysed by MALDI TOF/TOF mass spectrometry. The bar graph depicts the comparative quantitation of a histone H4 peptide from residues 4 to 17, which includes 4 lysines that are potentially acetylated. The relative amount of unmodified (none) and monoacetylated (mono) versions of the peptide was summed up and compared to the amount of di-, tri-, and tetraacetylated forms of the peptide. The peptide sequence and the potentially acetylated lysine residues are given on top of the graph.

galactose induced overexpression of the LexA-TAP fusion protein led to its non-specific binding to genomic chromatin fragments present in the cell extracts after lysis. These chromatin fragments further co-purified with the fusion protein. Proteins present in the different purifications were separated on an SDS-PAGE and stained with colloidal Coomassie Blue (Figure 15A). Bands corresponding to the individual histone proteins were excised from the gel. After in gel derivatization with propionic anhydride and digestion with trypsin, peptides were eluted and analyzed by MALDI-TOF/TOF analysis. As an example, Figure 15B summarizes the results obtained for histone H4 peptide 4-17 acetylation. In good agreement with the Western blot analysis, this histone modification was enriched in the preparation containing the purified 5S rRNA gene circle (compare quantitation in Figure 15B with Western blot in Figure 14B, panel H4-ac).

This result showed that the histone modification state at individual chromatin domains can be determined by mass spectrometry.

3.2.2 Specific non-histone chromatin components are selectively enriched in purifications of distinct rDNA domains

Samples of a control purification and purified chromatin domains including the E-pro region, the 5S rRNA gene, the ARS region, the 18S rRNA gene and the 35S rRNA gene were separated by SDS-PAGE and subjected to more sensitive silver staining to detect low abundant proteins in the purification. In good agreement with the previous analysis (see Figure 14), histone bands were not detected in the control purification indicating that these proteins are specifically enriched in the purified rDNA ring preparations (Figure 16A, compare lane 1 with lanes 2-6). Interestingly, silver staining also visualizes the DNA present in the different purifications (Figure 16A, bands in the high molecular weight

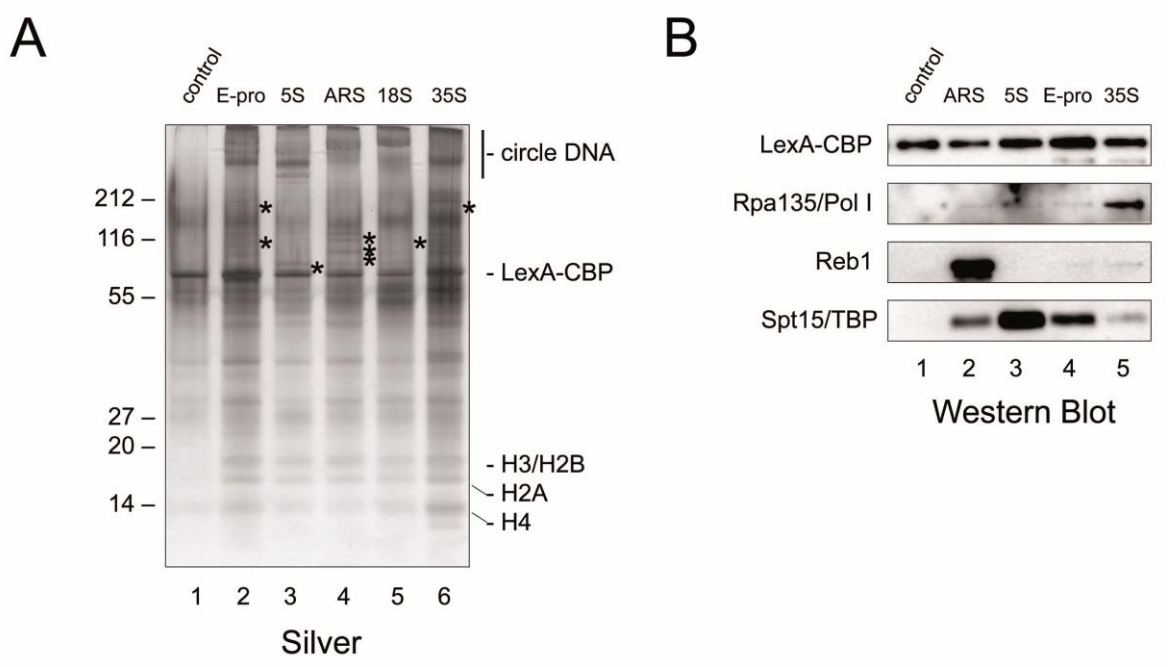

Figure 16 Protein analysis of affinity-purified rDNA chromatin domains reveals specific enrichment of distinct rDNA chromatin-associated proteins. A) Proteins associated with affinity purified rDNA circles from the yeast strains y2378, y2384, y2379, y2383, y2380 and y2381 (the respective chromatin domain is indicated on top of each lane) were separated on a 4-12% NuPAGE Novex Bis-Tris precast gel (Invitrogen) and protein bands visualized by Silver staining. Positions of marker proteins of a protein size marker are indicated on the left. Positions of the LexA-fusion protein after TEV protease cleavage (LexA-CBP), histone proteins H3, H2B, H2A and H4 and silver stained nucleic acids derived from chromatin circles (circle DNA) are indicated on the right. Selected protein bands that are specific to individual rDNA chromatin preparations and not present in the control purification are marked with an asterisk. B) Western blot analysis of specific rDNA chromatin components after affinity purification of distinct rDNA chromatin domains. Polypeptides present in the respective chromatin preparation (indicated on top of each lane) were separated on a 10% SDS PAGE, transferred to a PVDF membrane and subjected to Western blot analysis with antibodies recognizing the CBP moiety of the TAP-tagged LexA fusion protein (loading control), the Rpa135 subunit of Pol I, the Reb1 protein or the TATA-box binding protein (Spt15/TBP).

range marked as circle DNA on the right). Furthermore, silver staining revealed other specific protein bands present in each individual chromatin circle purification, but not in the control purification (Figure 16A, a selection of these bands is marked with asterisks), indicating that other non-histone rDNA chromatin components are co-purified with the distinct rDNA chromatin domains.

In order to address this possibility, samples of a control purification and purified chromatin domains including the ARS region, the 5S rRNA gene, the E-pro region and the 35S rRNA gene were further subjected to Western blot analyses with antibodies raised against some potential rDNA interaction partners (Figure 16B). Consistent with the results presented in Figure 14A, the analysis with an antibody recognizing the CBP moiety of the LexA fusion protein indicated similar amounts of the bait protein in all purifications (Figure 16B, panel LexA-CBP, lanes 1-5). An antibody directed against the second-largest subunit of Pol I, Rpa135, detected this protein specifically in the 35S rRNA gene purification (Figure 16B, panel Rpa135/Pol I, lane 5). Specific enrichment of the RNA polymerase I enhancer binding protein 1 (Reb1) in the purification of the ARS domain (Figure 16B, panel Reb1, lane 2) was also observed. Accordingly, the ARS containing rDNA circle is the only domain containing a Pol I promoter-proximal Reb1 binding site which supports robust Reb1 binding *in vivo* ((Kawauchi et al., 2008; Goetze et al., 2010; Reiter et al., 2012). The TATA binding protein (Spt15/TBP) was detected in all purifications containing rDNA domains (Figure 16B, panel Spt15/TBP). For the 35S rRNA and 5S rRNA genes which are transcribed by Pol I and Pol III, respectively, and the Pol II driven E-pro, this finding can be explained by the fact that TBP is involved in transcription initiation of all three RNA polymerases (Vannini and Cramer, 2012). Accordingly, TBP association with these loci *in vivo* has been previously reported (Merz et al., 2008, Goetze et al., 2010). A potential role for yeast TBP in replication has also been described (Lue and Kornberg, 1993; Stagljar et al., 1999), and TBP interaction with the ARS region is suggested by ChIP and ChEC experiments (data not shown). Interestingly, TBP appeared to be enriched in purified 5S rRNA gene chromatin preparations (Figure 16B, panel Spt15/TBP, lane 3). This observation might reflect earlier findings that Pol III genes have a high TBP occupancy when compared to other genomic locations *in vivo* (Roberts et al., 2003).

These findings indicate that, besides the histones as the prominent proteins enriched in the rDNA chromatin preparations (Figure 14A), other potential rDNA chromatin interacting proteins are co-purified with chromatin circles derived from distinct regions of the rDNA locus. Western blot analysis confirms that some known rDNA chromatin components stay associated to the chromatin rings during the purification procedure.

3.2.3 Comparative mass spectrometry reveals distinct proteomes for individual rDNA chromatin domains

3.2.3.1 Strategy for semiquantitative comparative analysis of rDNA chromatin composition using the iTRAQ technology

In order to investigate the composition of purified rDNA chromatin domains in an unbiased, antibody independent manner, mass spectrometry and the isobaric tag for relative and absolute quantitation (iTRAQ) technology was used (Ross et al., 2004; Zieske, 2006). Protein samples derived from control and chromatin ring purifications were digested with trypsin and the resulting peptides were separately labeled using two different isotopic iTRAQ reagents. These reagents consist of an amine reactive group which reacts with N-terminal amino groups and ε-amino groups of lysine residues. The two differentially labeled samples are combined and the mixture of peptides is separated

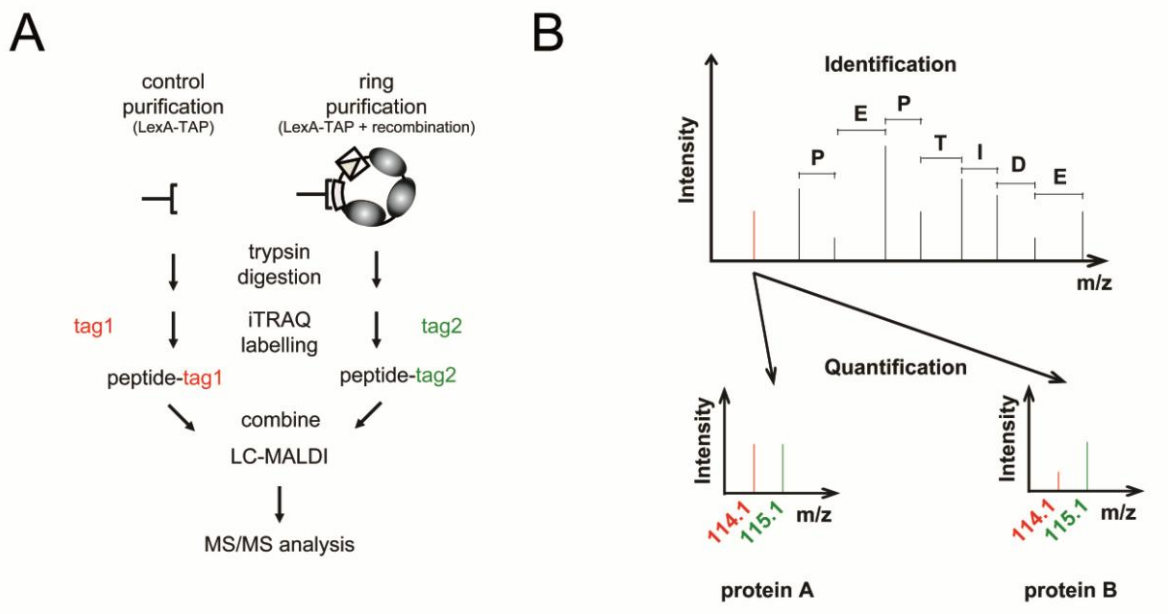

Figure 17 Schematic representation of the iTRAQ strategy for the proteomic analysis of rDNA chromatin domains. A) Workflow of the comparative mass spectrometry approach. Proteins co-purified with LexA-TAP (bracket connected to a line) in the control strain carrying an rDNA locus without recombination elements and the different chromatin circle strains are digested with trypsin and the resulting peptides are labeled with two different iTRAQ reagents (tag 1 and tag 2). The differentially labeled peptides are combined and analyzed by MALDI TOF/TOF mass spectrometry. B) Representative MS/MS spectrum of a selected PEPTIDE after analysis of iTRAQ samples. In the MS/MS mode, selected peptides are fragmented by collision with gas molecules (collision induced dissociation). The fragmentation results in different peptide fragments (P, E, P, T, I, D, E), which are used for identification of the respective PEPTIDE by MASCOT database search. The peptide fragments from both samples have an equal m/z and sum up to one signal peak. However, the reporter ions are released from the peptides and exhibit different masses representing the two samples. The area of each reporter ion peak is used for quantitation. In the two examples shown, protein A is equally present in both the control and the circle purification (resulting in a tag2 to tag1 iTRAQ ratio of 1), while the reporter ion of protein B shows a strong increase in the circle purification compared to the control purification (resulting in a tag2 to tag1 iTRAQ ratio greater than 1). The molecular masses of the reporter ions derived from tag1 (red) and tag2 (green) label the x-axis in the graphs on the bottom.

by nano-flow reversed phase chromatography following analysis by MALDI-TOF/TOF mass spectrometry (see Figure 17A for a schematic representation of the workflow). The isobaric labeling allows the relative quantification of peptides present in the two different samples based on ratios of reporter ions in the low m/z region of the resulting MS/MS spectra (see Figure 17B for a cartoon of a representative MS/MS spectrum).

3.2.3.2 Comparative analysis of proteins co-purifying with LexA-TAP from strains with and without recombined rDNA chromatin domains

In the following, the relative abundance of peptides in three independent biological replicates of the individual rDNA domain purifications each compared to a separate control purification was determined (Figure 18). It was possible to define distinct proteomes co-purifying with the four segments of the rDNA locus: the ARS region, the 5S rRNA gene, the E-pro region and the 35S rRNA gene. The identified proteins were classified in eight different groups according to their biological function. For each group the relative fraction of identified peptides present in the respective rDNA domain purification was calculated and is depicted in Figure 18A. In all purifications, a similar fraction of peptides of housekeeping proteins and ribosomal proteins (36%-43%) was detected. Peptides from proteins belonging to these groups had very similar iTRAQ ratios and were considered as background contaminants after the single step affinity purification. The average iTRAQ ratio of these two groups was subsequently used for normalization (see below). Peptides from proteins involved in chromatin/transcription (including RNA polymerases), replication and ribosome biogenesis were clearly overrepresented with regard to their abundance in the yeast proteome. There was also a substantial fraction of proteins with still unknown functions identified in these analyses (Figure 18A).

The iTRAQ ratios of all identified proteins were divided by the average iTRAQ ratio of housekeeping proteins and ribosomal proteins for each single comparison of control and circle purification. After this normalization, the average iTRAQ ratios of the replicate purifications were calculated and plotted against the total number of peptides identified in the replicate experiments (Figure 18B, graphs ARS, 5S, E-pro, 35S). In this graphical representation, the groups of housekeeping proteins and ribosomal proteins form a cluster in the center in each of the diagrams (Figure 18B, light gray squares and gray diamonds in all graphs). The four canonical histones were detected with a large number of peptides and with a high iTRAQ ratio arguing for a strong enrichment of these proteins in comparison to the control purification. This is consistent with their abundance in the different rDNA chromatin purifications (Figure 14A, Figure 15A, and Figure 16A).

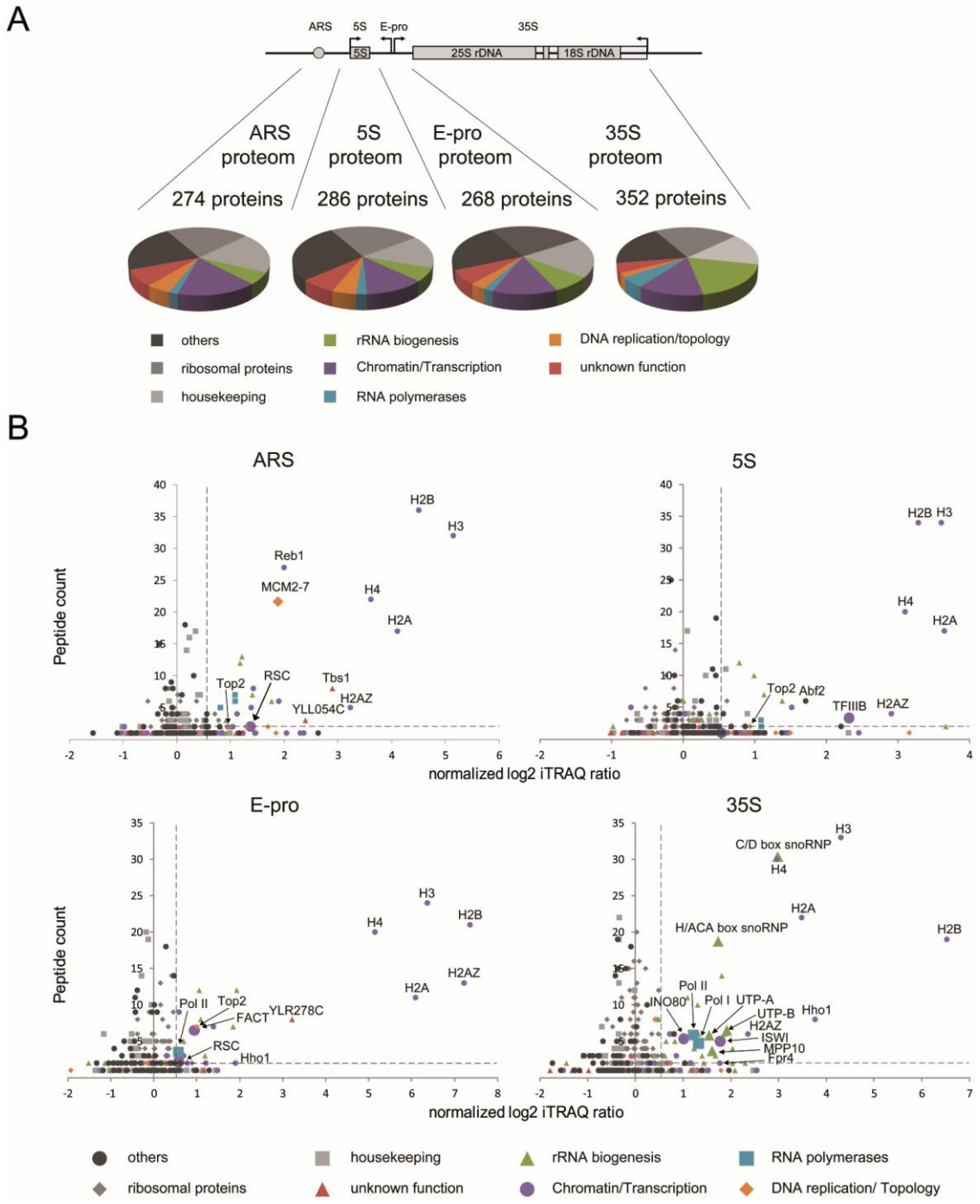

Figure 18 Proteome analysis of affinity purified rDNA chromatin domains. A) Proteins co-purifying with ARS, 5S, E-pro or 35S rDNA chromatin domains were subjected to comparative iTRAQ analysis with the proteins co-purified in the control strain. Identified proteins were categorized in 8 different groups according to their biological function. The pie charts depict the relative abundance of peptides of each group as the fraction of the total peptides identified in the analysis and summarize the results of three independent biological replicates for each individual rDNA domain. B) The iTRAQ ratios of individual circle versus control purifications for ARS, 5S, E-pro and 35S rDNA domain were divided through the median iTRAQ ratio of proteins belonging to the group of ribosomal proteins and housekeeping proteins in order to correct the ratios to similar enrichment of background contaminants. The average iTRAQ ratio of identified proteins was calculated from three independent replicates of each domain and plotted against the total number of identified iTRAQ labeled peptides of all replicate comparisons (smaller icons). If more than 50% of the components of a multi-protein complex were identified in the analysis, the average iTRAQ ratio and average peptide count of the respective uniqe complex components was calculated and plotted accordingly (larger icons). Only proteins/complexes which have been identified with an average iTRAQ ratio of at least 1.5 and with a (average) peptide count greater than 1 (indicated by dashed lines in the graphs) were considered as enriched in these analysis and are labeled in the graphs. Note the log2 scale of the x-axis.

Consequently, these proteins cluster within the upper-right corner of all graphs (Figure 18B, H2A, H2B, H3, H4 in all graphs). The yeast homolog of the vertebrate histone variant H2A.Z, Htz1, was also identified in all chromatin preparations of the different subdomains of the rDNA locus. Interestingly, the yeast homolog of the vertebrate linker histone H1,

Hho1, for which a role in 35S rRNA gene chromatin has been described in the past (Freidkin and Katcoff, 2001; Levy et al., 2008), appeared to be enriched in the 35S rRNA gene circle preparations (Figure 18B, graph 35S). Hho1 was not identified in ARS chromatin preparations.

Topoisomerase II (Top2), a protein which has been suggested to have roles in the nucleolus and in particular in RNA Pol I transcription (reviewed in (Drygin et al., 2010)) was identified in all rDNA chromatin preparations (Figure 18B, graph 35S).
In the proteome co-purifying with the ARS domain, all subunits of the hexameric MCM2-7 complex, the putative replicative helicase involved in both initiation and elongation steps of eukaryotic DNA replication (reviewed in Costa and Onesti, 2008), were identified with a large peptide count and positive iTRAQ ratio in comparison to the control purification (Figure 18B, graph ARS, Table 1). Additionally, Reb1 was identified with multiple peptides and a high average iTRAQ ratio consistent with the results of the Western blot analysis (Figure 16B, panel Reb1, lane 2). Interestingly, 10 out of 17 subunits of the Remodel the Structure of Chromatin (RSC) chromatin remodeling complex were detected in the proteome of the ARS chromatin ring (Figure 18B, graph ARS, Table 1). Furthermore, two proteins of unknown function, Tbs1 and Yll054c were significantly enriched in some of the ARS purifications (Figure 18B, graph ARS, Table 1).
In the proteome co-purifying with the 5S rRNA gene circle, the Pol III specific initiation complex TFIIIB (Bdp1, Brf1 and Spt15/TBP) were identified (Figure 18B, graph 5S, Table 1). Additionally, 2 out of 6 subunits of the TFIIIC complex (Tfc4 and Tfc7) were specifically detected in the 5S rRNA gene ring purification but did not meet our criteria to include the complex in Figure 18B or Table 1. Again, the observed enrichment of TBP was in good agreement with the results of the Western blot analysis (Figure 16B, panel Spt15/TBP, lane 3). A homolog of the vertebrate HMG1 and HMG2 proteins, Abf2, which was originally identified as ARS1 binding factor 2 and is predominantly localized to mitochondria being involved in maintenance of mitochondrial DNA ((Diffley and Stillman, 1991) was also enriched in these purifications (Figure 18B, graph 5S, Table 1).
Consistent with the function of E-pro as a bidirectional Pol II dependent promoter (Kobayashi and Ganley, 2005), several Pol II subunits were specifically identified in the E-pro proteome, but did not meet our criteria (except Rpo21) to include the complex in Figure 18B graph E-pro or Table 1. This purification further contained Spt16 and Pob3,

Table 1 Protein complexes/factors specifically enriched in three replicates of different rDNA chromatin preparations.

Only proteins with an average iTRAQ ratio of at least 1.5, identified with at least 2 peptides are depicted. If at least 50% of multi-protein complex components were identified, identified subunits are underlined and additional proteins are depicted which

* are identified with an average iTRAQ ratio of at least 1.5 and one peptide

** are identified with an average iTRAQ ratio greater than one and at least two peptides

		domain			
Biological function	**Enriched proteins/ complexes**	**ARS**	**5S**	**E-pro**	**35S**
Histones		H2A, H2B, H3, H4, H2AZ	H2A, H2B, H3, H4, H2AZ	H2A, H2B, H3, H4, H2AZ, Hho1	H2A, H2B, H3, H4, H2AZ, Hho1
DNA replication/ topology	MCM2-7 complex	Mcm2, Mcm3, Mcm4, Mcm5, Mcm6, Mcm7			Mcm6*
	Topoiso-merase	Top2	Top2	Top2	Top2**
	others	Smc5, Smc6			Smc5, Smc6*
Chromatin remodeling	RSC complex	Htl1*, Npl6*, Rsc1*, Rsc58*, Rsc6, Rsc8, Sfh1, Sth1, Arp7*, Act1**		Rsc58, Rsc6, Rsc8	Rsc8
	ISW1 complex	Isw1, Ioc2			Isw1, Ioc2**, Ioc3*
	INO80 complex	Rvb1, Rvb2, Arp4	Rvb2	Ies3, Rvb1, Rvb2	Ino80, Ies1**, Ies2*, Ies3*, Rvb1, Rvb2, Arp4, Arp8**
Transcription factors/ complexes	FACT	Pob3		Spt16, Pob3	
	TFIIIB		Bdp1, Brf1*, Spt15		
	others	Reb1, Stb4, Spt5, Hal9			
RNA Polymerases	Pol I				Rpa190, Rpa135, Rpa49, Rpa34, Rpa12
	Pol II	Rpo21, Rpb2	Rpo21	Rpo21	Rpo21, Rpb2, Rpb3**, Rpb4
	common Pol I/Pol III				Rpc19*, Rpc40
	common all	Rpo26	Rpo26		Rpb5, Rpb8, Rpo26, Rpb10
rRNA biogenesis	UTP-A/ t-UTP				Nan1, Utp4, Utp5, Utp8, Utp9, Utp10, Utp15
	UTP-B/ Pwp2				Utp6, Utp13, Utp21
	MPP10				Mpp10, Imp3, Imp4
	C/D box	Nop1, Nop56, Nop58,	Nop1, Nop56, Nop58,	Nop1, Nop56, Nop58,	Nop1, Nop56, Nop58,

	snoRNP	Snu13	Snu13	Snu13	Snu13, Rrp9
	H/ACA box snoRNP	Cbf5, Gar1, Nhp2		Cbf5, Gar1	Cbf5, Gar1, Nhp2, Nop10
	others		Dbp10		Bfr2, Emg1, Enp1, Kre33, Krr1, Prp43, Rok1, Sof1, Bud21, Dip2, Nop14, Utp22, Dbp10, Ebp2, Erb1, Has1, Nop12, Nop6, Rrp5, Rrs1, Srp40
Unknown function		Tbs1, Yll054c	Ylr241w	Ylr278c	
Others		Rpl40a, Yku80	Dnl4, Lat1, Abf2, Vps1, Crn1	Rpp1a, Pab1, Hsl1, Sum1	Fpr3, Tif2, Fpr4, Pab1, Yra1, Sum1, Yhb1, Mss116

two subunits of the Facilitate Chromatin Transcription (FACT) complex (Figure 18B, graph E-pro, Table 1). Another protein of unknown function, Ylr278c was enriched in the E-pro proteome (Figure 18B, graph E-pro, Table 1).

The largest proteome with a total of 352 proteins co-purified with the 35S rRNA gene circle (Figure 18A). Among these proteins, 11 out of 14 subunits of Pol I were identified (Figure 18B, graph 35S, Table 1). Moreover, Rrn5 a component of the Pol I specific initiation complex UAF of very low abundance was identified in one analysis but with only one peptide. Strikingly, 8 of the 12 subunits of Pol II were identified in these purifications (Figure 18B, graph 35S, Table 1). Pol II has been described to transcribe the 35S rRNA gene region in some situations in yeast (Conrad-Webb and Butow, 1995; Vu et al., 1999; Siddiqi et al., 2001; Cioci et al., 2003; Goetze et al., 2010), and in vertebrates (Gagnon-Kugler et al., 2009). Three out of four subunits of the chromatin remodeling complex ISW1 were also found to be enriched in 35S rRNA gene chromatin (Figure 18B, graph 35S, Table 1), in accordance with the reported interaction of ISW1 with the 35S rRNA gene *in vivo* (Jones et al., 2007; Mueller and Bryk, 2007). Notably, all subunits of the INO80 remodeling complex were also detected in the 35S chromatin preparations (Figure 18B, graph 35S, Table 1). The 35S proteome revealed strong enrichment of components of the SSU processome including subunits of the UTP-A/t-UTP, UTP-B/Pwp2 and MPP10 submodules. In addition, a large set of other 90S preribosome and U3 snoRNP components, as well as constituents of the H/ACA box and CD box snoRNPs were identified in this type of analysis (Figure 18B, graph 35S, Table 1). These proteins are thought to bind co-transcriptionally to the nascent rRNA chains during Pol I transcription (Mougey et al., 1993; Osheim et al., 2004; Wery et al., 2009, Hierlmeier et al., 2012). This suggests that the co-transcriptional assembly of rRNA biogenesis factors

on nascent transcripts extending Pol I trapped in elongation is preserved upon affinity purification.

In summary, these analyses show that distinct proteomes co-purify with defined chromosomal domains of the yeast rDNA locus. For many of the identified factors *in vivo* interaction with the respective domain has already been reported, validating the approach to isolate native chromatin. There is also good evidence that even large ribonucleoprotein complexes (RNPs) which presumably represent co-transcriptional assembly intermediates with nascent transcripts can be isolated with this method. Interestingly, distinct chromatin remodeling complexes were shown to be associated with specific rDNA domains, indicating that these complexes are recruited to special features of the respective domain, as for example histone modifications, other chromatin components, or DNA sequence elements. Finally, some proteins of unknown function were also identified in these purifications, which may be components of the individual chromatin domains *in vivo* (see below).

3.3 Selected complexes and factors identified by the proteome analysis interact with rDNA chromatin *in vivo*

In order to verify interaction of some of the factors identified in the native chromatin peparations with the rDNA *in vivo,* Chromatin Endogenous Cleavage (ChEC) analysis was performed (Schmid et al., 2004). To this end, yeast strains were created expressing the respective factors in fusion with micrococcal nuclease (MNase) from their endogenous chromosomal location. After crosslinking the cells with formaldehyde, nuclei were prepared and calcium was added to induce cleavage by the MNase fusion proteins in the proximity of their respective DNA-binding sites. After DNA isolation, specific cleavage events can be mapped with high precision to the DNA sequence by indirect end-labeling Southern blot analysis (Figure 19).

Two chromatin remodeling complexes, INO80 and ISW1, were specifically identified in 35S rRNA gene chromatin preparations (see above). Whereas interaction of the ISW1 complex with the rDNA locus had previously been observed (Jones et al., 2007), the INO80 complex had not yet been reported to associate with this genomic region. We performed ChEC analyses with yeast strains expressing MNase fusion proteins of ISW1 components, Isw1 and Ioc4, as well as INO80 components, Ies1, Ies4, Arp4, and Taf14 (Figure 19A and B, lanes 1-30). For all of the different components tested, we observed calcium dependent cleavage within the Pol I promoter region and in the 35S rRNA

coding sequence (Figure 19A, lanes 1-30, cleavage sites in the promoter region are labeled with asterisks on the right). Notably, the cleavage mediated by MNase fusion proteins of the ISW1 component Ioc4 and of the INO80 component Taf14 was very weak (Figure 19A, lanes 16-20 and 26-30). It is important to mention that Taf14 is a component of a number of different complexes, including mediator, transcription factor TFIID, the nucleosomal histone H3 acetyltransferase (NuA3), INO80 and also SWI/SNF.

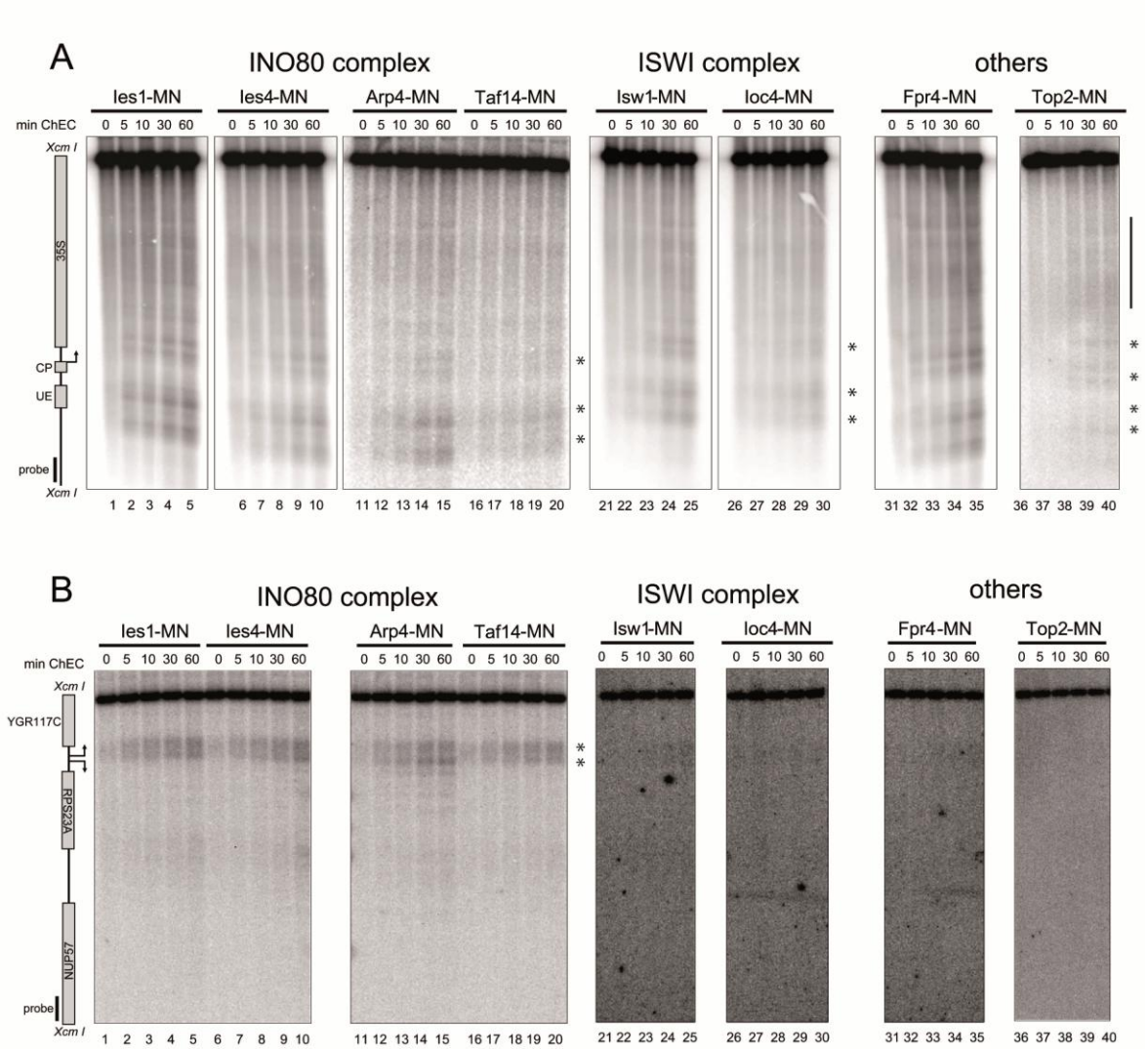

Figure 19 Selected complexes and factors identified by mass spectrometry interact with rDNA chromatin *in vivo*. A-B) ChEC analysis with yeast strains y2157 (Ies1-MN), y2158 (Ies4-MN), y2159 (Arp4-MN), y2160 (Taf14-MN), y2259 (Isw1-MN), y2260 (Ioc4-MN), y2258 (Fpr4-MN) and y2264 (Top2-MN) expressing Isw1, Ioc4, Ies1, Ies4, Arp4, Taf14, Fpr4 or Top2 as MNase fusion proteins from their endogenous chromosomal location. Yeast strains were grown at 30°C in YPD to exponential phase and crosslinked with formaldehyde. Nuclei were prepared and incubated in the absence (0 min ChEC) or presence of calcium for the times indicated on top of each panel (5, 10, 30, 60 min ChEC). DNA was isolated, digested with the restriction enzyme endonuclease *Xcm*I and subjected to indirect endlabeling Southern blot analysis with radioactively labeled probes rDNp (A) or NUP57 (B). Cartoons of the genomic regions analyzed in the different experiments are depicted on the left. Asterisks and black bars on the right label specific MN-fusion protein mediated cleavage events as detailed in the text.

Moreover, Arp4 is a shared subunit of the INO80, NuA4 histone acetyltransferase and Swr1 complexes. However, other complex-specific subunits of these chromatin-modifying and transcription initiation complexes were not specifically enriched in the 35S rRNA gene ring purifications. This result suggests that Taf14 and Arp4 interact with 35S rRNA gene chromatin as components of the INO80 complex. As a control for specificity of MNase fusion protein mediated cleavage events, the Southern blot membrane was also hybridized with a probe recognizing the coding sequence of the NUP57 gene on chromosome VII (Figure 19B). For MNase fusion proteins of the ISW1 components, Isw1 and Ioc4, cleavage at this genomic location was almost undetectable (Figure 19B, lanes 21-30). MNase fusion proteins of INO80 complex components instead showed specific cleavage at an intergenic region containing divergent promoters for the *RPS23A* and the *YGR117C* genes (Figure 19B, lanes 1-20), suggesting that INO80 might influence chromatin structure at this location.

ChEC experiments were also performed in yeast strains expressing MNase fusion proteins of Fpr4 for which rDNA association had been demonstrated in ChIP experiments (Kuzuhara and Horikoshi, 2004) and Topoisomerase 2 (Top2) for which no direct interaction with rDNA *in vivo* had been so far reported. Specific cleavage events were observed at the Pol I promoter and in the 35S rRNA coding sequence (Figure 19A, lanes 31-40, cleavage events within are labeled with asterisks and a black bar on the right). Cleavage of these factors was low within the region of chromosome VII detected with the probe recognizing the *NUP57* gene (Figure 19B, lanes 31-40).

Three proteins without annotated function, Tbs1, Yll054c as well as Ylr278c, were specifically and strongly enriched in ARS and E-pro domain purifications, respectively (see Figure 18B, graphs ARS and E-pro, Table 1). Interestingly, all three proteins bear an N-terminal Zn-finger domain and share predicted structural homology to the centromere-binding protein Cep3 (see Figure 20A for a schematic representation, http://toolkit.tuebingen.mpg.de/hhpred). In ChEC experiments with strains expressing the respective factors as MNase fusion proteins, Yll054c-MNase mediated cleavage could not be observed within the intergenic spacer region of the rDNA, (Figure 20B Yll054c-MN, lanes 1-5), which does not support (although cannot exclude) that the protein is a component of rDNA chromatin *in vivo*. However, two weak Tbs1-MNase induced cleavage events were observed within the region of the ribosomal autonomous replication sequence (Figure 20B Tbs1-MN, lanes 6-10, cleavage event within the region marked by asterisks on the right). One of these cleavage sites (upper asterisk) appears to be hypersensitive producing a low abundant fragment even in the absence of calcium-

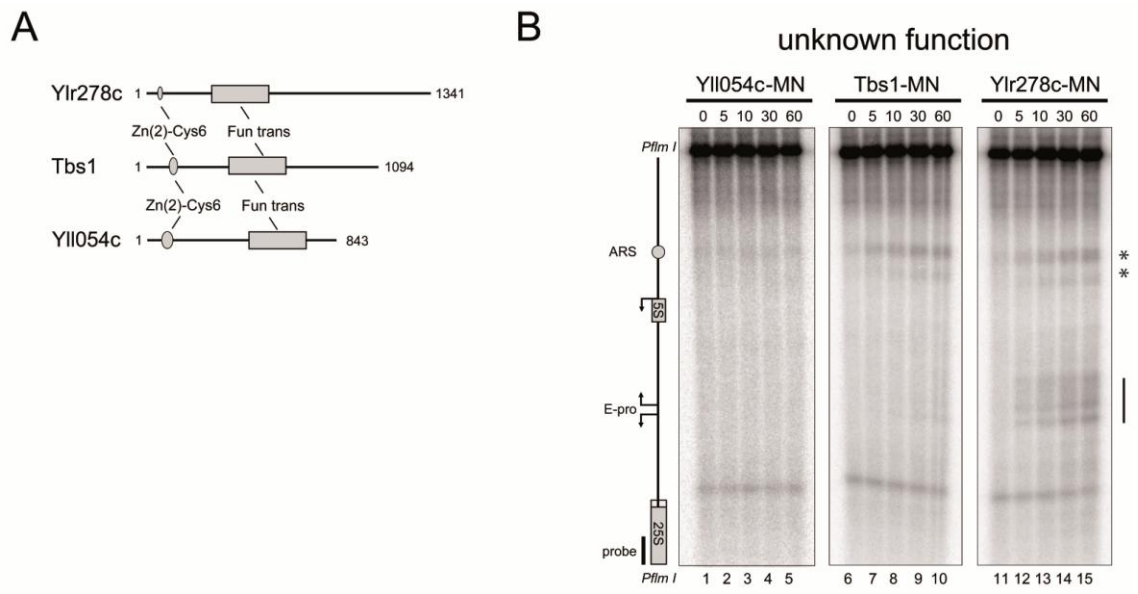

Figure 20 Tbs1 and Ylr278c proteins are associated with ARS and E-pro regions of the rDNA locus *in vivo*. A) Schematic representation of structural motifs within the amino acid sequence of Ylr278c, Tbs1 and Yll054c. The positions of a Zn(2)-Cys6 finger domain shared by all 3 proteins and a region sharing structural homology with a domain of centromere protein 3 (Cep3, fun-trans) are depicted as grey circles and grey boxes, respectively. B) Yeast strains y2707, y2633 and y2634 expressing Yll054c, Tbs1 or Ylr278c as a MNase fusion protein (Yll054c-MN, Tbs1-MN, Ylr278c-MN) were cultured and treated with formaldehyde as described (Figure 19). ChEC was performed with crude nuclei in the absence and presence of calcium for the indicated times. DNA was isolated, digested with the restriction enzyme endonuclease *Pfl*MI and analyzed in a Southern blot by indirect end labelling with the probe rDNA_IGS. A cartoon of the genomic region analyzed, including the positions of the 25S, ARS, 5S and E-pro regions, is depicted on the left. Two asterisks and a black line on the right label Tbs1-MN or Ylr278c-MN mediated cleavage events at the ARS and E-pro regions of the IGS region of the rDNA locus.

mediated cleavage in all ChEC experiments (Figure 20B Yll054c-MN, Tbs1-MN, and Ylr278c-MN, lanes 1, 6, and 11, cleavage event marked by the upper asterisk on the right). We note also a very faint Tbs1-MNase mediated cleavage event in the E-pro containing region (Figure 20B Tbs1-MN, cleavage event within the region marked by a black bar on the right). As for Tbs1-MNase, Ylr278c-MNase showed a weak cleavage pattern within the ARS region (Figure 20B Ylr278c-MN, cleavage event within the region marked by asterisks on the left). However, ChEC analysis with Ylr278c-MNase expressing strains led to stronger cutting events within the E-pro region (Figure 20B Ylr278c-MN, cleavage event within the region marked by a black bar on the left).

Although, rDNA interaction of Yll054c, identified in the ARS domain purification, could not be validated by this approach, we provide evidence for new rDNA *in vivo* interactions for the INO80 complex, Top2, Tbs1 and Ylr278c in good correlation with the finding that these proteins were identified in the MS-analyses with either the 35S, ARS or E-pro domains (Figure 18B graphs ARS and E-pro, Table 1). This indicates that the purification approach may be useful for the unbiased identification of protein-chromatin *in vivo* interactions.

3.4 Important structural and conformational chromatin features of specific rDNA chromatin domains are conserved upon isolation

3.4.1 Gel filtration analysis of the circular 5S rDNA and E-pro region suggests structural differences

Besides providing insights in histone modification state and protein composition of native chromatin, the purification strategy is amenable to structural and conformational analysis of the isolated domains. Gel filtration analysis of native *PHO5* promoter chromatin circles was previously reported to partially separate chromatin circles in correlation with the number of nucleosomes associated with the circular DNA molecules (Griesenbeck et al., 2003). Isolated *PHO5* promoter chromatin circles from yeast strains repressed in *PHO5* expression are decorated with ~3 nucleosomes, whereas activated *PHO5* promoter circles are (on average) associated with only one nucleosome (Boeger et al., 2003). Accordingly, gel filtration analysis of activated and repressed *PHO5* promoter circles showed overlapping, but distinct elution profiles from the column, with peaks in fractions 4 and 7, respectively (see Figure 5A in (Griesenbeck et al., 2003), Figure 3 (Boeger et al., 2008) and Figure 21A and B, panels *PHO5*). The *PHO5* promoter circle has a size of ~ 0.8kb, which is very similar to the size of E-pro (~ 0.7kb) and 5S rDNA (~ 0.8kb) chromatin circles after recombination. Thus, gel filtration experiments were performed with the different rDNA chromatin circles and the *PHO5* repressed and activated promoter circle and the resulting elution profiles were compared (Figure 21). Interestingly, the E-pro chromatin circle showed a similar gel filtration profile as the activated *PHO5* promoter circle (Figure 21A, compare panel E-pro with panel *PHO5* activated and Figure 21B, compare light grey squares in panel rDNA with light grey squares in panel *PHO5*), indicating that this chromatin circle with a size of 0.7kb has a similar nucleosome-depleted configuration as the *PHO5* promoter circle under activating conditions. This result is consistent with the SDS-PAGE analysis of affinity purified rDNA chromatin domains presented in Figure 14A where only a slight enrichment of histone molecules was observed when a E-pro purification was compared to a control purification (Figure 14A, compare lane 2 with lane 1).

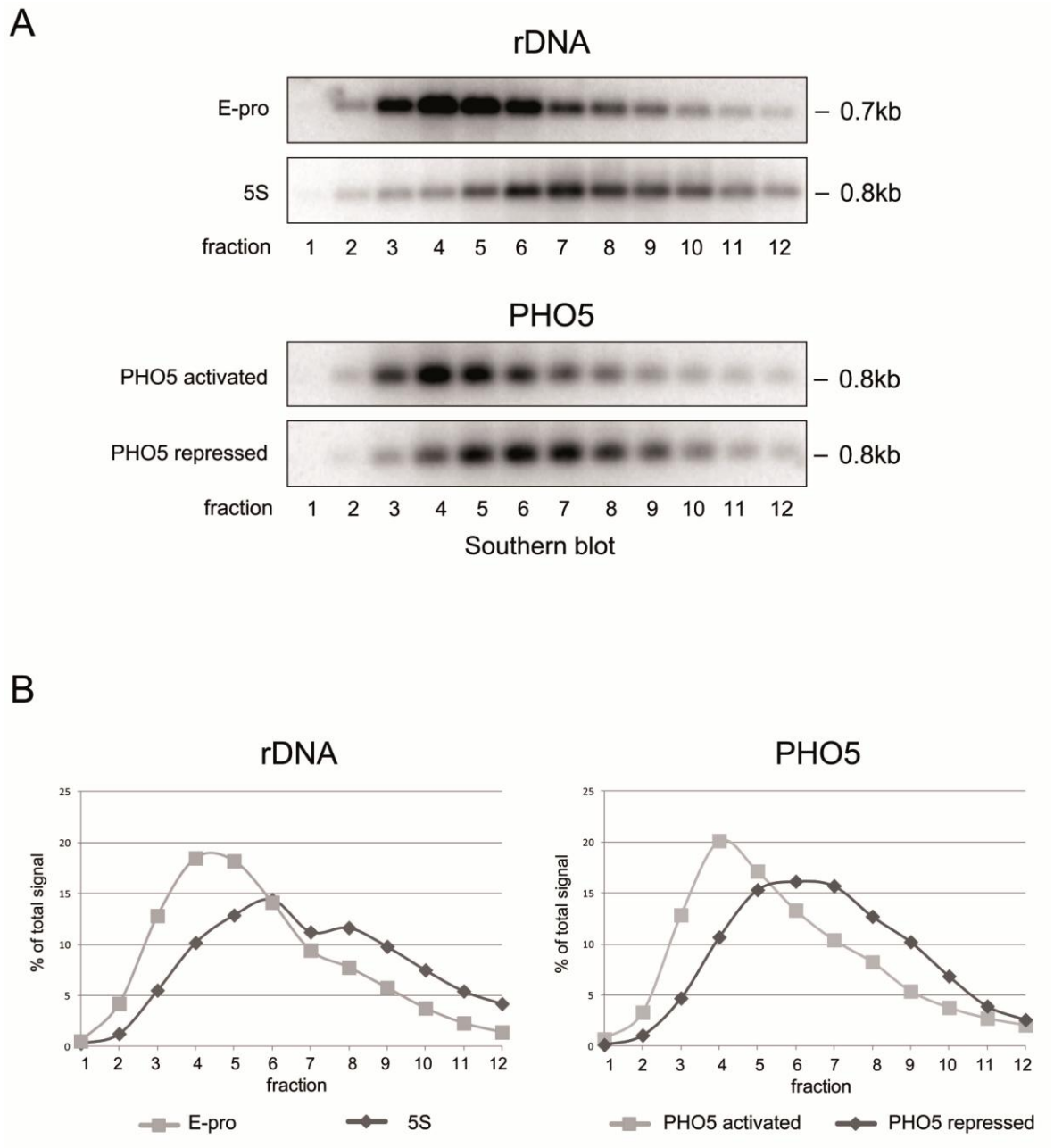

Figure 21 Gel filtration analysis of distinct chromatin circles indicates differences in the average number of associated nucleosomes. (A) Gel filtration of E-pro and 5S rDNA chromatin circles in comparison to activated and repressed *PHO5* promoter chromatin circles. rDNA chromatin circles isolated from yeast strains y2268 (E-pro), y1997 (5S), and *PHO5* promoter chromatin circles activated and repressed in *PHO5* expression isolated from yeast strains yM30.3 and yM64.1 were transformed with plasmid K355 for inducible expression of R recombinase in the absence of the recombinant LexA-TAP molecule. The chromatin circles were partially purified by differential centrifugation as described in (Griesenbeck et al., 2003; Boeger et al., 2008). A TSK-G4000SW column was used to fractionate rDNA and *PHO5* promoter circles from the individual preparations. DNA eluting in different fractions (1 to 12) from the column was extracted, linearized with NcoI and subjected to 1% agarose gel electrophoresis, and analyzed by blot hybridization with different probes detecting the E-pro, 5S or *PHO5* promoter regions. The size of the analyzed chromatin circle is indicated on the right of each panel. B) The percentage of total radioactivity of each fraction was calculated and plotted for each gel filtration experiment on the ordinate. The numbers of the fractions are indicated on the abscissa.

The gel filtration profile of 5S rRNA gene containing chromatin circles showed a broad distribution with peaks in fractions 6 and 8 (Figure 21A, panel 5S and Figure 21B, grey

diamonds in panel rDNA). The pattern was similar, but not identical, to the observed profile of repressed *PHO5* promoter circles (Figure 21B, compare grey diamonds in panel rDNA with grey diamonds in panel *PHO5*). The heterogenous gel filtration profile of 5S rRNA gene chromatin circles might be explained by multiple, alternative nucleosome configurations and/or chromatin states at the 5S rRNA gene containing region of rDNA chromatin (see below).

3.4.2 Single molecule electron microscopic analysis of 5S rRNA gene circles suggests a heterogeneous population of different chromatin states

The gel filtration analysis of 5S rRNA gene containing chromatin circles indicated heterogeneity in the shape of the chromatin domain which might reflect variable nucleosome numbers or configurations on individual molecules. To investigate this possibility, we tried to map nucleosome positions on individual 5S circles using a previously published technique (Cech and Pardue, 1977; Cech et al., 1977). Isolated 5S rRNA gene circles were crosslinked with psoralen. As mentioned in the introduction, psoralen intercalates into double-stranded nucleic acids and establishes covalent crosslinks between the two DNA strands upon irradiation with long wave UV light. DNA assembled into a nucleosome is protected from psoralen incorporation leaving a “footprint” of the nucleosome of around 150bp of uncrosslinked DNA flanked by crosslinked linker regions (see Figure 22A for a schematic representation). DNA isolated from psoralen treated 5S rRNA gene rings was spread onto carbon-coated copper grids under denaturing conditions and analyzed by electron microscopy. In the resulting electron micrographs, denatured 5S rRNA gene circle DNA was visualized as circular molecules with single-stranded DNA bubbles (see Figure 22A, representative electron micrograph on the right). Length measurements of the single stranded DNA stretches indicated that these positions have presumably been occupied by nucleosome core particles in the chromatin ring (Figure 22A, 150bp scale to approximately 50nm). We observed a high heterogeneity in the number of bubbles associated with individual 5S rRNA gene circles (data not shown, see below).

In order to align the positions of the observed single-stranded DNA bubbles with respect to the 5S rRNA gene sequence present on the molecules, the DNA had to be linearized. Therefore, purified psoralen crosslinked 5S circle DNA was subjected to digestion with the restriction enzyme *Nco*I. *Nco*I has a single restriction site and cuts the circular DNA such that the 5S rRNA coding sequence is located in the center of the resulting linear

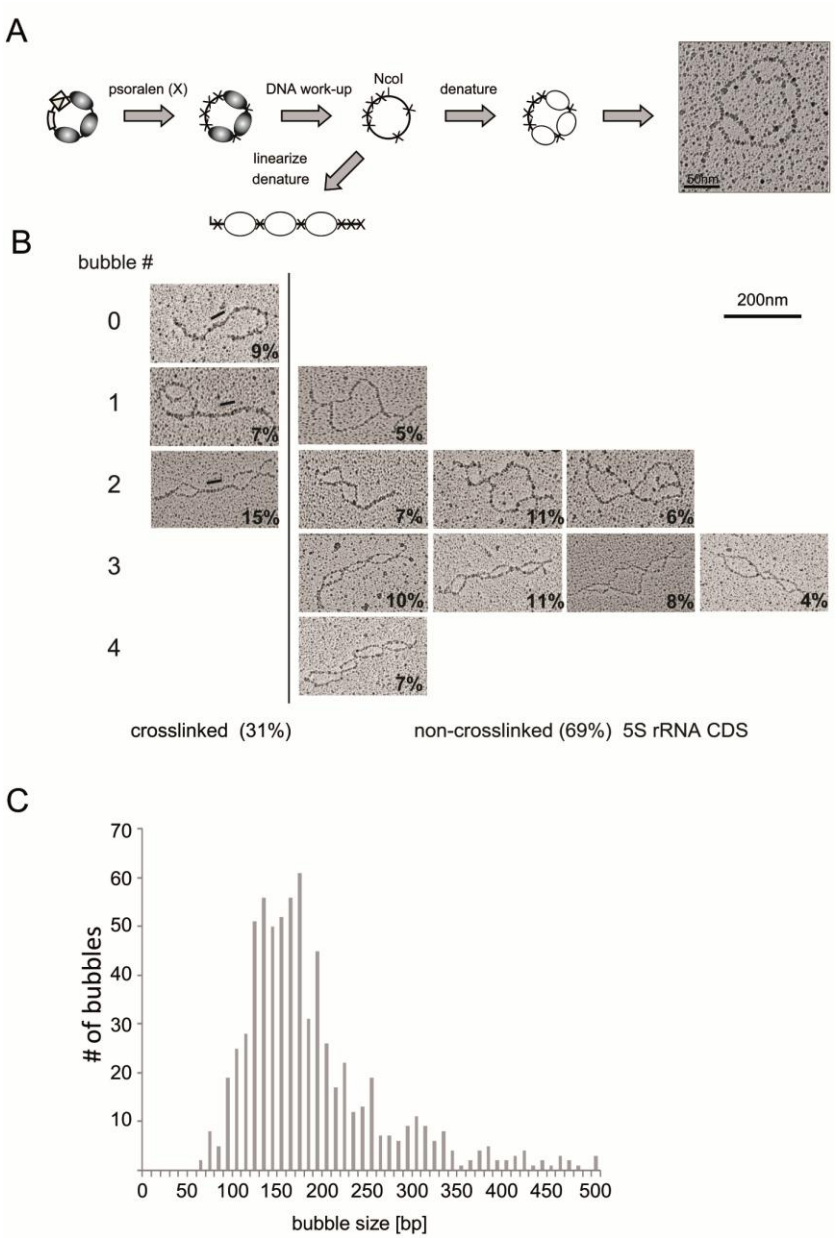

Figure 22 Determination of nucleosome positions on the 5S rRNA gene domain by single molecule EM analysis. A) Schematic representation of sample preparation. Isolated chromatin circles were subjected to psoralen crosslinking (indicated by black crosses). Psoralen intercalates into nucleosome-free DNA and forms a covalent bond between the DNA single strands upon UV-irradiation. After DNA isolation, crosslinked molecules were relaxed with a nicking endonuclease, denatured and analyzed by electron microscopy under denaturing conditions. Nucleosome positions can be deduced from single stranded DNA stretches with a length of around 50nm because nuclesomal DNA has been protected from psoralen incorporation due to its tight interaction with the histone octamer. The panel on the right shows a representative electron micrograph of a circular 5S rRNA gene DNA molecule on which non-crosslinked single-stranded bubbles indicate that the 5S rRNA gene domain was assembled into 4 nucleosomes. The scale bar in the lower right corner of the electron micrograph represents 50nm. B) To define nucleosome positions within the 5S rRNA gene domain, purified psoralen crosslinked DNA was linearized with the restriction endonuclease *Nco*I prior to denaturation and EM analysis. A total of 334 molecules from two independent biological replicates of the purification was analyzed and categorized in 12 different classes according to number (given on the left), size and position of the observed single stranded bubbles. Representative electron micrographs for molecules of each class are shown. The scale bar in the upper left corner represents 200nm. The percentage of each class in the total population of molecules is depicted in the lower right corner of the micrographs. 3 out of 12 classes contained a crosslinked DNA region at the position of the 5S rRNA coding sequence (leftmost electron micrographs, separated by a black line from molecules that were not crosslinked in this region). The position of the crosslinked 5S rRNA coding sequence is indicated by a black bar in the corresponding electron micrographs. C) The bar graph depicts bubble size distribution (in bp) in the total population of 701 single-stranded DNA bubbles observed in the 334 molecules.

DNA fragment. A total of 334 molecules were evaluated and classified into 12 different groups according to the number, position and size of the individual single stranded DNA bubbles (Figure 22B). None of these classes was enriched in the population, indicating a heterogeneous chromatin structure within the region flanking and encompassing the 5S rRNA gene.

Only 47% of the analyzed bubbles had a size of 130-180bp, which is in the expected size range of a nucleosome core particle (Figure 22C). A minor fraction of DNA bubbles (10%) had a size of 260-360bp, which can be explained by inefficient crosslinking of the linker DNA between two nucleosomes. However, we noticed that many DNA bubbles (26%) had an intermediate size of 180-260bp, which could not be explained by nucleosomal protection of the circle DNA against psoralen incorporation. It is possible that these psoralen inaccessibilities were the consequence of binding of chromatin components other than nucleosomes to the DNA. Interestingly, the profile of bubble size distribution closely resembles the one reported for the endogenous rDNA intergenic spacer region obtained after treatment of yeast cells with psoralen and isolation and EM analysis of the respective rDNA fragment (see Figure 5A in Dammann et al., 1993). The 5S rRNA gene region analyzed here is part of the rDNA segment investigated in this earlier study indicating that structural features of IGS chromatin are preserved upon isolation. Three different molecule classes showed a psoralen crosslinked stretch of DNA in the center of the linearized 5S rRNA gene ring (Figure 22B, column on the left, position of the 5S rRNA gene marked by a black bar). These 3 classes represented 31% of the total population of molecules. It has been reported that the Pol III transcribed tRNA genes belong to the most prominent nucleosome depleted regions in the genome and that nucleosome depletion correlates with transcriptional activity (Rao et al., 2005; Parnell et al., 2008). Therefore, the molecules with a nucleosome-free region at the Pol III-dependent 5S rRNA gene might represent the transcriptional active state of the gene. Consistently, the percentage of nucleosome-free 5S rRNA genes (Figure 22B, 31%) approximately matches the percentage of active 5S rRNA genes determined by electron microscopy of Miller chromatin spreads in different strains ((French et al., 2008), Table 2, 21-30%).

3.4.3 Restriction endonuclease accessibility analysis of 5S rRNA gene chromatin confirms the results of the single molecule approach

The single molecule EM analysis suggested that psoralen protection pattern of the purified 5S rRNA gene chromatin circles resembled the psoralen protection pattern of rDNA segments encompassing this region on the yeast chromosome (see above). In order to verify this result by an independent approach, we analyzed restriction enzyme accessibility of DNA in 5S rRNA gene chromatin on the isolated domain or on the yeast chromosome (Figure 23). Accessibility of DNA is impaired, when the DNA is assembled in nucleosomes, although there might be factors other than nucleosomes which interfere with efficient restriction enzyme cleavage (Simpson, 1998). Five different enzymes with recognition sites within the 5S rRNA gene sequence and in the flanking regions were used, respectively. Yeast nuclei and purified chromatin rings were incubated in the presence of the enzymes; DNA was isolated and analyzed in a Southern blot. Overall restriction enzyme DNA accessibilities were very similar at the isolated chromatin circles and at the chromosome (Figure 23A, compare upper and lower panel on the left, see Figure 23B on the right for quantitation). However, a subtle difference was observed with restriction enzymes cutting at the edges of the 5S rRNA gene coding sequence (Figure 23A and B, see *Hae*III and *Dde*I). Importantly, the restriction enzme *Sfc*I which has a single restriction site in the center of the 5S rRNA coding sequence cut 33-36% of the 5S rRNA gene DNA on the isolated circles and on the chromosome (Figure 23A and B, *Sfc*I). This correlated well with the results of the single molecule EM analysis, in which 31% of the 5S rRNA genes were psoralen accessible at this location (Figure 22B). These data support that important structural properties of the 5S rRNA gene chromatin are preserved upon purification. The rather intermediate restriction enzyme accessibilities further support a heterogenous nucleosome number and distribution on the 5S rRNA gene domain ((Boeger et al., 2008) see also 3.4.1 and 3.4.2).

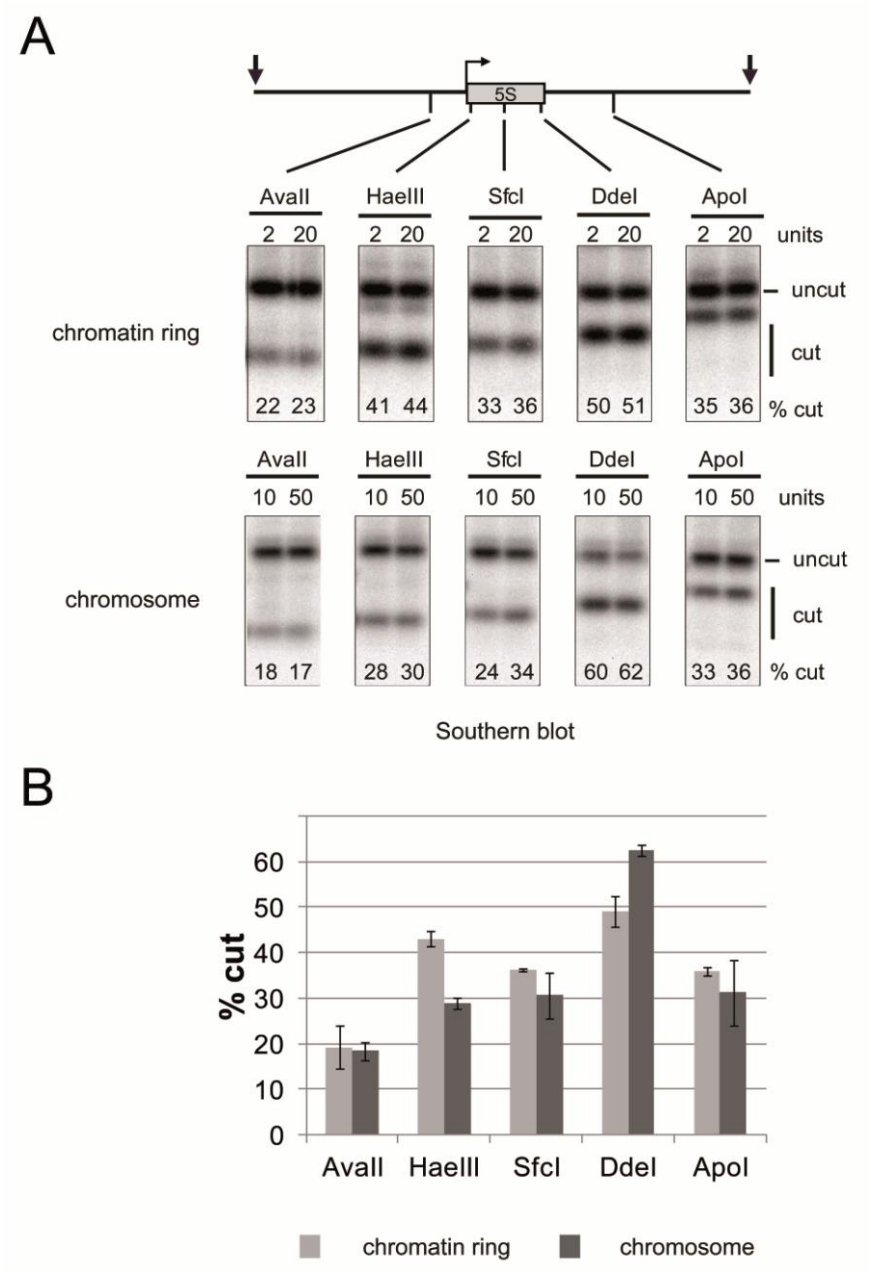

Figure 23 Restriction endonuclease accessibilities in chromatin at purified 5S rRNA gene circles and at the chromosome. A) Purified chromatin circles or isolated nuclei from yeast strains y1997 or y1599/y2124, respectively, were digested with increasing amounts (indicated on top of each pair of lanes) of the indicated restriction enzymes, as detailed in the Material and Methods section. DNA was isolated, digested with the restriction enzyme endonucleases *Nco*I (chromatin ring) or *Pvu*I/*Sph*I (chromosome) and subjected to indirect endlabeling Southern blot analysis with the radioactively labeled probe 5S_REA. A schematic representation of the 5S rRNA gene locus with the restriction sites used to probe chromatin structure and the restriction sites for the secondary restriction digest (arrows pointing downward) is given on the top. The positions of uncut and cut fragments are shown on the right of the panels. Numbers on the bottom of each panel give the percentage of accessibility for each restriction site. B) After quantitation of Southern blot signals the percentage of DNA cut at the highest restriction enzyme concentration was calculated and is displayed in a bar diagram. Average values and standard deviations are from two independent biological replicates.

3.5 Chromatin domains of single copy genes can be enriched in sufficient amounts and purity to perform mass spectrometric analysis

After recombination, rDNA domains are present in high copy number in the yeast genome. The yields obtained in the above preparations suggested that it is possible to apply the purification strategy to single copy gene loci. Specific enrichment of the single copy *PHO5* gene has been reported earlier (Griesenbeck et al., 2003). However, mass spectrometric analysis failed so far due to limited purity (and/or quantity) of the isolated material. In this study, *PHO5* gene chromatin was purified from a strain in which a 2.2kb region of chromosome II encompassing the *PHO5* promoter region and the *PHO5* ORF as well as a cluster of *LEXA* binding sites was flanked with recognition sites of R recombinase ((Boeger et al., 2003), see Figure 24A for a schematic representation). When compared to the purification of rDNA chromatin domains, the purification protocol for single copy genes contained three major modifications: i) expression of the LexA-TAP fusion protein was controlled by the basal *CYC1* promoter (Mumberg et al., 1995). This led to a substantial reduction of the cellular levels of the fusion protein when compared to LexA-TAP expressed under the *TEF2* promoter to prevent non-specific binding of LexA to bulk genomic chromatin fragments (see 3.1.2.2) ii) a fivefold excess of cells over the amount of cells used for the purification of the rDNA domains had to be used and iii) after IgG purification and elution with TEV protease, a second affinity purification step via Calmodulin sepharose matrix was performed. Figure 24B shows a representative DNA analysis of purified *PHO5* gene rings after the tandem affinity purification. Agarose gel electrophoresis and SybrSafe staining revealed a single DNA band at the expected size of the *PHO5* gene circle of 2.2kb (Figure 24B, panel SybrSafe, lane 2). No DNA was detected when the same procedure was applied to a control yeast strain lacking *LEXA* binding sites and RS elements at the *PHO5* locus (Figure 24B, panel SybrSafe, lane 1). Quantification of the DNA amount of purified *PHO5* gene circles after TAP-purification by qPCR analysis indicated a total yield of 10-15% after two subsequent affinity purifications (data not shown), which is superior to the yield obtained from purifications of rDNA chromatin domains after a single affinity step (0.5-5%, see 3.1.2.4). A possible explanation is that, at the beginning of the purification, the extraction of rDNA domains (including higher recombination products) from cell extracts is much more inefficient compared to the single-copy *PHO5* gene circles. Analysis of the protein content in the

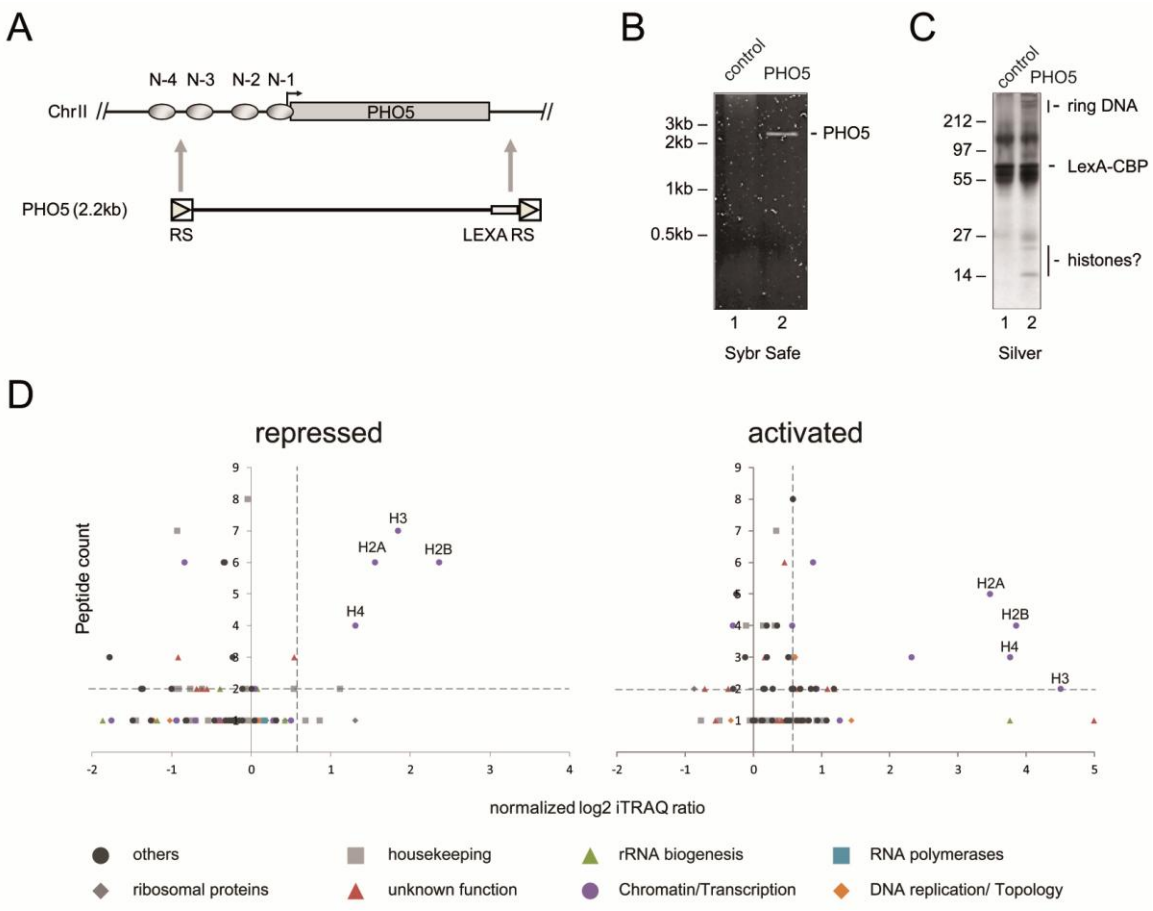

Figure 24 Chromatin domains of single copy genes can be enriched to perform mass spectrometric analysis. A) Genetic manipulation of the *PHO5* locus. The cartoon on the top is a schematic representation of the *PHO5* locus on chromosome II. *PHO5* (grey rectangle), coding region for *PHO5*; N-1 to -4 (filled ovals), positioned nucleosomes on the repressed *PHO5* promoter, an arrow indicates the direction of transcription and start sites used by RNA polymerase II. Grey arrows pointing from the bottom towards the rDNA cartoon mark the sites of insertion for RS elements and *LEXA* DNA binding sites to frame the *PHO5* gene. Recombination releases a 2.2kb chromatin ring. B) DNA and protein analysis of purified *PHO5* gene circles. Yeast strains y455 (*PHO5*) and y465 (control) carrying either a *PHO5* locus tagged with a cluster of *LEXA* DNA binding sites and flanked by RS elements (*PHO5*) or a *PHO5* locus lacking these modifications (control), were transformed with plasmid K2048 for constitutive expression of LexA-TAP and conditional expression of R Recombinase. After recombination, cells were subjected to tandem affinity purification as detailed in Materials and Methods section. Samples of the eluates from calmodulin sepharose beads were subjected to DNA analysis (panel on the left) and protein analysis (panel on the right). DNA was isolated, digested with *Nco*I, and analyzed in a 1% agarose gel stained with SybrSafe. The respective sample analyzed is indicated on top of each lane. Positions of DNA size markers are given on the left. The position of the 2.2kb NcoI fragment of the *PHO5* gene circle is given on the right. Proteins co-purifying with the *PHO5* chromatin domain were separated in an SDS PAGE gradient gel (4-12%) and stained with silver. The respective sample analyzed is indicated on top of each lane. Positions and sizes of marker proteins are indicated on the left. The positions of LexA-calmodulin binding peptide fusion protein (LexA-CBP), and histones, as well as the circle DNA (visualized by silver staining) are given on the right. Purification was performed from 5 $x10^{11}$ cells. 5% and 10% of the eluate were used for DNA analysis and protein analysis, respectively. C) Graphical summary of the enrichment of proteins in the *PHO5* gene circle purifications. Proteins co-purifying with *PHO5* gene circles isolated from cells in which *PHO5* transcription was repressed (y464), or constitutively activated (y465) were subjected to iTRAQ analysis in direct comparison with purifications of the corresponding control strains (y454, or y455, respectively). Data was evaluated as described in the Legend to Figure 18.

purified samples by SDS-PAGE and Silver staining revealed some enrichment of proteins migrating with the mobility of histone proteins in the sample containing the purified *PHO5* domain (Figure 24B, panel Silver, lane 2). These protein bands were not

detected in the control purification (Figure 24B, panel Silver, compare lane 2 with lane 1). We also assessed the protein composition of purified *PHO5* gene rings by comparative semiquantitative mass spectrometry as described above (Figure 24C). Thus, chromatin circles were purified from two different strains in which transcription of the *PHO5* gene was either repressed or constitutively activated (Boeger et al., 2003). *PHO5* promoter chromatin structure is very different on chromatin circles isolated from these two strains ((Boeger et al., 2003; Griesenbeck et al., 2003) see also 3.4.1). Each of the purifications was performed in duplicate. The canonical histone proteins were specifically enriched in the *PHO5* chromatin circle purifications in comparison to purifications from the respective control strains (Figure 24C). By applying the criteria for specific enrichment of proteins in such analyses (3.2.3.2) we did not observe significant co-purification of other chromatin components with activated or repressed *PHO5* chromatin.

Taken together, these results indicate that native chromatin derived from a single copy gene locus allows the specific identification of associated histone molecules. This might open the door to fully define the specific posttranslational histone modification state of chromatin at virtually every gene in yeast

4 Discussion

4.1 A single-step purification strategy allows robust enrichment of native rDNA chromatin

Compositional and structural analysis of defined genomic regions of interest is critical to our understanding of chromosome biology and gene regulation in the context of chromatin. Various strategies have been employed to isolate and analyze the composition of defined chromosomal domains to derive an unbiased description of chromatin at selected genomic locations (Higashinakagawa et al., 1977; Zhang and Hörz, 1982; Workman and Langmore, 1985; Boffa et al., 1995; Griesenbeck et al., 2003; Simpson et al., 2004; Ghirlando and Felsenfeld, 2008). Most of these attempts suffered from low recovery or insufficient purity of the isolated material, which made the intended downstream analyses difficult. In this work, site-specific recombination *in vivo* and subsequent affinity purification was used in order to derive an unbiased, antibody-independent description of the interacting proteome of selected chromosomal domains. Furthermore, the native purification procedure allowed the analysis of posttranslational modifications of histone molecules interacting with different regions of the yeast rDNA locus and initial structural analysis of nucleosome configurations on 5S rRNA gene chromatin domains by electron microscopy.

4.1.1 Yield and specificity of rDNA chromatin isolation procedure compare well with alternative chromatin purification strategies

In the beginning of this work, the rDNA chromatin preparations suffered from technical difficulties mainly due to problems at the level of the affinity chromatography. Three major modifications of the original protocol for purification of distinct chromosomal domains (Griesenbeck et al., 2004) greatly improved yield and purity of the chromatin preparation: i) a single-step purification protocol with IgG coated magnetic beads (Oeffinger et al., 2007) showed superior retention of rDNA chromatin circles compared to IgG sepharose and calmodulin agarose affinity matrices (see Figure 11B and C) ii) the

reduction of the expression level of the LexA-TAP fusion protein by exchanging the stronger inducible *GAL1-10* promoter for the constitutive *TEF2* promoter (Mumberg et al., 1995) substantially decreased the background purification of bulk chromatin fragments (see Figure 12 and Figure 15A, lane bulk), and iii) the stable chromosomal integration of the R recombinase and LexA-TAP expression cassette allowed to grow cells in full medium as opposed to using an expression plasmid requiring growth in minimal medium (see 3.1.2.3). In this way, around 200-500ng of purified rDNA chromatin circles could be obtained from one litre of exponentially growing yeast cultures (~5 x 10^{10} cells) which corresponds to a recovery between 0.5-5% of the total cellular amount of individual rDNA domains. The yield and specificity of distinct rDNA chromatin preparations (see Figure 13 for a representative DNA analysis of individual rDNA domains) compares well with most currently available chromatin purification methods that allow mass spectrometric identification of locus-specific chromatin associated proteins. Interestingly, the PICh approach introduced by Déjardin and colleagues (see 2.2.3.3) requires only 1/10^{th} of the cell number for the purification of rDNA domains (~ 3 x 10^9 HeLa cells) in order to identify the proteins associated with the multi-copy telomeric regions of the genome (Déjardin and Kingston, 2009). However, the recovery likely relies on the presence of many repetitive sequences which might make the affinity purification for every other locus than telomeres difficult because multiple different oligonucleotides covering the genomic locus of interest have to be used for efficient purification of DNA fragments. The PICh protocol was recently extended to the analysis of proteins associated to the *Drosophila* telomere-associated sequence (TAS) repeats (Antão et al., 2012). The TAS repeats show more complex sequences with ~30-fold less target sequences for a 25bp capture probe. However, it is questionable if this method is suitable for the purification of chromatin and subsequent mass spectrometric analysis of associated proteins when DNA sequences which are only present at a few or one copy per cell are targeted. Moreover, the approach is based on stabilization of nucleoprotein and protein-protein interactions by formaldehyde treatment, which excludes further functional and biochemical analysis of the purified material. However, the PICh procedure has also certain advantages compared to the native purification strategy presented in this work. Introduction of RS sites and LEXA binding sites in a chromosomal region of interest requires sophisticated genetic engineering methods which are not available in all model organisms. Instead, the PICh procedure relies on a DNA hybridization technique with a specific oligonucleotide complementary to the region of interest and thus, does not require genetic modifications of the genomic locus of interest. In general, this makes the method applicable to any model organism of choice.

The isolation of native mini-chromosomes by Lac-Repressor mediated affinity purification (Akiyoshi et al., 2009; Unnikrishnan et al., 2010, 2012) represents a similar approach to the LexA-TAP-mediated recovery of chromatin circles uncoupled from adjacent chromosomal regions by site-specific recombination *in vivo* presented in this work. In contrast to PICh, both strategies allow the purification of specific chromatin regions under native conditions and the isolated material is amenable to further structural and biochemical studies. However, the use of high-copy plasmids has two undesirable side-aspects: First, transfer of a chromosomal sequence into a standard cloning vector changes its natural genomic context, which may have functional consequences: certain autonomous replication sequences function as replication origins in plasmids, but not in their original chromosomal positions (Broach and Pringle, 1991). One possible explanation is that plasmids do not contain all required sequences in order to faithfully reproduce chromosomal events, or that there are differences in the episomal chromatin structure when compared to chromatin at the endogenous locus. The second problem is that the copy number of sequences on the extrachromosomal plasmids may differ from their genomic copy number. This is critical, if the plasmid encoded DNA-sequences are in large excess and the chromatin structure of the sequence of interest depends on a factor present in the cell in limiting amounts. The latter scenario has been reported for the transcriptional activation of the yeast *PHO5* gene present on a minichromosome (Haswell and O'Shea, 1999). Excision of the chromatin domain from its chromosomal context circumvents the second concern, but the integration of RS sites and *LEXA* binding sites and the site-specific recombination process of the targeted chromosomal region may induce changes to the local chromatin structure of the domains. However, previous studies of purified chromatin domains derived from the single-copy *PHO5* and *HMR* genes indicated that the genetic modifications and the recombination event as well as the purification procedure had no influence on the number and distribution of nucleosomes on the targeted genomic region (Ansari et al., 1999; Boeger et al., 2003; Griesenbeck et al., 2003). Results of the current work also supported this observation because restriction enzyme accessibilities of 5S rRNA gene chromatin in its chromosomal context were comparable to restriction enzyme accessibilities in purified 5S rRNA gene chromatin circles (Figure 23A and B). Moreover, psoralen-crosslinking analysis of purified chromatin circles including the 18S rRNA coding sequence and an entire rDNA repeat showed two distinct bands with different mobilities originating from open or closed 35S rRNA genes in Southern blot analysis. The ratio of open and closed 35S rRNA genes in purified chromatin samples was in fact identical to the ratio of open and closed 35S rRNA genes observed in isolated nuclei (data not shown and Figure

10A), indicating that the open and closed 35S rRNA gene chromatin states are preserved upon the purification.
Taken together, these analyses suggest that rDNA domains can be uncoupled from adjacent chromosomal regions by site-specific recombination and subsequently isolated and purified conserving characteristic structural properties of the respective chromatin region.

4.1.2 Pol I associated chromatin purified after formaldehyde crosslinking *in vivo* shows similarities and differences when compared to native 35S rRNA gene chromatin

The application of a native purification protocol raises concerns about dissociation of important chromatin components due to the (more or less) stringent detergent and salt concentrations used during the isolation procedure (see 5.2.12). Thus, the proteome data from the native purification of 35S chromatin circles were in part validated by a complementary approach conducted in our department by Jorge Pérez-Fernandez, Astrid Bruckmann and Rainer Deutzmann, in which RNA Pol I and RNA Pol II associated chromatin was purified from cells treated with formaldehyde to stabilize transient interactions prior to cell lysis and purification (Hierlmeier et al., 2012). After cell lysis, chromatin fragments were sheared by sonication and purified via affinity purification of Pol I- or Pol II-protein A fusion proteins using IgG coupled to magnetic beads. The co-purifying proteomes were compared by iTRAQ labeling and MALDI TOF/TOF mass spectrometry as described above (Figure 25, Table 2). An obvious problem of this approach is that common factors that specifically co-purify with both RNA Pol I and RNA Pol II associated chromatin are indistinguishable from background contaminants of the purification in this type of analysis. However, the only essential function of yeast Pol I is the transcription of the 35S rRNA gene (Nogi et al., 1991) and no other Pol I target loci have been described. Therefore, the above approach likely co-purifies actively transcribed 35S rRNA gene chromatin together with Pol I. Table 2 compares the proteins enriched in the Pol I purification with the proteins enriched in the purification of native 35S rRNA gene chromatin. Whereas only the actively transcribed nucleosome depleted chromatin state should be enriched in the Pol I purification, the native chromatin purification should not discriminate between the two different 35S rRNA chromatin states, and additionally contain the transcriptional inactive, nucleosomal 35S rRNA gene chromatin state. Accordingly, a large overlap between the Pol I purification and the 35S rRNA gene chromatin purification was observed. Many Pol I subunits were identified in

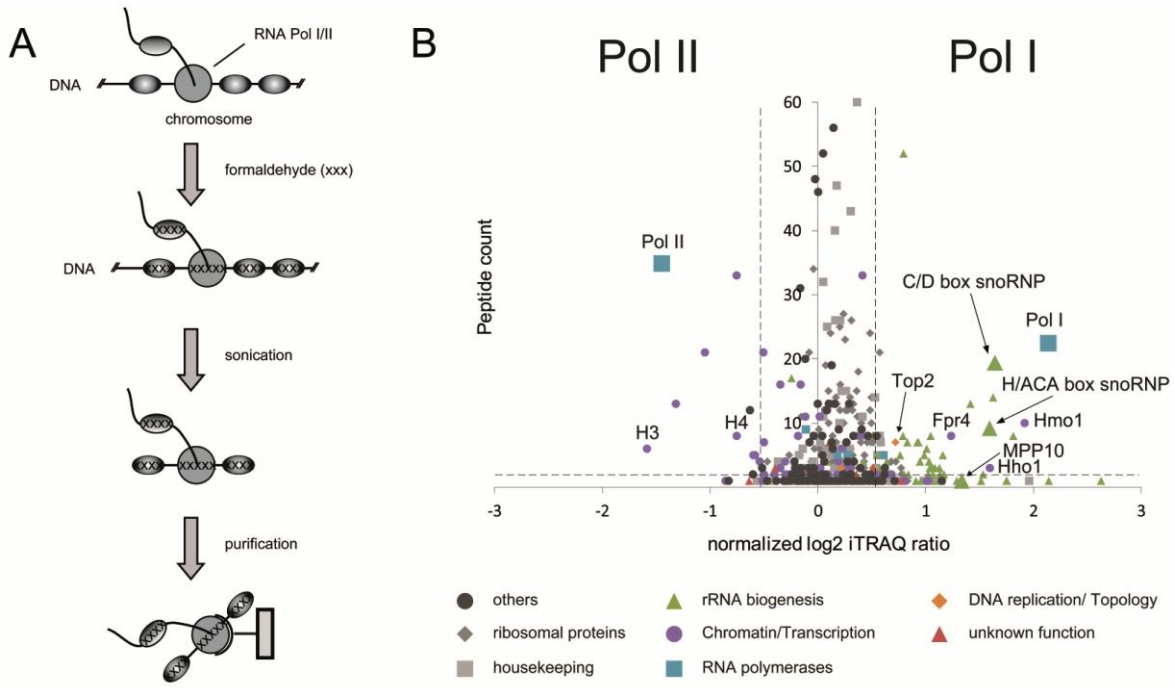

Figure 25 Pol I associated chromatin purified after formaldehyde crosslinking *in vivo* shows similarities and differences when compared to native 35S rRNA gene chromatin. A) Strategy for purification of chromatin fragments associated with Pol I and Pol II. Yeast strains, y2423 or y2424, expressing either the Pol I subunit Rpa135, or the Pol II subunit Rpb2 subunit as fusion proteins with a C-terminal protein A-tag from their endogenous chromosomal location were treated with formaldehyde. After cell lysis, chromatin is fragmented and solubilized by sonication and chromatin fragments bound by the two polymerases were purified via IgG coated magnetic beads. After elution under denaturing conditions, proteins were subjected to iTRAQ analysis as described in the legend to Figure 18. B) Graphical summary of the differential enrichment of proteins co-purifying with chromatin fragments bound by Pol I or Pol II. Proteins co-purifying with Rpa135-protein A (Pol I,) or Rpb2-protein A (Pol II) from strains y2423 or y2424, which have been treated with formaldehyde prior to purification, were subjected to comparative iTRAQ analysis. Data were evaluated as described in the Legend to Figure 18B.

both of the two different purifications. Three other chromatin components, Hho1, Top2 and Fpr4, which were enriched in the native 35S rRNA gene chromatin preparation, were also found in the Pol I purification from formaldehyde treated cells (Figure 25, Table 2). An almost identical subset of proteins belonging to the UTP-A/t-UTP, UTP-B and MPP10 complexes were present in both preparations, again suggesting that these factors are predominantly associated with the transcriptional active state of 35S rRNA gene chromatin. Notably, more components of the UTP-A, UTP-B and UTP-C complexes were identified in the native 35S rRNA gene preparation than in the Pol I purification after formaldehyde crosslink (Table 2). In contrast, additional rRNA biogenesis factors seemed to be enriched in the Pol I chromatin purification after formaldehyde fixation, indicating that the chemical crosslink stabilizes these large complexes. Similarly, the HMG-box protein, Hmo1, a component of actively transcribed 35S rRNA genes (Merz et al., 2008; Wittner et al., 2011) was only identified with chromatin fragments crosslinked to Pol I, but was not detected in the native chromatin purification (Table 2). This is presumably due to the relatively stringent buffer conditions used during the native isolation procedure which may lead to dissociation of Hmo1 from the 35S rRNA gene

Table 2 Comparison of protein complexes/factors enriched in purifications of native 35S rDNA chromatin rings and of Pol I from formaldehyde crosslinked cells
Only proteins with an average iTRAQ ratio of at least 1.5, identified with at least 2 peptides are depicted. If at least 50% of multi-protein complex components were identified, identified subunits are underlined and additional proteins are depicted which
* are identified with an average iTRAQ ratio of at least 1.5 and one peptide
** are identified with an average iTRAQ ratio greater than one and at least two peptides

Biological function	Enriched proteins/ complexes	Native purification of 35S circles	Purification of crosslinked Pol I
Histones		H2A, H2B, H3, H4, H2AZ, Hho1	Hho1
Topology	Topoiso-merase	Top2**	Top2
HMG-box		-	Hmo1
Chromatin remodeling	ISW1 complex	Isw1, Ioc2**, Ioc3*	-
	INO80 complex	Ino80, Ies1**, Ies2*, Ies3*, Rvb1, Rvb2, Arp4, Arp8**	Rvb1**
RNA Polymerase I	Pol I	Rpa190, Rpa135, Rpa49, Rpa34, Rpa12	Rpa190, Rpa135, Rpa49, Rpa43, Rpa34, Rpa14, Rpa12
	common Pol I/Pol III	Rpc19*, Rpc40	Rpc19, Rpc40
	common all	Rpb5, Rpb8, Rpo26, Rpb10	Rpb5, Rpb8**, Rpo26**, Rpb10**
rRNA biogenesis	UTP-A/ t-UTP	Nan1, Utp4, Utp5, Utp8, Utp9, Utp10, Utp15	Nan1*, Utp9, Utp15
	UTP-B/ Pwp2	Utp6, Utp13, Utp21	Utp21**
	MPP10	Mpp10, Imp3, Imp4	Imp4*
	C/D box snoRNP	Nop1, Nop56, Nop58, Snu13, Rrp9	Nop1, Nop56, Nop58, Snu13, Rrp9*
	H/ACA box snoRNP	Cbf5, Gar1, Nhp2, Nop10	Cbf5, Gar1, Nhp2, Nop10
	Others	Bfr2, Emg1, Enp1, Kre33, Krr1, Prp43, Rok1, Sof1, Bud21, Dip2, Nop14, Utp22, Dbp10, Ebp2, Erb1, Has1, Nop12, Nop6, Rrp5, Rrs1, Srp40	Bfr2, Cms1**, Ecm16**, Enp2, Esf2*, Hca4*, Kre33, Kri1, Krr1, Lcp5*, Prp43, Sof1*, Mrd1*, Nop14, Nop9*, Sas10, , Utp14 Brx1, Drs1, Ebp2, Erb1, Has1, Mak21*, Nip7, Nog1*, Nop12, Nop15, Nop2, Nop4*, Nop6, Nop7, Puf6*, Rlp7**, Rpf2*, Rrp14, Rrp5, Rrs1**, Ssf1*, Tif6, Srp40*,
Others		Fpr3, Tif2, Fpr4, Pab1, Yra1, Sum1, Yhb1, Mss116	Rps11b, Rps8a, Rpl32, Rpl36, Rpl37, Rpl8b, Tif3, Fpr4, Nhp6b, Dps1, Gsp2,

domain. As another difference, histone molecules were enriched in the native chromatin purification and in the chromatin crosslinked to Pol II, but not in the chromatin

crosslinked to Pol I (compare Figure 18B, all graphs, with Figure 25B). This adds further evidence that Pol I transcribes a nucleosome depleted DNA template, and that the transcriptional inactive 35S rRNA gene chromatin state is nucleosomal (Merz et al., 2008). Accordingly, chromatin remodeling complexes which should act on nucleosomal substrates are only enriched in the native 35S rRNA gene chromatin purification but not in the Pol I associated chromatin preparation (Table 2, ISW1 and INO80).

Taken together, the comparison between the results of the two different chromatin purification approaches indicate that many of the rRNA gene interacting factors can be isolated by the native purification procedure without the necessity of prior stabilization of DNA-protein, RNA-protein, or protein-protein interactions by crosslinking reagents. It is also noteworthy that the establishment of strains carrying a *LEXA* DNA-binding cluster at distinct sites in the genome and constitutively expressing the recombinant LexA-TAP fusion protein is fully compatible with an approach in which these cells are treated with formaldehyde prior to affinity purification of the fusion protein bound to fragmented chromatin. In fact such a complementary approach has been recently established for the isolation of chromatin at specific chromosomal regions from a mouse cell line (Hoshino and Fujii, 2009) and for identification of proteins and histone posttranslational modifications at the single copy *GAL1-10* promoter region in yeast (Byrum et al., 2012).

4.2 The purification approach allows the unbiased identification of new protein components of chromatin *in vivo*

Besides confirming many of the known rDNA-protein interactions, the proteome analyses identified several new factors and for most of them, *in vivo* interaction with the respective chromosomal regions could be demonstrated (Figure 19A and Figure 20B). Interestingly, two of the newly identified factors, Tbs1 and Ylr278c with interaction sites at the ribosomal ARS and the E-pro region, respectively, belong both to a class of yeast transcription factors bearing a Zn-finger domain and sharing predicted structural homology to the centromere-binding protein Cep3 (Figure 20A). Another protein belonging to this class of transcription factors, Yll054c, specifically co-purified with chromatin containing the ribosomal ARS region but *in vivo* interaction with rDNA could not be confirmed (Figure 20B, Yll054c-MN). Tbs1 and Ylr278c are both gene products of unknown function and it is tempting to speculate about possible rDNA chromatin-related functions of the gene products. The cleavage mediated by Tbs1-MNase fusion protein

was specific in the rARS region (Figure 20B) but rather weak compared to cleavage events observed by other rDNA chromatin components like histone- or RNA polymerase I-MNase fusion proteins (Merz et al., 2008). This may indicate that Tbs1 is only associated to a subpopulation of ribosomal ARS regions under the investigated experimental conditions. Interestingly, it was shown that replication initiation only occurs at specific ARSs placed downstream of transcriptionally active 35S rRNA genes (Dammann et al., 1995). However, the molecular mechanism for the selective activation of sequence-identical replication origins in the multicopy rDNA locus is unclear and it is likely that the local chromatin structure and the absence or presence of specific protein components like Tbs1 (or Yll054c) has a critical influence on the functional state of the ribosomal ARS. Tbs1 is not an essential gene and thus, it would be interesting to compare the distribution of active ribosomal ARSs in wildtype and *TBS1* knockout situation.

Ylr278c-MN showed distinct cleavage events in the E-pro region of the rDNA locus (Figure 20B). Transcription from this bidirectional Pol II promoter produces non-coding RNAs and promotes the dissociation of cohesin, thereby allowing unequal recombination and changes in rDNA copy number after the formation of DNA double-strand breaks (Kobayashi et al., 2001, 2004). The double strand breaks are introduced by Fob1-dependent pausing of the DNA replication machinery at RFB sites (Kobayashi et al., 1998, 2004; Burkhalter and Sogo, 2004). Interestingly, the NAD^+ dependent histone deacetylase Sir2 (Imai et al., 2000; Landry et al., 2000; Smith et al., 2000) represses the transcriptional activity from E-pro (Kobayashi and Ganley, 2005). A DNA-binding protein in the E-pro region like Ylr278c may have an influence on the transcriptional activity of the Pol II promoter, thereby regulating the rDNA copy number by the mechanism mentioned above. Initial experiments in a *YLR278C* knockout strain with a wildtype rDNA copy number did not show a significant change in the number of rDNA repeats (data not shown). However, it is still possible that the *YLR278C* gene product has a selective influence on transcriptionally active or inactive E-pro promoters and it will be interesting to investigate rDNA chromatin-related functions of this factor in the future.

Interestingly, specific association of chromatin remodeling complexes with the different rDNA regions was also detected *in vivo* (Figure 19A), indicating that they are differentially recruited to these chromosomal locations. This is remarkable, since detection of the DNA-association of chromatin remodeling complexes in ChIP experiments is often difficult. The specific interaction of these multi protein complexes with distinct domains, which are in close proximity on the chromosome, suggests that

other factors might help to recruit the remodelers to the respective region. It is likely that certain histone modifications participate in this recruitment. Accordingly, the analyses show that the different chromatin domains carry differential histone modification pattern (Figure 14B and Figure 15B). The ISW1 complex was previously reported to be associated with 35S rRNA gene chromatin *in vivo* (Jones et al., 2007; Mueller and Bryk, 2007) and it was speculated that the remodeling enzyme creates a dynamic chromatin structure allowing passage of multiple elongating Pol I complexes across a nucleosomal rDNA chromatin template. However, our laboratory demonstrated that actively transcribed 35S rRNA genes are largely devoid of histone molecules (Merz et al., 2008), which is in apparent conflict to the model provided by Proudfoot and co-workers (Jones et al., 2007). The ChIP proteome analysis of Pol I associated chromatin could not detect specific enrichment of ISW1 and INO80 subunits (Table 2), suggesting that the chromatin-remodeling complexes are not *per se* constituents of open, transcriptionally active rDNA chromatin. Recently, it was shown that RNA polymerase I transcription is required to convert the nucleosomal chromatin state of 35S rRNA genes into the open, nucleosome-depleted configuration (Wittner et al., 2011). However, it is still an open question if histone chaperones or other factors are involved in Pol I transcription-dependent nucleosome eviction and the identified ISW1 and INO80 remodeling complexes may assist Pol I during the initial passage of the nucleosomal 35S rRNA gene chromatin.

The INO80 complex has been implicated in the DNA damage response and maintenance of genome integrity, because *INO80* mutants show hypersensitivities to methyl methanesulfonate (MMS), a DNA alkylating agent, and to hydroxyurea (HU), an inhibitor of ribonucleotide reductase that causes depletion of deoxynucleoside triphosphate (dNTP) pools (Shen et al., 2000). Moreover, INO80 is enriched at DNA double-strand breaks and interacts with γ-H2AX to facilitate the DNA damage response (Downs et al., 2004; Morrison et al., 2004). The closed state of 35S rRNA gene chromatin, the identified potential target substrate of the INO80 complex, was also shown to be important for genome integrity (Ide et al., 2010) and it will be interesting to further investigate the significance of this correlation in the future.

4.3 The native purification strategy is compatible with downstream structural and biochemical analysis of the isolated material

The purification technique makes native chromatin amenable to further downstream analyses. Along these lines, initial structural studies primarily focusing on the possibility to define nucleosome positions on defined chromosomal regions were conducted in this work. The statistical analysis of the results indicate a large heterogeneity of different nucleosomal states on a 700bp long DNA fragment encompassing the Pol III transcribed 5S rRNA gene (Figure 22B and C). The statistical evaluation of the single molecule analyses is in agreement with restriction enzyme accessibilities in purified 5S rRNA gene chromatin circles and in 5S rRNA gene chromatin on the chromosome in isolated nuclei likely reflecting the *in vivo* situation (Figure 23A and B). The results further corroborate previous findings that actively transcribed 5S rRNA genes may be nucleosome depleted.
In the current study, a heterogeneous population of 5S rRNA genes in different transcriptional states has been subjected to EM analysis. The purification of 5S rDNA chromatin circles was performed from an unsynchronized population of yeast cells and the observed heterogeneity of chromatin states may in part be explained by the possibility that individual classes of molecules correspond to a specific stage of the cell cycle. In the future, the same kind of experiments can be carried out in the course of the cell cycle with a synchronized culture of yeast cells to test this hypothesis. On this way, it will be interesting to correlate specific structural states of the chromatin with the transcriptional activity of the locus. Moreover, methods like gel filtration or density sedimentation may also be useful to separate different chromatin populations and to analyze the composition of chromatin in different transcriptional states. Along these lines, gel filtration analysis of rDNA chromatin domains derived from the E-pro region and the 5S rRNA gene yielded a broad elution profile (Figure 21A and B). It will be interesting to analyze individual fractions by electron microscopy. Meanwhile, similar single molecule analyses have been performed with purified single copy gene loci in distinct transcriptional states revealing important insights in the chromatin configuration and dynamics at the *PHO5* promoter upon transcriptional activation (Brown et al, 2012). In addition to information about nucleosome positions, EM studies with native chromatin may yield insights in higher order structures adopted by the different chromatin domains in different functional states.

Another important aspect which has not been addressed in the present study is the use of the purified chromatin domains in functional *in vitro* studies. Preliminary analyses showed that purified chromatin domains can be subjected to *in vitro* transcription reactions (data not shown). This might eventually help to improve the understanding of transcription in the context of chromatin. It will be also interesting to investigate the requirements for the transition between different rDNA chromatin states *in vitro*. Along these lines, purified chromatin rings have been successfully used to identify specific enzymes required for the chromatin transition at the Pol II dependent *PHO5* promoter upon transcriptional activation (Ehrensberger and Kornberg, 2011).

4.4 Outlook

The specific enrichment of canonical histone proteins in the *PHO5* chromatin circle purifications in comparison to purifications from the respective control strains (Figure 24B and C) indicates that the presented approach is applicable to virtually any genomic locus in yeast. Furthermore, some transcription factors and components of the SWI/SNF chromatin remodeling complex were specifically detected in the purification containing the activated *PHO5* chromatin (data not shown). Although these results are encouraging, more experiments are needed to significantly confirm the compositional differences between activated and repressed *PHO5* chromatin. In the near future, a reasonable aim will be to define the posttranslational modification state of histone molecules derived from *PHO5* chromatin circles isolated under activated and repressed conditions.

In summary, this technique has the potential to provide many new insights in chromatin structure and dynamics and may be a useful tool for researchers to advance chromatin research at their specific locus of interest.

5 Material and methods

5.1 Material

5.1.1 Chemicals

All chemicals and solvents used in this work were purchased at the highest available purity from Sigma-Aldrich, Merck, Fluka, Roth or J.T.Baker, except agarose electrophoresis grade (Invitrogen), 5-FOA (Toronto Research chemicals), bromphenol blue (Serva), G418/Geneticin (Gibco), milk powder (Sukofin), Nonidet P-40 substitute (NP40) (USB Corporation), Tris ultrapure (USB Corporation) and Tween 20 (Serva).
Ingredients for growth media were purchased from BD Biosciences (Bacto Agar, Bacto Peptone, Bacto Tryptone and Bacto Yeast Extract), Sunrise Science Products (Yeast nitrogen base (YNB), amino acids and adenine), Sigma-Aldrich (D(+)-glucose, amino acids and uracil) and Chemos GmbH (D(+)-Raffinose). Water was always purified with an Elga Purelab Ultra device prior to use.

5.1.2 Buffers and media

Unless stated otherwise, all solutions have been prepared in water that has a resistivity of 18.2 MΩ-cm and total organic content of less than five parts per billion. The pH values were measured at room temperature. Percentage is mass per volume (m/v) and pH was adjusted with HCl or NaOH if not indicated otherwise.

media & buffer	**Ingredients**	**concentration**
LB medium	Tryptone	10g/l
	Yeast extract	5g/l
	NaCl	5g/l
	1M NaOH	1ml/l
	Agar (plates)	20g/l
	Autoclave	

LB/Amp	Ampicillin in LB medium,	50µg/ml
YP	Yeast extract Peptone Agar (plates) Autoclave	10g/l 20g/l 20g/l
YPD medium	YP + Glucose	20g/l
YPR medium	YP + Raffinose	20g/l
YPG medium	YP + Galactose	20g/l
YPD with Geneticin	YPD + Geneticin (Gibco) in YPD	400mg/l
YPAD	YPD + Adenine hemisulfate salt	100mg/l
HHY-Leu/Ura/His	Tyrosin Isoleucine Phenylalanine Glutamate Threonine Aspartate Valine Serine Arginine Adenine Tryptophane Methionine Lysine	0.6g/l 0.8g/l 0.5g/l 1g/l 2g/l 1g/l 1.5g/l 4g/l 0.2g/l 0.4g/l 0.4g/l 0.2g/l 0.3g/l
Synthetic medium (SC)	YNB HHY Uracile Histidine Leucine Agar (plates) Autoclave	6.7g/l 1.29g/l 35mg/l 20mg/l 100mg/l 20g/l
SCD-Leu	SC without Leucine + Glucose	20g/l
SCR-Leu	SC without Leucine + Raffinose	20g/l
SCG-Leu	SC without Leucine + Galactose	20g/l
SCD-Ura	SC without Uracil + Glucose	20g/l
SCG-Leu + 5-FOA	SCG-Leu + 5-Fluoroorotic acid	1g/l

IR buffer	Tris-HCl pH 8 EDTA	50mM 20mM
IRN buffer	Tris-HCl pH 8 EDTA NaCl	50mM 20mM 0.5M
TBE buffer	Tris Boric acid EDTA	90mM 90mM 1mM
10 x DNA loading buffer	Bromphenol blue Xylen cyanol Glycerine	0.25% 0.25% 40%
TE buffer	Tris-HCl pH 8 EDTA	10mM 1mM
20 x SSC	NaCl Tri-sodium citrate dehydrate pH7 with HCl	3M 0.3M
Buffer MB	Tris-HCl pH 8.0 KCl MgAc Triton X-100 Tween 20 DTT	20mM 200mM 5mM 0.5% 0.1% 1mM
Buffer CWB	Tris-HCl pH 8.0 KCl MgAc Triton X-100 Tween 20 $CaCl_2$ DTT	20mM 200-300mM 5mM 0.5% 0.1% 2mM 1mM
Buffer CEB	Tris-HCl pH8.0 KCl EDTA EGTA Triton X-100 Tween 20 DTT	20mM 400mM 1mM 10mM 0.5% 0.1% 1mM

Buffer A	Tris-HCl pH 7.4 Spermine Spermidine KCl EDTA	15mM 0.2mM 0.5mM 80mM 2-4mM
Buffer Ag	Buffer A without EDTA EGTA	 0.1mM
Buffer GF	HEPES pH7.4 KCl EDTA Glycerol Spermidine Spermine β-mercaptoethanol	25mM 200mM 2mM 10% (w/v) 0.125mM 0.05mM 5mM
Protease Inhibitors 100x	Benzamidine PMSF	33mg/ml 17mg/ml
4 x Upper Tris	Tris SDS Bromphenol blue pH 6.8 with HCl	0.5M 0.40%
4 x Lower Tris	Tris SDS pH 8.8 with HCl	1.5M 0.40%
Transfer buffer (Western Blot)	Tris Glycine Methanol	25mM 192mM 20%
10 x Electrophoresis buffer (SDS-PAGE)	Tris Glycin SDS	250mM 1.9 M 1.00%
10 x PBS	NaCl KCl $Na_2HPO_4 \cdot 2H_2O$ KH_2PO_4 pH 7.4 with HCl or NaOH	1.37M 27mM 10mM 20mM
PBST	PBS	1x

	Tween 20	0.05%
ChIP Lysis buffer	HEPES pH 7.5	50mM
	NaCl	140mM
	EDTA	5mM
	EGTA	5mM
	Triton X-100	1%
	DOC	0.10%
ChIP Wash buffer I	HEPES pH 7.5	50mM
	NaCl	500mM
	EDTA	2mM
	Triton X-100	1%
	DOC	0.10%
ChIP Wash buffer II	Tris-HCl pH 8	10mM
	LiCl	250mM
	EDTA	2mM
	Nonidet P40	0.50%
	DOC	0.50%
HU buffer SDS	SDS	5%
	Tris-HCl pH 6.8	200mM
	EDTA	1mM
	β-mercapto-ethanol	1mM
	Urea	1.5%
	Bromophenolblue; store at -20°C	8M
SORB	LiOAc	100mM
	Tris-HCl pH 8	10mM
	EDTA pH 8	1mM
	Sorbitol	1M
	pH 8 with HOAc	
PEG	LiOAc	100mM
	Tris-HCl pH 8	10mM
	EDTA pH 8	1mM
	Polyethylene glycol PEG3350 (Sigma)	40%

5.1.3 Nucleic acids

A. Nucleotides

For synthesis of DNA molecules, the “desoxynucleotide solution mix” by New England Biolabs was used which contains each of the four desoxynucleotides in 10mM concentration.

B. Oligonucleotides

#	**sequence (5` → 3`)**	**function**	**gene/locus**
611	AGGCGAAGAAAACCCACAAA	Primer used for qPCR amplifying a region in NOC1 locus together with 612	*NOC1*
612	GTCGTCAGCATCCTCGTCAG	Primer used for qPCR amplifying a region in NOC1 locus together with 611	*NOC1*
613	CATGATCAGATGGGGCTTGA	Primer used for qPCR amplifying a region in PDC1 locus together with 614	*PDC1*
614	ACCGGTGGTAGCGACTCTGT	Primer used for qPCR amplifying a region in PDC1 locus together with 613	*PDC1*
623	CCTCGAGGGAGCTTGCAT	Primer used for verification of 35S circle recombination together with 685	*35S rRNA gene*
685	TCCAAAGTGACAGGTGCCC	Primer used for verification of 35S circle recombination together with 623	*35S rRNA gene*
688	TCATCTTATGTGCGCTGCTT	Primer used for qPCR amplifiying a region in PHO5 promoter together with 689	*PHO5*
689	CAGTTGCGTTCTATGCGAAA	Primer used for qPCR amplifiying a region in PHO5 promoter together with 688	*PHO5*
710	TGGAGCAAAGAAATCACCGC	Primer used for qPCR amplifying a region in 25S rDNA together with primer 711	*25S_2*
711	CCGCTGGATTATGGCTGAAC	Primer used for qPCR amplifying a region in 25S rDNA together with primer 710	*25S_2*
712	GAGTCCTTGTGGCTCTTGGC	Primer used for qPCR amplifying a region in 18S rDNA together with primer 713	*18S_2*
713	AATACTGATGCCCCCGACC	Primer used for qPCR amplifying a region	*18S_2*

		in 18S rDNA together with primer 712	
920	GCCATATCTACCAGAAAGCACC	Primer used for qPCR amplifying a region in 5S rDNA together with primer 921	*5S*
921	GATTGCAGCACCTGAGTTTCG	Primer used for qPCR amplifying a region in 5S rDNA together with primer 920	*5S*
1040	GCACTTGCTTCAGGACCATA	Primer used to verify genomic MNase tag to chromosomal genes in ChEC approach	*MNase CDS*
2099	TGTCCTCCACCCATAACACC	Primer to obtain template for Southern probe preparation from yeast genomic DNA together with primer 2100	*5S*
2100	ATTTAGCATAGGAAGCCAAG	Primer to obtain template for Southern probe preparation from yeast genomic DNA together with primer 2099	*5S*
2286	GATGGTACCGATCAGCATTACATGAAAATCAGTTGCTAAAATGGTTATCCAAACGTACGCTGCAGGTCGAC	Primer to obtain amplicon of pYM13 for genomic integration of TAP KanMX6 together with primer 1495	*RRN5*
2287	GATGGTACCACAGGGTAATGGAGATCAAACAAGAGACTTTGGCACATCAATGGAATTGCGTACGCTGCAGGTCGAC	Primer to obtain amplicon of pYM13 for genomic integration of TAP KanMX6 together with primer 1745	*FOB1*
2288	GATGGTACCAAGTTTCTCCAAGAAGATTAATTACGACGCCATTGACGGTTTGTTTAGGCGTACGCTGCAGGTCGAC	Primer to obtain amplicon of pYM13 for genomic integration of TAP KanMX6 together with primer 1683	*BRF1*
2289	GATGGTACCGAAGCCAAGTGGTGGATTTGCATCATTAATAAAAGATTTCAAGAAAAAACGTACGCTGCAGGTCGAC	Primer to obtain amplicon of pYM13 for genomic integration of TAP KanMX6 together with primer 1724	*NET1*
2290	GATGGTACCGCGATGTCTATTTGAAAGTCTCTCAAATGAGGCAGCTTTAAAAGCGAACCGTACGCTGCAGGTCGAC	Primer to obtain amplicon of pYM13 for genomic integration of TAP KanMX6 together with primer 1689	*RPO31*
2291	GATGGTACCAAGATTTATAGAATAAAAGAGAGGATAGTGCTAAGCAATGTCCGCCCTATGCGT	Primer to obtain amplicon of pYM13 for genomic integration of TAP KanMX6 together with primer 2292	*TFC7*

	ACGCTGCAGGTCGAC		
2292	CTACCGCGGATGCACCTGTGTTCTTTAAATAAGGTTGCTGCTGCTACAAAATACATAATCGATGAATTCGAGCTCG	Primer to obtain amplicon of pYM13 for genomic integration of TAP KanMX6 together with primer 2291	*TFC7*
2411	GATGGTACCGAAGAAATTAGAAGATGCTGAGGGCCAAGAAAATGCTGCTTCTTCAGAATCGTACGCTGCAGGTCGAC	Primer to obtain amplicon of K643 for genomic integration of MNase-3xHA KanMX6 together with primer 2413	*RIM1*
2412	GATGGTACCAAGAGTACAAAAAAGCTATCCAAGAATATAATGCTCGCTACCCTCTCAACTCGTACGCTGCAGGTCGAC	Primer to obtain amplicon of K643 for genomic integration of MNase-3xHA KanMX6 together with primer 2414	*ABF2*
2413	CTACCGCGGGATAAAAAATATCGAGGAAGAGTCGAAATAAGCAAGCGTAAATATTACAAATCGATGAATTCGAGCTCG	Primer to obtain amplicon of K643 for genomic integration of MNase-3xHA KanMX6 together with primer 2411	*RIM1*
2414	GACCTCGAGTAGGAACGGAAAGAATAAAGGCATAAAAAACATTGTGAGAGTACCGCGGTATCGATGAATTCGAGCTCG	Primer to obtain amplicon of K643 for genomic integration of MNase-3xHA KanMX6 together with primer 2412	*ABF2*
2494	GATGGTACCACGCGCGGAAATTGATGACGAAGAAGCAACCGCCATGTTTAAGCTGGAGTCGTACGCTGCAGGTCGAC	Primer to obtain amplicon of K643 for genomic integration of MNase-3xHA KanMX6 together with primer 2495	*IES1*
2495	CTACCGCGGTTCTTAAATGTATGTATGTGTGTGTGTGTGTGTGTGCGTATTGTTCTATTATCGATGAATTCGAGCTCG	Primer to obtain amplicon of K643 for genomic integration of MNase-3xHA KanMX6 together with primer 2494	*IES1*
2496	GATGGTACCTCCTGAAGTAAAACAACTTGAAAAAGAAGGAGAGGATGGACTGGACTCATCGTACGCTGCAGGTCGAC	Primer to obtain amplicon of K643 for genomic integration of MNase-3xHA KanMX6 together with primer 2497	*IES4*
2497	CTACCGCGGAACTAGAAAGTGTGGGGCCCTGAGAACAACTTTAAGCTGTTGACATTACCATCG	Primer to obtain amplicon of K643 for genomic integration of MNase-3xHA KanMX6 together with primer 2496	*IES4*

	ATGAATTCGAGCTCG		
2498	GATGGTACCGGAATACGAAGAGGTGGGCGTCGAAAGATTGCTTAACGATAGGTTTAGATCGTACGCTGCAGGTCGAC	Primer to obtain amplicon of K643 for genomic integration of MNase-3xHA KanMX6 together with primer 2499	*ARP4*
2499	CTACCGCGGCAAACTGCTAAACTGAAAGGCGACTTGTCATTCAACAACGTTTTCTATTCATCGATGAATTCGAGCTCG	Primer to obtain amplicon of K643 for genomic integration of MNase-3xHA KanMX6 together with primer 2498	*ARP4*
2500	GATGGTACCTGAGGGATTATTGAAAAGTCTATGGGACTACGTTAAGAAAAATACCGAGTCGTACGCTGCAGGTCGAC	Primer to obtain amplicon of K643 for genomic integration of MNase-3xHA KanMX6 together with primer 2501	*TAF14*
2501	CTACCGCGGTTTATTTATACAAACATAAAAGCGCGCATTTAACGCCCTTTTACCTTTTAATCGATGAATTCGAGCTCG	Primer to obtain amplicon of K643 for genomic integration of MNase-3xHA KanMX6 together with primer 2500	*TAF14*
2502	GATGGTACCAAGTCTTGAAGATCTGGACAAGGAAATGGCGGACTATTTCGAAAAGAAATCGTACGCTGCAGGTCGAC	Primer to obtain amplicon of K643 for genomic integration of MNase-3xHA KanMX6 together with primer 2503	*YRA1*
2503	CTACCGCGGAATTAAATTTAATAAAACCAAATTAAATCAAACAAAAAATTGACAATTAAATCGATGAATTCGAGCTCG	Primer to obtain amplicon of K643 for genomic integration of MNase-3xHA KanMX6 together with primer 2502	*YRA1*
2504	GACCTCGAGGAAGATGGTCGAGATATTGAGAAACGCTAGTCAAATCGTCTCCTCTGTTTCGTACGCTGCAGGTCGAC	Primer to obtain amplicon of K643 for genomic integration of MNase-3xHA KanMX6 together with primer 2505	*VPS1*
2505	CTACCGCGGGAGAAATACTCAAAACCAAGCTTGAGTCGACCGGTATAGATGAGGAAAACATCGATGAATTCGAGCTCG	Primer to obtain amplicon of K643 for genomic integration of MNase-3xHA KanMX6 together with primer 2504	*VPS1*
2506	CTGGAGCTCGGATCCGAGTTTATCATTATCAATACT	Primer to obtain amplicon from GPD promoter of yeast genomic DNA together with primer 2510	*GPD*

2507	CTGGAGCTCGGATCCCAAAGCGCCAGTTCATTTGGCG	Primer to obtain amplicon from CYC1 promoter of yeast genomic DNA together with primer 2511	*CYC1*
2508	CTGGAGCTCGGATCCCACCCAGACCGCGACAAATTA	Primer to obtain amplicon from TEF2 promoter of yeast genomic DNA together with primer 2512	*TEF2*
2509	CTGGAGCTCGGATCCTATTTCAGGGAGATTAACGTA	Primer to obtain amplicon from ADH1 promoter of yeast genomic DNA together with primer 2513	*ADH1*
2510	AGTTCTAGATCGAAACTAAGTTCTTGGTGT	Primer to obtain amplicon from GPD promoter of yeast genomic DNA together with primer 2506	*GPD*
2511	AGTTCTAGAGTGTTTGTGTGTCTATAGAAG	Primer to obtain amplicon from CYC1 promoter of yeast genomic DNA together with primer 2507	*CYC1*
2512	AGTTCTAGACGTTGACCGTATATTCTAAAA	Primer to obtain amplicon from TEF2 promoter of yeast genomic DNA together with primer 2508	*TEF2*
2513	AGTTCTAGAATGCTTGGTATAGCTTGAAAT	Primer to obtain amplicon from ADH1 promoter of yeast genomic DNA together with primer 2509	*ADH1*
2586	GGTTTTATATACAGCACCATGGAAG	Primer used for verification of 5S circle recombination together with 2587	*5S*
2587	CATGAAAGTTGGTCGGTAGG	Primer used for verification of 5S circle recombination together with 2586	*5S*
2663	GATGGTACCTCCTGCTAACTCTGAATTGACATTTGATGTTAAATTGGTCTCCATGAAATCGTACGCTGCAGGTCGAC	Primer to obtain amplicon of K643 for genomic integration of MNase-3xHA KanMX6 together with primer 2672	*FPR4*
2664	GATGGTACCGCCGAGCTTTAGTGAAGACGTAAAGGAAGAAGAAAGCAAAGTAGGAGCATCGTACGCTGCAGGTCGAC	Primer to obtain amplicon of K643 for genomic integration of MNase-3xHA KanMX6 together with primer 2673	*IOC4*
2665	GATGGTACCAACTGAACAGTTGGTAGCAGAGAAAATTCCGGAAAACGAAACCACTCATTCGTA	Primer to obtain amplicon of K643 for genomic integration of MNase-3xHA KanMX6 together with primer 2674	*ISW1*

	CGCTGCAGGTCGAC		
2666	GATGGTACCAGACCATTGTATCGTCGTTGGTAGATACATGAGAAGCGGTTTGAAGAAATCGTACGCTGCAGGTCGAC	Primer to obtain amplicon of K643 for genomic integration of MNase-3xHA KanMX6 together with primer 2675	*NOP1*
2667	GATGGTACCCAGATCAAGAAATACCGCTTCTTTCGCTGGTTCAAAGAAAACATTTGATTCGTACGCTGCAGGTCGAC	Primer to obtain amplicon of K643 for genomic integration of MNase-3xHA KanMX6 together with primer 2676	*NSR1*
2668	GATGGTACCAATATCTCATGAAACGGAATTCATGAATTTCTGGATAAATGTCTTACCATCGTACGCTGCAGGTCGAC	Primer to obtain amplicon of K643 for genomic integration of MNase-3xHA KanMX6 together with primer 2677	*RSC4*
2669	GATGGTACCTGATGAAGAGGAAAACCAAGGATCAGATGTTTCGTTCAATGAAGAGGATTCGTACGCTGCAGGTCGAC	Primer to obtain amplicon of K643 for genomic integration of MNase-3xHA KanMX6 together with primer 2678	*TOP2*
2670	GATGGTACCTGATCTTGTGAAGTTTTGCATGGGAGTGGCAGCTTTTGTGACCACCGCGTCGTACGCTGCAGGTCGAC	Primer to obtain amplicon of K643 for genomic integration of MNase-3xHA KanMX6 together with primer 2679	*UTP21*
2671	GATGGTACCATGGGATAAAACAGGAACTGTCGATGAAATAATAAAATTTTTATCTGAATCGTACGCTGCAGGTCGAC	Primer to obtain amplicon of K643 for genomic integration of MNase-3xHA KanMX6 together with primer 2680	*YTA7*
2672	CTACCGCGGTTGTATATAGTATTATAGATACATATATCAATACGTATGCATTAAGGACCATCGATGAATTCGAGCTCG	Primer to obtain amplicon of K643 for genomic integration of MNase-3xHA KanMX6 together with primer 2663	*FPR4*
2673	CTACCGCGGTTCCCCTCTATTGTTCAAAAGCAGAGTACATCAACTGCAATAGCAACAGGATCGATGAATTCGAGCTCG	Primer to obtain amplicon of K643 for genomic integration of MNase-3xHA KanMX6 together with primer 2664	*IOC4*
2674	CTACCGCGGAGCATGGTGTAGGATATATTAAAAAAAATCGAAATATAAAAAAAGAAGGTATCGAT	Primer to obtain amplicon of K643 for genomic integration of MNase-3xHA KanMX6 together with primer 2665	*ISW1*

	GAATTCGAGCTCG		
2675	CTACCGCGGAATAATTGAGCAAGCTACCAGAAACTTTTGACTAATTTCCTTTATTCAACATCGATGAATTCGAGCTCG	Primer to obtain amplicon of K643 for genomic integration of MNase-3xHA KanMX6 together with primer 2666	*NOP1*
2676	CTACCGCGGTTAACGTAAAAAGAGAAAAAATTGAAATTGAAATTCATTTCATTTTCTCAATCGATGAATTCGAGCTCG	Primer to obtain amplicon of K643 for genomic integration of MNase-3xHA KanMX6 together with primer 2667	*NSR1*
2677	CTACCGCGGTATATAGATACATGCATATGATGGGAAGACTATGAAGAGAGAGATAGTCAATCGATGAATTCGAGCTCG	Primer to obtain amplicon of K643 for genomic integration of MNase-3xHA KanMX6 together with primer 2668	*RSC4*
2678	CTACCGCGGTCTGATATAAACATATAAAAAGAATGGCGCTTTCTCTGGATAAATATTATATCGATGAATTCGAGCTCG	Primer to obtain amplicon of K643 for genomic integration of MNase-3xHA KanMX6 together with primer 2669	*TOP2*
2679	CTACCGCGGAAAAATATACAATCTGCCTTTGTTACTAATATACTTGTTCTATATAATGCATCGATGAATTCGAGCTCG	Primer to obtain amplicon of K643 for genomic integration of MNase-3xHA KanMX6 together with primer 2670	*UTP21*
2680	CTACCGCGGTATATGAACTAACTACATTTAAGAATTATATAAACATTATGGACTCCTGCATCGATGAATTCGAGCTCG	Primer to obtain amplicon of K643 for genomic integration of MNase-3xHA KanMX6 together with primer 2671	*YTA7*
2686	GATGGTACCCCTGCAGGATGTCGAAAGCTACATATAA	Primer to obtain amplicon from URA3 gene together with primer 2687	*URA3*
2687	CTACCGCGGCCTGCAGGTTAGTTTTGCTGGCCGCATCT	Primer to obtain amplicon from URA3 gene together with primer 2686	*URA3*
3034	CCACCTACCGACCAACTTTC	Primer to obtain template for Southern probe preparation from yeast genomic DNA together with primer 3035	*5S*
3035	GAGGTGTTATGGGTGGAGGA	Primer to obtain template for Southern probe preparation from yeast genomic DNA together with primer 3035	*5S*
3036	GCAAGCTCCCTCGAGTACAA	Primer to obtain template for Southern	*E-Pro*

		probe preparation from yeast genomic DNA together with primer 3037	
3037	GGAAAGCGGGAAGGAATAAG	Primer to obtain template for Southern probe preparation from yeast genomic DNA together with primer 3036	*E-Pro*
3038	AATACTGCCGCCGAAATTCT	Primer to obtain template for Southern probe preparation from yeast genomic DNA together with primer 3039	*rARS*
3039	ATGCAAGCTCCCTCGACA	Primer to obtain template for Southern probe preparation from yeast genomic DNA together with primer 3038	*rARS*
3149	GATGGTACCTTTTTTTTACGATCGGGATTTCTTCTTCAAGAATGTGTGTGTAAAAATGTCGTACGCTGCAGGTCGAC	Primer to obtain amplicon of K643 for genomic integration of MNase-3xHA KanMX6 together with primer 3150	*TBS1*
3150	CTACCGCGGCGCGTATGCATATGTATTAGTTAAATTACTCGAATGTCCTTTATATAATAATCGATGAATTCGAGCTCG	Primer to obtain amplicon of K643 for genomic integration of MNase-3xHA KanMX6 together with primer 3149	*TBS1*
3177	GATGGTACCTGGCTATGAACATTACACCACGTTTATATACCGATCGTTCGAGAGATTTTCGTACGCTGCAGGTCGAC	Primer to obtain amplicon of pYM13 for genomic integration of TAP KanMX6 together with primer 3178	*RPB2*
3178	CTACCGCGGAATGAAATGTTTTTTATTATTTTACTTTCTTAGAGTTACAACATTATTTCATCGATGAATTCGAGCTCG	Primer to obtain amplicon of pYM13 for genomic integration of TAP KanMX6 together with primer 3177	*RPB2*
3179	GATGGTACCCTGAGCTATCCGCAATGGGTATAAGATTGCGTTATAATGTAGAGCCCAAACGTACGCTGCAGGTCGAC	Primer to obtain amplicon of pYM13 for genomic integration of TAP KanMX6 together with primer 3180	*RPA135*
3180	CTACCGCGGCCAAGCCTTCATTTACCATTCTATATCAATTTGGAAAGAAGGGTATTTCTATCGATGAATTCGAGCTCG	Primer to obtain amplicon of pYM13 for genomic integration of TAP KanMX6 together with primer 3179	*RPA135*
3243	GATGGTACCTCCGGTAGAAGA	Primer to obtain amplicon of K643 for	*YLR278C*

	CTTTTGGACGATTAATGATGACTACGGCTTTTTAACGTCGTACGCTGCAGGTCGAC	genomic integration of MNase-3xHA KanMX6 together with primer 3244	
3244	CTACCGCGGAAAAAAAAAAAAAGGAATGAGTTTGTACATACTATTATATTAATGTAGTAATCGATGAATTCGAGCTCG	Primer to obtain amplicon of K643 for genomic integration of MNase-3xHA KanMX6 together with primer 3243	*YLR278C*
3249	TGACGGAAATACGCTTCAGA	Primer used for qPCR amplifying a region in rARS together with 3250	*rARS*
3250	GCCAGATGAAAGATGAATAGACA	Primer used for qPCR amplifying a region in rARS together with 3250	*rARS*
3251	GGGTAACCCAGTTCCTCACTT	Primer used for qPCR amplifying a region in rARS together with 3252	*rARS*
3252	TTGGTTTTGGTTTCGGTTGT	Primer used for qPCR amplifying a region in rARS together with 3251	*rARS*
3253	ACCTCTCTCCGTATCCTCGT	Primer used for qPCR amplifying a region in rARS together with 3254	*ARS416*
3254	GACGACTTGAGGCTGATGGT	Primer used for qPCR amplifying a region in rARS together with 3253	*ARS416*
3255	GGGTGGTGTGATCTTTAACCA	Primer used for qPCR amplifying a region in rARS together with 3256	*ARS1215*
3256	GGCCTTGTAATTCAGTTTGTTCA	Primer used for qPCR amplifying a region in rARS together with 3255	*ARS1215*
3257	GCAGCTCCAAAAGAAAGGAA	Primer used for qPCR amplifying a region in rARS together with 3258	*ARS522*
3258	GTTTACCGGGGATGATGATG	Primer used for qPCR amplifying a region in rARS together with 3257	*ARS522*
3280	GATGGTACCAATTGATCTTGATAAGCTACTTGGAATTTTCCCTAACCTGAGTAACTTTTCGTACGCTGCAGGTCGAC	Primer to obtain amplicon of K643 for genomic integration of MNase-3xHA KanMX6 together with primer 3281	*YLL054C*
3281	CTACCGCGGAGCATTAGTTTACTAACTTTCTCCTCGTATCTTTCAAATTTGTATTCCCCATCGATGAATTCGAGCTCG	Primer to obtain amplicon of K643 for genomic integration of MNase-3xHA KanMX6 together with primer 3280	*YLL054C*

C. DNA size markers

2-log ladder (NEB)
size of fragments (bp): 10000, 8000, 6000, 5000, 4000, 3000, 2000, 1500, 1200, 1000, 900, 800, 700, 600, 500/517, 400, 300, 200, 100

1kB ladder (NEB)
size of fragments (bp): 10002, 8001, 6001, 5001, 4001, 3001, 2000, 1500, 1000, 517, 500

100bp ladder (NEB)
size of fragments (bp): 1517, 1200, 1000, 900, 800, 700, 600, 500, 517, 400, 300. 200, 100

D. DNA probes for Southern blot detection

name	**synthesis**	**locus**	**restriction enzyme**	**fragment size (kb)**
3.5kb rDNA	digest of pNOY373 with *Nco*I and purification of 3.5kb fragment	rDNA	EcoRI	2.6, 1.9, 0.7
rDNp	PCR from genomic DNA using primers 817 and 818	rDNA	XcmI	4.9
GAL1	PCR from genomic DNA using primers 1163, 1164	GAL1-10	EcoRI	1.9
NUP57	PCR from genomic DNA using primers 1167, 1168	NUP57	XcmI	4.2
rDNA_IGS	PCR from genomic DNA using primers 711, 1558	rDNA	PflMI	9.2
IGS2	PCR from genomic DNA using primers 1161, 1162	rDNA	XcmI	4.3
LEXA	PCR from plasmid pM49.2 using primers 597, 598	LEXA	-	-
5S	PCR from genomic DNA using primers 2099, 2100	5S	-	-
5S_REA	PCR from genomic DNA using primers 3034, 3035	5S	NcoI PvuI/SphI	0.77 0.74

IGS2	PCR from genomic DNA using primers 1161, 1162	rDNA	XcmI	4.3

E. Plasmids

To generate pT30, oligonucleotides 1045 and 1046 were annealed and cloned into AflII digested plasmid K773 (pT28) (Reiter et al., 2012). Plasmid K366 (pT2) (Reiter et al., 2012) was digested SacII and DraIII and the resulting 8.812bp fragment was ligated with the 1.507bp SacII and Dra III fragment of pT30, yielding pT32. Plasmid K450 (pKM4) (Reiter et al., 2012) was digested with BamHI and SbfI and cloned into BamHI and SbfI digested YEplac195 (Gietz and Sugino, 1988) yielding plasmid K451 (pKM5). A 4.439bp MluI-SbfI fragment of pT32 was inserted into the 10.203bp MluI-SbfI backbone of K451 (pKM5), yielding K673 (pT34). Plasmid K375 (pT11) was digested with PstI and BamHI and the resulting 4.526bp fragment was cloned into the BamHI and PstI digested backbone of K673 (pT34) resulting in plasmid K674 (pT36).

For construction of plasmids containing a modified IGS region of the rDNA locus, a BamHI/NotI fragment of pNOY373 (Wai et al., 2000) was cloned into BamHI and NotI digested pBlueskript KS (Stratagene) resulting in plasmid K1560 (pBlueskript BamHI NotI 5S). A NotI/BsrGI fragment containing the E-pro region, a BseRI/SphI fragment containing the 5S rDNA gene and a SphI/BamHI fragment containing the ARS element from K1560 were blunted and cloned into HpaI and XhoI digested, blunted plasmid pM49.2 (Griesenbeck et al., 2004) yielding K1578 (pUS6), pMW5a, and pUS1, respectively. The resulting plasmids were digested with BamHI and PstI for pUS6 and pMW5a or with BamHI and SbfI for pUS1, blunted and reinserted into NotI and BsrGI digested, blunted, BsrGI and SphI digested, blunted or SphI and BamHI digested, blunted K1560 yielding pUS9b, pBlueskript_5S-RS and K1577 (pUS3), respectively. The self-complementary oligonucleotide 2629 was annealed and ligated with SacII restricted pUS9b in order to introduce a NotI restriction site yielding K2024 (pUS9b_NotI). pBlueskript_5S-RS was digested with NotI and SmaI and the resulting 2.158bp fragment was cloned into NotI/SmaI digested pNOY373 yielding pNOY373_5S-RS. pUS9b_NotI was digested with NotI and BamHI and cloned into NotI and BamHI digested pNOY373 yielding pUS11. pUS3 was digested with NotI and EcoRI and the blunted 2.197bp fragment was ligated with NotI and BamHI digested blunted pNOY373 yielding pUS5. pNOY373_5S-RS was digested with SmaI and PstI and the 9.457bp fragment was cloned into PstI and BamHI digested pT4 (Reiter et al., 2012) yielding K1185 (pAG43). pUS5 was linearized with PstI and ligated with PstI linearized pT4 resulting in K2026 (pUS7). pUS11 was digested with BamHI and PstI and cloned into BamHI and PstI

digested pT4 resulting in K2027 (pUS12). Generation of plasmids K375, K389, K1185 and K1785 has been described in (Reiter et al., 2012).

A set of plasmids for inducible expression of R recombinase and constitutive expression of LexA-TAP was constructed. The *CYC1*, *TEF2 or ADH1* promoter regions, differing largely in their expression strength, were amplified with primer pairs 2507/2511, 2508/2512 or 2509/2513 from yeast genomic DNA. The PCR products were digested with XbaI and XhoI and cloned into XbaI and XhoI digested pBlueskript KS yielding plasmids pBlueskript_CYC1, pBlueskript_TEF2 or pBlueskript_ADH1. The KpnI/XbaI fragment of plasmid pJSS3 (Griesenbeck et al., 2004) containing the coding sequence of LexA-TAP was cloned into KpnI and XbaI digested pBlueskript_CYC1, pBlueskript_TEF2 or pBlueskript_ADH1 resulting in pBlueskript_CYC1 LexA-TAP, pBlueskript_TEF2 LexA-TAP or pBlueskript_ADH1 LexA-TAP. The plasmids were digested with BamHI and KpnI and the resulting fragments were blunted and cloned into SmaI linearized pB3 (Griesenbeck et al., 2004) yielding K2048 (pSH15), K2049 (pSH17) or K2050 (pSH19).
Another plasmid K929 (pKG7) allows inducible expression of R recombinase and LexA-TAP both under control of the bidirectional *GAL1-10* promoter. To this end, plasmid K356 (pJSS3) (Griesenbeck et al., 2004) was linearized with BssHII and the resulting 7.891bp fragment was blunted and ligated with SmaI linearized plasmid K355 (pB3) yielding K363 (pR2). K363 was digested with SpeI and the resulting 11.239bp fragment was religated yielding K929 (pKG7). The plasmids K2048 (pSH15), K2049 (pSH17), K2050 (pSH19) and K929 (pKG7) allow ectopic expression of R Recombinase under control of the inducible *GAL1-10* promoter and expression of the LexA-TAP protein under control of the constitutive *CYC1*, *TEF2, ADH1* or inducible *GAL1-10* promoter, respectively. The transformed plasmids have to be maintained in the yeast cell, which is accomplished by a selectable *LEU2* marker gene present on all the expression plasmids. However, cells must be grown in minimal medium lacking leucine in order to obtain uniform cell populations including the plasmid.
In order to conduct the chromatin preparations from yeast cells grown in full medium, the expression cassettes for R recombinase and LexA-TAP were flanked with homologous sequences of the yeast *URA3* gene. To this end, the *URA3* coding sequence was amplified with primer pair 2686, 2687 from yeast genomic DNA. The PCR product was digested with KpnI and SacII and cloned into KpnI and SacII digested pBlueskript KS yielding K2051 (pBlueskript_URA3). Plasmids pSH15 and pSH17 were digested with BssSI and the resulting 9.314bp or 9428bp fragments were blunted and cloned into StuI linearized plasmid K2051 yielding K2054 (pSH23) and K2052 (pSH21). K2052 (pSH21) was digested with HindIII and PflFI, blunted and religated yielding K2053 (pSH22). The

plasmids K2052 (pSH21) and K2054 (pSH23) allow genomic integration of the expression cassettes for R Recombinase under control of the inducible *GAL1-10* promoter and the LexA-TAP protein under control of the constitutive *TEF2* or *CYC1* promoters, respectively. Plasmid K2053 (pSH22) allows genomic integration of the expression cassette for R Recombinase under control of the *GAL1-10* promoter without LexA-TAP expression. The plasmids were digested with SbfI and the resulting DNA fragments were transformed in the yeast cells allowing the stable chromosomal integration of the expression cassette at the endogenous *URA3* locus by homologous recombination. Mutant clones for positive integration were selected on SCD-LEU plates for the *LEU2* marker present on the expression cassettes.

plasmid	**#**	**Cloning**	**Function**	**Reference**
pBluescript KS (+/-)	1		LacZ T3 and T7 promoter M13 - 20 T7 and SK primer Col E 1 - Origin f1ori (+or -)	Stratagene
pB3.1	K355	Leu2 marker framed with RS-sites, lexA SOS-box eliminated by *Bae*I-digest of pB2 and religation after blunting with Klenow	Shuttle vector for RecR-expression in yeast under the control of the *GAL1* promoter.	Joachim Griesenbeck
pJSS3.1	K356	LexA, plectin spacer, TAP tags amplified by PCR subcloned into the pCR2.1-TOPO. Final three-part ligation product subcloned into the E.coli-yeast centromeric shuttle vector p416-GPD (ATCC no. 87360).	Yeast expression vector for LexA-TAP under control of a glyceraldehydes-phosphate dehydrogenase (*GPD*) promoter	Joachim Griesenbeck
pT11	K375		E. coli/yeast shuttle vector used to construct strains with modified *RDN1* locus with *LEXA* binding sites and RS sites flanking the whole rDNA repeat	Joachim Griesenbeck

pT25	K389		E. coli/yeast shuttle vector used to construct strains with modified *RDN1* locus with *LEXA* binding sites and RS sites flanking the *RDN1* 35S CDS and promoter	
pKM9	K643	PCR with primers 839, 840 from pYM1 (V36; 3xHA-Tag) via *Bbs*I, *Bss*HII in *Bbs*I, *Bss*HII from pFA6a-MN-KanMX6 (K456)	(PCR-) template, cloning	Katharina Merz
pT36	K674		E. coli /yeast shuttle vector used to construct strains with modified *RDN1* locus with *LEXA* binding sites and RS sites flanking the *RDN1* 18S CDS including ETS1 and promoter	Joachim Griesenbeck
pAG43	K1185	insertion of a modified rDNA repeat containing a RS_3xLexA_5S_RS excision cassette from SmaI/PstI pNOY373_5S-RS@2 into BamHI_blunt/PstI pT4	E. coli /yeast shuttle vector used to construct strains with modified *RDN1* locus with *LEXA* binding sites and RS sites flanking the *RDN1* 5S CDS	Joachim Griesenbeck
pUS7	K2026		E. coli /yeast shuttle vector used to construct strains with modified *RDN1* locus with *LEXA* binding sites and RS sites flanking the ARS	Ulrike Stöckl
pUS12	K2027		E. coli /yeast shuttle vector used to construct strains with modified *RDN1* locus with *LEXA*	Ulrike Stöckl

			binding sites and RS sites flanking the E-Pro	
pSH_RIM1	K2046	PCR with primers 2411, 2413 from pKM9 via *Kpn*I and *Sac*II in pBluescript KS	genomic C-terminal MNase tagging by recombination, linearisation with *Kpn*I, *Sac*II	this study
pSH_ABF2	K2047	PCR with primers 2412, 2414 from pKM9 via *Kpn*I and *XhoI* in pBluescript KS	genomic C-terminal MNase tagging by recombination, linearisation with *Kpn*I, *Xho*I	this study
pSH_IES1	K2055	PCR with primers 2494, 2495 from pKM9 via *Kpn*I and *Sac*II in pBluescript KS	genomic C-terminal MNase tagging by recombination, linearisation with *Kpn*I, *Sac*II	this study
pSH_IES4	K2056	PCR with primers 2496, 2497 from pKM9 via *Kpn*I and *Sac*II in pBluescript KS	genomic C-terminal MNase tagging by recombination, linearisation with *Kpn*I, *Sac*II	this study
pSH_ARP4	K2057	PCR with primers 2498, 2499 from pKM9 via *Kpn*I and *Sac*II in pBluescript KS	genomic C-terminal MNase tagging by recombination, linearisation with *Kpn*I, *Sac*II	this study
pSH_TAF14	K2058	PCR with primers 2500, 2501 from pKM9 via *Kpn*I and *Sac*II in pBluescript KS	genomic C-terminal MNase tagging by recombination, linearisation with *Kpn*I, *Sac*II	this study
pSH_YRA1	K2059	PCR with primers 2502, 2503 from pKM9 via *Kpn*I and *Sac*II in pBluescript KS	genomic C-terminal MNase tagging by recombination, linearisation with *Kpn*I,	this study

			*Sac*II	
pSH_VPS1	K2060	PCR with primers 2504, 2505 from pKM9 via *Xho*I and *Sac*II in pBluescript KS	genomic C-terminal MNase tagging by recombination, linearisation with *Xho*I, *Sac*II	this study
pSH15	K2048	PCR with primers 2507, 2511 from yeast genomic DNA via *XbaI*, *XhoI* in pBluescript KS resulting in pBluescript_CYC1; LexA-TAP from pJSS3 via *KpnI*, *XbaI* into pBluescript_CYC1 resulting in pBluescript_CYC1 LexATAP; CYC1 LexATAP via blunted BamHI, KpnI into SmaI digested pB3.1 resulting in pSH15	Constitutive expression of LexA-TAP under control of *CYC1* promoter and inducible expression of R Recombinase under control of *GAL1-10* promoter; *LEU2* selection marker framed with RS sites	this study
pSH17	K2049	PCR with primers 2508, 2512 from yeast genomic DNA via *XbaI*, *XhoI* in pBluescript KS resulting in pBluescript_TEF2; LexA-TAP from pJSS3 via *KpnI*, *XbaI* into pBluescript_TEF2 resulting in pBluescript_TEF2 LexATAP; TEF2 LexATAP via blunted BamHI, KpnI into SmaI digested pB3.1 resulting in pSH17	Constitutive expression of LexA-TAP under control of *TEF2* promoter and inducible expression of R Recombinase under control of GAL1-10 promoter; LEU2 selection marker framed with RS sites	this study
pSH19	K2050	PCR with primers 2509, 2513 from yeast genomic DNA via *XbaI*, *XhoI* in pBluescript KS resulting in pBluescript_ADH1; LexA-TAP from pJSS3 via *KpnI*, *XbaI* into pBluescript_ADH1 resulting in pBluescript_ADH1 LexATAP; ADH1 LexATAP via	Constitutive expression of LexA-TAP under control of *ADH1* promoter and inducible expression of R Recombinase under control of *GAL1-10* promoter; *LEU2*	this study

		blunted BamHI, KpnI into SmaI digested pB3.1 resulting in pSH19	selection marker framed with RS sites	
pSH_FPR4	K2061	PCR with primers 2663, 2672 from pKM9 via *Kpn*I and *Sac*II in pBluescript KS	genomic C-terminal MNase tagging by recombination, linearisation with *Kpn*I, *Sac*II	this study
pSH_IOC4	K2062	PCR with primers 2664, 2673 from pKM9 via *Kpn*I and *Sac*II in pBluescript KS	genomic C-terminal MNase tagging by recombination, linearisation with *Kpn*I, *Sac*II	this study
pSH_ISW1	K2063	PCR with primers 2665, 2674 from pKM9 via *Kpn*I and *Sac*II in pBluescript KS	genomic C-terminal MNase tagging by recombination, linearisation with *Kpn*I, *Sac*II	this study
pSH_NOP1	K2064	PCR with primers 2666, 2675 from pKM9 via *Kpn*I and *Sac*II in pBluescript KS	genomic C-terminal MNase tagging by recombination, linearisation with *Kpn*I, *Sac*II	this study
pSH_NSR1	K2065	PCR with primers 2667, 2676 from pKM9 via *Kpn*I and *Sac*II in pBluescript KS	genomic C-terminal MNase tagging by recombination, linearisation with *Kpn*I, *Sac*II	this study
pSH_RSC4	K2066	PCR with primers 2668, 2677 from pKM9 via *Kpn*I and *Sac*II in pBluescript KS	genomic C-terminal MNase tagging by recombination, linearisation with *Kpn*I, *Sac*II	this study
pSH_TOP2	K2067	PCR with primers 2669, 2678 from pKM9 via *Kpn*I and *Sac*II in pBluescript KS	genomic C-terminal MNase tagging by recombination,	this study

			linearisation with *Kpn*I, *Sac*II	
pSH_UTP21	K2068	PCR with primers 2670, 2679 from pKM9 via *Kpn*I and *Sac*II in pBluescript KS	genomic C-terminal MNase tagging by recombination, linearisation with *Kpn*I, *Sac*II	this study
pSH_YTA7	K2069	PCR with primers 2671, 2680 from pKM9 via *Kpn*I and *Sac*II in pBluescript KS	genomic C-terminal MNase tagging by recombination, linearisation with *Kpn*I, *Sac*II	this study
pBluescript_URA3	K2051	PCR with primers 2686, 2687 from yeast genomic DNA via *Kpn*I and *Sac*II in pBluescript KS	genomic *URA3* gene flanked with SbfI sites for genomic integration of expression cassettes in *URA3* locus	this study
pSH21	K2052	*BssSI* digested and blunted pSH17 via *StuI* in pBluescript_URA3	Genomic integration of *TEF2* LexA-TAP *GAL1-10* RecR expression cassette by recombination in *URA3* locus, linearization with *SbfI*	this study
pSH22	K2053	*HindIII, PflFI* digestion of pSH21, blunting and re-ligation	Genomic integration of *GAL1-10* RecR expression cassette by recombination in *URA3* locus, linearization with *SbfI*	this study
pSH23	K2054	*BssSI* digested and blunted pSH15 via *StuI* in pBluescript_URA3	Genomic integration of *CYC1* LexA-TAP *GAL1-10* RecR expression cassette by recombination in *URA3* locus, linearization with	this study

			Sbfl	
pSH_TBS 1	K2072	PCR with primers 3149, 3150 from pKM9 via *Kpn*I and *Sac*II in pBluescript KS	genomic C-terminal MNase tagging by recombination, linearisation with *Kpn*I, *Sac*II	this study
pSH_YLR 278C	K2073	PCR with primers 3243, 3244 from pKM9 via *Kpn*I and *Sac*II in pBluescript KS	genomic C-terminal MNase tagging by recombination, linearisation with *Kpn*I, *Sac*II	this study
pSH_YLL 054C	K2074	PCR with primers 3280, 3281 from pKM9 via *Kpn*I and *Sac*II in pBluescript KS	genomic C-terminal MNase tagging by recombination, linearisation with *Kpn*I, *Sac*II	this study

5.1.4 Enzymes and polypeptides

All enzymes were used with the provided buffers.

GoTaq Polymerase	PROMEGA
Herculase	SRATAGENE
HotStar Taq	QUIAGEN
T4-DNA –polymerase	NEW ENGLAND BIOLABS
Restriction endonucleases	NEW ENGLAND BIOLABS
Antarctic phosphatase	NEW ENGLAND BIOLABS
T4-DNA-ligase	NEW ENGLAND BIOLABS
Zymolyase 100T	SEIKAGAKU CORPORATION
Proteinase K	SIGMA-ALDRICH
RNAse A	INVITROGEN
Trypsin	ROCHE
Protein-Marker Broad Range	NEW ENGLAND BIOLABS
Prestained ColorPlus Protein-Marker	NEW ENGLAND BIOLABS

5.1.5 Antibodies

antibody	origin	dilution	manufacturer
Anti H3	rabbit	1:1000	Abcam
Anti H3K4me3	rabbit	1:1000	Abcam
Anti-H3K36me3	rabbit	1:1000	Abcam
Anti-H4Ac	rabbit	1:1000	Millipore
Anti-A135	rabbit	1:5000	Buhler et al, 1980
Anti-TBP	rabbit	1:5000	
Anti-Reb1	rabbit	1:5000	
Anti CBP	goat	1:2500	Santa Cruz Biotechnology
Anti-PAP	rabbit	1:3000	Roche
3F10 anti-HA	monoclonal rat	1:5000	Roche
Anti-rat (peroxidase-conjugated)	goat	1:2500	Dianova
Anti-rabbit (peroxidase-conjugated)	goat	1:3000	Dianova
Anti-mouse (peroxidase-conjugated)	goat	1:5000	Dianova
Anti-goat (peroxidase-conjugated)	donkey	1:5000	Santa Cruz Biotechnology

5.1.6 Organisms

A. host bacteria

For cloning, the electro-competent *E. coli* strain “XL1BlueMRF” by Stratagene is used. genotype: Δ(mcrA)183, Δ(mcrCB-hsdSMR-mrr)173, endA1, supE44, thi-1, recA1, gyrA96, relA1, lac, λ-, [F’, proAB, lacIqZΔM15, tn10(tetr)+].

B. Yeast strains

Establishment of strains expressing MNase fusion proteins

Strains expressing yeast proteins with a C-terminal MNase carrying a triple hemagglutinin (3xHA) epitope from their chromosomal location were generated as described previously (Merz et al., 2008). Expression of the MNase fusion protein was

verified by Western blot analysis with antibodies 3F10 (Roche) recognizing the C-terminal 3xHA-tag of the fusion proteins (data not shown, see also (Merz et al., 2008)). None of the strains expressing MNase fusion proteins showed an obvious growth phenotype (data not shown).

Modification of the endogenous rDNA locus

A previously described method was used to genetically modify the endogenous rDNA locus (Wai et al., 2000), such that each rDNA repeat contained the specific insertion of RS elements and *LEXA* binding sites. To this end, the plasmids K375 (pT11), K389 (pT25), K674 (pT36), K1185 (pAG43), K1785 (pT11-WT), K2026 (pUS7), K2027 (pUS12) were digested with SpeI. The resulting DNA fragments contained a wildtype rDNA repeat (K1785) or a modified rDNA repeat, in which either the ARS (K2026), the 5S rRNA gene (K1185), the E-pro region (K2027), the 18S rRNA coding sequence (K674), the 35S rRNA gene (K389) or a complete rDNA repeat (K375) are flanked by RS elements and include *LEXA* binding sites. These fragments also contained sequences for integration and expansion of the modified rDNA repeats as described earlier (Wai et al., 2000). After transformation into yeast strain NOY989, mutant clones containing a re-expanded modified rDNA locus were selected as described (Wai et al., 2000).

name	**Genotype**	**reference or source**
NOY505	MATa ade2-1 ura3-1 trp1-1 leu2-3,112 his3-11 can1-100	(Nogi et al 1991)
NOY989	MATa ade2-1 ura3-1 trp1-1 leu2-3,112 his3-11 can1-100 rdnΔ::URA3/pNOY353	(Wai et al., 2000)
yS18	MATα; his3-11; his3-15; leu2-3; leu2-112; canr; ura3Δ5	(Sengstang et al, 1987)
yM7.8	MATα; his3-11; his3-15; leu2-3; leu2-112; canr; ura3Δ5; pho80::his3	(Boeger et al. 2003)
yM2.1	MATα; his3-11; his3-15; leu2-3; leu2-112; canr; ura3Δ5; pho5:RS-3xLexA-RS	(Boeger et al., 2003)
yM8.14	MATα; his3-11; his3-15; leu2-3; leu2-112; canr; ura3Δ5; pho80::his3; pho5:RS-3xLEXA-RS	(Boeger et al., 2003)
yM30.3	MATα; his3-11; his3-15; leu2-3; leu2-112; canr; ura3Δ5; pho80::his3; pho5 Promoter: RS-3xLEXA-RS; <TATA>	Hinrich Boeger

yM64.1	MATα; his3-11; his3-15; leu2-3; leu2-112; canr; ura3Δ5; pho5 Promoter: RS-3xLEXA-RS; <TATA>	Hinrich Boeger
y908	MATa; ade2-1; ura3-1; trp1-1; leu2-3,112; his3-11; can1-100; rdn:L_5S_RS_35S_3xLEXA_RS_L	this study
y909	MATa; ade2-1; ura3-1; trp1-1; leu2-3,112; his3-11; can1-100; rdn:L_5S_25S_RS_18S_3xLEXA_RS_L	this study
y1599	MATa; ade2-1; ura3-1; trp1-1; leu2-3,112; his3-11; can1-100; rdn ITS1-WT	(Reiter et al., 2012)
y1997	MATa; ade2-1; ura3-1; trp1-1; leu2-3,112; his3-11; can1-100; rdn:L_RS_5S_LEXA_RS_35S_L	this study
y2124	MATa; ade2-1; ura3-1; trp1-1; leu2-3,112; his3-11; can1-100; rdn:L_5S_35S_L	this study
y2125	MATa ade2-1 ura3-1 trp1-1 leu2-3,112 his3-11 can1-100; RIM1-MNase-3xHA:kanMX6	this study
y2126	MATa ade2-1 ura3-1 trp1-1 leu2-3,112 his3-11 can1-100; ABF2-MNase-3xHA:kanMX6	this study
y2157	MATa ade2-1 ura3-1 trp1-1 leu2-3,112 his3-11 can1-100; IES1-MNase-3xHA:kanMX6	this study
y2158	MATa ade2-1 ura3-1 trp1-1 leu2-3,112 his3-11 can1-100; IES4-MNase-3xHA:kanMX6	this study
y2159	MATa ade2-1 ura3-1 trp1-1 leu2-3,112 his3-11 can1-100; TAF14-MNase-3xHA:kanMX6	this study
y2160	MATa ade2-1 ura3-1 trp1-1 leu2-3,112 his3-11 can1-100; ARP4-MNase-3xHA:kanMX6	this study
y2161	MATa ade2-1 ura3-1 trp1-1 leu2-3,112 his3-11 can1-100; YRA1-MNase-3xHA:kanMX6	this study
y2162	MATa ade2-1 ura3-1 trp1-1 leu2-3,112 his3-11 can1-100; VPS1-MNase-3xHA:kanMX6	this study
y2258	MATa ade2-1 ura3-1 trp1-1 leu2-3,112 his3-11 can1-100; FPR4-MNase-3xHA:kanMX6	this study
y2259	MATa ade2-1 ura3-1 trp1-1 leu2-3,112 his3-11 can1-100; ISW1-MNase-3xHA:kanMX6	this study
y2260	MATa ade2-1 ura3-1 trp1-1 leu2-3,112 his3-11 can1-100; IOC4-MNase-3xHA:kanMX6	this study
y2261	MATa ade2-1 ura3-1 trp1-1 leu2-3,112 his3-11 can1-100; NOP1-MNase-3xHA:kanMX6	this study

y2262	MATa ade2-1 ura3-1 trp1-1 leu2-3,112 his3-11 can1-100; NSR1-MNase-3xHA:kanMX6	this study
y2263	MATa ade2-1 ura3-1 trp1-1 leu2-3,112 his3-11 can1-100; RSC4-MNase-3xHA:kanMX6	this study
y2264	MATa ade2-1 ura3-1 trp1-1 leu2-3,112 his3-11 can1-100; TOP2-MNase-3xHA:kanMX6	this study
y2265	MATa ade2-1 ura3-1 trp1-1 leu2-3,112 his3-11 can1-100; UTP21-MNase-3xHA:kanMX6	this study
y2266	MATa ade2-1 ura3-1 trp1-1 leu2-3,112 his3-11 can1-100; YTA7-MNase-3xHA:kanMX6	this study
y2267	MATa; ade2-1; ura3-1; trp1-1; leu2-3,112; his3-11; can1-100; rdn:L_ RS_LEXA_rARS_RS_5S_35S_L	this study
y2268	MATa; ade2-1; ura3-1; trp1-1; leu2-3,112; his3-11; can1-100; rdn:L_5S_RS_E-Pro_LEXA_RS_35S_L	this study
y2345	MATa; ade2-1; ura3-1; trp1-1; leu2-3,112; his3-11; can1-100; rdn:L_RS_5S_35S_LEXA_RS_L	this study
y2378	MATa; ade2-1; ura3-1; trp1-1; leu2-3,112; his3-11; can1-100; rdn:L_5S_35S_L; URA3::LEU2 pTEF2 LEXA-TAP pGAL RecR	this study
y2379	MATa; ade2-1; ura3-1; trp1-1; leu2-3,112; his3-11; can1-100; rdn:L_RS_5S_LEXA_RS_35S_L; URA3::LEU2 pTEF2 LEXA-TAP pGAL RecR	this study
y2380	MATa; ade2-1; ura3-1; trp1-1; leu2-3,112; his3-11; can1-100; rdn:L_5S_25S_RS_18S_LEXA_RS_L; URA3::LEU2 pTEF2 LEXA-TAP pGAL RecR	this study
y2381	MATa; ade2-1; ura3-1; trp1-1; leu2-3,112; his3-11; can1-100; rdn:L_5S_RS_35S_LEXA_RS_L; URA3::LEU2 pTEF2 LEXA-TAP pGAL RecR	this study
y2382	MATa; ade2-1; ura3-1; trp1-1; leu2-3,112; his3-11; can1-100; rdn:L_RS_5S_35S_LEXA_RS_L; URA3::LEU2 pTEF2 LEXA-TAP pGAL RecR	this study
y2383	MATa; ade2-1; ura3-1; trp1-1; leu2-3,112; his3-11; can1-100; rdn:L_RS_LEXA_rARS_RS_5S_35S_L; URA3::LEU2 pTEF2 LEXA-TAP pGAL RecR	this study
y2384	MATa; ade2-1; ura3-1; trp1-1; leu2-3,112; his3-11; can1-100; rdn:L_5S_RS_E-Pro_LEXA_RS_35S_L; URA3::LEU2 pTEF2 LEXA-TAP pGAL RecR	this study

y2385	MATa; ade2-1; ura3-1; trp1-1; leu2-3,112; his3-11; can1-100; rdn:L_5S_25S_RS_18S_LEXA_RS_L; URA3::LEU2 pGAL RecR	this study
y2386	MATa; ade2-1; ura3-1; trp1-1; leu2-3,112; his3-11; can1-100; rdn:L_5S_RS_35S_LEXA_RS_L; URA3::LEU2 pGAL RecR	this study
y2387	MATa; ade2-1; ura3-1; trp1-1; leu2-3,112; his3-11; can1-100; rdn:L_RS_5S_LEXA_RS_35S_L; URA3::LEU2 pGAL RecR	this study
y2388	MATa; ade2-1; ura3-1; trp1-1; leu2-3,112; his3-11; can1-100; rdn:L_5S_35S_L; URA3::LEU2 pGAL RecR	this study
y2389	MATa; ade2-1; ura3-1; trp1-1; leu2-3,112; his3-11; can1-100; rdn:L_RS_LEXA_rARS_RS_5S_35S_L; URA3::LEU2 pGAL RecR	this study
y2390	MATa; ade2-1; ura3-1; trp1-1; leu2-3,112; his3-11; can1-100; rdn:L_5S_RS_E-Pro_LEXA_RS_35S_L; URA3::LEU2 pGAL RecR	this study
y2391	MATa; ade2-1; ura3-1; trp1-1; leu2-3,112; his3-11; can1-100; rdn:L_RS_5S_35S_LEXA_RS_L; URA3::LEU2 pGAL RecR	this study
y2423	MATa; his3Δ-1; leu2Δ-0; met15Δ-0; ura3Δ-0; Rpa135-TEV-Prot-A::KanMX6	(Hierlmeier et al., 2012)
y2424	MATa; his3Δ-1; leu2Δ-0; met15Δ-0; ura3Δ-0; Rpb2-TEV-Prot-A::KanMX6	(Hierlmeier et al., 2012)
y2470	MATa; ade2-1; ura3-1; trp1-1; leu2-3,112; his3-11; can1-100; uaf30::URA3_KL; rdn:L_5S_35S_L; URA3::LEU2 pTEF2 LEXA-TAP pGAL RecR	this study
y2473	MATa; ade2-1; ura3-1; trp1-1; leu2-3,112; his3-11; can1-100; uaf30::URA3_KL; rdn:L_5S_RS_35S_LEXA_RS_L; URA3::LEU2 pTEF2 LEXA-TAP pGAL RecR	this study
y2618	MATa ade2-1 ura3-1 trp1-1 leu2-3,112 his3-11 can1-100; TBS1-MNase-3xHA:kanMX6	this study
y2619	MATa; ade2-1; ura3-1; trp1-1; leu2-3,112; his3-11; can1-100; rdn:L_5S_35S_L; URA3::LEU2 pTEF2 LEXA-TAP pGAL RecR; TBS1-MNase-3xHA:kanMX6	this study
y2620	MATa; ade2-1; ura3-1; trp1-1; leu2-3,112; his3-11; can1-100; rdn:L_RS_LEXA_rARS_RS_5S_35S_L; URA3::LEU2 pTEF2 LEXA-TAP pGAL RecR; TBS1-MNase-3xHA:kanMX6	this study
y2625	MATa ade2-1 ura3-1 trp1-1 leu2-3,112 his3-11 can1-100; YLR278C-MNase-3xHA:kanMX6	this study

y2626	MATa; ade2-1; ura3-1; trp1-1; leu2-3,112; his3-11; can1-100; rdn:L_5S_35S_L; URA3::LEU2 pTEF2 LEXA-TAP pGAL RecR; YLR278C-MNase-3xHA:kanMX6	this study
y2627	MATa; ade2-1; ura3-1; trp1-1; leu2-3,112; his3-11; can1-100; rdn:L_5S_RS_E-Pro_LEXA_RS_35S_L; URA3::LEU2 pTEF2 LEXA-TAP pGAL RecR; YLR278C-MNase-3xHA:kanMX6	this study
y2628	MATα; his3-11; his3-15; leu2-3; leu2-112; canr; ura3Δ5; URA3::LEU2 pCYC1 LEXA-TAP pGAL RecR	this study
y2629	MATα; his3-11; his3-15; leu2-3; leu2-112; canr; ura3Δ5; pho5:RS-3xLexA-RS; URA3::LEU2 pCYC1 LEXA-TAP pGAL RecR	this study
y2630	MATα; his3-11; his3-15; leu2-3; leu2-112; canr; ura3Δ5; pho80::his3; pho5:RS-3xLexA-RS; URA3::LEU2 pCYC1 LEXA-TAP pGAL RecR	this study
y2632	MATα; his3-11; his3-15; leu2-3; leu2-112; canr; ura3Δ5; pho80::his3; URA3::LEU2 pCYC1 LEXA-TAP pGAL RecR	this study
y2633	MATa; ade2-1; ura3-1; trp1-1; leu2-3,112; his3-11; can1-100; rdn:L_5S_35S_L; URA3::LEU2 pGAL RecR; TBS1-MNase-3xHA:kanMX6	this study
y2634	MATa; ade2-1; ura3-1; trp1-1; leu2-3,112; his3-11; can1-100; rdn:L_5S_35S_L; URA3::LEU2 pGAL RecR; YLR278C-MNase-3xHA:kanMX6	this study
y2635	MATa; ade2-1; ura3-1; trp1-1; leu2-3,112; his3-11; can1-100; rdn:L_RS_LEXA_rARS_RS_5S_35S_L; URA3::LEU2 pGAL RecR; TBS1-MNase-3xHA:kanMX6	this study
y2636	MATa; ade2-1; ura3-1; trp1-1; leu2-3,112; his3-11; can1-100; rdn:L_5S_RS_E-Pro_LEXA_RS_35S_L; URA3::LEU2 pGAL RecR; YLR278C-MNase-3xHA:kanMX6	this study
y2706	MATa ade2-1 ura3-1 trp1-1 leu2-3,112 his3-11 can1-100; YLL054C-MNase-3xHA:kanMX6	this study
y2707	MATa; ade2-1; ura3-1; trp1-1; leu2-3,112; his3-11; can1-100; rdn:L_5S_35S_L; URA3::LEU2 pGAL RecR; YLL054C-MNase-3xHA:kanMX6	this study
y2708	MATa; ade2-1; ura3-1; trp1-1; leu2-3,112; his3-11; can1-100; rdn:L_RS_LEXA_rARS_RS_5S_35S_L; URA3::LEU2 pGAL RecR; YLL054C-MNase-3xHA:kanMX6	this study

5.1.7 Equipment

device	**manufacturer**
Eraser	Raytest
4800 Proteomics Analyzer MALDI TOF/TOF	Applied Biosystems
ÄKTA™FPLC System	GE Healthcare
BAS cassette 2040	Fuji
BAS-III imaging plate	Fuji
Biofuge Fresco refrigerated tabletop centrifuge	Hereaus
Biofuge Pico tabletop centrifuge	Hereaus
Blacklight blue lamps 15 W	Sankyo-Denki
Branson Sonifier 250	Branson
C412 centrifuge	Jouan
CT422 refrigerated centrifuge	Jouan
DNA cross-linking system Fluo-Link tFL20.M	Vilber Loumat
Electrophoresis system model 45-2010-i	Peqlab Biotechnologie GmBH
Electroporation device Micropulser	Biorad
Gel Max UV transilluminator	INTAS
Hybridisation tubes	Bachofer, Rettberg
Hybridisation oven	Peqlab Biotechnologie GmBH
IKA-Vibrax VXR	IKA
Incubators	Memmert
LAS-3000 chemiluminescence imager	Fuji
NanoDrop ND-1000 spectrophotometer	Peqlab Biotechnologie GmBH
PCR Sprint thermocycler	Hybaid
peqSTAR 96 Universal Gradient	Peqlab Biotechnologie GmBH
Power Pac 3000 power supplies	Biorad
Rotor Gene RG-3000	Corbett Research
Shake incubators Multitron / Minitron	Infors
Stratalinker 1800	Stratagene
Sub-cell Gt Agarose Gel Electrophoresis System	Biorad
Thermomixer® Dry Block Heating Shaker	Eppendorf
Trans-Blot SD Semi-dry transfer cell	Biorad
BcMag Separator-24	Bioclone Inc.

BcMag Separator-50	Bioclone Inc.
Tefal Prep`line 810031 Coffee Grinder	Tefal
Ultimate 3000 nanoHPLC	Dionex
Ultrospec 3100pro spectrophotometer	Amersham

5.1.8 Consumables

Consumable	**manufacturer**
BM Chemiluminescence Blotting Substrate (POD)	Roche
ColorPlus Prestained Protein Marker, Broad Range (7-175 kDa)	New England Biolabs
Protein Marker, Broad Range (2-212 kDa)	New England Biolabs
Filter paper 3MM	Whatman
Gene pulser cuvettes	BioRad
Glass beads (0.75-1 mm)	Roth
Immobilon-P transfer membrane	Millipore
Multiwell plates (24 wells)	Sarstedt
Positive TM membrane	MP Biomedicals
ProbeQuant™ G-50 Micro Columns	GE Healthcare
Protein G SepharoseTM 4 Fast Flow	GE Healthcare
Calmodulin Affinity Resin	Stratagene
Protein Assay Dye Reagent Concentrate	Biorad
BcMag™ Epoxy-Activated magnetic beads	Bioclone Inc.
Ni-NTA Superflow	Quiagen
rabbit IgG	Sigma
Salmon Sperm DNA (10 mg/ml)	Invitrogen
SimplyBlue™ SafeStain	Invitrogen
TSK Gel 4000SW	Tosoh Bioscience
TSK Gel 5000PW	Tosoh Bioscience
SYBR Green	Roche
SYBR Safe DNA Gel Stain	Invitrogen

5.1.9 Software

software	**producer**
4000 Series Explorer	Applied Biosystems
Acrobat 7.0 Professional v.7.0.9	Adobe
Data Explorer v.4.5 C	Applied Biosystems
GPS Explorer v.3.5	Applied Biosystems
Image Reader LAS-3000 v.2.2	Fujifilm
Mascot	Matrix Science
Microsoft Office 2007	Microsoft
ND-1000 v.3.5.2	Peqlab Biotechnologie GmBH
Illustrator CS3	Adobe
MultiGauge v.3.0	Fujifilm
Rotor-Gene 6000	Corbett Research
Image Reader FLA-3000 v.1.8	Fujifilm

5.2 Methods

5.2.1 Enzymatic manipulation of DNA

A. Polymerase chain reaction (PCR)

PCR was performed in 30-50µl reactions. Each reaction contained the DNA to be amplified, 0.25mM desoxynucleotides, 20pmol of each the forward and the reverse primer, PCR buffer to a final concentration 1x with 1.5mM $MgCl_2$ and 2.5U GoTaq polymerase. The components were mixed in a 0.2 or 0.5ml reaction tube. Semi-hotstart was performed to eliminate primer-dimers, mispriming and secondary structure of the primer molecules. The reaction tubes are placed into the PCR machine block when the temperature has reached 80°C. DNA is initially denatured by heating the samples 3 minutes to 95°C. Amplification is performed in 35 cycles. Each cycle consists of denaturation of double-stranded DNA (45 seconds at 95°C), annealing of primers to matching DNA sequences (30 seconds at 3°C below melting temperature of the primers)

and amplification (1min per 1kb at 72°C). When all cycles are complete, amplification is continued for 10 minutes at 72°C. Temperature is then lowered to 4°C for storage.

B. Sequence specific restriction endonucleases

Restriction enzyme digestion was performed in buffer and temperature conditions as indicated by NEB. Control digestions for cloning were performed in 50µl reactions with 1µl of restriction enzyme per 1µg of DNA. Total glycerol concentration (present in restriction enzyme storage buffer) should not exceed 5%.

C. DNA Ligation

In order to clone DNA sequences into vectors, quantity of purified DNA fragments digested with restriction endonuclease(s) was measured by UV spectrometry (see 5.2.3). A three-time to five-time excess of insert DNA compared to the vector DNA fragment was incubated in a 20 µl ligase reaction (400U T4 DNA ligase NEB, 50 mM Tris-HCl, 10 mM $MgCl_2$, 1 mM ATP, 10 mM Dithiothreitol, 25 µg/ml BSA) 1 h at room temperature or overnight at 16°C. 1 to 3µl of ligation reaction was used for *E. coli* transformation (see 5.2.8).

5.2.2 Purification of nucleic acids

A. Plasmid Isolation

Plasmid DNA was isolated from *E. coli* cultures with kits. Pelleted cells are lysed with a buffer containing NaOH and SDS. Genomic DNA and proteins are precipitated when the alkaline lysate is neutralized with KOAc. The supernatant which still contains the plasmids is transferred to an anion exchange column which binds the DNA in low salt conditions. Remaining RNA and proteins are washed away. Then, plasmid DNA is eluted with high salt buffers, desalted by isopropanol precipitation and resuspended in TE or water.
Minipreps (up to 5ml of *E. coli* culture) were prepared with the Quiagen Quiaprep Spin miniprep kit. Midipreps (50ml of *E. coli* culture, yield up to 100µg of DNA) were prepared with the Invitrogen PureLink Quick Plasmid midiprep kit. Preparation was performed as indicated in the manual.

B. Isolation of genomic DNA from yeast

A culture of yeast cells was grown overnight in 5ml YPD. Cells were spun down and resuspended in 500µl H_2O. Cells were spun down again and resuspended in 500µl 1M sorbitol, 0.1M EDTA. 3µl of 2% zymolyase (10mM Tris-HCl pH8.0, 5% glucose, 2% zymolyase) were added and incubated for 60 minutes at 37°C. Spheroblasts were spun down at 5000g for 5 minutes (table-top centrifuge). After addition of 500µl IR buffer and 50µl 10% SDS, the samples were vortexed until lysis is complete (about 1 minute at full speed). Samples were incubated for 30 minutes at 65°C. For precipitation of nucleic acids, 200µl of 5M KOAc were added and samples were kept on ice for 20 minutes. Samples were spun down at 16600g for 20minutes at 4°C, the resulting supernatant was transferred to a new microtube. 1.5µl of RNAseA (100mg/ml) was added and samples were incubated at room temperature over night. After addition of 750µl 2-propanol, DNA was precipitated at room temperature for 5 minutes and pelleted (13000rpm, 5minutes in table-top centrifuge). The pellet was washed once with ice-cold 70% EtOH and spun again (13000rpm, 5minutes in table-top centrifuge). The supernatant was discarded and the DNA pellet air-dried to eliminate remnants of ethanol. The dry pellet was resuspended in 50µl TE buffer.

C. Phenol Extraction

DNA from aqueous samples was extracted by phenol-chloroform. About one volume of Phenol-chloroform-isoamyl alcohol (25:24:1) was added to the sample. Samples were vortexed until the solution gets milky. Samples were centrifuged for at least 5 minutes at room temperature. An aliquot of the upper aqueous phase was transferred to a new reaction tube. The white layer of denatured protein in between the upper aqueous and the lower phenol phase should not be disturbed.

D. Ethanol precipitation

If samples do not yet contain at least 0.25M salt (e.g. 0.5x IRN buffer is sufficient), an equal volume of IRN was added to the sample. DNA is precipitated by addition of 2.5 new volumes of 100% ethanol; to precipitate small amounts of DNA, glycogen (2µl of 5mg/ml) can be supplemented. Samples were frozen (-20°C) for at least 1 hour and DNA was pelleted at full speed for 20 minutes at 4°C. To eliminate salt, the pellet can be washed with ice-cold 70% ethanol. The supernatant was discarded, the pellet air-dried and resuspended in TE or water.

E. Purification of PCR products

DNA samples from restricition digests and PCR products were purified with the “QIAquick PCR purification Kit” (Qiagen). DNA above an exclusion size (depending on experimental conditions) was bound to a silicate gel column while smaller DNA molecules, salts, nucleotides, enzymes and glycerol were removed. DNA was eluted with 2mM or 10mM Tris-HCl, pH 8.0.

5.2.3 Quantitative and qualitative analysis of nucleic acids

A. UV spectrometry

Concentration of pure DNA samples was measured by nanodrop UV spectroscopy at 260nm wavelength ($1OD_{260}$ = 50µg/ml). To determine contamination with proteins and RNA, absorbance was concomitantly measured at 280nm. The ratio of OD_{260}/OD_{280} of pure DNA is between 1.8 and 2.0.

B. Agarose gel electrophoresis

Agarose gel electrophoresis was used to separate DNA fragments of different lengths. Electrophoresis was performed routinely with 1.0% (w/v) agarose, 1xTBE gels containing SybrSafe (except for psoralen crosslinked DNA samples), and 1xTBE as electrophoresis buffer. To determine the lengths of the fragments, 1µg of DNA standard (2log ladder) was used in a concentration of 500µg/ml in 1xDNA loading buffer. Electrophoresis was performed at 3 to 5 volts per cm.

C. Southern Blot

DNA was transferred from an agarose gel to a positively charged nylon membrane (Positive$_{TM}$ Membrane, MP Biomedicals) by Southern blot. For denaturation of double-stranded DNA, the gel was incubated twice for 15 minutes in 0.5M NaOH, 1.5M NaCl on a shaker. Subsequently, the gel was incubated twice for 15 minutes in transfer buffer (1M NH_4OAc). The DNA was transferred upwards with capillary flow of transfer buffer through a blotting pile. The pile consisted of from bottom to top: a bridge of 2 thin Whatman papers placed over a reservoir of 1M NH_4OAc (Whatman 3MM, Whatman,

17x34cm) framed with parafilm to prevent bypass of capillary flow, the gel (upside down), the membrane, three thin Whatman papers (15x20cm) and recycling paper towels (about 10cm). All layers apart from the recycling paper towels were soaked in 1M NH_4OAc. The pile was covered with a glass or plastic plate. A weight (about 0.5kg) assured that the capillary transfer was not interrupted. It is important that no air bubbles remain between the membrane and the gel. Blotting was performed overnight or for at least 6h (1% gel). Afterwards, the DNA was crosslinked to the membrane ($0.3J/cm_2$). In this step, thymine bases are covalently bound to the amino groups of the membrane. The membrane can be dried and stored at room temperature.

D. Hybridisation

Up to four blots can be stacked into one hybridization tube, separated by meshes. Membranes were wetted with 2x SSC and prehybridised for 1h at hybridization temperature (65°C) with hybridization buffer (0.5M sodium phosphate buffer pH 7.2, 7% SDS). The buffer used for prehybridization was discarded and new prewarmed hybridization buffer (15ml) was poured into the tube. The probe was mixed with salmon sperm DNA (end concentration 100µg/ml), boiled at 95°C for five minutes and pipetted into the tube. Hybridization occured over night at hybridization temperature with gentle rotation in a hybridization oven. The blots should be covered with liquid, stick to the wall of the tube and not roll.
After hybridization, the probe in hybridization buffer can be stored at -20°C and reused. First, blots were rinsed once with 30ml 3x SSC, 0.1% SDS. Blots were washed at hybridization temperature while rotating the tube in the hybridization oven. Three washing buffers with decreasing salt- and rising SDS-concentration were used in the following order:

Wash 1 0.3x SSC, 0.1% SDS
Wash 2 0.1x SSC, 0.1% SDS
Wash 3 0.1x SSC, 1.5% SDS

Each wash step was repeated twice for 15 min. Afterwards, the blots were dried and stored at room temperature.

E. Detection of radioactive probes

A BAS-III imaging plate (IP) was erased with the Eraser (Raytest). The blot was put into a BAS cassette 2040 and the IP was taken out of the eraser in the dark and put onto the blot. The time of exposure depends on the radioactive signal. IPs were scanned with 100µM resolution in a phosphor imager (FLA3000 by Fujifilm).

F. Quantification of Southern Blots with *MultiGauge*

For quantitative analysis of Southern blots, the software program *MultiGauge 3.0* (fujifilm) was used. A square area is positioned over the bands of interest for profile analysis. The software calculates the signal intensity and plots it over the length of the band. Background (horizontal) is subtracted automatically. Signals are quantified by integration of the surface area below signal peaks. Values are given as QL or PSL. QL stands for quantum level and is a raw value; it is calculated by dividing the recorded emission by a constant factor. PSL stands for photo-stimulated luminescence; this value is proportional to the amount of radiation recorded from an image plate but does not give an absolute quantification of the volume of radiation (for reference and further information, see MultiGauge manual). For quantification the ratio of signal intensities of the band corresponding to restriction fragments can be calculated.

G. Quantitative real-time PCR (qPCR)

qPCR was used to measure the amount of a specific DNA fragment with high accuracy. The amount of DNA present at the end of each single PCR cycle was detected by measuring the fluorescence of SYBR-Green (Roche). SYBR-Green is a dye that shows fluorescence when bound to DNA double helices, but not in solution (excitation at 509nm, emission at 526nm). Therefore, the intensity of the fluorescence signal allows direct measurement of the amount of DNA present in a sample. qPCR reactions were performed in 0.1ml, the reaction volume was 20µl. The reaction contained 4µl of DNA sample and 16µl of master mix. The master mix contained 4pmol of the forward and the reverse primer, 0.25µl of a 1:400000 SYBR-Green stock solution in DMSO, 0.4U HotStarTaq-polymerase (Qiagen) and premix. Premix consisted of $MgCl_2$ (to adjust a final concentration of 2.5mM in the qPCR reaction), dNTPs (final concentration 0.2mM in the qPCR reaction) and 10 x PCR buffer (Qiagen; 1 x final concentration in the qPCR reaction). SYBR-Green was thawed in the dark. qPCR was performed in a Rotor-Gene RG3000 system (Corbett Research). SYBR-Green was excited at 480nm; fluorescence was recorded at 510nm. Data was evaluated by analysing the data with the comparative quantitation module of the RotorGene analysis software.

5.2.4 Manipulation of *Escherichia coli*

A. Preparation of electrocompetent bacteria

An overnight culture of *E. coli* XL1-Blue in SOB medium (OD600 approx. 3) was diluted 1:100 in SOB prewarmed to 37°C; this culture was grown with vigorous aeration at 300 rpm and 37°C for about 3 h, until the OD_{600} reached a value between 0.4 and 0.6. Then, the culture was chilled on ice for 15 min before being centrifuged for 10 min at 1000 g and 4°C in a GS3 rotor. Centrifugation was repeated after resuspension of the pellet in 400 ml ice-cold, sterile water and, after that, in 200 ml ice-cold, sterile water. The washed pellet was resuspended in 10 ml cold, sterile 10% (v/v) glycerol, transferred to a Falcon tube, and centrifuged at 5000 g and 4°C for 10 min. After resuspension of the pellet in 1.5 ml cold, sterile 10% (v/v) glycerol, 50–100 µl aliquots were stored at –80°C.

B. Transformation by electroporation

The required number of aliquots plus a background control aliquot was thawed on ice and pipetted into a chilled 0.2 cm electroporation cuvette. About 1ng of a plasmid miniprep or up to 3 µl of a ligation sample were pipetted into the cell drop. Pulsing was performed with programme EC2 in a micropulser. Immediately after the pulse, 1 ml 37°C LB medium was added and the sample was transferred in a microreaction tube following an incubation step for 30-60 min at 37°C. 100µl of the supernatant was plated on LB-Amp. The residual cells were spun down for one minute at 5000 rpm in a microfuge. About 800µl were discarded and the pellet was resuspended in the remaining supernatant, plated onto LB-Amp and incubated overnight at 37°C.

C. Liquid culture

A single colony was picked from a plate or a piece of frozen culture was scratched from the glycerol stock. Cells were transferred into a sterile tube containing 5ml of LB-Amp (50µg/ml ampicilline). The culture was incubated at 37°C over night.

5.2.5 Manipulation of *Saccharomyces cerevisae*

A. Preparation of competent yeast cells

50ml of an exponentially growing yeast culture was pelleted (500g, 5min at room temperature). The pellet was washed at room temperature with 25ml autoclaved H_2O, then with 5ml SORB. The pellet was resuspended in 500µl SORB, transferred to a reaction tube and repelleted. The supernatant was completely removed, the pellet then resuspended in 360µl SORB. 40µl of salmon sperm DNA was boiled at 95°C for 5 minutes and added to the cell suspension. After mixing, 50µl aliquots were transferred to fresh reaction tubes and placed at -80°C for storage.

B. Transformation of competent yeast cells

The required number of competent cell aliquots plus a background control was thawed on ice. DNA (2-5µg per transformation in about 1µg/µl concentration) was added to the cells and the sample was mixed. 6 volumes of PEG were added; samples were mixed thoroughly and incubated at room temperature for about 30 minutes. 1/9 of total volume (cells plus DNA plus PEG) of pure, sterile DMSO was added, samples were mixed and heat-shocked at 42°C for about 15 minutes. Cells were pelleted (2000rpm, 2minutes at room temperature in table-top centrifuge), the supernatant completely removed and the pellet resuspended in 1ml appropriate rich medium (without antibiotics). Cells were grown at 30°C for about 2 to 3 hours. After that, cells were pelleted, 9/10 of the supernatant was discarded. The cell pellet was resuspended in the remaining supernatant and plated on selective agar plates. When cells are selected for resistance to Geneticin, they should be replica-plated to identify positive clones.

C. Liquid culture

Yeast cultures were inoculated with a single colony from plates or with a piece of frozen culture ice from a -80°C glycerol stock. Cultures were grown in the respective medium at optimal growth temperature (30°C). Precultures were grown in sterile plastic tubes (10ml tube volume, 4ml maximal culture volume). Larger cultures were grown in glass flasks; the culture volume should not exceed 1/3 of the flask volume.

D. Permanent culture in glycerol

2ml of a freshly stationary yeast culture were mixed with 1ml of sterile 50% glycerol and separated to two aliquots. Cells were frozen on dry ice and stored at -80°C.

E) Establishment of MNase fusion strains

For each target gene, a PCR was performed with overhang primers. The primers are composed of a 5' sequence complementary to the target gene (50bp immediately before or after the stop codon) and 3' sequence complementary to pKM9 (S3 and S2 adapter, priming before and after the MNase-HA_3-KanMX cassette). The PCR was performed with a proofreading enzyme (Herculase); the PCR product was cloned into pBluescript and sequenced. After verification of sequence correctness, the plasmid was prepared with a Midi-prep kit. The insert was excised with restriction enzyme digestion and transformed into competent yeast cells. The KanMX marker was used for selection on Geneticin plates; initial plates were replica-plated. To screen for positive clones, colonies were stroked out, protein was isolated (denaturing protein isolation) and analyzed for HA signals of correct size (molecular weight of the protein factor plus 22kDa for the tag) by Western blot. None of the MNase tags led to an obvious growth phenotype.

F) Establishment of yeast strains with integrated RS and *LEXA* binding sites in the rDNA locus

A previously described method was used to genetically modify the endogenous rDNA locus (Wai et al., 2000), such that each rDNA repeat contained the specific insertion of RS elements and *LEXA* binding sites. To this end, the plasmids K375 (pT11), K389 (pT25), K674 (pT36), K1185 (pAG43), K1785 (pT11-WT), K2026 (pUS7), K2027 (pUS12) were digested with SpeI. The resulting DNA fragments contained a wildtype rDNA repeat (K1785) or a modified rDNA repeat, in which either the ARS (K2026), the 5S rRNA gene (K1185), the E-pro region (K2027), the 18S rRNA coding sequence (K674), the 35S rRNA gene (K389) or a complete rDNA repeat (K375) are flanked by RS elements and include *LEXA* binding sites. These fragments also contained sequences for integration and expansion of the modified rDNA repeats as described earlier (Wai et al., 2000). After transformation into yeast strain NOY989, mutant clones containing a re-expanded modified rDNA locus were selected as described (Wai et al., 2000).

5.2.6 Formaldehyde crosslinking (FA-X) of yeast cultures

Yeast cells were cultivated overnight at 30°C and then crosslinked in exponential phase (final OD_{600} = 0.4-0.6). Unless noted otherwise, Yeast Peptone Dextrose (YPD) medium

was used as growth medium and supplemented with adenine if the strain is auxotrophic for adenine. Formaldehyde was added to a final concentration of 1% and cells were fixed for 15 minutes at growth temperature while shaking. Excess formaldehyde was quenched with glycine (final concentration 125mM) for at least five minutes at room temperature. Cells were harvested in 50ml tubes (4,200 × g, 5min at 4°C in a microcentrifuge), suspended in 1ml of water, and transferred into 1.5ml microtubes. Yeast cells were collected by centrifugation (6,000 × g, 2min at 4°C in a microcentrifuge; supernatant was discarded), and the pellets were frozen in liquid nitrogen and stored at −20°C. Alternatively, cells were used immediately without freezing.

5.2.7 Preparation of nuclei

All steps were performed on ice. Cells were washed in 0.6ml of buffer A and 1× Protease inhibitors and then collected by centrifugation (16,000 × g, 2min at 4°C in a microcentrifuge; supernatant was discarded). The washing step was repeated three times. Finally, cells were suspended in 350µl of buffer A, 1× Protease inhibitors and ~500µl of glass beads were added. Note: There must be enough buffer solution to cover the beads by a thin layer. Cell disruption was done for 10min at maximum speed on the Vibrax shaker at 4°C. To collect the cell lysates, the bottom and cap of microtubes were pierced with a hot needle and placed in a 15ml tube. After centrifugation (130 × g, 1 min at 4°C) the glass beads remained in the microtubes and were discarded. The crude cell lysates, which were collected in the 15ml tubes, were transferred into new 1.5ml microtubes and centrifuged at 16,000 × g for 2min at 4°C (microcentrifuge). The supernatants were discarded and the pellets (containing crude nuclei) were suspended in 0.6ml of buffer A and 1× Protease inhibitors. After another centrifugation step (16,000 × g for 2min at 4°C) supernatants were removed. Buffer A contains 2mM EDTA, which inhibits premature MNase activation if Ca^{2+} is released from the endoplasmic reticulum. The EDTA concentration can be increased up to 4mM without affecting the quality of the experiment. The nuclei pellets can be frozen in liquid nitrogen and stored at -80°C or were used immediately in a ChEC assay.

5.2.8 Chromatin Endogenous Cleavage (ChEC)

Nuclei isolated from formaldehyde-crosslinked cells were suspended in buffer Ag and 1×Protease inhibitors in a total volume of 550–600µl (The volume to suspend crude nuclei is calculated such that it exceeds the summed volume of all samples of the ChEC

time course by at least 50µl), and pre-incubated at 30°C, thermomixer set at 750rpm, for 3min. After vigorous vortexing, one 80µl aliquot of the nuclei suspensions were transferred to new tubes and used as a control (0min ChEC): no calcium was added. For the rest of the nuclei suspensions, MNase-fusion proteins were activated by the addition of $CaCl_2$ (2µl of 0.1M stock solution per 100µl reaction volume; the final concentration is 2mM) and incubated at 30°C with constant shaking (thermomixer set at 750rpm). At different time intervals, 80µl aliquots were taken, transferred to 1.5ml microtubes containing 100µl of IRN buffer and mixed to stop the MNase activity (The incubation time in $CaCl_2$ containing buffer is carefully chosen and depends on the protein that is tagged with MNase. Namely, for very abundant proteins it is advisable to add naked, linear plasmid DNA to the nuclei to have an exogenous control for unspecific digestion. It is conceivable that MNase fusion proteins cut DNA surrounding their binding site and, thus, releasing themselves in the solvent and cutting more DNA non-specifically, like free MNases. After Southern blotting the membrane can be hybridised with the plasmid-specific probe to monitor the amount of nonspecific degradation. It is important to mix the suspension before taking aliquots because nuclei sediment.). Samples mixed with IRN can be kept at room temperature. At the end of the time course, 100µl of IRN were added to the “0 min ChEC” aliquots.

5.2.9 DNA workup of ChEC samples

Nuclei are treated with 2µl of RNase A (20 mg/ml), mixed, and incubated at 37°C for at least 1h. 10µl of 10% SDS and 2µl of Proteinase K (20mg/ml) are added, mixed, and samples are incubated for 1h at 56°C. Formaldehyde crosslink is reversed by incubation at 65°C overnight. DNA is extracted with phenol–chloroform–isoamyl alcohol. 1× volume of IRN and 2.5× volume of ethanol are added and DNA is precipitated at −20°C for at least 20min. DNA is collected by centrifugation at 16,000 × g for 20min at 4°C. DNA is dried for 5–10min at room temperature and resuspended in 25µl of TE buffer.

5.2.10 Restriction digest and agarose gel electrophoresis of ChEC samples

12µl of each sample were digested with the appropriate restriction enzyme in a final volume of 20µl as recommended by the manufacturer overnight. 10× DNA loading buffer

was added to the samples prior to loading on a 1% agarose gel (250ml, 15 × 20 cm) containing 1x SybrSafe stain. DNA prepared from the ChEC assay was separated at 6V/cm during 6h in 1xTBE running buffer. After electrophoresis, the DNA from the agarose gels was transferred to a positively charged membrane by Southern blot as described in 5.2.3.

5.2.11 Chromatin Immuno Precipitation (ChIP)

ChIP was performed mainly as described (Hecht and Grunstein, 1999). Formaldehyde fixed cells from 50ml of an exponentially growing yeast culture were washed (1min, 13000 rpm, 4°C) with 1ml of cold ChIP lysis buffer and suspended in 400µl of ChIP lysis buffer, EGTA and EDTA in the buffer suppress MNase activity. Glass beads (Ø 0.75-1.0 mm, Roth) were added and cells were disrupted on a VXR basic IKA Vibrax orbital shaker for 3x15min with 2000-2200rpm at 4°C. DNA was sonicated in a volume of 1ml ChIP lysis buffer using a Branson Sonifier 250 to obtain an average DNA fragment size of 500bp. Cell debris was removed by centrifugation (20min, 13000rpm, 4°C). The chromatin extracts were split into three aliquots. 40µl of each aliquot served as an input control, 200µl of each aliquot were incubated for 90min at 4°C with 1µg of a monoclonal α-HA antibody (3F10, Roche) and 125µl of Protein G sepharose (Amersham) to enrich the MNase-HA_3-tagged proteins bound by the antibody. After immunoprecipitation, the beads were washed three times with ChIP lysis buffer, twice with ChIP washing buffer I and twice with ChIP washing buffer II followed by a final washing step with TE buffer. 250µl of buffer IRN were added to the beads (IPs) and to the input samples. DNA was isolated as described for ChEC experiments (see 5.2.9). Both, DNA derived from Input and IP were resuspended in 50µl of TE buffer. Relative DNA amounts present in Input and IP DNA were determined by quantitative PCR using a RotorGene 3000 system (Corbett Research) and the comparative analysis software module. Primer pairs used for amplification are listed in 5.1.3 B. Input DNA was diluted 1:500, and IP DNA was diluted 1:100 prior to analysis. Retention of specific DNA-fragments was calculated as the fraction of total Input DNA. The mean values and error bars were derived from three independent ChIP experiments analysed in triplicate quantitative PCR reactions.

5.2.12 Purification of specific chromatin circles from *S. cerevisiae*

A. Cell culture and recombination of chromatin circles

Yeast cells competent for excision of chromatin domains by R Recombinase were cultivated overnight at 30°C in YPR or SCR medium. Recombination was induced at a cell density of 5-7 x 10^7 cells/ml (OD_{600} of 0.8-1.0) by adding galactose to a final concentration of 2% (wt/vol). Cells were grown for an additional 1.5 h at 30°C before harvesting to allow proper expression of R Recombinase and formation of chromatin circles. After induction, cells were harvested by centrifugation (10 min, 9000 x g at 4°C), yielding a wet weight between 3 and 4 g per litre of cell culture. After washing twice with water, cells were pelleted in sealed 20 ml syringes by centrifugation (5 min, 3000 x g at 4°C). Syringes were unsealed, supernatants were decanted, and cells were extruded into liquid nitrogen. The resulting “cell spaghetti” were stored at –80°C until use.

B. Cell lysis by coffee grinder

A commercial coffee grinder (TEFAL, Prep`line) was pre-cooled by grinding 30-50g of dry ice for two times. The resulting powder of dry ice was discarded. Appropriate amount of frozen cells (3-4g of rDNA circles or 18-20g of PHO5 circles) were mixed with ~ 60g of dry ice and ground in the coffee mill. The coffee grinder is run for 3x1 min, with short intervals in between. Occasional tapping with a spatula against the outside of the mill prevents ground cells from sticking in a layer to the inside wall of the grinder. The fine powder of ground yeast can be stored at –80°C.

C. Affinity purification of chromatin circles using IgG coupled magnetic beads

After evaporation of dry ice, the powder is dissolved in 0.75ml of cold buffer MB with 1x Protease Inhibitors per 1g of ground yeast cells. The cell lysate was cleared from cell debris by centrifugation for 30min in a microcentrifuge (13.000rpm; 4°C). The protein concentration of the cleared lysate was determined using the Bradford assay. The whole amount of cell lysate (typically 1ml per 1g of yeast cells with 15-20mg/ml of total protein) was incubated with 2x200µl (for rDNA circles) or 1x200µl (for *PHO5* circles) of equilibrated (3x washing with 0.5ml buffer MB) IgG coupled magnetic beads slurry in 2x 1.5ml microcentrifuge tubes (rDNA circles) or 50ml Falcon tube (*PHO5* circles) and

rotated for 1h at 4°C. The beads were washed 5 times with 750µl cold buffer MB with 1x Protease Inhibitors. Between each washing step, the beads were gently rotated for 10min. Finally, the beads were washed with cold buffer MB without Protease Inhibitors. Chromatin circles were released by proteolytic cleavage for 2h or over night at 4°C with 10µg 6xHis-tagged recombinant TEV protease (100µg/ml dissolved in buffer MB without Protease Inhibitors) in a total volume of 100µl. The supernatant was transferred in a new microtube and residual chromatin circles were washed from the beads once with another 100µl buffer MB.

D. Depletion of TEV protease by Ni-NTA affinity chromatography

For rDNA chromatin circles, the 6xHis tagged TEV protease was depleted from the sample by Ni-NTA affinity chromatography. 40µl of equilibrated (3x washing with 0.5ml buffer MB) Ni-NTA slurry was incubated with the elution sample from 5.2.12.C by gentle rotation in a sealed BioRad 5ml batch column for 30min. The column was unsealed and the sample was passed in a new microtube. This step removed virtually all of the recombinant TEV protease.

E. Calmodulin affinity purification

For *PHO5* chromatin circles, the TEV elution was adjusted to a total volume of 400µl with buffer MB and supplemented with 2mM $CaCl_2$. The elution sample was applied to 200µl Calmodulin affinity slurry that had been equilibrated with buffer MB for at least 2h. Beads were incubated for 1h at 4°C and washed 4x with 1ml buffer CWB. Chromatin circles were eluted from Calmodulin beads by

1) applying 100µl CEB and the column was eluted by gravity flow
2) after closing the outlet of the column, 200µl CEB were applied and vortexed for 20 minutes at 4°C in a Vibrax at about 1000rpm; the column was eluted by gravity flow
3) further 100µl CEB were applied and the column eluted by gravity flow

All elution steps were combined resulting in a total volume of 400µl.

F. DNA and protein analysis of the purification

For DNA analysis, 20µl from each step of the purification is supplemented with 80µl H_2O and 100µl IRN buffer. RNA is digested with 3µl RNAseA (10mg/ml) for 1h at 37˚C. Afterwards, SDS (final concentration 0.5%) is added together with 3µl of Proteinase K (20mg/ml stock) and incubated for 1h at 56˚C. DNA is isolated by phenol-chloroform

extraction, precipitated with ethanol and resuspended in 20µl TE buffer. DNA circles were linearized by digestion with an appropriate restriction enzyme for 2h or over night at 37°C in a final volume of 30µl. The DNA samples were analyzed by Agarose gel electrophoresis, Southern blot or qPCR analysis.
For protein analysis, 10µl from each step of the purification were added to 20µl of SDS-sample buffer. The samples were loaded on SDS-Polyacrylamide gels and subjected to Western blotting or Silver staining.

5.2.13 Endonuclease digestion analysis of purified chromatin domains

For restriction enzyme endonuclease digestion of chromosomal and affinity purified chromatin domains, crude nuclei were prepared as described in (Reiter et al., 2012) and 5S rRNA chromatin circles were purified as detailed above. An aliquot of the crude nuclei corresponding to ~ 2 x 10^8 cells or 1.25% of the TEV elution were adjusted to a final volume of 100µl with the recommended conditions for the restriction enzyme (NEB). Digestion was performed for 60 min at the recommended temperature with 10 or 50 U for nuclei and 2 or 20 U for chromatin circles of the indicated restriction endonucleases. The reaction was terminated by adding the same volume of IRN buffer (50mM Tris-HCl, pH8, 20mM EDTA, 500mM NaCl). After treatment with RNase A (at a final concentration of 0.33mg/ml for 1h at 37°C), Proteinase K and SDS were added to a final concentration of 0.33mg/ml and 0.5% and incubation was continued for 1h at 56°C. After phenol/chloroform extraction, DNA was precipitated with ethanol by using 40 µg of glycogen as a carrier. The DNA was resuspended in 20µl H_2O and DNA molecules were linearized by digestion with 20U PvuI/SphI (nuclei) or 20U NcoI (chromatin circles) over night at 37°C in a final volume of 30µl. The DNA samples were then subjected to indirect-end labelling Southern blot analysis.

5.2.14 Micrococcus nuclease digestion of purified chromatin domains

For micrococcal nuclease digestion, 500 attomol of affinity-purified chromatin circles are adjusted to 2mM $MgCl_2$, 3mM $CaCl_2$ in a final volume of 850µl with MNase buffer containing 1µg of salmon sperm DNA (Invitrogen)/ml. As an input control, a sample is withdrawn before addition of the enzyme. Digestion is started by addition of 3.5U of

micrococcal nuclease (Sigma) and incubation at 30°C. After defined times of incubation digestion is terminated by the addition of the same volume of IRN buffer to each 200µl aliquot. After addition of 2.8 U of Proteinase K (Sigma), samples are incubated for 30 minutes at 56°C and further purified by phenol/chloroform extraction. DNA is precipitated with ethanol by using 100µg of glycogen/ml as a carrier. The DNA is resuspended in 20µl and samples are subjected to analysis by Southern blot.

5.2.15 Gel filtration chromatography of chromatin circles

For gel filtration chromatography of chromatin circles, yeast cell spaghetti were lysed by the “coffee grinder” method as described in 3.2.12 B. After evaporation of dry ice, the powder was dissolved with 1.25ml buffer GF with 1x Protease Inhibitors per 1g of yeast cell spaghetti. The cell lysate was cleared from cell debris by centrifugation for 20min in a microcentrifuge (13.000rpm; 4°C). A 500µl fraction of the resulting supernatant was loaded on a TSK Gel 4000SW or TSK Gel 5000PW column (Tosoh Bioscience) using an ÄKTA FPLC system. Separation was performed in buffer GF with a flow rate of 1ml/min and 500µl fractions were collected.

5.2.16 Protein-biochemical methods

A) Denaturing protein extraction of yeast cells

About 1ml (or less, depends on abundance of the desired protein) of an overnight yeast liquid culture was spun down. Cells were resuspended in 1ml ice-cold water. Samples were chilled on ice and supplemented with 150µl of pre-treatment solution (1.85M NaOH, 1M β-mercapto-ethanol) for 15 minutes on ice. Proteins were precipitated with 150µl 55% trichloroacetic acid for 10 minutes on ice and pelleted (13000rpm, 10minutes at 4°C in table-top centrifuge). The supernatant was discarded and the pellet resuspended in 30-50µl HU-buffer (5% SDS, 200mM Tris pH6.8, 1mM EDTA, 2.13mM β-mercapto-ethanol, 8M urea, bromophenolblue; store at -20°C). If colour turns yellow, the pH of the suspension is too acidic and must be neutralised with ammonia gas until the colour turns (dark) blue again. Proteins were denatured for 10 minutes at 65°C while shaking. Insoluble cell particles were pelleted (13000 rpm, 1min at room temperature). An adequate volume of the supernatant was analysed by Western blot.

B. Methanol chloroform precipitation of proteins

Protein precipitation for subsequent mass spectrometric analyses was performed using the chloroform/methanol precipitation method (Wessel and Flügge, 1984). The volume of the sample was adjusted to 150 µl with H_2O, followed by the addition of four volumes (600 µl) methanol, one volume (150 µl) chloroform and 3 volumes (450 µl) H_2O. After each of these addition steps, the sample was mixed well by vortexing. The resulting phases were separated by centrifugation in a table top centrifuge for 5 min, 13000 rpm. The upper phase was discarded while carefully avoiding loss of the interphase which contains the precipitated proteins. Upon addition of another three volumes of methanol (450 µl) and vortexing, the proteins were pelleted by centrifugation (5 min, 13000 rpm). The supernatant was completely removed and the protein pellet dried for 10 min at room temperature.

C. SDS-Polyacrylamide gel electrophoresis

Proteins were separated according to molecular weight by vertical, discontinuous SDS-PAGE according to Laemmli (1970). The discontinuous system consisted of a lower separating gel and an upper stacking gel:

separating gel	6%	8%	10%	12.5%	14.5%
H_2O	5.5ml	4.82ml	4.2ml	3.3ml	2.68ml
4x Lower Tris	2.5ml	2.5ml	2.5ml	2.5ml	2.5ml
30% Acrylamide (AA) + 0.8% Bis-AA	2.0ml	2.68ml	3.3ml	4.2ml	4.82ml
10% SDS	100µl				
TEMED	5µl				
25% APS	50µl				

stacking gel	6%	4%
H_2O	2.75ml	3.05ml
4x Upper Tris	1.25ml	1.25ml
30% AA + 0.8% bAA	1.00ml	0.65ml
10% SDS	100µl	
TEMED	5µl	
25% APS	50µl	

Pre-stained marker (NEB) was used as a molecular weight marker. The bands were stained blue so they were visible in the gel and on the membrane. Gels were run at 140V for 1.5h or until the bromophenolblue band reached the lower border of the gel.

Samples for mass spectrometric analyses were separated on 4-12 % gradient NuPAGE Bis-Tris gels (Life Technologies) using the NuPAGE MES SDS running buffer (Invitrogen) complemented with NuPAGE antioxidant (Life Technologies). Gel electrophoresis was performed according to the manufacturer's instructions except for the voltage applied. Instead of running the gels at constant 200 V, a constant current of 50 mA was applied while limiting the voltage to a maximum of 180 V.

D. Coomassie staining

To visualize the total protein content of a polyacrylamide gel, it was stained with SimplyBlue SafeStain (Invitrogen) according to the manufacturer's instructions. This stain is a commercially available pure (*i.e.* keratin-free) Coomassie G-250 stain. Briefly, the gel was washed 3 times 5 min with H_2O to remove SDS and buffer salts which interfere with the binding of the stain to the proteins. Staining was performed for 1 h at RT on a shaker, before destaining with H_2O.

E. Silver staining

To stain polyacrylamide gels with low protein content, the more sensitive silver staining was preferred over the Coomassie staining. The proteins were fixed in the gel by incubation in fixation-solution (50 % (v/v) methanol, 12 % (v/v) acetic acid, 0.02 % (v/v) formaldehyde) for 1 h or over night (RT). Afterwards the gel was washed in 50 % (v/v) ethanol for 20 min and incubated in 0.8 mM $Na_2S_2O_3$ for 1 min, directly followed by three 20 seconds wash steps with H_2O. Next, the gel was incubated in staining-solution (12 mM $AgNO_3$, 0.03 % (v/v) formaldehyde) for 20 min and washed two times for 20 seconds with H_2O. The stained protein bands became visible upon incubation with developing solution (566 mM Na_2CO_3, 0.02 % (v/v) formaldehyde, 0.016 mM $Na_2S_2O_3$). The development was stopped with 1 % acetic acid.

F. Western blot

After SDS-PAGE, proteins are associated with SDS and therefore negatively charged. Consequently, proteins can be blotted by semi-dry transfer to a PVDF-membrane by electric current (BIORAD semi-dry transfer apparatus). Three layers of thin Whatman paper were soaked in blotting buffer (25mM Tris, 190mM glycine, 20% methanol, pH8.3) and piled on the lower electrode (anode) of the semi-transfer device. The membrane (Immobilon PSQ 0.2µm, Millipore) was first soaked in methanol, then in blotting buffer and subsequently put onto the pile of Whatman papers. Air bubbles were carefully removed as they prevent the flow of the electric current. The membrane must be kept wet (with blotting buffer) all the time. The gel apparatus was disassembled, the gel was transferred onto the membrane. Air bubbles were removed and the gel was covered with three more layers of soaked Whatman paper. The blot was run at 24V for 1.5h. After blotting, the marker bands and lanes should be marked with a pen.

G. Ponceau staining

Western blots can be stained with Ponceau (0.5% Ponceau in 1% acetic acid) to control if proteins transfer worked properly. Staining was performed for one to three minutes at room temperature in a tray. Afterwards, the membrane was washed with water.

H. Detection of proteins by chemiluminescence

The membrane was blocked with blocking solution (5% milk powder in 1x PBST) to prevent unspecific binding of the antibody. Blocking was performed in a tray for 1h at room temperature or overnight at 4°C while shaking. The membrane was wrapped into a 50ml falcon tube containing the first antibody dilution (appropriate dilution in 1x PBST with 5% milk powder, 3ml for large membrane) and rotated at room temperature for 1h. After three five-minute washes with 1x PBST in a tray, the membrane was wrapped into a 50ml falcon tube with the second antibody (appropriate dilution in 1x PBST with 5% milk powder, 3ml for large membrane) and rotated at room temperature for half an hour. The membrane was washed three times for five minutes with 1x PBST. The secondary antibody was coupled to horseradish peroxidase (POD), which catalyses the oxidation of diacylhydrazides via an activated intermediate that decays to the ground state by emission of light in the visible range. The membrane was put between two sheets of a thin plastic bag (Roth) and covered with a liquid film of reaction substrates (BM chemiluminescence blotting substrate (POD), Roche). The position of the PSM bands

and lanes were marked with a fluorescent pen. Detection followed immediately after addition of the substrate in a LAS-3000 fluorescence reader (Fuji).

I. Quantification of Western blots with Multi Gauge

For quantitative analysis of Western blot signals the profile quantitation module of the MultiGauge 3.0 (Fuji) software was used. After background subtraction signal intensities of the individual peaks were obtained by computing the integral of the peak area.

5.2.17 Analysis of histone modifications by MALDI TOF/TOF mass spectrometry

A. Destaining of the gel bands

The Coomassie stained protein bands corresponding to histones H3 and H4 were excised from the gel and the gel pieces destained by subsequent incubation with 200µl H_2O for 5 min at RT, 200µl 0.1M NH_4HCO_3 for 5 min at RT and 200µl 0.1M NH_4HCO_3, 30% acetonitrile for 15 min at 37°C with continous shaking in a thermomixer. The last washing step was repeated if the gel pieces were still blue.

B. Propionylation

After washing the gel pieces for further two times with 200µl of 70% MeOH for 5 min at RT, 11-15µl (as little as possible, but enough to cover the gel pieces) of 0.71M propionic anhydride (Sigma) in 70% MeOH were added to each sample. After incubation for 2 min at RT, 30-40µl of 1M NH_4HCO_3 were added to each reaction and incubated for 25 min at RT. The lid of the tubes should be opened from time to time to release CO_2 from the reaction and the pH of the reaction should stay between 7.0 and 8.0. If the pH decreases below 7.0, addition of 1M NH_4HCO_3 in small aliquots buffers the reaction. After washing the gel pieces for two times with 200µl 70% MeOH for 1-2 min at RT, the propionylation reaction is repeated with freshly prepared 0.71M propionic anhydride in 70% MeOH for 30 min.

C. Trypsin digestion

After washing the gel pieces for 3 times with 200µl 0.1M NH_4HCO_3 for 5 min at RT, with 200µl H_2O for 5 min at RT and 200µl 0.1M NH_4HCO_3, 50% acetonitrile for 15 min at 37°C with continous shaking in a thermomixer, the gel pieces are shrinked by incubation with 100µl 100% acetonitrile for 2 x 2 min at RT. Proteins were then digested with trypsin (Roche Applied Science) according manufacturer's instructions over night at 37°C.

D. MALDI TOF/TOF mass spectrometry

0.5-1µl aliquots of each sample were spotted in triplicates on to a stainless steel MALDI target plate, allowed to dry, overlaid with 0.5µl freshly prepared, ice-cold 5 mg/ml alpha-cyano-4-hydroxy cinnamic acid (for mass spectrometry, Fluka) in 50% acetonitrile/0.3% TFA, dried again and analysed by MALDI-TOF/TOF in a 4800 instrument from Applied Biosystems, operated according manufacturer's instructions. Full MS spectra were acquired in the reflector modus, with m/z from 700 to 2000 (H4) or 700 to 2500 (H3); focus on 1500 (H4) or 1600 (H3) and 50x50 spectra were acquired per spot. For the tandem MS/MS spectra, the peptide 4-17 of H4 was fragmented in PSD modus whereas the peptides of H3 were fragmented with CID; in all the cases the isolation window width 1.0 Da; an inclusion list was used for parent ion selection (tolerance 0.3 Da) and 85x45 shots per spectra were acquired. For all MS and MS/MS spectra, the laser intensity was manually adjusted for optimized S/N.
Spectra were processed with mMass 5.2.0 (Strohalm et al., 2008, 2010). After recalibration by using signals of the histones (peptides 46-55 and 79-92 for H4 and peptides 64-69 and 27-40 unmodified for H3), the relative proportion of a given modification for the peptides of interest was calculated by dividing the absolute intensity of the signal corresponding to that modification through the sum of the intensities for all the signals corresponding to any modified species from the same peptide. The results for all the MALDI replicas of each measurement were averaged.

5.2.18 Comparative iTRAQ MALDI TOF/TOF mass spectrometry

A. Trypsin digest and iTRAQ labelling

The lyophilised protein samples were resuspended in 20µl dissolution buffer (iTRAQ^{TM} labelling kit (Life Technologies) and reduced with 5mM Tris-(2-carboxyethyl)phosphine at

60°C for 1h. Cysteins were blocked with 10mM methyl-methanethiosulfonate (MMTS) at room temperature for 10min. After trypsin digestion for 20h at 37°C, tryptic peptides of the purifications of interest were labelled with different combinations of the four iTRAQ™ reagents according to the manufacturer (Life Technologies). The differentially labelled peptides were combined and lyophilized.

B. Peptide separation and automated spotting of the peptide fractions

The combined differentially labelled peptides were dissolved for 2h in 0.1%TFA and loaded on a nano-flow HPLC-system (Dionex) harbouring a C18-Pep-Mep column (LC-Packings). The peptides were separated by a gradient of 5% to 95% of buffer B (80% acetonitrile/0.05% TFA) and fractions were mixed with 5 volumes of CHCA (alpha-cyano-4-hydroxy cinnamic acid; Sigma) matrix (2mg/ml in 70% acetonitrile/0.1%TFA) and spotted online via the Probot system (Dionex) on a MALDI-target.

C. MALDI TOF/TOF analysis

MS/MS analyses were performed on an Applied Biosystems 4800 Proteomics Analyzer. MALDI-TOF/TOF mass spectrometer operated in positive ion reflector mode and evaluated by searching the NCBInr protein sequence database with the Mascot search engine (Matrix Science) implemented in the GPS Explorer software (Applied Biosystems). Laser intensity was adjusted due to laser condition and sample concentration. The ten most intense peptide peaks per spot detected in the MS mode were further fragmented yielding the respective MS/MS spectra.

D. iTRAQ data evaluation

Only proteins identified by peptides with a Confidence Interval > 95% were included in the analysis. The peak area for iTRAQ™ reporter ions were interpreted and corrected by the GPS-Explorer software (Applied Biosystems) and Excel (Microsoft). An average iTRAQ ratio of all peptides of a given protein was calculated and outliers were deleted by manual evaluation.

6 References

Adkins, M.W., Howar, S.R., and Tyler, J.K. (2004). Chromatin disassembly mediated by the histone chaperone Asf1 is essential for transcriptional activation of the yeast PHO5 and PHO8 genes. Mol. Cell *14*, 657–666.

Ahmad, K., and Henikoff, S. (2002). The Histone Variant H3.3 Marks Active Chromatin by Replication-Independent Nucleosome Assembly. Molecular Cell *9*, 1191–1200.

Akiyoshi, B., Nelson, C.R., Ranish, J.A., and Biggins, S. (2009). Quantitative proteomic analysis of purified yeast kinetochores identifies a PP1 regulatory subunit. Genes Dev. *23*, 2887–2899.

Almer, A., and Hörz, W. (1986). Nuclease hypersensitive regions with adjacent positioned nucleosomes mark the gene boundaries of the PHO5/PHO3 locus in yeast. EMBO J. *5*, 2681–2687.

Almer, A., Rudolph, H., Hinnen, A., and Hörz, W. (1986). Removal of positioned nucleosomes from the yeast PHO5 promoter upon PHO5 induction releases additional upstream activating DNA elements. EMBO J *5*, 2689–2696.

Ansari, A., Cheng, T.-H., and Gartenberg, M.R. (1999). Isolation of Selected Chromatin Fragments from Yeast by Site-Specific Recombinationin Vivo. Methods *17*, 104–111.

Ansari, A., and Gartenberg, M.R. (1999). Persistence of an alternate chromatin structure at silenced loci in vitro. Proc. Natl. Acad. Sci. U.S.A. *96*, 343–348.

Antão, J.M., Mason, J.M., Déjardin, J., and Kingston, R.E. (2012). Protein landscape at Drosophila melanogaster telomere-associated sequence repeats. Mol. Cell. Biol. *32*, 2170–2182.

Arents, G., Burlingame, R.W., Wang, B.C., Love, W.E., and Moudrianakis, E.N. (1991). The nucleosomal core histone octamer at 3.1 A resolution: a tripartite protein assembly and a left-handed superhelix. Proc. Natl. Acad. Sci. U.S.A. *88*, 10148–10152.

Argos, P., Landy, A., Abremski, K., Egan, J.B., Haggard-Ljungquist, E., Hoess, R.H., Kahn, M.L., Kalionis, B., Narayana, S.V., and Pierson, L.S. (1986). The integrase family of site-specific recombinases: regional similarities and global diversity. EMBO J *5*, 433–440.

Banerjee, S., and Cantor, C.R. (1990). Nucleosome assembly of simian virus 40 DNA in a mammalian cell extract. Mol. Cell. Biol. *10*, 2863–2873.

Banks, G.C., Li, Y., and Reeves, R. (2000). Differential in vivo modifications of the HMGI(Y) nonhistone chromatin proteins modulate nucleosome and DNA interactions. Biochemistry *39*, 8333–8346.

Bannister, A.J., Schneider, R., and Kouzarides, T. (2002). Histone methylation: dynamic or static? Cell *109*, 801–806.

Barbaric, S., Münsterkötter, M., Goding, C., and Hörz, W. (1998). Cooperative Pho2-Pho4 interactions at the PHO5 promoter are critical for binding of Pho4 to UASp1 and for efficient transactivation by Pho4 at UASp2. Mol. Cell. Biol. *18*, 2629–2639.

Barbaric, S., Reinke, H., and Hörz, W. (2003). Multiple Mechanistically Distinct Functions of SAGA at the PHO5 Promoter. Molecular and Cellular Biology *23*, 3468 –3476.

Barbaric, S., Walker, J., Schmid, A., Svejstrup, J.Q., and Hörz, W. (2001). Increasing the rate of chromatin remodeling and gene activation--a novel role for the histone acetyltransferase Gcn5. EMBO J. *20*, 4944–4951.

Barski, A., Cuddapah, S., Cui, K., Roh, T.-Y., Schones, D.E., Wang, Z., Wei, G., Chepelev, I., and Zhao, K. (2007). High-Resolution Profiling of Histone Methylations in the Human Genome. Cell *129*, 823–837.

Becker, P.B. (2006). Gene regulation: A finger on the mark. Nature *442*, 31–32.

Becker, P.B., and Wu, C. (1992). Cell-free system for assembly of transcriptionally repressed chromatin from Drosophila embryos. Mol. Cell. Biol. *12*, 2241–2249.

Ben-Shem, A., Garreau de Loubresse, N., Melnikov, S., Jenner, L., Yusupova, G., and Yusupov, M. (2011). The structure of the eukaryotic ribosome at 3.0 Å resolution. Science *334*, 1524–1529.

Berger, A.B., Decourty, L., Badis, G., Nehrbass, U., Jacquier, A., and Gadal, O. (2007). Hmo1 is required for TOR-dependent regulation of ribosomal protein gene transcription. Mol. Cell. Biol. *27*, 8015–8026.

Birch, J.L., and Zomerdijk, J.C.B.M. (2008). Structure and function of ribosomal RNA gene chromatin. Biochem. Soc. Trans. *36*, 619–624.

Boeger, H., Griesenbeck, J., and Kornberg, R.D. (2008). Nucleosome retention and the stochastic nature of promoter chromatin remodeling for transcription. Cell *133*, 716–726.

Boeger, H., Griesenbeck, J., Strattan, J.S., and Kornberg, R.D. (2003). Nucleosomes unfold completely at a transcriptionally active promoter. Mol. Cell *11*, 1587–1598.

Boffa, L.C., Carpaneto, E.M., and Allfrey, V.G. (1995). Isolation of active genes containing CAG repeats by DNA strand invasion by a peptide nucleic acid. Proceedings of the National Academy of Sciences *92*, 1901 –1905.

Boffelli, D., De Santis, P., Palleschi, A., and Savino, M. (1991). The curvature vector in nucleosomal DNAs and theoretical prediction of nucleosome positioning. Biophysical Chemistry *39*, 127–136.

Bonenfant, D., Towbin, H., Coulot, M., Schindler, P., Mueller, D.R., and van Oostrum, J. (2007). Analysis of dynamic changes in post-translational modifications of human histones during cell cycle by mass spectrometry. Mol. Cell Proteomics *6*, 1917–1932.

Brewer, B.J., and Fangman, W.L. (1988). A replication fork barrier at the 3' end of yeast ribosomal RNA genes. Cell *55*, 637–643.

Brewer, B.J., Lockshon, D., and Fangman, W.L. (1992). The arrest of replication forks in the rDNA of yeast occurs independently of transcription. Cell *71*, 267–276.

Broach, J.R., and Pringle, J.R. (1991). The Molecular and Cellular Biology of the Yeast Saccharomyces: Genome dynamics, protein synthesis, and energetics (CSHL Press).

Bryk, M., Banerjee, M., Murphy, M., Knudsen, K.E., Garfinkel, D.J., and Curcio, M.J. (1997). Transcriptional silencing of Ty1 elements in the RDN1 locus of yeast. Genes Dev. *11*, 255–269.

Burkhalter, M.D., and Sogo, J.M. (2004). rDNA enhancer affects replication initiation and mitotic recombination: Fob1 mediates nucleolytic processing independently of replication. Mol. Cell *15*, 409–421.

Butala, M., Žgur-Bertok, D., and Busby, S.J.W. (2008). The bacterial LexA transcriptional repressor. Cellular and Molecular Life Sciences *66*, 82–93.

Buttinelli, M., Di Mauro, E., and Negri, R. (1993). Multiple nucleosome positioning with unique rotational setting for the Saccharomyces cerevisiae 5S rRNA gene in vitro and in vivo. Proc. Natl. Acad. Sci. U.S.A. *90*, 9315–9319.

Byrum, S.D., Raman, A., Taverna, S.D., and Tackett, A.J. (2012). ChAP-MS: A Method for Identification of Proteins and Histone Posttranslational Modifications at a Single Genomic Locus. Cell Rep *2*, 198–205.

Camerini-Otero, R.D., Sollner-Webb, B., and Felsenfeld, G. (1976). The organization of histones and DNA in chromatin: evidence for an arginine-rich histone kernel. Cell *8*, 333–347.

Carr, A., and Biggin, M.D. (1999). An in vivo UV crosslinking assay that detects DNA binding by sequence-specific transcription factors. Methods Mol. Biol. *119*, 497–508.

Carruthers, L.M., and Hansen, J.C. (2000). The Core Histone N Termini Function Independently of Linker Histones During Chromatin Condensation. J. Biol. Chem. *275*, 37285–37290.

Caserta, M., Agricola, E., Churcher, M., Hiriart, E., Verdone, L., Di Mauro, E., and Travers, A. (2009). A translational signature for nucleosome positioning in vivo. Nucleic Acids Res. *37*, 5309–5321.

Cech, T., and Pardue, M.L. (1977). Cross-linking of DNA with trimethylpsoralen is a probe for chromatin structure. Cell *11*, 631–640.

Cech, T., Potter, D., and Pardue, M.L. (1977). Electron microscopy of DNA cross-linked with trimethylpsoralen: a probe for chromatin structure. Biochemistry *16*, 5313–5321.

Cerutti, H., and Casas-Mollano, J.A. (2009). Histone H3 phosphorylation: universal code or lineage specific dialects? Epigenetics *4*, 71–75.

CHAO, F.C. (1957). Dissociation of macromolecular ribonucleoprotein of yeast. Arch. Biochem. Biophys. *70*, 426–431.

CHAO, F.C., and SCHACHMAN, H.K. (1956). The isolation and characterization of a macro-molecular ribonucleoprotein from yeast. Arch. Biochem. Biophys. *61*, 220–230.

Chaw, Y.F., Crane, L.E., Lange, P., and Shapiro, R. (1980). Isolation and identification of cross-links from formaldehyde-treated nucleic acids. Biochemistry *19*, 5525–5531.

Cioci, F., Vu, L., Eliason, K., Oakes, M., Siddiqi, I.N., and Nomura, M. (2003). Silencing in yeast rDNA chromatin: reciprocal relationship in gene expression between RNA polymerase I and II. Mol. Cell *12*, 135–145.

Clapier, C.R., and Cairns, B.R. (2009). The biology of chromatin remodeling complexes. Annu. Rev. Biochem. *78*, 273–304.

Conconi, A., Losa, R., Koller, T., and Sogo, J.M. (1984). Psoralen-crosslinking of soluble and of H1-depleted soluble rat liver chromatin. J. Mol. Biol. *178*, 920–928.

Conconi, A., Widmer, R.M., Koller, T., and Sogo, J.M. (1989). Two different chromatin structures coexist in ribosomal RNA genes throughout the cell cycle. Cell *57*, 753–761.

Conrad-Webb, H., and Butow, R.A. (1995). A polymerase switch in the synthesis of rRNA in Saccharomyces cerevisiae. Mol. Cell. Biol. *15*, 2420–2428.

Costa, A., and Onesti, S. (2008). The MCM complex: (just) a replicative helicase? Biochem. Soc. Trans. *36*, 136–140.

Costas, C., de la Paz Sanchez, M., Stroud, H., Yu, Y., Oliveros, J.C., Feng, S., Benguria, A., López-Vidriero, I., Zhang, X., Solano, R., et al. (2011). Genome-wide mapping of Arabidopsis thaliana origins of DNA replication and their associated epigenetic marks. Nat. Struct. Mol. Biol. *18*, 395–400.

Dammann, R., Lucchini, R., Koller, T., and Sogo, J.M. (1993). Chromatin structures and transcription of rDNA in yeast Saccharomyces cerevisiae. Nucleic Acids Research *21*, 2331 –2338.

Dammann, R., Lucchini, R., Koller, T., and Sogo, J.M. (1995). Transcription in the yeast rRNA gene locus: distribution of the active gene copies and chromatin structure of their flanking regulatory sequences. Mol. Cell. Biol. *15*, 5294–5303.

Davey, C.A., Sargent, D.F., Luger, K., Maeder, A.W., and Richmond, T.J. (2002). Solvent mediated interactions in the structure of the nucleosome core particle at 1.9 a resolution. J. Mol. Biol. *319*, 1097–1113.

Davie, J.R., Lin, R., and Allis, C.D. (1991). Timing of the appearance of ubiquitinated histones in developing new macronuclei of Tetrahymena thermophila. Biochem. Cell Biol. *69*, 66–71.

Davie, J.R., and Murphy, L.C. (1990). Level of ubiquitinated histone H2B in chromatin is coupled to ongoing transcription. Biochemistry *29*, 4752–4757.

Dean, A., Pederson, D.S., and Simpson, R.T. (1989). Isolation of yeast plasmid chromatin. Meth. Enzymol. *170*, 26–41.

Deckert, J., Khalaf, R.A., Hwang, S.M., and Zitomer, R.S. (1999). Characterization of the DNA binding and bending HMG domain of the yeast hypoxic repressor Rox1. Nucleic Acids Res. *27*, 3518–3526.

Déjardin, J., and Kingston, R.E. (2009). Purification of proteins associated with specific genomic Loci. Cell *136*, 175–186.

Dhalluin, C. (1999). Structure and ligand of a histone acetyltransferase bromodomain. Nature *399*, 491–496.

Diffley, J.F., and Stillman, B. (1991). A close relative of the nuclear, chromosomal high-mobility group protein HMG1 in yeast mitochondria. Proc. Natl. Acad. Sci. U.S.A. *88*, 7864–7868.

Dimitrov, S.I., and Moss, T. (2001). UV laser-induced protein-DNA crosslinking. Methods Mol. Biol. *148*, 395–402.

Dong, L., and Xu, C.W. (2004). Carbohydrates induce mono-ubiquitination of H2B in yeast. J. Biol. Chem. *279*, 1577–1580.

Downs, J.A., Allard, S., Jobin-Robitaille, O., Javaheri, A., Auger, A., Bouchard, N., Kron, S.J., Jackson, S.P., and Côté, J. (2004). Binding of Chromatin-Modifying Activities to Phosphorylated Histone H2A at DNA Damage Sites. Molecular Cell *16*, 979–990.

Dragan, A.I., Read, C.M., Makeyeva, E.N., Milgotina, E.I., Churchill, M.E.A., Crane-Robinson, C., and Privalov, P.L. (2004). DNA binding and bending by HMG boxes: energetic determinants of specificity. J. Mol. Biol. *343*, 371–393.

Dragon, F., Gallagher, J.E.G., Compagnone-Post, P.A., Mitchell, B.M., Porwancher, K.A., Wehner, K.A., Wormsley, S., Settlage, R.E., Shabanowitz, J., Osheim, Y., et al. (2002). A large nucleolar U3 ribonucleoprotein required for 18S ribosomal RNA biogenesis. Nature *417*, 967–970.

Drew, H.R., and Travers, A.A. (1985). DNA bending and its relation to nucleosome positioning. Journal of Molecular Biology *186*, 773–790.

Drouin, G., and de Sá, M.M. (1995). The concerted evolution of 5S ribosomal genes linked to the repeat units of other multigene families. Mol. Biol. Evol. *12*, 481–493.

Drygin, D., Rice, W.G., and Grummt, I. (2010). The RNA polymerase I transcription machinery: an emerging target for the treatment of cancer. Annu. Rev. Pharmacol. Toxicol. *50*, 131–156.

Duerksen, J.D., and McCarthy, B.J. (1971). Distribution of deoxyribonucleic acid sequences in fractionated chromatin. Biochemistry *10*, 1471–1478.

Ehrensberger, A.H., and Kornberg, R.D. (2011). Isolation of an activator-dependent, promoter-specific chromatin remodeling factor. Proceedings of the National Academy of Sciences *108*, 10115 –10120.

Elion, E.A., and Warner, J.R. (1986). An RNA polymerase I enhancer in Saccharomyces cerevisiae. Mol. Cell. Biol. *6*, 2089–2097.

Fan, J.Y., Gordon, F., Luger, K., Hansen, J.C., and Tremethick, D.J. (2002). The essential histone variant H2A.Z regulates the equilibrium between different chromatin conformational states. Nature Structural & Molecular Biology *9*, 172–176.

Felsenfeld, G., and Groudine, M. (2003). Controlling the double helix. Nature *421*, 448–453.

Franklin, S.G., and Zweidler, A. (1977). Non-allelic variants of histones 2a, 2b and 3 in mammals. , Published Online: 17 March 1977; | Doi:10.1038/266273a0 *266*, 273–275.

Freidkin, I., and Katcoff, D.J. (2001). Specific distribution of the Saccharomyces cerevisiae linker histone homolog HHO1p in the chromatin. Nucleic Acids Res. *29*, 4043–4051.

French, S.L., Osheim, Y.N., Cioci, F., Nomura, M., and Beyer, A.L. (2003). In exponentially growing Saccharomyces cerevisiae cells, rRNA synthesis is determined by the summed RNA polymerase I loading rate rather than by the number of active genes. Mol. Cell. Biol. *23*, 1558–1568.

French, S.L., Osheim, Y.N., Schneider, D.A., Sikes, M.L., Fernandez, C.F., Copela, L.A., Misra, V.A., Nomura, M., Wolin, S.L., and Beyer, A.L. (2008). Visual analysis of the yeast 5S rRNA gene transcriptome: regulation and role of La protein. Mol. Cell. Biol. *28*, 4576–4587.

FRENSTER, J.H., ALLFREY, V.G., and MIRSKY, A.E. (1963). REPRESSED AND ACTIVE CHROMATIN ISOLATED FROM INTERPHASE LYMPHOCYTES. Proc. Natl. Acad. Sci. U.S.A. *50*, 1026–1032.

Fromont-Racine, M., Senger, B., Saveanu, C., and Fasiolo, F. (2003). Ribosome assembly in eukaryotes. Gene *313*, 17–42.

Gadal, O., Labarre, S., Boschiero, C., and Thuriaux, P. (2002). Hmo1, an HMG-box protein, belongs to the yeast ribosomal DNA transcription system. EMBO J. *21*, 5498–5507.

Gagnon-Kugler, T., Langlois, F., Stefanovsky, V., Lessard, F., and Moss, T. (2009). Loss of human ribosomal gene CpG methylation enhances cryptic RNA polymerase II transcription and disrupts ribosomal RNA processing. Mol. Cell *35*, 414–425.

Gale, J.M., and Smerdon, M.J. (1988). Photofootprint of nucleosome core DNA in intact chromatin having different structural states. J. Mol. Biol. *204*, 949–958.

Gall, J.G., Wu, Z., Murphy, C., and Gao, H. (2004). Structure in the amphibian germinal vesicle. Experimental Cell Research *296*, 28–34.

Gallagher, J.E.G., Dunbar, D.A., Granneman, S., Mitchell, B.M., Osheim, Y., Beyer, A.L., and Baserga, S.J. (2004). RNA polymerase I transcription and pre-rRNA processing are linked by specific SSU processome components. Genes Dev. *18*, 2506–2517.

Garcia, B.A., Barber, C.M., Hake, S.B., Ptak, C., Turner, F.B., Busby, S.A., Shabanowitz, J., Moran, R.G., Allis, C.D., and Hunt, D.F. (2005). Modifications of human histone H3 variants during mitosis. Biochemistry *44*, 13202–13213.

Gartenberg, M.R. (1999). Formation of extrachromosomal DNA rings in Saccharomyces cerevisiae using site-specific recombination. Methods Mol. Biol. *94*, 125–133.

Gartenberg, M.R. (2012). Generation of DNA circles in yeast by inducible site-specific recombination. Methods Mol. Biol. *833*, 103–113.

Geiduschek, E.P., and Kassavetis, G.A. (2001). The RNA polymerase III transcription apparatus. J. Mol. Biol. *310*, 1–26.

Germond, J.E., Bellard, M., Oudet, P., and Chambon, P. (1976). Stability of nucleosomes in native and reconstituted chromatins. Nucleic Acids Res. *3*, 3173–3192.

Ghirlando, R., and Felsenfeld, G. (2008). Hydrodynamic Studies on Defined Heterochromatin Fragments Support a 30-nm Fiber Having Six Nucleosomes per Turn. Journal of Molecular Biology *376*, 1417–1425.

Gietz, R.D., and Sugino, A. (1988). New yeast-Escherichia coli shuttle vectors constructed with in vitro mutagenized yeast genes lacking six-base pair restriction sites. Gene *74*, 527–534.

Gilmour, D.S., Rougvie, A.E., and Lis, J.T. (1991). Protein-DNA cross-linking as a means to determine the distribution of proteins on DNA in vivo. Methods Cell Biol. *35*, 369–381.

Glikin, G.C., Ruberti, I., and Worcel, A. (1984). Chromatin assembly in Xenopus oocytes: in vitro studies. Cell *37*, 33–41.

Goetze, H., Wittner, M., Hamperl, S., Hondele, M., Merz, K., Stoeckl, U., and Griesenbeck, J. (2010). Alternative Chromatin Structures of the 35S rRNA Genes in Saccharomyces cerevisiae Provide a Molecular Basis for the Selective Recruitment of RNA Polymerases I and II. Molecular and Cellular Biology *30*, 2028 –2045.

Goldknopf, I.L., Sudhakar, S., Rosenbaum, F., and Busch, H. (1980). Timing of ubiquitin synthesis and conjugation into protein A24 during the HeLa cell cycle. Biochem. Biophys. Res. Commun. *95*, 1253–1260.

Goodier, J.L., Fan, H., and Maraia, R.J. (1997). A Carboxy-Terminal Basic Region Controls RNA Polymerase III Transcription Factor Activity of Human La Protein. Mol. Cell. Biol. *17*, 5823–5832.

Gopaul, D.N., and Duyne, G.D. (1999). Structure and mechanism in site-specific recombination. Curr. Opin. Struct. Biol. *9*, 14–20.

Gottesfeld, J.M. (1977). Methods for fractionation of chromatin into transcriptionally active and inactive segments. Methods Cell Biol. *16*, 421–436.

Gottschling, D.E., Aparicio, O.M., Billington, B.L., and Zakian, V.A. (1990). Position effect at S. cerevisiae telomeres: reversible repression of Pol II transcription. Cell *63*, 751–762.

Granneman, S., and Baserga, S.J. (2004). Ribosome biogenesis: of knobs and RNA processing. Experimental Cell Research *296*, 43–50.

Gregory, P.D., Schmid, A., Zavari, M., Lui, L., Berger, S.L., and Hörz, W. (1998). Absence of Gcn5 HAT activity defines a novel state in the opening of chromatin at the PHO5 promoter in yeast. Mol. Cell *1*, 495–505.

Griesenbeck, J., Boeger, H., Strattan, J.S., and Kornberg, R.D. (2003). Affinity Purification of Specific Chromatin Segments from Chromosomal Loci in Yeast. Molecular and Cellular Biology *23*, 9275 –9282.

Griesenbeck, J., Boeger, H., Strattan, J.S., and Kornberg, R.D. (2004). Purification of defined chromosomal domains. Meth. Enzymol. *375*, 170–178.

Guillemette, B., Bataille, A.R., Gévry, N., Adam, M., Blanchette, M., Robert, F., and Gaudreau, L. (2005). Variant histone H2A.Z is globally localized to the promoters of inactive yeast genes and regulates nucleosome positioning. PLoS Biol. *3*, e384.

Guillemette, B., Drogaris, P., Lin, H.-H.S., Armstrong, H., Hiragami-Hamada, K., Imhof, A., Bonneil, E., Thibault, P., Verreault, A., and Festenstein, R.J. (2011). H3 lysine 4 is acetylated at active gene promoters and is regulated by H3 lysine 4 methylation. PLoS Genet. *7*, e1001354.

Hacques, M.F., Muller, S., De Murcia, G., Van Regenmortel, M.H., and Marion, C. (1990). Use of an immobilized enzyme and specific antibodies to analyse the accessibility and role of histone tails in chromatin structure. Biochem. Biophys. Res. Commun. *168*, 637–643.

Haeusler, R.A., and Engelke, D.R. (2006). Spatial organization of transcription by RNA polymerase III. Nucleic Acids Res. *34*, 4826–4836.

Hall, D.B., Wade, J.T., and Struhl, K. (2006). An HMG protein, Hmo1, associates with promoters of many ribosomal protein genes and throughout the rRNA gene locus in Saccharomyces cerevisiae. Mol. Cell. Biol. *26*, 3672–3679.

Hanson, C.V., Shen, C.K., and Hearst, J.E. (1976). Cross-linking of DNA in situ as a probe for chromatin structure. Science *193*, 62–64.

Harbison, C.T., Gordon, D.B., Lee, T.I., Rinaldi, N.J., Macisaac, K.D., Danford, T.W., Hannett, N.M., Tagne, J.-B., Reynolds, D.B., Yoo, J., et al. (2004). Transcriptional regulatory code of a eukaryotic genome. Nature *431*, 99–104.

Haswell, E.S., and O'Shea, E.K. (1999). An in vitro system recapitulates chromatin remodeling at the PHO5 promoter. Mol. Cell. Biol. *19*, 2817–2827.

Hecht, A., and Grunstein, M. (1999). Mapping DNA interaction sites of chromosomal proteins using immunoprecipitation and polymerase chain reaction. Meth. Enzymol. *304*, 399–414.

Hewish, D.R., and Burgoyne, L.A. (1973). Chromatin sub-structure. The digestion of chromatin DNA at regularly spaced sites by a nuclear deoxyribonuclease. Biochem. Biophys. Res. Commun. *52*, 504–510.

Higashinakagawa, T., Wahn, H., and Reeder, R.H. (1977). Isolation of ribosomal gene chromatin. Developmental Biology *55*, 375–386.

Hirst, K., Fisher, F., McAndrew, P.C., and Goding, C.R. (1994). The transcription factor, the Cdk, its cyclin and their regulator: directing the transcriptional response to a nutritional signal. EMBO J. *13*, 5410–5420.

Hizume, K., Nakai, T., Araki, S., Prieto, E., Yoshikawa, K., and Takeyasu, K. (2009). Removal of histone tails from nucleosome dissects the physical mechanisms of salt-induced aggregation, linker histone H1-induced compaction, and 30-nm fiber formation of the nucleosome array. Ultramicroscopy *109*, 868–873.

Hong, L., Schroth, G.P., Matthews, H.R., Yau, P., and Bradbury, E.M. (1993). Studies of the DNA binding properties of histone H4 amino terminus. Thermal denaturation studies reveal that acetylation markedly reduces the binding constant of the H4 "tail" to DNA. J. Biol. Chem. *268*, 305–314.

Hörz, W., and Zachau, H.G. (1980). Deoxyribonuclease II as a probe for chromatin structure. I. Location of cleavage sites. J. Mol. Biol. *144*, 305–327.

Hoshino, A., and Fujii, H. (2009). Insertional chromatin immunoprecipitation: a method for isolating specific genomic regions. J. Biosci. Bioeng. *108*, 446–449.

Howe, L., Ranalli, T.A., Allis, C.D., and Ausió, J. (1998). Transcriptionally active Xenopus laevis somatic 5 S ribosomal RNA genes are packaged with hyperacetylated histone H4, whereas transcriptionally silent oocyte genes are not. J. Biol. Chem. *273*, 20693–20696.

Huyen, Y., Zgheib, O., Ditullio, R.A., Jr, Gorgoulis, V.G., Zacharatos, P., Petty, T.J., Sheston, E.A., Mellert, H.S., Stavridi, E.S., and Halazonetis, T.D. (2004). Methylated lysine 79 of histone H3 targets 53BP1 to DNA double-strand breaks. Nature *432*, 406–411.

Ide, S., Miyazaki, T., Maki, H., and Kobayashi, T. (2010). Abundance of Ribosomal RNA Gene Copies Maintains Genome Integrity. Science *327*, 693 –696.

Imai, S., Armstrong, C.M., Kaeberlein, M., and Guarente, L. (2000). Transcriptional silencing and longevity protein Sir2 is an NAD-dependent histone deacetylase. Nature *403*, 795–800.

Ioshikhes, I.P., Albert, I., Zanton, S.J., and Pugh, B.F. (2006). Nucleosome positions predicted through comparative genomics. Nat. Genet. *38*, 1210–1215.

Ito, T., Tyler, J.K., and Kadonaga, J.T. (2003). Chromatin assembly factors: a dual function in nucleosome formation and mobilization? Genes to Cells *2*, 593–600.

Jacobson, R.H., Ladurner, A.G., King, D.S., and Tjian, R. (2000). Structure and function of a human TAFII250 double bromodomain module. Science *288*, 1422–1425.

Jenuwein, T., and Allis, C.D. (2001). Translating the histone code. Science *293*, 1074–1080.

Johnson, E.S. (2004). Protein modification by SUMO. Annu. Rev. Biochem. *73*, 355–382.

Jones, H.S., Kawauchi, J., Braglia, P., Alen, C.M., Kent, N.A., and Proudfoot, N.J. (2007a). RNA polymerase I in yeast transcribes dynamic nucleosomal rDNA. Nat. Struct. Mol. Biol. *14*, 123–130.

Jothi, R., Cuddapah, S., Barski, A., Cui, K., and Zhao, K. (2008). Genome-wide identification of in vivo protein-DNA binding sites from ChIP-Seq data. Nucleic Acids Res. *36*, 5221–5231.

Kaplan, N., Moore, I.K., Fondufe-Mittendorf, Y., Gossett, A.J., Tillo, D., Field, Y., LeProust, E.M., Hughes, T.R., Lieb, J.D., Widom, J., et al. (2009). The DNA-encoded nucleosome organization of a eukaryotic genome. Nature *458*, 362–366.

Kasahara, K., Ohtsuki, K., Ki, S., Aoyama, K., Takahashi, H., Kobayashi, T., Shirahige, K., and Kokubo, T. (2007). Assembly of regulatory factors on rRNA and ribosomal protein genes in Saccharomyces cerevisiae. Mol. Cell. Biol. *27*, 6686–6705.

Kassavetis, G.A., Braun, B.R., Nguyen, L.H., and Peter Geiduschek, E. (1990). S. cerevisiae TFIIIB is the transcription initiation factor proper of RNA polymerase III, while TFIIIA and TFIIIC are assembly factors. Cell *60*, 235–245.

Kawauchi, J., Mischo, H., Braglia, P., Rondon, A., and Proudfoot, N.J. (2008). Budding yeast RNA polymerases I and II employ parallel mechanisms of transcriptional termination. Genes & Development *22*, 1082 –1092.

Keener, J., Dodd, J.A., Lalo, D., and Nomura, M. (1997). Histones H3 and H4 are components of upstream activation factor required for the high-level transcription of yeast rDNA by RNA polymerase I. Proc. Natl. Acad. Sci. U.S.A. *94*, 13458–13462.

Kennedy, E.J., Pillus, L., and Ghosh, G. (2005). Pho5p and newly identified nucleotide pyrophosphatases/ phosphodiesterases regulate extracellular nucleotide phosphate metabolism in Saccharomyces cerevisiae. Eukaryotic Cell *4*, 1892–1901.

Keys, D.A., Lee, B.S., Dodd, J.A., Nguyen, T.T., Vu, L., Fantino, E., Burson, L.M., Nogi, Y., and Nomura, M. (1996). Multiprotein transcription factor UAF interacts with the upstream element of the yeast RNA polymerase I promoter and forms a stable preinitiation complex. Genes Dev. *10*, 887–903.

Keys, D.A., Vu, L., Steffan, J.S., Dodd, J.A., Yamamoto, R.T., Nogi, Y., and Nomura, M. (1994). RRN6 and RRN7 encode subunits of a multiprotein complex essential for the initiation of rDNA transcription by RNA polymerase I in Saccharomyces cerevisiae. Genes Dev. *8*, 2349–2362.

Khorasanizadeh, S. (2004). The Nucleosome: From Genomic Organization to Genomic Regulation. Cell *116*, 259–272.

Kim, J., Daniel, J., Espejo, A., Lake, A., Krishna, M., Xia, L., Zhang, Y., and Bedford, M.T. (2006). Tudor, MBT and chromo domains gauge the degree of lysine methylation. EMBO Rep. *7*, 397–403.

Kim, Y., Shen, C.-H., and Clark, D.J. (2004). Purification and nucleosome mapping analysis of native yeast plasmid chromatin. Methods *33*, 59–67.

Kobayashi, T., and Ganley, A.R.D. (2005). Recombination regulation by transcription-induced cohesin dissociation in rDNA repeats. Science *309*, 1581–1584.

Kobayashi, T., Heck, D.J., Nomura, M., and Horiuchi, T. (1998). Expansion and contraction of ribosomal DNA repeats in Saccharomyces cerevisiae: requirement of replication fork blocking (Fob1) protein and the role of RNA polymerase I. Genes Dev. *12*, 3821–3830.

Kobayashi, T., Hidaka, M., Nishizawa, M., and Horiuchi, T. (1992). Identification of a site required for DNA replication fork blocking activity in the rRNA gene cluster in Saccharomyces cerevisiae. Mol. Gen. Genet. *233*, 355–362.

Kobayashi, T., Horiuchi, T., Tongaonkar, P., Vu, L., and Nomura, M. (2004). SIR2 regulates recombination between different rDNA repeats, but not recombination within individual rRNA genes in yeast. Cell *117*, 441–453.

Kobayashi, T., Nomura, M., and Horiuchi, T. (2001a). Identification of DNA cis elements essential for expansion of ribosomal DNA repeats in Saccharomyces cerevisiae. Mol. Cell. Biol. *21*, 136–147.

Koberna, K., Malínský, J., Pliss, A., Masata, M., Vecerova, J., Fialová, M., Bednár, J., and Raska, I. (2002). Ribosomal genes in focus: new transcripts label the dense fibrillar components and form clusters indicative of “Christmas trees” in situ. J. Cell Biol. *157*, 743–748.

Korber, P., Barbaric, S., Luckenbach, T., Schmid, A., Schermer, U.J., Blaschke, D., and Hörz, W. (2006). The Histone Chaperone Asf1 Increases the Rate of Histone Eviction at the Yeast PHO5 and PHO8 Promoters. Journal of Biological Chemistry *281*, 5539 – 5545.

Kornberg, R.D. (1974). Chromatin structure: a repeating unit of histones and DNA. Science *184*, 868–871.

Kornberg, R.D., LaPointe, J.W., and Lorch, Y. (1989). Preparation of nucleosomes and chromatin. Meth. Enzymol. *170*, 3–14.

Kornberg, R.D., and Lorch, Y. (1995). Interplay between chromatin structure and transcription. Curr. Opin. Cell Biol. *7*, 371–375.

Kos, M., and Tollervey, D. (2010). Yeast pre-rRNA processing and modification occur cotranscriptionally. Mol. Cell *37*, 809–820.

Kouzarides, T. (2002). Histone methylation in transcriptional control. Current Opinion in Genetics & Development *12*, 198–209.

Krebs, J.E. (2007). Moving marks: Dynamic histone modifications in yeast. Molecular BioSystems *3*, 590.

Krebs, J.E., Fry, C.J., Samuels, M.L., and Peterson, C.L. (2000). Global role for chromatin remodeling enzymes in mitotic gene expression. Cell *102*, 587–598.

Kressler, D., Hurt, E., and Baβler, J. (2010). Driving ribosome assembly. Biochimica Et Biophysica Acta (BBA) - Molecular Cell Research *1803*, 673–683.

Krogan, N.J., Kim, M., Tong, A., Golshani, A., Cagney, G., Canadien, V., Richards, D.P., Beattie, B.K., Emili, A., Boone, C., et al. (2003). Methylation of Histone H3 by Set2 in Saccharomyces cerevisiae Is Linked to Transcriptional Elongation by RNA Polymerase II. Molecular and Cellular Biology *23*, 4207 –4218.

Kubicek, S., and Jenuwein, T. (2004). A crack in histone lysine methylation. Cell *119*, 903–906.

Kulkens, T., Riggs, D.L., Heck, J.D., Planta, R.J., and Nomura, M. (1991). The yeast RNA polymerase I promoter: ribosomal DNA sequences involved in transcription initiation and complex formation in vitro. Nucleic Acids Res. *19*, 5363–5370.

Kuo, M.H., vom Baur, E., Struhl, K., and Allis, C.D. (2000). Gcn4 activator targets Gcn5 histone acetyltransferase to specific promoters independently of transcription. Mol. Cell *6*, 1309–1320.

Kurdistani, S.K., and Grunstein, M. (2003). Histone acetylation and deacetylation in yeast. Nat. Rev. Mol. Cell Biol. *4*, 276–284.

Kuzuhara, T., and Horikoshi, M. (2004). A nuclear FK506-binding protein is a histone chaperone regulating rDNA silencing. Nat. Struct. Mol. Biol. *11*, 275–283.

Lachner, M., O'Carroll, D., Rea, S., Mechtler, K., and Jenuwein, T. (2001). Methylation of histone H3 lysine 9 creates a binding site for HP1 proteins. Nature *410*, 116–120.

Lalo, D., Steffan, J.S., Dodd, J.A., and Nomura, M. (1996). RRN11 encodes the third subunit of the complex containing Rrn6p and Rrn7p that is essential for the initiation of rDNA transcription by yeast RNA polymerase I. J. Biol. Chem. *271*, 21062–21067.

Landry, J., Sutton, A., Tafrov, S.T., Heller, R.C., Stebbins, J., Pillus, L., and Sternglanz, R. (2000). The silencing protein SIR2 and its homologs are NAD-dependent protein deacetylases. Proc. Natl. Acad. Sci. U.S.A. *97*, 5807–5811.

Lee, B.M., and Mahadevan, L.C. (2009). Stability of histone modifications across mammalian genomes: implications for "epigenetic" marking. J. Cell. Biochem. *108*, 22–34.

Lee, T.I., Johnstone, S.E., and Young, R.A. (2006). Chromatin immunoprecipitation and microarray-based analysis of protein location. Nat Protoc *1*, 729–748.

Lee, W., Tillo, D., Bray, N., Morse, R.H., Davis, R.W., Hughes, T.R., and Nislow, C. (2007). A high-resolution atlas of nucleosome occupancy in yeast. Nature Genetics *39*, 1235–1244.

Lee, Y., Erkine, A.M., Van Ryk, D.I., and Nazar, R.N. (1995). In vivo analyses of the internal control region in the 5S rRNA gene from Saccharomyces cerevisiae. Nucleic Acids Res. *23*, 634–640.

Léger-Silvestre, I., Trumtel, S., Noaillac-Depeyre, J., and Gas, N. (1999). Functional compartmentalization of the nucleus in the budding yeast Saccharomyces cerevisiae. Chromosoma *108*, 103–113.

Levy, A., Eyal, M., Hershkovits, G., Salmon-Divon, M., Klutstein, M., and Katcoff, D.J. (2008). Yeast linker histone Hho1p is required for efficient RNA polymerase I processivity and transcriptional silencing at the ribosomal DNA. Proc. Natl. Acad. Sci. U.S.A. *105*, 11703–11708.

Li, B., Carey, M., and Workman, J.L. (2007). The Role of Chromatin during Transcription. Cell *128*, 707–719.

Li, B., Howe, L., Anderson, S., Yates, J.R., and Workman, J.L. (2003). The Set2 Histone Methyltransferase Functions through the Phosphorylated Carboxyl-terminal Domain of RNA Polymerase II. Journal of Biological Chemistry *278*, 8897 –8903.

Linskens, M.H., and Huberman, J.A. (1988). Organization of Replication of Ribosomal DNA in Saccharomyces Cerevisiae. Mol. Cell. Biol. *8*, 4927–4935.

Lohr, D. (1983). Chromatin structure differs between coding and upstream flanking sequences of the yeast 35S ribosomal genes. Biochemistry *22*, 927–934.

Loidl, P. (1994). Histone acetylation: facts and questions. Chromosoma *103*, 441–449.

Lucchini, R., and Sogo, J.M. (1994). Chromatin structure and transcriptional activity around the replication forks arrested at the 3' end of the yeast rRNA genes. Mol. Cell. Biol. *14*, 318–326.

Lue, N.F., and Kornberg, R.D. (1993). A possible role for the yeast TATA-element-binding protein in DNA replication. Proc. Natl. Acad. Sci. U.S.A. *90*, 8018–8022.

Luger, K., Mader, A.W., Richmond, R.K., Sargent, D.F., and Richmond, T.J. (1997a). Crystal structure of the nucleosome core particle at 2.8[thinsp][angst] resolution. Nature *389*, 251–260.

Luger, K., and Richmond, T.J. (1998). The histone tails of the nucleosome. Curr. Opin. Genet. Dev. *8*, 140–146.

Luo, Y., Pfuetzner, R.A., Mosimann, S., Paetzel, M., Frey, E.A., Cherney, M., Kim, B., Little, J.W., and Strynadka, N.C.J. (2001). Crystal Structure of LexA: A Conformational Switch for Regulation of Self-Cleavage. Cell *106*, 585–594.

Maresca, T.J., and Heald, R. (2006). The long and the short of it: linker histone H1 is required for metaphase chromosome compaction. Cell Cycle *5*, 589–591.

Martin, C., and Zhang, Y. (2005). The diverse functions of histone lysine methylation. Nature Reviews Molecular Cell Biology *6*, 838–849.

Mavrich, T.N., Jiang, C., Ioshikhes, I.P., Li, X., Venters, B.J., Zanton, S.J., Tomsho, L.P., Qi, J., Glaser, R.L., Schuster, S.C., et al. (2008). Nucleosome organization in the Drosophila genome. Nature *453*, 358–362.

McConaughy, B.L., and McCarthy, B.J. (1972). Fractionation of chromatin by thermal chromatography. Biochemistry *11*, 998–1003.

McGhee, J.D., and von Hippel, P.H. (1975a). Formaldehyde as a probe of DNA structure. I. Reaction with exocyclic amino groups of DNA bases. Biochemistry *14*, 1281–1296.

McGhee, J.D., and von Hippel, P.H. (1975b). Formaldehyde as a probe of DNA structure. II. Reaction with endocyclic imino groups of DNA bases. Biochemistry *14*, 1297–1303.

McStay, B., and Grummt, I. (2008). The epigenetics of rRNA genes: from molecular to chromosome biology. Annu. Rev. Cell Dev. Biol. *24*, 131–157.

Meneghini, M.D., Wu, M., and Madhani, H.D. (2003). Conserved histone variant H2A.Z protects euchromatin from the ectopic spread of silent heterochromatin. Cell *112*, 725–736.

Merz, K., Hondele, M., Goetze, H., Gmelch, K., Stoeckl, U., and Griesenbeck, J. (2008). Actively transcribed rRNA genes in S. cerevisiae are organized in a specialized chromatin associated with the high-mobility group protein Hmo1 and are largely devoid of histone molecules. Genes & Development *22*, 1190 –1204.

Messner, S., and Hottiger, M.O. (2011). Histone ADP-ribosylation in DNA repair, replication and transcription. Trends in Cell Biology *21*, 534–542.

Miller, O.L., Jr (1981). The nucleolus, chromosomes, and visualization of genetic activity. J. Cell Biol. *91*, 15s–27s.

Miller, O.L., Jr, and Beatty, B.R. (1969). Visualization of nucleolar genes. Science *164*, 955–957.

Morrison, A.J., Highland, J., Krogan, N.J., Arbel-Eden, A., Greenblatt, J.F., Haber, J.E., and Shen, X. (2004). INO80 and γ-H2AX Interaction Links ATP-Dependent Chromatin Remodeling to DNA Damage Repair. Cell *119*, 767–775.

Mougey, E.B., O'Reilly, M., Osheim, Y., Miller, O.L., Jr, Beyer, A., and Sollner-Webb, B. (1993). The terminal balls characteristic of eukaryotic rRNA transcription units in chromatin spreads are rRNA processing complexes. Genes Dev. *7*, 1609–1619.

Mueller, J.E., and Bryk, M. (2007). Isw1 acts independently of the Isw1a and Isw1b complexes in regulating transcriptional silencing at the ribosomal DNA locus in Saccharomyces cerevisiae. J. Mol. Biol. *371*, 1–10.

Mueller, R.D., Yasuda, H., Hatch, C.L., Bonner, W.M., and Bradbury, E.M. (1985). Identification of ubiquitinated histones 2A and 2B in Physarum polycephalum. Disappearance of these proteins at metaphase and reappearance at anaphase. J. Biol. Chem. *260*, 5147–5153.

Mumberg, D., Müller, R., and Funk, M. (1995). Yeast vectors for the controlled expression of heterologous proteins in different genetic backgrounds. Gene *156*, 119–122.

Musters, W., Knol, J., Maas, P., Dekker, A.F., van Heerikhuizen, H., and Planta, R.J. (1989). Linker scanning of the yeast RNA polymerase I promoter. Nucleic Acids Res. *17*, 9661–9678.

Neelin, J.M., Mazen, A., and Champagne, M. (1976). The fractionation of active and inactive chromatins from erythroid cells of chicken. FEBS Letters *65*, 309–314.

Nelson, T., Wiegand, R., and Brutlag, D. (1981). Ribonucleic acid and other polyanions facilitate chromatin assembly in vitro. Biochemistry *20*, 2594–2601.

Németh, A., and Längst, G. (2008). Chromatin organization of active ribosomal RNA genes. Epigenetics *3*, 243–245.

Nguyen, A.T., and Zhang, Y. (2011). The diverse functions of Dot1 and H3K79 methylation. Genes Dev. *25*, 1345–1358.

Nogi, Y., Yano, R., and Nomura, M. (1991). Synthesis of large rRNAs by RNA polymerase II in mutants of Saccharomyces cerevisiae defective in RNA polymerase I. PNAS *88*, 3962–3966.

Nomura, M. (2001). Ribosomal RNA genes, RNA polymerases, nucleolar structures, and synthesis of rRNA in the yeast Saccharomyces cerevisiae. Cold Spring Harb. Symp. Quant. Biol. *66*, 555–565.

Nourani, A., Utley, R.T., Allard, S., and Côté, J. (2004). Recruitment of the NuA4 complex poises the PHO5 promoter for chromatin remodeling and activation. EMBO J *23*, 2597–2607.

Oakes, M., Aris, J.P., Brockenbrough, J.S., Wai, H., Vu, L., and Nomura, M. (1998). Mutational analysis of the structure and localization of the nucleolus in the yeast Saccharomyces cerevisiae. J. Cell Biol. *143*, 23–34.

Oeffinger, M., Wei, K.E., Rogers, R., DeGrasse, J.A., Chait, B.T., Aitchison, J.D., and Rout, M.P. (2007). Comprehensive analysis of diverse ribonucleoprotein complexes. Nat Meth *4*, 951–956.

Ogawa, N., DeRisi, J., and Brown, P.O. (2000). New components of a system for phosphate accumulation and polyphosphate metabolism in Saccharomyces cerevisiae revealed by genomic expression analysis. Mol. Biol. Cell *11*, 4309–4321.

Olins, A.L., and Olins, D.E. (1974). Spheroid chromatin units (v bodies). Science *183*, 330–332.

Olins, D.E., and Olins, A.L. (2003). Chromatin history: our view from the bridge. Nat. Rev. Mol. Cell Biol. *4*, 809–814.

Osheim, Y.N., French, S.L., Keck, K.M., Champion, E.A., Spasov, K., Dragon, F., Baserga, S.J., and Beyer, A.L. (2004). Pre-18S Ribosomal RNA Is Structurally Compacted into the SSU Processome Prior to Being Cleaved from Nascent Transcripts in Saccharomyces cerevisiae. Molecular Cell *16*, 943–954.

Oshima, Y. (1997). The phosphatase system in Saccharomyces cerevisiae. Genes Genet. Syst. *72*, 323–334.

Oudet, P., Gross-Bellard, M., and Chambon, P. (1975). Electron microscopic and biochemical evidence that chromatin structure is a repeating unit. Cell *4*, 281–300.

Palmer, D.K., O'Day, K., Wener, M.H., Andrews, B.S., and Margolis, R.L. (1987). A 17-kD Centromere Protein (CENP-A) Copurifies with Nucleosome Core Particles and with Histones. J Cell Biol *104*, 805–815.

Parnell, T.J., Huff, J.T., and Cairns, B.R. (2008). RSC regulates nucleosome positioning at Pol II genes and density at Pol III genes. EMBO J. *27*, 100–110.

Pederson, D.S., Venkatesan, M., Thoma, F., and Simpson, R.T. (1986). Isolation of an episomal yeast gene and replication origin as chromatin. Proc. Natl. Acad. Sci. U.S.A. *83*, 7206–7210.

Peterson, C.L., and Laniel, M.-A. (2004). Histones and histone modifications. Current Biology *14*, R546–R551.

Philippsen, P., Thomas, M., Kramer, R.A., and Davis, R.W. (1978). Unique arrangement of coding sequences for 5 S, 5.8 S, 18 S and 25 S ribosomal RNA in Saccharomyces cerevisiae as determined by R-loop and hybridization analysis. J. Mol. Biol. *123*, 387–404.

Phillips, N.B., Nikolskaya, T., Jancso-Radek, A., Ittah, V., Jiang, F., Singh, R., Haas, E., and Weiss, M.A. (2004). Sry-directed sex reversal in transgenic mice is robust with respect to enhanced DNA bending: comparison of human and murine HMG boxes. Biochemistry *43*, 7066–7081.

Pickart, C.M. (2001). Mechanisms Underlying Ubiquitination. Annual Review of Biochemistry *70*, 503–533.

Planta, R.J. (1997). Regulation of ribosome synthesis in yeast. Yeast *13*, 1505–1518.

Pokholok, D.K., Harbison, C.T., Levine, S., Cole, M., Hannett, N.M., Lee, T.I., Bell, G.W., Walker, K., Rolfe, P.A., Herbolsheimer, E., et al. (2005). Genome-wide Map of Nucleosome Acetylation and Methylation in Yeast. Cell *122*, 517–527.

Prieto, J.-L., and McStay, B. (2007). Recruitment of factors linking transcription and processing of pre-rRNA to NOR chromatin is UBF-dependent and occurs independent of transcription in human cells. Genes Dev. *21*, 2041–2054.

Puig, O., Caspary, F., Rigaut, G., Rutz, B., Bouveret, E., Bragado-Nilsson, E., Wilm, M., and Séraphin, B. (2001). The Tandem Affinity Purification (TAP) Method: A General Procedure of Protein Complex Purification. Methods *24*, 218–229.

Raisner, R.M., Hartley, P.D., Meneghini, M.D., Bao, M.Z., Liu, C.L., Schreiber, S.L., Rando, O.J., and Madhani, H.D. (2005). Histone variant H2A.Z marks the 5' ends of both active and inactive genes in euchromatin. Cell *123*, 233–248.

Rao, B., Shibata, Y., Strahl, B.D., and Lieb, J.D. (2005). Dimethylation of histone H3 at lysine 36 demarcates regulatory and nonregulatory chromatin genome-wide. Mol. Cell. Biol. *25*, 9447–9459.

Raska, I. (2003). Oldies but goldies: searching for Christmas trees within the nucleolar architecture. Trends Cell Biol. *13*, 517–525.

Reeck, G.R., Simpson, R.T., and Sober, H.A. (1972). Resolution of a Spectrum of Nucleoprotein Species in Sonicated Chromatin. Proc Natl Acad Sci U S A *69*, 2317–2321.

Reinke, H., and Hörz, W. (2003). Histones are first hyperacetylated and then lose contact with the activated PHO5 promoter. Mol. Cell *11*, 1599–1607.

Reiter, A., Hamperl, S., Seitz, H., Merkl, P., Perez-Fernandez, J., Williams, L., Gerber, J., Németh, A., Léger, I., Gadal, O., et al. (2012). The Reb1-homologue Ydr026c/Nsi1 is required for efficient RNA polymerase I termination in yeast. The EMBO Journal.

Rhode, P.R., Elsasser, S., and Campbell, J.L. (1992). Role of multifunctional autonomously replicating sequence binding factor 1 in the initiation of DNA replication and transcriptional control in Saccharomyces cerevisiae. Mol. Cell. Biol. *12*, 1064–1077.

Rigaut, G., Shevchenko, A., Rutz, B., Wilm, M., Mann, M., and Seraphin, B. (1999). A generic protein purification method for protein complex characterization and proteome exploration. Nat Biotech *17*, 1030–1032.

Roberts, D.N., Stewart, A.J., Huff, J.T., and Cairns, B.R. (2003). The RNA Polymerase III Transcriptome Revealed by Genome-Wide Localization and Activity–occupancy Relationships. PNAS *100*, 14695–14700.

Rogakou, E.P., Pilch, D.R., Orr, A.H., Ivanova, V.S., and Bonner, W.M. (1998). DNA double-stranded breaks induce histone H2AX phosphorylation on serine 139. J. Biol. Chem. *273*, 5858–5868.

Ross, P.L., Huang, Y.N., Marchese, J.N., Williamson, B., Parker, K., Hattan, S., Khainovski, N., Pillai, S., Dey, S., Daniels, S., et al. (2004). Multiplexed protein quantitation in Saccharomyces cerevisiae using amine-reactive isobaric tagging reagents. Mol. Cell Proteomics *3*, 1154–1169.

Santisteban, M.S., Kalashnikova, T., and Smith, M.M. (2000). Histone H2A.Z regulats transcription and is partially redundant with nucleosome remodeling complexes. Cell *103*, 411–422.

Savage, M., and Bonner, J. (1978). Fractionation of chromatin into template-active and template-inactive portions. Methods Cell Biol. *18*, 1–21.

Schalch, T., Duda, S., Sargent, D.F., and Richmond, T.J. (2005). X-ray structure of a tetranucleosome and its implications for the chromatin fibre. Nature *436*, 138–141.

Scheer, U., and Hock, R. (1999). Structure and function of the nucleolus. Curr. Opin. Cell Biol. *11*, 385–390.

Schmid, M., Arib, G., Laemmli, C., Nishikawa, J., Durussel, T., and Laemmli, U.K. (2006). Nup-PI: the nucleopore-promoter interaction of genes in yeast. Mol. Cell *21*, 379–391.

Schmid, M., Durussel, T., and Laemmli, U.K. (2004). ChIC and ChEC: Genomic Mapping of Chromatin Proteins. Molecular Cell *16*, 147–157.

Schwartz, B.E., and Ahmad, K. (2005). Transcriptional Activation Triggers Deposition and Removal of the Histone Variant H3.3. Genes Dev. *19*, 804–814.

Sengstag, C., and Hinnen, A. (1988). A 28-bp segment of the Saccharomyces cerevisiae PHO5 upstream activator sequence confers phosphate control to the CYC1-lacZ gene fusion. Gene *67*, 223–228.

Shen, X., Mizuguchi, G., Hamiche, A., and Wu, C. (2000). A chromatin remodelling complex involved in transcription and DNA processing. Nature *406*, 541–544.

Siddiqi, I.N., Dodd, J.A., Vu, L., Eliason, K., Oakes, M.L., Keener, J., Moore, R., Young, M.K., and Nomura, M. (2001). Transcription of chromosomal rRNA genes by both RNA polymerase I and II in yeast uaf30 mutants lacking the 30 kDa subunit of transcription factor UAF. EMBO J. *20*, 4512–4521.

Simpson, R.T. (1990). Nucleosome positioning can affect the function of a cis-acting DNA element in vivo. Nature *343*, 387–389.

Simpson, R.T. (1998). Chromatin structure and analysis of mechanisms of activators and repressors. Methods *15*, 283–294.

Simpson, R.T., Ducker, C.E., Diller, J.D., and Ruan, C. (2004). Purification of native, defined chromatin segments. Meth. Enzymol. *375*, 158–170.

Smith, C.M., Gafken, P.R., Zhang, Z., Gottschling, D.E., Smith, J.B., and Smith, D.L. (2003). Mass spectrometric quantification of acetylation at specific lysines within the amino-terminal tail of histone H4. Anal. Biochem. *316*, 23–33.

Smith, J.S., and Boeke, J.D. (1997). An unusual form of transcriptional silencing in yeast ribosomal DNA. Genes Dev. *11*, 241–254.

Smith, J.S., Brachmann, C.B., Celic, I., Kenna, M.A., Muhammad, S., Starai, V.J., Avalos, J.L., Escalante-Semerena, J.C., Grubmeyer, C., Wolberger, C., et al. (2000). A phylogenetically conserved NAD+-dependent protein deacetylase activity in the Sir2 protein family. Proc. Natl. Acad. Sci. U.S.A. *97*, 6658–6663.

Sogo, J.M., and Thoma, F. (1989). Electron microscopy of chromatin. Meth. Enzymol. *170*, 142–165.

Springer, M., Wykoff, D.D., Miller, N., and O'Shea, E.K. (2003). Partially phosphorylated Pho4 activates transcription of a subset of phosphate-responsive genes. PLoS Biol. *1*, E28.

Stagljar, I., Hübscher, U., and Barberis, A. (1999). Activation of DNA replication in yeast by recruitment of the RNA polymerase II transcription complex. Biol. Chem. *380*, 525–530.

van Steensel, B., Delrow, J., and Henikoff, S. (2001). Chromatin profiling using targeted DNA adenine methyltransferase. Nat. Genet. *27*, 304–308.

van Steensel, B., and Henikoff, S. (2000). Identification of in vivo DNA targets of chromatin proteins using tethered dam methyltransferase. Nat. Biotechnol. *18*, 424–428.

Steger, D.J., Haswell, E.S., Miller, A.L., Wente, S.R., and O'Shea, E.K. (2003). Regulation of chromatin remodeling by inositol polyphosphates. Science *299*, 114–116.

Stein, A., Whitlock, J.P., Jr, and Bina, M. (1979). Acidic polypeptides can assemble both histones and chromatin in vitro at physiological ionic strength. Proc. Natl. Acad. Sci. U.S.A. *76*, 5000–5004.

Stinchcomb, D.T., Struhl, K., and Davis, R.W. (1979). Isolation and characterisation of a yeast chromosomal replicator. Nature *282*, 39–43.

Strahl, B.D., and Allis, C.D. (2000). The language of covalent histone modifications. Nature *403*, 41–45.

Strohalm, M., Hassman, M., Kosata, B., and Kodícek, M. (2008). mMass data miner: an open source alternative for mass spectrometric data analysis. Rapid Commun. Mass Spectrom. *22*, 905–908.

Strohalm, M., Kavan, D., Novák, P., Volný, M., and Havlícek, V. (2010). mMass 3: a cross-platform software environment for precise analysis of mass spectrometric data. Anal. Chem. *82*, 4648–4651.

Stros, M., Muselíková-Polanská, E., Pospísilová, S., and Strauss, F. (2004). High-affinity binding of tumor-suppressor protein p53 and HMGB1 to hemicatenated DNA loops. Biochemistry *43*, 7215–7225.

Sun, Z.-W., and Allis, C.D. (2002). Ubiquitination of histone H2B regulates H3 methylation and gene silencing in yeast. Nature *418*, 104–108.

Svaren, J., and Hörz, W. (1997). Transcription factors vs nucleosomes: regulation of the PH05 promoter in yeast. Trends in Biochemical Sciences *22*, 93–97.

Taipale, M., Rea, S., Richter, K., Vilar, A., Lichter, P., Imhof, A., and Akhtar, A. (2005). hMOF histone acetyltransferase is required for histone H4 lysine 16 acetylation in mammalian cells. Mol. Cell. Biol. *25*, 6798–6810.

Tan, M., Luo, H., Lee, S., Jin, F., Yang, J.S., Montellier, E., Buchou, T., Cheng, Z., Rousseaux, S., Rajagopal, N., et al. (2011). Identification of 67 histone marks and histone lysine crotonylation as a new type of histone modification. Cell *146*, 1016–1028.

Telford, D.J., and Stewart, B.W. (1989). Micrococcal nuclease: its specificity and use for chromatin analysis. Int. J. Biochem. *21*, 127–137.

Thoma, F., Bergman, L.W., and Simpson, R.T. (1984). Nuclease digestion of circular TRP1ARS1 chromatin reveals positioned nucleosomes separated by nuclease-sensitive regions. Journal of Molecular Biology *177*, 715–733.

Tolkunov, D., and Morozov, A.V. (2010). Genomic studies and computational predictions of nucleosome positions and formation energies. Adv Protein Chem Struct Biol *79*, 1–57.

Tongaonkar, P., French, S.L., Oakes, M.L., Vu, L., Schneider, D.A., Beyer, A.L., and Nomura, M. (2005). Histones are required for transcription of yeast rRNA genes by RNA polymerase I. Proc. Natl. Acad. Sci. U.S.A. *102*, 10129–10134.

Toussaint, M., Levasseur, G., Tremblay, M., Paquette, M., and Conconi, A. (2005). Psoralen photocrosslinking, a tool to study the chromatin structure of RNA polymerase I--transcribed ribosomal genes. Biochem. Cell Biol. *83*, 449–459.

Tremethick, D.J. (2007). Higher-Order Structures of Chromatin: The Elusive 30 nm Fiber. Cell *128*, 651–654.

Trendelenburg, M.F. (1983). Progress in visualization of eukaryotic gene transcription. Hum. Genet. *63*, 197–215.

Trumtel, S., Léger-Silvestre, I., Gleizes, P.E., Teulières, F., and Gas, N. (2000). Assembly and functional organization of the nucleolus: ultrastructural analysis of Saccharomyces cerevisiae mutants. Mol. Biol. Cell *11*, 2175–2189.

Tschochner, H., and Hurt, E. (2003). Pre-ribosomes on the road from the nucleolus to the cytoplasm. Trends Cell Biol. *13*, 255–263.

Unnikrishnan, A., Akiyoshi, B., Biggins, S., and Tsukiyama, T. (2012). An Efficient Purification System for Native Minichromosome from Saccharomyces cerevisiae. Methods Mol. Biol. *833*, 115–123.

Unnikrishnan, A., Gafken, P.R., and Tsukiyama, T. (2010). Dynamic changes in histone acetylation regulate origins of DNA replication. Nat Struct Mol Biol *17*, 430–437.

Vannini, A., and Cramer, P. (2012). Conservation between the RNA polymerase I, II, and III transcription initiation machineries. Mol. Cell *45*, 439–446.

Venema, J., and Tollervey, D. (1999). RIBOSOME SYNTHESIS IN Saccharomyces cerevisiae. Annual Review of Genetics *33*, 261–311.

Villar-Garea, A., and Imhof, A. (2006). The analysis of histone modifications. Biochim. Biophys. Acta *1764*, 1932–1939.

Vitolo, J.M., Thiriet, C., and Hayes, J.J. (2000). The H3-H4 N-terminal tail domains are the primary mediators of transcription factor IIIA access to 5S DNA within a nucleosome. Mol. Cell. Biol. *20*, 2167–2175.

Vogelauer, M., Cioci, F., and Camilloni, G. (1998). DNA protein-interactions at the Saccharomyces cerevisiae 35 S rRNA promoter and in its surrounding region. J. Mol. Biol. *275*, 197–209.

Vogelauer, M., Wu, J., Suka, N., and Grunstein, M. (2000). Global histone acetylation and deacetylation in yeast. Nature *408*, 495–498.

Vu, L., Siddiqi, I., Lee, B.S., Josaitis, C.A., and Nomura, M. (1999). RNA polymerase switch in transcription of yeast rDNA: role of transcription factor UAF (upstream activation factor) in silencing rDNA transcription by RNA polymerase II. Proc. Natl. Acad. Sci. U.S.A. *96*, 4390–4395.

Wade, P.A. (2001). Transcriptional control at regulatory checkpoints by histone deacetylases: molecular connections between cancer and chromatin. Hum. Mol. Genet. *10*, 693–698.

Wagner, E.J., and Carpenter, P.B. (2012). Understanding the language of Lys36 methylation at histone H3. Nature Reviews Molecular Cell Biology *13*, 115–126.

Wai, H., Johzuka, K., Vu, L., Eliason, K., Kobayashi, T., Horiuchi, T., and Nomura, M. (2001). Yeast RNA polymerase I enhancer is dispensable for transcription of the chromosomal rRNA gene and cell growth, and its apparent transcription enhancement from ectopic promoters requires Fob1 protein. Mol. Cell. Biol. *21*, 5541–5553.

Wai, H.H., Vu, L., Oakes, M., and Nomura, M. (2000). Complete deletion of yeast chromosomal rDNA repeats and integration of a new rDNA repeat: use of rDNA deletion strains for functional analysis of rDNA promoter elements in vivo. Nucleic Acids Research *28*, 3524 –3534.

Warner, J.R. (1989). Synthesis of ribosomes in Saccharomyces cerevisiae. Microbiol. Rev. *53*, 256–271.

Warner, J.R. (1999). The economics of ribosome biosynthesis in yeast. Trends Biochem. Sci. *24*, 437–440.

Waterborg, J.H. (2000). Steady-state levels of histone acetylation in Saccharomyces cerevisiae. J. Biol. Chem. *275*, 13007–13011.

Wery, M., Ruidant, S., Schillewaert, S., Leporé, N., and Lafontaine, D.L.J. (2009). The nuclear poly(A) polymerase and Exosome cofactor Trf5 is recruited cotranscriptionally to nucleolar surveillance. RNA *15*, 406–419.

Wessel, D., and Flügge, U.I. (1984). A method for the quantitative recovery of protein in dilute solution in the presence of detergents and lipids. Anal. Biochem. *138*, 141–143.

West, M.H., and Bonner, W.M. (1980). Histone 2A, a heteromorphous family of eight protein species. Biochemistry *19*, 3238–3245.

White, C.L., Suto, R.K., and Luger, K. (2001). Structure of the yeast nucleosome core particle reveals fundamental changes in internucleosome interactions. EMBO J. *20*, 5207–5218.

Wittner, M., Hamperl, S., Stöckl, U., Seufert, W., Tschochner, H., Milkereit, P., and Griesenbeck, J. (2011). Establishment and Maintenance of Alternative Chromatin States at a Multicopy Gene Locus. Cell *145*, 543–554.

Woodcock, C.L., and Ghosh, R.P. (2010). Chromatin Higher-Order Structure and Dynamics. Cold Spring Harb Perspect Biol *2*,.

Workman, J.L., and Langmore, J.P. (1985). Nucleoprotein hybridization: a method for isolating specific genes as high molecular weight chromatin. Biochemistry *24*, 7486–7497.

Wu, R.S., and Bonner, W.M. (1981). Separation of basal histone synthesis from S-phase histone synthesis in dividing cells. Cell *27*, 321–330.

Wysocka, J., Swigut, T., Milne, T.A., Dou, Y., Zhang, X., Burlingame, A.L., Roeder, R.G., Brivanlou, A.H., and Allis, C.D. (2005). WDR5 associates with histone H3 methylated at K4 and is essential for H3 K4 methylation and vertebrate development. Cell *121*, 859–872.

Yuan, G.-C., Liu, Y.-J., Dion, M.F., Slack, M.D., Wu, L.F., Altschuler, S.J., and Rando, O.J. (2005). Genome-Scale Identification of Nucleosome Positions in S. Cerevisiae. Science *309*, 626–630.

Zhang, A.P.P., Pigli, Y.Z., and Rice, P.A. (2010). Structure of the LexA-DNA complex and implications for SOS box measurement. Nature *466*, 883–886.

Zhang, H., Roberts, D.N., and Cairns, B.R. (2005). Genome-wide dynamics of Htz1, a histone H2A variant that poises repressed/basal promoters for activation through histone loss. Cell *123*, 219–231.

Zhang, X.Y., and Hörz, W. (1982). Analysis of highly purified satellite DNA containing chromatin from the mouse. Nucleic Acids Res *10*, 1481–1494.

Zhang, Y., and Reinberg, D. (2001). Transcription Regulation by Histone Methylation: Interplay Between Different Covalent Modifications of the Core Histone Tails. Genes Dev. *15*, 2343–2360.

Zhou, H., Li, D., Song, L., Liu, R., Chen, J., and Huang, X. (2008). Thr11 phosphorylated H3 is associated with centromere DNA during mitosis in MCF-7 cells. Mol. Cell. Biochem. *311*, 45–50.

Zieske, L.R. (2006). A perspective on the use of iTRAQ reagent technology for protein complex and profiling studies. J. Exp. Bot. *57*, 1501–1508.

7 Abbreviations

5-FOA	5-fluoro-orotic acid
ADP	adenosine triphosphate
Amp	ampicilline
APS	ammonium persulfate
ATP	adenosine triphosphate
ARS	autonomous replication sequence
Bbd	bar-body deficient
bp	base pair(s)
CBP	calmodulin binding peptide
CEN	centromere
CDS	coding sequence
CF	core factor
ChEC	chromatin endogenous cleavage
ChIC	chromatin immunocleavage
ChIP	chromatin immunoprecipitation
CoA	coenzym A
CE	core element
C-terminal	carboxy-terminal
Da	Dalton
Dam	DNA adenine methyltransferase
DamID	DNA adenine methyltransferase identification
DFC	dense fibrillar component
DNA	desoxyribonucleic acid
dNTP	2-desoxyribonucleotide 5' triphosphate
E. coli	*Escherichia coli*
EDTA	ethylene diamine tetra acetate
EGTA	ethylene glycol tetraacetic acid
E-pro	expansion promoter
E/T	enhancer/terminator
FC	fibrillar component
g	gram(s)
GC	granular component
h	hour(s)
HAT	histone acetyltransferase
HDAC	histone deacetylase
HDM	histone demethylase
HMT	histone methyltransferase
IGS	intergenic spacer
k	kilo
kb	kilo base pair(s)
l	liter(s)
LB	lysogeny broth
MCM	minichromosome maintenance
ORC	origin recognition complex
me	methyl
mg	milligram(s)
min	minute(s)
ml	milliliter(s)
MNase	micrococcal nuclease
mM	millimolar (mmol/l)

MW	molecular weight
M	molar (mol/l)
NAD^+	nicotinamidadenine dinucleotide
NDR	nucleosome-depleted region
NER	nucleotide excision repair
N-terminal	amino-terminal
NTS	non-transcribed strand
nm	nanometer(s)
OD	optical density
ORF	open reading frame
P	promoter
PAGE	poly acryl amide electrophoresis
PBS	phophate buffered saline
PCR	polymerase chain reaction
PIC	pre-initiation complex
PICh	proteomics of isolated chromatin fragments
pH	negative decadic logarithm of [H+]
Pol	RNA polymerase
PRMT	protein arginine methyltransferase
PTM	posttranslational modification
qPCR	quantitative real-time PCR
rDNA	ribosomal DNA
RFB	replication fork barrier
RNA	ribonucleic acid
RNP	ribonucleoprotein
RP	ribosomal protein
rpm	rotations per minute
rRNA	ribosomal RNA
RT	room temperature
S	sedimentation coefficient
SAM	S-adenosyl methionine
S. cerevisiae	Saccharomyces cerevisiae
SDS	sodium dodecyl sulfate
snoRNA	small nucleolar RNA
SUMO	small ubiquitin-like modifiers
TAP	tandem affinity purification
Taq	Thermus aquaticus
TAS	Telomere-associated sequence
TBP	TATA-box binding protein
TEL	telomere
TEMED	tetramethylethylenediamine
TEV	tobacco etch virus (protease)
Tris	tris(hydroxy methyl) amino methane
TSS	transcription start site
U	unit(s)
UAF	upstream activating factor
UE	upstream element
UBP	ubiquitin proteases
UV	ultra violet
WT	wild-type

8 Publications

Hamperl, S., Brown, CR., Pérez-Férnandez, J., Bruckmann, A., Wittner, M., Huber, K., Villar Garea, A., Babl, V., Stöckl, U., Deutzmann, R., Boeger, H., Milkereit, P., Tschochner, H. and Griesenbeck, J. Compositional and structural analysis of selected chromosomal domains from *S. cerevisae* (manuscript in preparation)

Hamperl, S., Brown, CR., Pérez-Férnandez, J., Wittner, M., Huber, K., Stöckl, U., Boeger, H., Milkereit, P., Tschochner, H. and Griesenbeck, J. Purification of specific chromatin domains derived from single-copy genes of Saccharomyces cerevisiae. Methods in Molecular Biology (in press)

Németh, A.; Pérez-Férnandez, J.; Merkl P; Hamperl S.; Gerber J.; Griesenbeck J. and Tschochner H. RNA polymerase I termination: where is the end? Biochimica et Biophysica Acta Gene Gene Regulatory Mechanisms (in press)

Hierlmeier, T., Merl, J., Sauert, M., Pérez-Férnandez, J., Schultz, P., Bruckmann, A., Hamperl, S., Ohmayer, U., Rachel, R., Jacob, A., Hergert, K., Deutzmann, R., Griesenbeck, J., Hurt, E., Basler, J. and Tschochner, H. Rrp5p, Noc1p and Noc2p form a protein module which is part of early large ribosomal subunit precursors in *S. cerevisiae* Nucleic Acids Research (under revision)

Reiter, A., Hamperl, S., Seitz, H., Merkl, P., Pérez-Férnandez, J., Williams, L., Gerber, J., Nemeth, A., Léger, I., Gadal, O., Milkereit, P., Griesenbeck, J., and Tschochner, H. (2012). Association of the Reb1-homolog Ydr026c/Nsi1 with the ribosomal RNA gene termination is required for efficient Pol I transcription in yeast. EMBO J *31*(16), 3480-93.

Wittner, M., Hamperl, S., Stöckl, U., Seufert, W., Tschochner, H., Milkereit, P., and Griesenbeck, J. (2011). Establishment and Maintenance of Alternative Chromatin States at a Multicopy Gene Locus. Cell *145*, 543–554.

Goetze, H., Wittner, M., Hamperl, S., Hondele, M., Merz, K., Stoeckl, U., and Griesenbeck, J. (2010). Alternative Chromatin Structures of the 35S rRNA Genes in Saccharomyces cerevisiae Provide a Molecular Basis for the Selective Recruitment of RNA Polymerases I and II. Molecular and Cellular Biology *30*, 2028 –2045.

9 Acknowledgements

Ich bedanke mich ganz herzlich bei allen Mitgliedern des „House of the Ribosome“ für die tolle Zusammenarbeit und enorme Hilfsbereitschaft in allen Belangen. Die tolle Arbeitsatmosphäre und die entspannten Kaffeepausen haben maßgeblich zum Erfolg dieser Arbeit beigetragen.

An erster Stelle möchte ich mich bei Achim für die spannende Themastellung und die „Rundumbetreuung“ dieser Arbeit zu jeder Tages- und Nachtzeit bedanken.

Ich möchte mich auch bei Herrn Dr. Helfried Mallow für die aufrichtigen und hilfreichen Ratschläge bedanken, der leider viel zu früh aus dem Leben geschieden ist.

Ganz besonders bedanken möchte ich mich sowohl bei Prof. Dr. Herbert Tschochner als auch bei Dr. Philipp Milkereit für die vielen produktiven Anregungen und ihre stete Bereitschaft über die Ergebnisse meiner Arbeit zu diskutieren. Insbesondere möchte ich mich auch für die Möglichkeit zur Teilnahme an den zahlreichen internationalen Konferenzen bedanken.

Prof. Dr. Hinrich Boeger und Dr. Chris Brown möchte ich für die Zusammenarbeit und die Möglichkeit eines Forschungsaufenthaltes an der UCSC danken. Vielen Dank für die herzliche Gastfreundschaft und nette wissenschaftliche Betreuung in dieser und auch nach dieser Zeit.

Entschuldigen möchte ich mich bei den Kollegen im Glaskasten, deren Arbeit manchmal mit lauterer Musik unterstützt wurde. Mein Dank gilt auch meinen Forschungspraktikanten Thomas Hackenberg, Sebastian Schwindl und Bachelor-Studentinnen Julia Pickl und Annika Frauenstein für die Hilfe bei dieser Arbeit.

Mein größter Dank gilt meinen Eltern Hans und Christa für ihre bedingungslose Unterstützung während des Studiums und der Promotion. Ohne Sie wäre diese Ausbildung nicht möglich gewesen und ich bin froh dass Sie auch voll und ganz hinter meinem weiteren Weg stehen.